EFFECTS OF TETANUS TOXIN ON SYNAPTIC PROTEINS IN MODELS OF TEMPORAL LOBE EPILEPSY

by

LUCY JANE FOSS

A thesis submitted to the University of Birmingham for the degree of DOCTOR OF PHILOSOPHY

Neuronal Networks Group

School of Clinical and Experimental Medicine

College of Medical and Dental Sciences

University of Birmingham

October 2013

ABSTRACT

Injection of tetanus toxin (TeNT), systemically or directly into the brain, has long been known to cause spastic paralysis or seizures respectively: thought to be due to disruption of inhibitory neurons and cleavage of vesicle associated membrane protein 2 (VAMP2). Here we investigate mechanisms involved in TeNT-induced chronic epilepsy in the first 16 days following injections *in vivo* and focally onto organotypic hippocampal slice cultures. Immunohistochemical analysis identified a spatial and temporal cleavage of both VAMP1 and VAMP2 progressing from day 2 post injection through to days 8 and 16. This was concentration dependent in slice cultures. VAMP1 has been shown to co-localise predominantly with inhibitory and VAMP2 with excitatory neurons. Contradicting previous results we have shown cleavage of both VAMP1 and VAMP2, disruption of both inhibition and excitation and direct effects of the toxin in the contralateral hippocampus. This indicates that inhibitory neurons and VAMP2 are not specifically targeted by TeNT. This project benefits from the combination of electrophysiological and immunohistochemical techniques to uncover functional changes induced by TeNT. It is also the first study of focally injected TeNT onto slice cultures and offers benefits for future long term studies of the effects of the toxin and drug screening.

ACKNOWLEDGEMENTS

I would like to send a huge thank you to Prof. Attila Sik and Prof. John Jefferys. Their knowledge and wisdom was unending and invaluable. I have learnt so much from both of them throughout my time under their supervision, not just about science. I must also thank Dr Alex Ferecsko, Dr Andrew Powell, Dr Premysl Jiruska, Dr Wei-Chih Chang and Dr Atif Saghir for their guidance in various techniques that were crucial to the work in this thesis.

It has been wonderful to have been part of the Neuronal Networks Group. Each person deserves an individual thank you, both past and present members. Each and every day was entertaining and not a day went by without laughter and some form of silliness! I am going to miss working and socialising with you all. I would also like to thank so many of my friends for getting me through the more challenging times. From Wednesdays spent in the pub with Ella, Jen and Sarah to my wonderful housemate Kali who I could always rely upon, and to 'the gang' who have all been great friends to me for the last seven years. You have all been there for me and are wonderful people.

A final massive thank you goes to my family for their endless support. They have always helped me achieve my best and I wouldn't have been able to do it all without them.

The Olympus Fluoview FV1000 confocal microscope used in this research was obtained through the Birmingham Science City Translational Medicine Clinical Research Infrastructure and Trials Platform, with support from Advantage West Midlands (AWM).

TABLE OF CONTENTS

LIST OF ILLUSTRATIONS

LIST OF TABLES

ABBREVIATIONS

AOI	Area of interest
BSA	Bovine serum albumin
CA	Cornu ammonis
CNS	Central nervous system
DAPI	4’,6-Diamidino-2-Phenylindole
DG	Dentate gyrus
FITC	Fluorescein Isothiocyanate
GBSS	Gey’s balanced salt solution
HBSS	Hank’s balanced salt solution
MEM	Minimum Essential Medium
NGS	Normal goat serum
O-LM interneuron	Stratum oriens lacunosum moleculare interneuron
PB	Phosphate buffer
PBS	Phosphate buffered salin
Str. lacunosum moleculare	Stratum lacunosum moleculare
Str. lucidum	Stratum lucidum

Str. oriens	Stratum oriens
Str. pyramidale	Stratum pyramidale
Str. radiatum	Stratum radiatum
TBS	Tris buffered saline
TBST	Tris buffered saline + Triton X-100
TeNT	Tetanus toxin
TLE	Temporal lobe epilepsy
VAMP	Vesicle associated membrane protein
Vti1a	Vps10p-tail-interactor-1a

1 INTRODUCTION

1.1 Epilepsy

Epilepsy is a disease that affects approximately 1% of the population (Elger, 2002; Majores *et al.*, 2007) and encompasses a large family of disorders (Fisher *et al.*, 2005). For the definition of epilepsy to be used, at least one epileptic seizure must have occurred; this being the clinical manifestation of a transient incidence of abnormal synchronous or excessive neuronal activity (Engel & Pedley, 1997; Blume *et al.*, 2001; Fisher *et al.*, 2005). The abnormal firing is often self-limiting and intermittent but the disease is characterised by a chronic predisposition to seizures occurring (Engel & Pedley, 1997; Fisher *et al.*, 2005). There are also further consequences for the sufferer, including neurobiological, psychological, cognitive and social effects (Engel & Pedley, 1997; Fisher *et al.*, 2005). This is a disease that can occur across all age groups and can be a result of various factors, including head injuries, tumours, febrile seizures, and even genetic predispositions (Engel, 2001; Gambardella *et al.*, 2009; Ruban *et al.*, 2009). Everyday-life can be severely affected for patients suffering from epilepsy and the ability to carry out normal activities can become constrained if seizures are not well managed.

Epilepsy encompasses a broad variety of symptoms that arise due to disruptions and disorders of brain function that can result from pathologic processes. It is not itself a specific disease or a single syndrome. Epilepsies tend to be categorised by the type of seizure that manifest and also by other clinical features that are associated. Seizure types, recurrence patterns, age of onset, EEG recordings, familial occurrence or not, associated clinical or neurological signs and prognosis are all important in identifying certain epileptic syndromes (Engel, 2006). There are more

than 40 seizure types associated with humans and within these, some are familial (where genetic determinants are found) (Engel, 2006). The classification of epilepsies and seizure types is likely to be updated as further insights into the syndromes are made (Berg & Scheffer, 2011). The relief of seizures by treatments including medication or surgery is not always the end point to the disability. Lives can still be affected by the psychological effects that remain after the treatment of the medical factors.

Of the multiple epilepsies, temporal lobe epilepsy (TLE) is the type that we investigate in this project.

1.1.1 Temporal lobe epilepsy

Temporal lobe epilepsy is the most common form of epilepsy (Engel, 2001; Choi *et al.*, 2008), encompassing about 30% of people suffering from the disease. TLE can consist of simple partial seizures or complex partial seizures, where consciousness is maintained in the former but lost during the latter type. These seizures originate and can stay in one hemisphere of the brain, however they can progress to include both sides of the brain at which point secondary generalisation has occurred (Sharma *et al.*, 2007). This form of epilepsy is often associated with morphological changes within the hippocampus know as hippocampal sclerosis, which affects approximately 60% of TLE patients (Blumcke *et al.*, 1999). For those who do not present with hippocampal sclerosis, the type of epilepsy is termed non-lesional TLE.

For 20-40% of epilepsy sufferers, drug treatments are ineffective, categorising their epilepsy as medically intractable (Loscher, 1997; French, 2007; Loscher & Brandt, 2010). This medically intractable epilepsy often involves numerous antiepileptics

being tried in mono- and combination therapies but to no avail (Loscher, 1997). Surgical resection is most commonly and most effectively used to treat TLE of all the epilepsies (Engel, 2001); however this is not a suitable option for all patients. In TLE compared to other epilepsies, patients have a much greater risk of being refractory with estimates in the range of 58-89% of cases, although variable worldwide (Loscher, 1997; Aull-Watschinger *et al.*, 2008; Cascino, 2008). For patients that have to endure seizures which are not well controlled, the continued research into epilepsy to understand the mechanisms and variances is vitally important. This provides the first step to finding drugs or other means of treatment that may be able to help people with drug refractory epilepsy. To be able to do this, *in vivo* animal models and *in vitro* based techniques provide key research tools.

Epilepsy is one of the main causes of neuropsychiatric disability, second to depression across the world (Engel & Pedley, 1997) and therefore deserves continuing research efforts. This project uses animal models of TLE to investigate the mechanisms of the disease further.

1.2 Animal models of epilepsy

Animal models are key tools for research into multiple diseases, including neurological diseases like epilepsy. An animal model is a representation of a disease, modelling different features or symptoms which allow an insight into the human disease.

There are numerous models of epilepsy. These range from injections of substances acting on various biochemical pathways, either systemically or directly into the brain; for example kainic acid, picrotoxin or tetanus toxin (TeNT); to electrical stimulation of

parts of the brain, to hyperthermia and post-trauma models (Sharma *et al.*, 2007). The different models are able to induce different types of seizures and can represent differing stages of the disease, for example length of time to onset, occurrence of a physical injury, frequency of seizures and morphological changes. We are yet to fully understand the underlying mechanisms in both human and animal models of epilepsy thus further research is required. There are animal models that model the lesional and non-lesional forms of TLE, and can represent acute or chronic spontaneous forms, dependent on the form of induction and time after administration (Vincent & Mulle, 2009).

The existence of multiple models is of great use as the ability to model varying symptoms and causes of the disease is increased. Each model of course has advantages and disadvantages to be considered but they are tools that can provide many answers.

1.2.1 Tetanus toxin-induced epilepsy

It has been known for a long time that TeNT causes seizures in many animals, including rats, mice and rabbits (Roux & Borrel, 1898). Injection of a minute amount of TeNT into one hippocampus of an adult rat causes a chronic spontaneous model of TLE. The model does not involve a status epilepticus as in many of the other substance injection models (Raedt *et al.*, 2009; Vermoesen *et al.*, 2010). It also results in minimal cell death, with only about 10% of injected animals showing the hippocampal sclerosis morphology (Jefferys *et al.*, 1992; Jefferys & Whittington, 1996; Jiruska *et al.*, 2010)(and unpublished data from our laboratory). This is compared with injections of pilocarpine (Turski *et al.*, 1984; Cavalheiro *et al.*, 1991) or kainic acid (Lothman & Collins, 1981) that cause severe pathology. The TeNT

model is therefore a useful tool for representing those patients that have seizures but without the associated hippocampal sclerosis. However, there still remain a number of unanswered questions about the epilepsy induced by intrahippocampal TeNT injection. The model produces spontaneous recurrent seizures in adult rats from 5-7 days after injection and recovery from seizures occurs by 6-8 weeks (Mellanby *et al.*, 1977; Brace *et al.*, 1985; Empson & Jefferys, 1993). Behavioural and learning impairments remain a feature after remission from the seizures (Brace *et al.*, 1985; Jefferys & Williams, 1987). The aim of this study is to further understand the mechanism by which TeNT causes the epilepsy, focussing on the early stage – up to 16 days after injection. Future experiments will address the later stages of this model in light of our findings.

1.2.2 Actions of tetanus toxin

To be able to understand the mechanisms involved in the epilepsy induced by injections of TeNT into the brain, we must first consider the actions of the toxin. The TeNT itself is an exotoxin from the bacterium *Clostridium tetani* with a molecular weight of ~150kDa (Helting & Zwisler, 1977; Chen *et al.*, 2008a). The clinical feature most commonly associated with infection by TeNT is trismus, which is better known as ‘lockjaw’ (Smith & Drew, 1995; Farrar *et al.*, 2000; Turillazzi *et al.*, 2009). The TeNT is a zinc protease which consists of a heavy and a light chain, of which both are needed for the model. Both chains play important and different roles in the pathogenesis of the toxin. The heavy chain (~98kDa) is important for the binding, internalisation and transport of the toxin and is an atoxic component (Helting & Zwisler, 1977; Figueiredo *et al.*, 1997; Jefferys & Walker, 2006; Chen *et al.*, 2008a). The light chain (~52kDa) is responsible for the protease action of the toxin (Helting &

Zwisler, 1977; Jefferys & Walker, 2006; Chen *et al.*, 2008a). The two chains are linked by a protease sensitive loop which tissue proteases cleave, leaving a disulphide bond between the two chains (Cook *et al.*, 2001). This disulphide bond is reduced following internalisation of the toxin and this allows the light chain to become free (Cook *et al.*, 2001; Yeh *et al.*, 2010). The normal pathogenesis of the toxin involves entry through a break in the skin or a wound. The toxin is taken into motoneurons by endocytosis and then travels in endosomes by retrograde axonal transport along these motoneurons into the spinal cord (Figueiredo *et al.*, 1997). Here the toxin is able to cross synapses between neurons and have its main action; the cleavage of vesicle associated membrane protein (VAMP; also known as synaptobrevin) in presynaptic terminals (Cook *et al.*, 2001; Jefferys & Walker, 2006).

The exact mechanism of entry into neurons of the central nervous system (CNS) remains uncertain. It is likely that there are different mechanisms involved in the entry into motoneurons and the subsequent entry into interneurons (Rossetto *et al.*, 2001; Yeh *et al.*, 2010; Blum *et al.*, 2012). Whilst some show that entry into inhibitory neurons occurs through synaptic vesicle recycling and the binding of TeNT to synaptic vesicle protein 2 (SV2) (Yeh *et al.*, 2010), others have shown that synaptic recycling may not be important and that binding to gangliosides is the suggested route (Chen *et al.*, 2009; Blum *et al.*, 2012). Disruption of SV2 isoforms (Yeh *et al.*, 2010) and gangliosides (Kitamura *et al.*, 1999) have both shown some resistance to the cleavage effects of TeNT in comparison with control animals therefore the question as to TeNT entry into neurons still remains. If SV2 was to be the entry route, Yeh *et al.* (2010) have shown that inhibitory and excitatory neurons largely possess different SV2 isoforms in the cortex. Inhibitory neurons were found to mostly co-

localise with SV2A, whereas SV2B was mostly present in excitatory neurons. This was the case in both spinal cord and cortical neurons however they also show that this differential expression does not correspond with a preference of the target to one population or the other. The hippocampus has been shown to express both SV2A and SV2B although their co-localisations with specific neuron populations has not been studied (Janz & Sudhof, 1999), but a lack of SV2B staining in the stratum lucidum (str. lucidum) and hilus would suggest that perhaps SV2B is not expressed in excitatory granule or mossy cells of the hippocampus.

1.2.3 Vesicle Associated Membrane Protein (VAMP) as the target for TeNT

The VAMPs belong to the group of soluble N-ethylmaleimide sensitive factor attachment protein receptors (SNARE) which are required for neurotransmitter release following vesicle fusion with the presynaptic membrane (Chen *et al.*, 2008a). A single hydrophobic C-terminal segment anchors the VAMP to the synaptic vesicle and the rest of the protein remains in the cytoplasm (Sollner *et al.*, 1993; Yamasaki *et al.*, 1994). For vesicle fusion to occur, a SNARE complex must be formed. This is through the interaction of a v-SNARE; those that sit within the vesicle membrane e.g. VAMP, and two t-SNAREs; those that reside in the target membrane, e.g. syntaxin1 and synaptosomal-associated protein 25 (SNAP-25) (Figure 1.1).

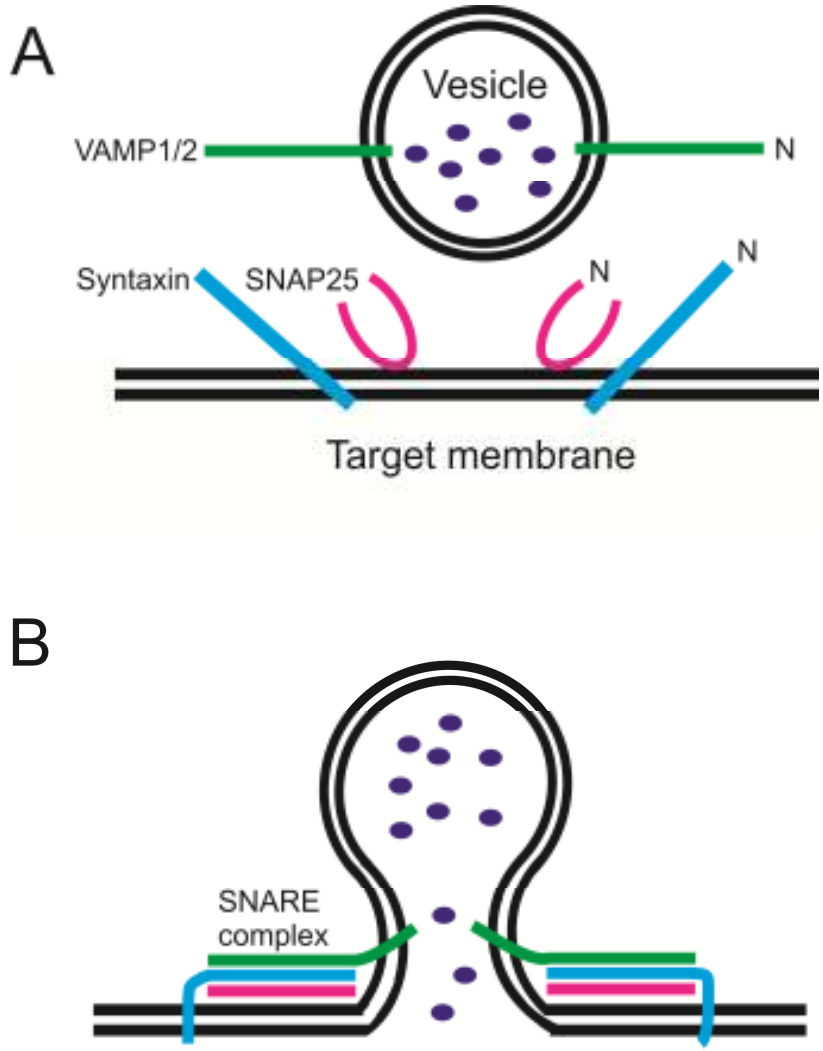

Figure 1.1. Schematic of vesicle fusion by formation of the SNARE complex. Panel A shows VAMP/synaptobrevin (v-SNARE) associated with synaptic vesicles and syntaxin and SNAP25 (t-SNAREs) associated with the target membrane (synaptic cleft). Panel B shows the formation of a SNARE complex and the resulting fusion of the vesicle membrane with that of the target membrane, allowing for neurotransmitter release. The SNARE complex is formed when the SNARE motifs of each of VAMP/synaptobrevin, syntaxin and SNAP25 are combined. Figure adapted from Sudhof (2004).

Botulinum toxins (BoNTs) and TeNT have specific cleavage sites on VAMP, syntaxin and/or SNAP25. These are represented in Figure 1.2. Interestingly, Hayashi *et al.* (1994) showed that the cleaved fragment of VAMP2 (cleaved by TeNT) was still able to form the stable complex with syntaxin and SNAP25 but if the complex had already

been formed, then the TeNT could not have its action. This showed that vesicles that had already docked and fused with the presynaptic membrane were unaffected by the protease action of the toxin. Humeau *et al.* (2000) also showed that there was a very tight window during the docking process of vesicles at the active zone in which the TeNT could have its action. Over time, the TeNT will continue to cleave the VAMP isoforms when they become available within the 'physiological window' (Humeau *et al.*, 2000).

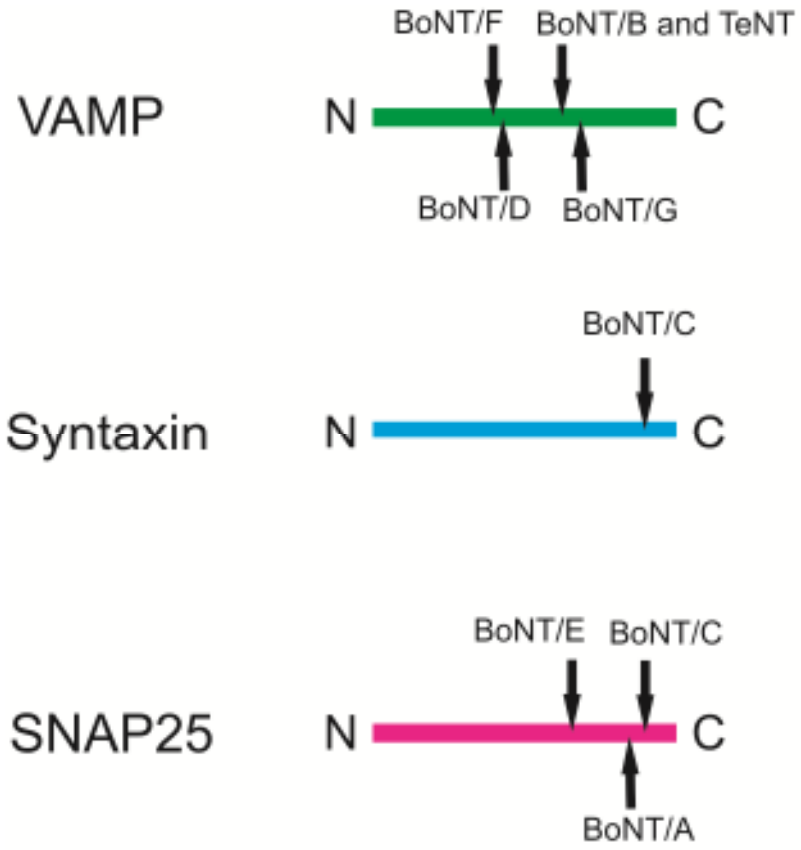

Figure 1.2. Sites of cleavage by TeNT and BoNTs. Representation of the cleavage sites of the seven different BoNTs and TeNT. These cleave VAMP/synpatobrevin, syntaxin and SNAP25 at distinct sites. BoNT/B and TeNT cleave at the same site on VAMP/synaptobrevin. Adapted from Humeau *et al.* (2000).

The use of toxins like tetanus and botulinum allowed for the discovery of the function of proteins involved in neurotransmitter release e.g. VAMP, and to further understand the mechanisms used (Schiavo *et al.*, 1992; Yamasaki *et al.*, 1994; Hussain & Davanger, 2011). New techniques have also allowed for TeNT light chain to be targeted to specific neurons in drosophila and rat brain to elucidate the function of subpopulations of neurons. These include use of the GAL4/UAS system in drosophila that has shown roles of specific neurons in circadian rhythm, visual fixation and locomotion (Xiong *et al.*, 2010; Chow *et al.*, 2011; Umezaki *et al.*, 2011; Alekseyenko *et al.*, 2013). Recombinant proteins have also been used to specifically target subpopulations of neurons in rats to show the neurons involved in rotational behaviour (Kobayashi *et al.*, 2008) and virally targeted TeNT in CA1 parvalbumin neurons has shown their importance in spatial reference memory (Murray *et al.*, 2011). Whilst intrahippocampal injections of TeNT have been predominantly carried out in rats, a recent study has shown epileptiform activity after TeNT into the visual cortex of mice (Mainardi *et al.*, 2012). Our laboratory is also currently undertaking intrahippocampal injections into mice for comparative studies to those in rats. These experiments emphasise the importance of TeNT as a tool to look at neuronal function and the resulting dysfunction of the network,

In the TeNT model of chronic recurrent epilepsy, the disruption of neurotransmission through the disruption of the formation of SNARE complexes after cleavage of VAMP accounts for changes in neuronal activity. This is thought to be through disturbances in the inhibition-excitation ratio. The literature regarding TeNT includes some discrepancies as to the target of the exotoxin. Most claim that VAMP2 alone is the target based on work by Schiavo *et al.* (1992), whereas others only state that

inhibitory neurons are preferentially targeted (Humeau *et al.*, 2000; Doheny *et al.*, 2002) due to the spastic paralysis caused after peripheral infection. Part of this project looks to resolve this discrepancy by looking at the distribution of the VAMP1 and VAMP2 isoforms at different time points throughout the *in vivo* and *in vitro* model and to further understand their roles in the induction of epilepsy.

1.2.4 Summary of TeNT model

This TeNT model has been shown to be complex and discrepancies exist between different theories as to the actions of the toxin. The aim of this project is to study, in detail, the changes that occur during the first 16 days of the model with a focus on the cleavage effects of the toxin using immunohistochemistry and the coupling of these results with functional electrophysiological recordings. This study focuses on three specific time points within the course of the TeNT-induced epileptic syndrome. Two days post injection was chosen as the first time point as it represents a stage before epileptic seizures have been witnessed and within *in vitro* slices, no epileptic activity could be stimulated (Jefferys, 1989). The 8 day post injection group were chosen as this is at a time when seizures have begun in most animals and the threshold for burst firing was at its lowest in acute *ex vivo* slices (Whittington & Jefferys, 1994). The day 16 group represents the time point when epileptic activity is at its peak in *ex vivo* slices (Whittington & Jefferys, 1994). The use of the hippocampus, an area which has a laminar structure allows for detailed analysis of the effects of the toxin.

1.3 The Hippocampus

The hippocampus contains a unique and specialised organisation and is the main focus of this study. It forms part of the temporal lobe and is a structure that is important in learning and memory. The hippocampal formation is made up of the cornu ammonis (CA) regions of which there are three; CA1-3; the hilus and the dentate gyrus (DG). The tri-synaptic pathway, in brief, carries information from external brain regions to the dentate gyrus, which in turn passes this information on to the CA3 which finally innervates the CA1. The innervations within the hippocampus are organised and complicated. The two hippocampi of the brain are connected via commissural projections. The projections of the CA3 make contact with both the ipsilateral and the contralateral CA1 and CA3 (Laurberg & Sorensen, 1981; Amaral & Lavenex, 2007). There are also commissural projections from the hilus to the contralateral inner molecular layer of the dentate gyrus (Laurberg & Sorensen, 1981) and weak projections between the CA1 on both sides of the brain (van Groen & Wyss, 1990; Gulyas *et al.*, 1998; Amaral & Lavenex, 2007).

The hippocampus consists of both inhibitory and excitatory neurons, of which the percentages are 10% and 90 % respectively (Freund & Buzsaki, 1996). Balance between the excitatory and inhibitory neurons is important when such interconnected networks exist between the different areas of individual hippocampi and between the two hippocampi. It is thought that an imbalance between the excitation-inhibition ratio could explain part of the mechanism of epilepsy. The principal excitatory cells in the hippocampal formation are the pyramidal cells of the CA1 and CA3, the granule cells of the dentate gyrus and the mossy cells of the hilus. There are multiple types of inhibitory neurons, which can be classed using multiple criteria, for example

neurochemical markers, firing properties and morphology (Freund & Buzsaki, 1996; Sugino *et al.*, 2006). Given that there are so many types and subclasses of neuron, the potential for disruption of the regulatory balance by a dysfunction or interruption of part of the neurotransmission mechanism is high.

1.3.1 Use of the hippocampus for investigation into the mechanisms involved in epilepsy

The hippocampus provides a useful research tool in that the cell layers are clearly defined and accessible in slices. *In vitro* techniques including using brain slices allow for an insight into the physiology and morphology of different brain structures in control and disease situations. For the purposes of modelling epilepsy, slices can be used that were obtained from an animal that had epilepsy induced *in vivo* or that had received a treatment in the *in vitro* setting to induce an epilepsy-like condition. Electrophysiology and immunohistochemical analyses can be carried out on these slices to gain an insight into the changes that occur during the course of the epilepsy model.

1.3.1.1 Acute ex vivo slices

Acute *ex vivo* slices are commonly used for studying the electrophysiological properties of the hippocampus following *in vivo* injection with either TeNT or control solutions (Jefferys, 1989; Empson & Jefferys, 1993; Vreugdenhil *et al.*, 2002). These slices allow application of drugs to isolate different features of the slices' properties as well as electrophysiological recordings from various regions and layers within the structure. However, a disadvantage of these slices is that they can only be used for electrophysiological recordings for about 24 hours after isolation from the animal. Following this the slices can be fixed and utilised for immunohistochemistry. The

slicing process causes a substantial degree of damage through deinnervation. The 24 hour time limit does not allow for any reorganisation or reinnervation of these denervated axons therefore recordings may not be as accurate a representation of the *in vivo* condition as would be preferable. Recordings and immunohistochemical analysis of *ex vivo* slices are used for part of this project however a technique that may go some way to overcoming the disadvantages associated with acute slices is that of organotypic hippocampal slice cultures, which are used for the remaining part of the project.

1.3.1.2 Organotypic hippocampal slice cultures

Organotypic hippocampal slice cultures are an *in vitro* technique that has been around for a number of decades (Gahwiler, 1981). A popular method involves a roller tube containing a hippocampal slice maintained in a plasma clot which goes through rotations in an incubator to alternate between being submerged in the clot and being in contact with the air. A second technique published in 1991 by Stoppini *et al.* (1991) had slices resting on a semi-permeable membrane at an interface between culture medium below the membrane and the humidified atmosphere of the incubator air above. No expensive rotating devices for the incubator were required with this method and no plasma clot was involved. New born animals are used for slice cultures with a greater success rate than with adult slices (Gahwiler *et al.*, 2001; Fuller & Dailey, 2007). This interface method is the method that we have used for the project.

Organotypic hippocampal slice cultures retain their organisation and viability for a number of weeks following isolation. From just one animal, up to 20 slices (400µm) can be cultured, with some being treated with control solution, and others with the

TeNT. This means that the animal acts as its own control. The cytoarchitecture of the hippocampus is preserved within slice cultures which provides a useful platform for manipulations of different areas. Kamada *et al.* (2004) show that the organisation of the pyramidal layers and granule cell layer within the slice are reorganised slightly but remain in the position that would be expected. The pyramidal cell layer of the CA1 reorganises to spread out into a flatter layer rather than the cells remaining piled on top of each other as is seen in the CA3 (Stoppini *et al.*, 1991; Buchs *et al.*, 1993), but this reorganisation is minimal. Another advantage of the organotypic slices is that they can be recorded from on multiple days. This allows for following changes within a slice at multiple time points. These slice cultures provide a way of refining and reducing the number of animals used in research and therefore acts as good practice. This technique has the potential to act as a medium throughput screen for antiepileptic drugs before they are used in live animals.

Organotypic hippocampal slice cultures are becoming commonly used to model a number of different disease states, including post trauma, oxygen and glucose deprivation and epilepsy. Most of these models induce the disease activity by exposing the whole slice to an agent, whether it be chemical such as kainic acid (Bausch & McNamara, 2004; Reid *et al.*, 2008) or glutamate (Ziobro *et al.*, 2011) put into the culture medium to induce epilepsy, perfusion with an epileptogenic agent (Albus *et al.*, 2008) or solution e.g. low-Mg^{2+} (Gutierrez *et al.*, 1999; Kovacs *et al.*, 1999; Wahab *et al.*, 2009), or depriving the whole slice of oxygen (Jung *et al.*, 2012). Either way, it is generally the entire slice that has been ‘treated’ with something.

Part of this project involved establishing a treatment method that can apply the TeNT in a focal manner to the organotypic slice, to mimic that of the injections of TeNT that

are carried out *in vivo*. As far as we are aware, this has not been done in slice cultures to date. A handful of groups have used TeNT with slice cultures for various experiments (Mitchell, 1998; Scheuber *et al.*, 2006) but none have applied it focally for an epilepsy model. The advantage of focal injections is that the activity of different areas of the hippocampus can be assessed following injection into a remote area. This will allow investigation into the spread of the effects of the toxin throughout the hippocampus from the injection site of the CA3. We will be able to follow this spread across the time course of the model and compare and contrast to results from *ex vivo* slices from animals that had received *in vivo* intrahippocampal TeNT injections.

There are a number of advantages to using organotypic slice cultures over acute slices and thus was the reason for attempting to establish a slice culture model of TeNT-induced epilepsy. Firstly they are a good representation of the connectivity that is present *in vivo* (Kim *et al.*, 2013) as the first week in culture allows the slice to recover from the isolation procedure and a degree of reorganisation occurs, unlike in acute slices. Admittedly recurrent connections are formed but De Simoni & Edwards (2006) have shown that cut axons do not sprout randomly but show some selectivity. Connections between the dentate gyrus and CA1 have however also been shown to form in slices that do not contain the entorhinal cortex (Gutierrez & Heinemann, 1999). This is thought to be because the afferent inputs to the dentate gyrus which arise from places like the entorhinal cortex have been cut and so new connections are formed within the remaining areas. In our slices, the entorhinal cortex remains attached to the hippocampus.

Overall, these slice cultures offer the possibility to study the effects of focal TeNT injections and to compare the results with the wealth of information that already exists from *in vivo* experiments and *ex vivo* slices.

1.4 Aims

The main aims of this project are to investigate the effects of TeNT on VAMP1 and VAMP2 within the hippocampus and therefore to further understand the mechanisms of epilepsy in the early stages of this model, up to 16 days post injection. Part of the work looks at these effects following *in vivo* intrahippocampal injections that induce chronic, spontaneous, recurrent epilepsy. Whilst there is a wealth of literature focussed on *in vivo* intrahippocampal TeNT injections, this is the first study to look at the spatiotemporal effects of the toxin on VAMP1 and VAMP2 expression in slices *ex vivo*. This was done over a timescale up to 16 days post injection. The next aim was to investigate VAMP immunopositive boutons around cells that had been recorded from at 8-16 days post injection. This was to correlate electrophysiology with immunohistochemistry to give a more detailed view of the changes within the first 16 days of the epileptic syndrome. The final stage of the project was to establish an *in vitro* model of the TeNT injections in organotypic hippocampal slice cultures. These are good representations of the *in vivo* situation with regards to organisation of the slices and connections, and offer advantages over the acutely prepared slices that are so commonly used where synaptic reorganisation is not possible in the time frame of experiments. Focal injections of an epileptogenic agent have not been characterised in organotypic hippocampal slice cultures to date and so information as to whether the effects of the TeNT can be replicated *in vitro* will offer important observations towards the uses of TeNT. Electrophysiological recordings were

compared to immunohistochemical analysis following injections, again to understand the spatiotemporal effects of the toxin.

1.4.1 Hypotheses

- VAMP2 will be cleaved within the first two weeks following *in vivo* intrahippocampal TeNT injection, the stage at which seizure onset occurs. VAMP1 will remain unaffected by the toxin given that Schiavo *et al.* (1992) have shown the TeNT cleavage site is not present in this isoform.

- Functional electrophysiological changes will be associated with local changes in VAMP expression

- Focal TeNT application onto organotypic hippocampal slice cultures *in vitro* will show comparable changes in electrophysiology and immunohistochemistry to that observed after *in vivo* injections.

2 MATERIALS AND METHODS

2.1 *In vivo* intrahippocampal TeNT injections for the investigation of the effects on VAMP1 and VAMP2

This section of the study aims to understand the spatiotemporal effects of TeNT injections on VAMP1 and VAMP2 within the early stages of the epileptic syndrome induced by these injections. This will consider the changes up to 16 days post injection and will look at both ipsilateral and contralateral hippocampi.

2.1.1 Surgery

Three experimental groups were used for this part of the study. The number of animals in each of the control experimental groups was 2. For the animals injected with TeNT: 6 were killed at 2 days post injection, 4 at 8 days post injection and 6 at 16 days post injection. The three experimental groups represented three different time points after surgery at which the rats were killed and their brains prepared for immunohistochemistry. All procedures were carried out under the Animals (Scientific Procedures) Act 1986.

Surgery was carried out by Dr Alex Ferecsko and Dr Premysl Jiruska. Adult male Sprague-Dawley rats were anaesthetised by inhalation of Isofluorane adjusted to block the pedal reflex while sustaining regular breathing. An intramuscular injection of the analgesic Buprenorphine (1ml/kg) was given to all rats. Rats were positioned in a stereotaxic frame and the skull exposed to drill a small burr hole at stereotaxic coordinates: -4.1mm anterior-posterior (AP) and -3.9mm lateral (Paxinos & Watson, 1998). A 1µl Hamilton syringe was positioned over the burr hole and lowered to a depth of -3.8mm below the cortical surface into the stratum radiatum (str. radiatum) of the dorsal CA3 area of the hippocampus (Figure 2.1). A 1µl injection of vehicle

solution, 0.05M phosphate buffered saline (PBS; Sigma-Aldrich, Dorset, UK) and 2% bovine serum albumin (BSA, Sigma-Aldrich), or TeNT-containing solution (25ng/µl (Sigma-Aldrich #B5002) in the PBS and BSA solution) was made at 200µl/min. The needle was left in place for 5mins following the injection to prevent backflow of the solution up the needle tract and allow for diffusion away from the injection site. The Hamilton syringe was removed and the skin above the midline sutured. Rats were housed individually for recovery and video monitoring.

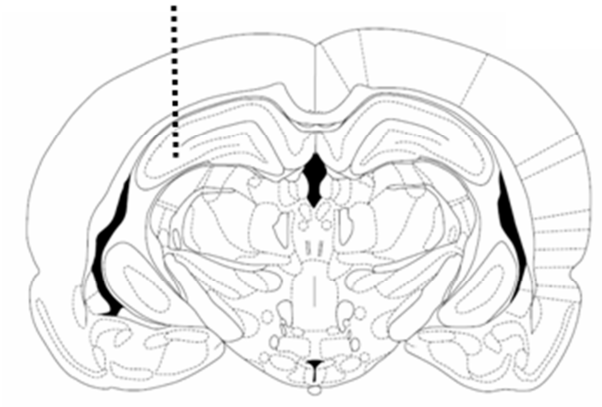

Figure 2.1. Injection site into rat brain. Coronal section at anterior-posterior co-ordinate –4.16mm within rat brain. Dotted line shows the targeted position of the injection: –3.9mm lateral and -3.8mm deep, corresponding to the right hand CA3 str. radiatum. Figure adapted from Paxinos & Watson (1998).

2.1.2 Video monitoring

Rats that had received the TeNT injection and were in the 8 and 16 day groups were video monitored individually from 5 days post injection. Those animals that were in the day 2 group were not video monitored as behavioural seizures have not been shown to occur at this early stage (Jiruska *et al.*, 2013). The monitoring equipment was infrared digital cameras (MSI 380i) coupled with Spike 2 software (CED,

Cambridge, UK). The video monitoring allowed for confirmation of the seizure syndrome using the Racine scale of seizure severity (Racine, 1972).

2.1.3 Histology

2.1.3.1 Perfusion, fixation and slicing

At the given time points of 2, 8 and 16 days post injection, the animals received an overdose of Euthatal (Merial Animal Health Limited, Essex, UK) and were perfused with saline at a speed of 1ml/min followed by 4% paraformaldehyde (Sigma-Aldrich) in 0.1M phosphate buffer (PB; Sigma-Aldrich). The brain was removed and post-fixed in 4% paraformaldehyde with gentle agitation for a further hour before storing in 0.1M PB at 4˚C.

The most anterior and posterior parts of the brain were removed and the central part glued to the block of the Vibratome Series 1000 (Technical Products International, St. Louis, MO, USA) for sectioning. Coronal sections of 80µm thickness were collected into 0.1M PB in 24 well plates. Only sections containing the hippocampus were collected. Slices were stored in 0.1M PB containing thimerosal (0.01%; Sigma-Aldrich) to avoid fungal infections.

2.1.3.2 Immunohistochemistry

Sections were washed 3 x 10 minutes in 0.1M PB followed by 2 x 15 minute washes in tris buffered saline (TBS; Sigma-Aldrich) + Triton X-100 (0.5%; Sigma-Aldrich) (TBST) for permeabilisation. The blocking solution of TBST and 5% normal goat serum (NGS; Burlingame, CA, USA) was added to the slices for 45 minutes at room temperature before incubating the respective slices in the primary antibody solution containing TBST, 2% NGS, 0.01% thimerosal and antibodies against either VAMP1

(rabbit, 1:500; Abcam, Cambridge, UK) or VAMP2 (rabbit, 1:1000; Synaptic Systems, Goettingen, Germany). The sections were incubated for three days at 4˚C. Sections were then washed 2 x 10 minutes in TBST and the secondary antibody solution added. This consisted of TBST, 0.01% thimerosal and Alexa 488 goat anti-rabbit IgG (1:1000; Molecular Probes, Paisley, UK). Sections were incubated overnight at 4˚C in the dark.

Finally, sections were washed 3 x 15min 0.1M PB and mounted on glass slides with glass coverslips using the home made anti-fade medium, Mowiol (Sigma-Aldrich). Immunofluorescent microscopy (Olympus BX61 microscope (Olympus, Essex, UK)) equipped with an EXi Blue digital camera (QImaging, Surrey, Canada) was used to reveal the labelling and tiled images at low magnification were taken to give a basic overview of the slice. An exposure time of two seconds and a light intensity of 75% were used to image all slices.

2.1.4 Analysis

2.1.4.1 Grey level analysis of VAMP1 and VAMP2 immunosignal

A grey level analysis was carried out on the low magnification images from the VAMP1 and VAMP2 immunostained slices using Image-Pro Plus software (MediaCybernetics, Maryland, USA). The Area of Interest (AOI) tool was used to outline the dentate gyrus (DG), CA2/3 and CA1 separately (Figure 2.2, Panel A). It should be noted that for VAMP1 the outer molecular layer of the dentate gyrus was not included as it had very low intensity immunostaining. The individual AOIs allowed for each area to be analysed separately. A further square AOI, placed in the contralateral subiculum was used as a marker for the brightest pixel intensity. This area was used as it is considered as part of the hippocampal formation yet does not

receive commissural projections from the ipsilateral hippocampal areas. CA1a neurons project to the subiculum just across the border from the CA1, whereas CA1c neurons project to the distal portions of the subiculum, e.g. further from the CA1, but only within the same side of the brain (Amaral *et al.*, 1991). It was hypothesised that this area would therefore be least affected, if at all, by the TeNT. The darkest intensity of pixels was considered as the threshold where all pixels in all areas were included (see Panel D in Figure 2.2). Both hippocampi (ipsilateral and contralateral) received identical staining conditions as the two sides of the brain were attached during immunostaining.

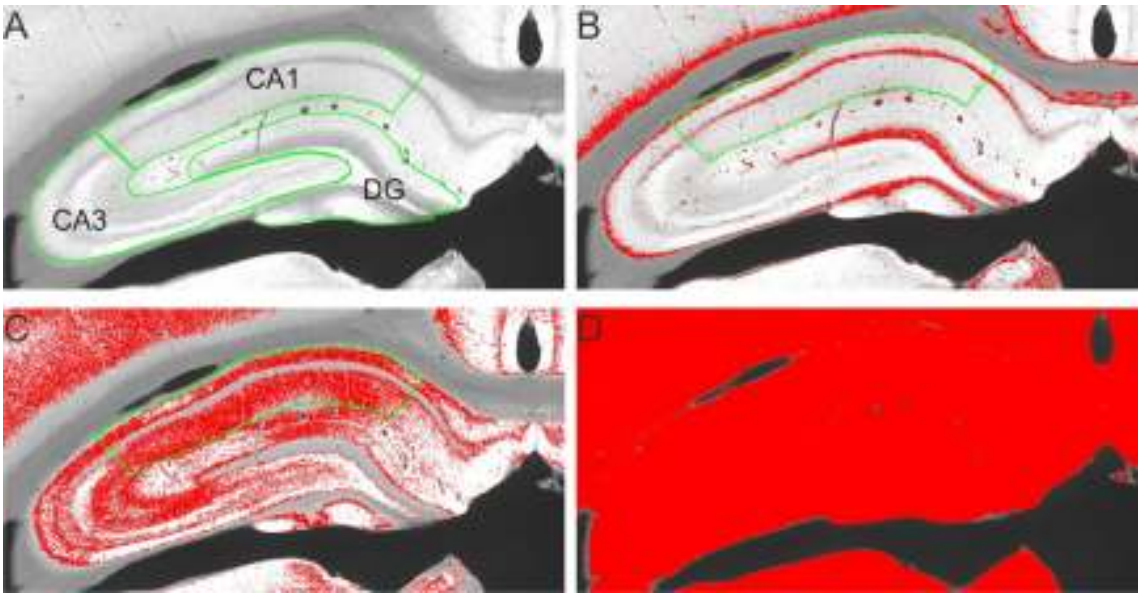

Figure 2.2. Grey level analysis. Panel A shows the outline made of each of the DG, CA2/3 and CA1. Panel B shows the pixels included in grey level 3 to be counted within the active AOI: the CA1 (outlined in green). Panel C shows the pixels included in grey level 5 and it can be seen that more pixels are present in this brighter intensity grey level than in grey level 3. Panel D shows the pixels included within the range of minimum and maximum pixel intensities for that slice.

The range between the highest and lowest pixel intensities (contralateral subiculum and all pixels included, respectively) for each individual slice was divided into 8 different grey levels. The Count/Size dialogue box within Image-Pro Plus was used and the Select Ranges tool allowed thresholds to be set for a particular count. The output for the count was set to give the sum of the area of the pixels in the selected intensity range for example grey level 3 (as shown in Panel B of Figure 2.2). The upper and lower limits for each grey level were set in the Select Ranges box and the area covered by the pixels in that range was collected. Once this had been done for each grey level, the AOI was converted to an object to measure the total area. This allowed the pixel intensities in each grey level to be represented as a percentage of the total area of the AOI. This was done for all three regions (CA1, CA2/3 and DG) in both the ipsilateral and contralateral hippocampi. The outputs allowed graphs to be made that show the distribution of the pixel intensities in the different regions of the hippocampus in control and TeNT injected animals. Any changes in the individual areas at different time points in the model and in different parts of the hippocampus (e.g. mid and posterior levels, dorsal and ventral) can also be determined.

2.1.4.2 First moment analysis

To allow for ease of comparisons of the distributions of pixel intensities in the different treatment groups (ipsilateral TeNT, contralateral TeNT, ipsilateral control and contralateral control) a form of analysis that gives a weighted average of the distribution was used. This is first moment analysis. Using a weighted average for each of the grey level spectrums allows an overall comparison of the treatment conditions to be made regarding the pixel intensities. Rather than having to compare each treatment within each grey level, the first moment looks at the distribution within

each treatment as a whole and can show if there has been a statistically significant shift towards darker or lighter intensity grey levels. If there has been a shift of the trace towards the darker grey levels, for example following cleavage of one of the VAMP isoforms, then the first moment will reflect this as a lower value.

The equation for calculating the first moment is as shown below where f is the grey level (1 through to 8) and I is the percentage of pixels in the given grey level.

$$mom_1 = \frac{\sum f.I}{\sum I}$$

The first moment for the individual hippocampal areas of each slice was calculated.

2.1.4.3 Reliability of measurements

The measurements from the grey level analysis would have benefitted from a number of steps to check reliability and repeatability. Resources did not allow for experiments to be carried out under blind conditions but a number of steps were included in the analysis to try and overcome this and remove human bias where possible, for example, the automation of the measurements. This included the thresholding tool to determine the upper and lower limits of the grey level analysis in specific and consistently chosen regions of the hippocampus. The contralateral hippocampus acting as an internal control was also important. Slices were incubated in antibody solutions with the ipsilateral and contralateral sides attached thus being exposed to the same conditions.

The boundaries of the different regions of the hippocampus were outlined by hand and thus there may be some margin of error regarding the exact regions but given that the regions are so large then this should not have too much of an implication on

the overall results. Ideally, to check the reliability of the results, duplication of the measurements could be carried out by a second person. This would include the duplication of the tracing of the areas of interest and the measurements of the grey levels.

2.1.4.4 Statistical analysis

Control values from each of the time points were compared within the individual hippocampal regions (one way ANOVA). No significant differences were found (see Appendix Section 7.1) and therefore the controls from all time points were pooled together within the individual regions. This was done separately for ipsilateral and contralateral controls. The low number of control slices at each time point was therefore no longer a problem.

Two way ANOVAs were used to compare the side (ipsilateral or contralateral) with the treatment (control or TeNT) within a hippocampal region, for example CA1, and within individual time points. SigmaPlot (Systat Software Inc., London, UK) was used to carry out all statistical analysis and a significance criterion of 0.05 was used unless otherwise stated, for example after correction for multiple comparisons. The Bonferroni correction for multiple comparisons was used when three tests representing days 2, 8 and 16 were carried out within an individual region, for example the comparisons within the CA1 mentioned above. This corrected the significance criterion to 0.0167 and reduced the chance of obtaining one or more false positives to 0.05. Whilst the data within the three individual time points was not used in more than one of the two-way ANOVAs within this grouping, the correction for multiple comparisons was still used to reduce the chance of Type I errors as the data was treated as a whole cohort rather than individually. For clarity within the

analysis, multiple univariate tests were used. This consisted of data from within individual time points being compared initially; two way ANOVAs of side versus treatment. This allowed for observations of the effects of the treatment at the specific time points and to identify the changes, if any, that occurred in the two sides of the brain during the duration of the epileptic syndrome. Following this, the three different time points were compared, but only within TeNT treated slices, as the controls had been grouped across the three different time points. Data is presented as mean ± standard error of the mean (SEM) unless indicated.

2.2 In vivo injections for functional analysis of TeNT effects

This section of the project aimed to look at VAMP1 and 2 immunohistochemistry in slices that had already been used to look at the electrophysiological effects of the toxin injected animals in comparison to controls. VAMP1 and 2 immunopositive boutons were counted to relate to the synaptic physiology. This was in order to test whether the changes in physiology that are seen in the TeNT model of epilepsy can be explained by the direct action of the toxin on VAMP1 and/or VAMP2.

2.2.1 Surgery

Two batches of animals were used, the first to investigate the ipsilateral hippocampus, the second to look at the contralateral side. Adult male Sprague-Dawley rats received a unilateral intrahippocampal injection of 1µl vehicle (0.05M PBS + 2% BSA) (6 rats for ipsilateral study and 8 for the contralateral) or TeNT-containing solution (2.5ng/µl toxin (Quadratech Diagnostics Ltd., Surrey, UK) in 0.05M PBS + 2% BSA) (5 rats for ipsilateral study and 6 for the contralateral group). Surgery was carried out by Dr Wei-Chih Chang and Dr Atif Saghir following the same protocol as described in Section 2.1.1. Animals were housed individually and allowed to recover. Spontaneous recurrent seizures began after a latent period of 5-7 days. Animals were killed and perfused with ~100ml cold sucrose ACSF (in mM: 204.8 sucrose, 2.5 KCl, 26 $NaHCO_3$, 1.2 $NaH_2PO_4H_2O$, 10 glucose, 5 $MgCl_2$, 0.1 $CaCl_2$) (by Dr Wei-Chih Chang) at 8-16 days post injection. Brains were then quickly removed and sectioned to 300µm along the coronal plane using a Vibrating Microtome 7000smz-2 (Campden Instruments, Loughborough, UK) with a cooling system and a specimen bath cooler at temperature of ~1°C. Individual slices were then transferred

to a gassed ACSF-filled holding chamber. Whole-cell patch clamp recordings were carried out from cells within the CA1, either at the subiculum end (CA1a) or the CA3 end (CA1c) (Dr Wei-Chih Chang and Dr Andrew Powell). Patched cells were filled with an internal solution containing Alexa 488 and neurobiotin. Each slice was fixed in 4% paraformaldehyde for 1 hour and then washed once with 0.1M PB before storage in 0.1M PB plus thimerosal (0.01%).

2.2.2 Histology

2.2.2.1 Re-sectioning 300µm slices to 80µm

A thickness of 300µm was not suitable for the staining protocols so the slices needed to be re-sectioned to a thickness of 80µm using a Vibratome Series 1000. A square of wax was first sectioned using the vibratome to ensure a completely flat surface, large enough for the section (containing just cortex and hippocampus) to be glued onto. The section was then superglued to the flat wax and submerged in 0.1M PB. The blade was carefully lowered in 10-20µm steps until it began to cut the surface of the slice. At this point 80µm thick sections were collected into 0.1M PB in a 24 well plate. Generally three 80µm and one 40µm thick sections were collected from a single 300µm slice. Sections were stored in fresh 0.1M PB with thimerosal (0.01%) at 4˚C in the fridge before immunohistochemistry.

2.2.2.2 Immunohistochemistry

The immunostaining procedure for these sections was very similar to that carried out on the slices used for grey level analysis, but with some slight modifications. Sections that were to be stained with the VAMP2 antibody were ready for the immunohistochemistry straight away following re-sectioning and storage, however tests with the VAMP1 antibody indicated that the slices needed to be fixed in 4%

paraformaldehyde for a further 5 hours to achieve ideal staining conditions. Aside from this, the initial part of the protocol was the same for both antibodies with initial washes in 0.1M PB and then TBST followed by 45 minutes in the blocking solution and a three day incubation in the primary antibody solution at 4˚C. The sections were incubated with either VAMP1 (1:800, Abcam) or VAMP2 (1:1000, Synaptic Systems).

The secondary antibody solution differed slightly to the previous experiments. For slices that did not contain recorded cells, the secondary antibody solution consisted of TBST, 0.01% thimerosal and Alexa 488 goat anti-rabbit IgG (1:1000; Molecular Probes) as previously. However, for sections that contained cells labelled with neurobiotin, Alexa 546 conjugated streptavidin (Molecular Probes) was added to the secondary antibody solution at a concentration of 1:200 to visualise filled cells. The sections were incubated overnight at 4˚C in the dark and then mounted onto glass slides with glass coverslips and Mowiol.

2.2.2.3 Microscopy

Immunofluorescent microscopy was carried out to reveal streptavidin labelled cells and the VAMP immunostaining. Images were taken at low magnification (4x and 10x objectives) with a light output of 25% and a 1 second exposure time. High magnification (oil immersion 100x objective) images were taken with a light output of 10% and an exposure time of 0.2 seconds.

High magnification images were taken in the strata pyramidale and radiatum of both the CA1 and the CA3. Only the CA1 contained cells that had been recorded from. These cells provided the position for the image to be taken and corresponded to either the CA1a or CA1c. If the cell body of the patched cell was present then this

was positioned in the centre of the field of vision. If it was not visible then the position was estimated by the dendrites that were visible or the position of the cell body in adjacent slices. Images of the str. pyramidale were taken with this layer running horizontally through the middle of the field of vision, with the strata oriens and radiatum present above and below respectively. For the str. radiatum images, the field of view was positioned so that the cell body layer was just out of view. A Z-stack with a total depth of 2μm made up of 10 images from the surface was taken using the fluorescein isothiocyanate (FITC) filter to look at the VAMP1 or 2 immunostaining. The Z-stacks in the CA3 were taken in the CA3b region in the same way as in CA1, but without the marker of the Alexa 546 conjugated streptavidin stained cell. Z-stacks were taken from the ipsilateral and contralateral sides of the first batch of animals, with the contralateral image positions being estimated and trying to match to the ipsilateral halves. Only the contralateral side of the second batch was used.

2.2.3 Analysis

2.2.3.1 Str. radiatum

Figure 2.3 shows a flow diagram with an overview of the image processing that was required before analysis. The purpose of these Z-stacks was to be able to count boutons that contain the vesicles that have been immunostained to reveal either VAMP1 or VAMP2. It is the vesicles within the boutons that are being visualised but we shall refer to these groups of vesicles as boutons from here onwards. The Z-stacks underwent 3D deconvolution using AutoQuant (MediaCybernetics, Maryland, USA) to reduce the distortion and produce a clearer image. Image-Pro Plus was then used to flatten the Z-stacks to one image using the Extended Depth of Field option, and the Max. Intensity Output without normalisation. Filters were applied to enhance

the image and aid the automatic counting of the boutons. The Median filter was applied first with a kernel size of 3x3 and 20 passes. Next the Flatten filter with the dark background setting and 7 pixels feature width was applied before the Despeckle filter, again with a kernel size of 3x3 and 20 passes with sensitivity of 1. A region of interest (sized 10x10μm) was placed in four different areas across the image. The software automatically counted the bright objects in the area followed by a watershed split giving an output of all the different areas of the counted objects. Only those objects that were within the size range of 0.1-<0.7μm^2 were included in the analysis as boutons. This range was chosen as it included objects that were deemed to be consistently sized and present and thus hypothesised to be boutons containing the vesicles. This was considered across a number of images before making the decision.

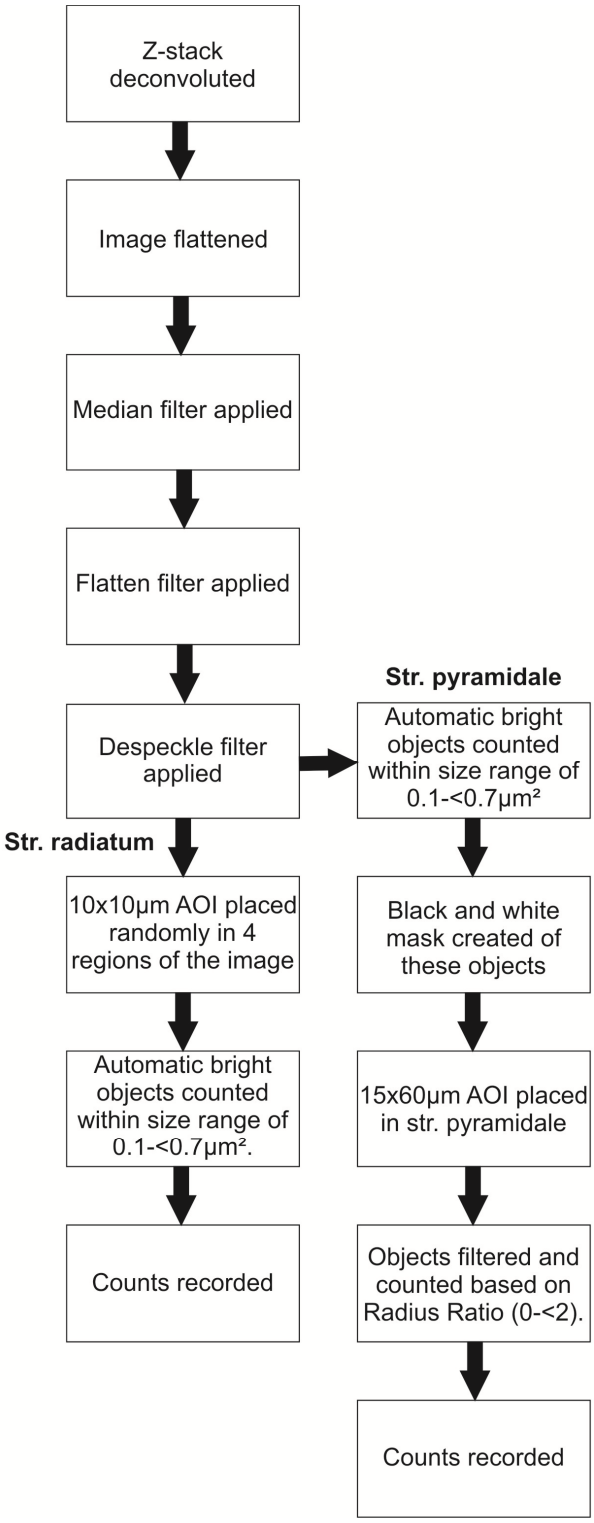

Figure 2.3. Image processing for the quantification of VAMP1 and VAMP2 immunopositive boutons. Flow diagram showing an overview of the image processing required to quantify boutons in the strata radiatum and pyramidale within high magnification *ex vivo* images.

2.2.3.2 Str. pyramidale

Counting of the boutons in the str. pyramidale had to be carried out in a slightly different way to that of the str. radiatum as shown in Figure 2.3. This was because the area contained a lot of dark space where the cell bodies were spread throughout the str. pyramidale layer, thus giving a less homogeneous layer. After the filters were applied, the boutons that were in the range of 0.1-<0.7μm^2 were counted using the bright objects counting system in Image-Pro Plus. These bright objects were then saved as a mask so that the background was black and the boutons white. This stage was an addition, different to the str. radiatum. In the case of the str. pyramidale images, randomly placing the AOI would not suffice (as was done in the str. radiatum) as there was a high chance that it could be placed in the centre of a dark cell body or out of the layer entirely. A large AOI, 15x60μm was placed within the str. pyramidale layer. This was of a size that covered about half the length of the image and was small enough to fit within the width of the str. pyramidale.

For the majority of images, it was very clear where the boutons were and they could be seen surrounding cell bodies. However, with some images where there were not very many boutons, some noise from the background was picked up as bright objects. Boutons needed to be counted, but in a way that excluded the background noise. Filtering based on Roundness was tried, where the value was calculated using the perimeter and the area. Here, a perfect circle was equal to 1, and anything else was >1. The problem here was that even background noise was sometimes being considered a perfect circle, or very close, when it was clearly not. This was because the perimeter and area could have been such that they satisfied the equation even when the image showed that the noise wasn't actually round. Instead, Radius Ratio

was chosen to filter the objects. This gave another indication of roundness but considered just the maximum and minimum radii. A perfect circle would again give a Radius Ratio equal to 1 (maximum radius divided by minimum radius). The cut-off for Radius Ratio was set at 2 to give some leeway to objects that weren't fully round. This did exclude a number of boutons, both in control and TeNT slices but it certainly made sure that the background noise was not included in the counts. This form of analysis was carried out in the CA1 and CA3 images, making sure in the CA3 images, that the AOI was put in the str. pyramidale and not in the adjacent str. lucidum.

Results from the bouton counts were compared with results from the electrophysiological recordings based on the positions of the cells (CA1a and CA1c), the side of the brain in which they were present and the treatment to which the animals had been exposed.

2.2.3.3 Statistical analysis

SigmaPlot was used for statistical analysis of the bouton counts within CA1a, CA1c and CA3. The t-test or Mann Whitney Rank Sum test was used with a significance criterion of 0.05. If a correction for multiple comparisons was needed then the Bonferroni correction was used (as in Section 2.1.4.4) and the adjusted significance criterion will be stated within the Results. Two way ANOVAs were not used in the analysis of the bouton counts as the data from some groups did not satisfy the conditions of normal distribution and equal variance. Thus multiple t-tests (for normally distributed data) or Mann Whitney Rank Sum tests (for non-normally distributed data) were required for comparison of the data.

2.3 Organotypic hippocampal slice cultures for the analysis of TeNT in vitro

This final set of experiments investigates whether injections of TeNT onto organotypic hippocampal slice cultures *in vitro* can reproduce the results seen following *in vivo* injections. Both electrophysiological and immunohistochemical experiments are undertaken.

2.3.1 Preparation of organotypic hippocampal slice cultures

2.3.1.1 Animals

The animals used for the setup of newborn organotypic hippocampal slice cultures were 5-6 day old Balb/C mice. All procedures were carried out under the Animals (Scientific Procedures) Act 1986.

Initially new born Balb/C mice aged between 5 and 10 days were used. The yield of slices that were suitable for use usually ranged from about 40-60% per animal. This meant that a number of slices from each animal showed degradation of quality throughout the days in culture and therefore could not be used for the experiments. Slices were classed as viable if the hippocampal structure could be clearly identified and showed an intact appearance under low magnification. Poor slices tended to have holes in the CA3 area, which seemed to be the most vulnerable, or show very dark patches, indicating dead cells. In preliminary recordings from untreated slices, it was rare to achieve recordings from these darkened areas suggesting that the cells were no longer living. Sometimes the cell layer of the CA3 became very close to the edge showing that there had been a recession of the tissue at the edge of the slice. Slices that displayed these characteristics were not treated as the circuitry could not be guaranteed and could vary from intact slices. The results of each set up were

variable between early batches. Best results were achieved from animals that were aged between 5 and 6 days, consistent with that in other studies (Gahwiler *et al.*, 2001; Fuller & Dailey, 2007). This age range of mice was used for collection of the results presented in this study. The yield of these slices was much better, with 60-80% of slices being usable.

Slices could be maintained with a change of medium twice a week if not out of the incubator for more than a couple of minutes. Slices had been maintained up to 50+ days in culture, which following immunohistochemistry, still showed the hippocampal architecture.

2.3.1.2 Chemicals and reagents

Culture medium consisted of: Minimum Essential Medium (MEM – with Earle's salts, without glutamine, 50%; GIBCO, Paisley, UK), Heat-Inactivated Horse Serum (25%; GIBCO), Hank's Balanced Salt Solution (HBSS, 25%; GIBCO), 45% D-glucose (~1%; Sigma-Aldrich), GlutaMAX (~1%; Sigma-Aldrich) and Penicillin-Streptomycin (~1%; Sigma-Aldrich). Dissection medium consisted of Gey's Balanced Salt Solution (GBSS; Sigma-Aldrich) and 45% D-glucose (1%; Sigma-Aldrich).

2.3.1.3 Culturing equipment

Two Millicell Cell Culture Inserts (30mm diameter, 0.4µm pore width; Millipore, Co. Cork, Ireland) were positioned on top of 1.2ml of culture medium in two wells of a 6 well plate for each brain that was dissected. The plate was put into the humidified atmosphere incubator (5% CO_2 and 37˚C) for at least 30 minutes before dissection began to allow the medium to equilibrate.

2.3.1.4 Dissection

The method used for the organotypic hippocampal slice cultures was based on that of Stoppini *et al*. (1991), with slight modifications. A 5-6 day old Balb/C mouse pup was killed using an approved Schedule 1 procedure: cervical dislocation followed by decapitation. An incision was made down the midline to expose the skull which was then opened to allow access to the brain. The brain was removed and placed into a sterile petri dish containing the dissection medium and hemisected under a Leica GZ6 dissection microscope. The midbrain was carefully removed to provide access to the hippocampus and using a pair of fine tweezers and a paddle pastette, the hippocampi from both hemispheres of the brain were gently eased away from the surrounding tissue. The hippocampi were then transferred straight to the platform of a McIlwain tissue chopper (The Mickle Laboratory Engineering Co. Ltd., Surrey, UK) and sliced to 400μm, with the long axis perpendicular to the blade. Slices were then transferred into another sterile petri dish containing dissection medium. Fine tweezers were used to separate the slices. Each Millicell insert received 8-10 slices which were positioned to avoid contact between the slices. Any excess liquid was removed and the plate returned to the incubator. The orientation of each of the slices was noted later on the day of dissection.

2.3.1.5 Maintenance of slice cultures

The medium in each well supporting the Millicell inserts was replaced every 3-4 days following 30 minutes of pre-warming in the incubator. Cultures were maintained for 10-14 days before any treatments were carried out.

2.3.2 Treatment solutions

The treatments consisted of an injection of either a vehicle solution for control slices (0.05M PBS and 2% BSA) or the TeNT solution at concentrations of 5, 25 or 50ng/µl toxin (Quadratech Diagnostics Ltd.) within the vehicle solution.

2.3.3 Optimisation of a focal treatment method

Having established that the culturing procedure produced viable slices, the next stage was to investigate how to carry out focal injections to the str. radiatum of the CA3. Organotypic hippocampal slice cultures have been used in other studies to look at epileptic activity following treatment with substances, for example kainic acid, but in these cases the entire slice was exposed to the treatment, with the substance being added to the culture medium. Other non-epilepsy based protocols employed a chamber to expose the entire well, for example, to a high oxygen environment. Again, here the entire slice is exposed. The aim of this project was to carry out focal injections like those in the *in vivo* model of TeNT induced epilepsy.

A number of factors were to be considered to establish this focal injection method; apparatus for delivering the injection, injection volume, controlled and consistent delivery of injection and maintaining the viability of slices during the injection process. The following sections will describe the different procedures that were tested to address these factors and how the final method was decided upon.

2.3.3.1 Methylene blue injections using hand held glass pipette

The first factor to be addressed was the volume of the injection and the apparatus for delivery. *In vivo*, 1µl of control or TeNT solution was injected into one hippocampus of an adult rat. Here, *in vitro* we were dealing with a single slice with thickness 100-

150µm from a new born mouse so the volume needed to be scaled down substantially. Testing started with injections of control solution containing methylene blue onto some fixed slices. Here a glass pipette (Wiretrol II, 10µl; Drummond Scientific Company, PA, USA) that had calibration marks at every 1µl was used. A plunger inserted into the end and pushed very gently was used to try to inject 0.25µl of the solution onto the slices. This produced a large amount of spread across the small slice and was therefore not suitable. Not only was the size of the injection a problem but also the accuracy at delivering a consistent volume with only judgement by eye.

2.3.3.2 Filter paper as a means of focal treatment

Next, it was thought that perhaps a small piece of filter paper soaked in the substance for treatment could provide a means of focal injection. The considerations here however included having a regular sized piece of filter paper and maintaining sterility of the slice. Would putting filter paper onto the slice cause any damage, for example introducing a barrier between the slice and the surrounding atmosphere? To fit onto just the str. radiatum of the CA3 it would have to be a very small piece of filter paper. It was tried a few times but was not taken any further.

2.3.3.3 Positioning a glass pipette in a holder to give better control.

The filter paper idea was dropped and we reverted back to using a glass pipette with a small tip size. To gain better control over the positioning of the glass pipette it was put in an electrode holder which was held in place on a clamp stand. This allowed for positioning of the pipette tip over the slice and then pushing on the plunger to eject the liquid. The tip was left in place on the slice for 5 minutes to mimic that of the injections that are carried out *in vivo.*

With tip sizes of around 20µm it was very difficult to withdraw the solution into the pipette. Tip sizes had to be increased to a minimum of 30µm to allow solution to enter. If it was difficult to get the solution in then it would be hard to be certain that it was coming out of the tip when it came to the injections. With tip sizes of 30-50µm, the injections could be made using the plunger but again it was difficult to control the volume. Even with a Vaseline coating around the plunger, it was not always a smooth movement. We needed to find a way to inject a smaller volume than 0.25µl and in a controlled manner.

2.3.3.4 Microinjections using a motorised pump

A microinjection pump is used with a Hamilton syringe in the *in vivo* injections so a variation of this idea was tried. The tip of the Hamilton syringe itself is very large in comparison to the str. radiatum of slice cultures and therefore would inject too large an area. We wanted to keep using a glass pipette to make sure that the tip size could be small enough. A Hamilton syringe was heat sealed to some rubber tubing which was in turn attached to the glass pipette supported by the electrode holder. However, liquid failed to be ejected from within the glass pipette. With such an elaborate setup it was likely that air was escaping somewhere or just being compressed. The end of the rubber tubing was put into a beaker of water to see if bubbles were released when the pump was set to inject but there weren't any, implying that the air was indeed being compressed rather than moved.

This setup needed simplifying. A paper was found Shao & Feldman (2007) that used a microinjection pump with a glass pipette and plunger clamped in place instead of the Hamilton syringe. In their study they were removing liquid rather than injecting it but the principal of the setup seemed consistent with what was required. This set up

was tried and immediately the injections proved easier to control. User defined settings were inputted into the MicroSyringe Pump Controller, relating to the length and volume of the glass pipette to work out the volume per step. Differing volumes were tested to see the spread of the injection solution across the slices. Volumes started at 150nl working downwards and with speeds ranging from 50nl/sec to 2nl/sec. Once we had established that 3nl was an injection volume that didn't disperse too much across fixed slices, the apparatus was set up to test on living slice cultures. To be able to control the pipette positioning on the slice, a USB camera was put in one of the eye pieces of a dissection microscope and connected to a computer. The software ScopePhoto (Scopetek, Zhejiang Province, China) was used to view and record the injections. It was difficult to manipulate the focus and lower the glass pipette whilst watching the computer screen at first but this got a little easier with practice. Injections of 3nl of control solution were made onto slice cultures with the tip left in place for 5 minutes on each slice. With the culture insert containing up to 10 slices and a 5 minute wait following injections, the plates were out of the incubator too long. The medium was going very pink with exposure to the low concentrations of carbon dioxide in the air. Instead, the plates were put back into the incubator between each injection to try and keep the slices in their ideal environment for as much time as possible. Later this was adapted by removing the 5 minute wait which seemed unnecessary due to the thin tissue and so any backflow of the TeNT would not occur (as was the reason for leaving it there *in vivo*).

To double check that consistent injections were occurring, fluorescent DiI was included in the injection solution (control) to see the spread of the solution across the slices. Volumes ranged from 3nl to 30nl. It was clear that the higher volume injections

produced larger diffusion areas when viewed under fluorescent microscopy. It was decided that the 16nl injection was not spreading too far and seemed better than 3nl which were not always clear as to whether the solution had come out the pipette. Injections were therefore carried out at a volume of 16nl and injection speed of 2nl/sec onto the slices. Slices were returned to the incubator between injections.

Having tried carrying out the injections in the hood using ScopePhoto to visualise the positioning of the pipette tip, it was clear that this was adding a level of unnecessary difficulty and extra time. The setup was therefore moved to a different flow hood to be able to view the slices directly down the dissection microscope rather than through ScopePhoto and the computer. This gave greater control and greatly sped up the process which meant that the slice cultures remained viable.

A final amendment to the method included cutting around the individual slices and placing these (and their attached membrane) on a new Millicell culture insert before carrying out the treatments. This meant that individual slices could easily be removed for electrophysiology or immunohistochemistry without disturbing the surrounding slices. Previously slices had been cut around when needed but this could have disturbed the toxin if the slices had been treated.

2.3.3.5 Final treatment procedure

Four hours prior to treatment, the membrane of the Millicell inserts was cut out from the surrounding plastic ring. Each individual slice and a small amount of the surrounding membrane were then cut out and all were positioned onto a new membrane. This meant that following treatment, each slice could be manipulated individually without disturbing the surrounding slices. This was important if the TeNT

was still present on the slice to avoid loss of toxicity. The medium was also changed at this point. Glass pipettes (Wiretrol II, 10µl; Drummond Scientific Company, PA, USA) were pulled on a Narishige PN-3 pipette puller (Narishige, Tokyo, Japan) and broken back to give a tip size of 30-40µm. A pipette was held in place by an electrode holder which was secured between the clamps of a MicroSyringe Pump (World Precision Instruments, FL, USA) which was in turn secured in a micromanipulator (Figure 2.4). A wire plunger was inserted into the top of the pipette with a Vaseline coat to aid the movement. The vehicle or TeNT solution was slowly withdrawn into the pipette. The MicroSyringe Pump was controlled by the Micro4™ MicroSyringe Pump Controller (World Precision Instruments, FL. USA) and user settings manually inputted.

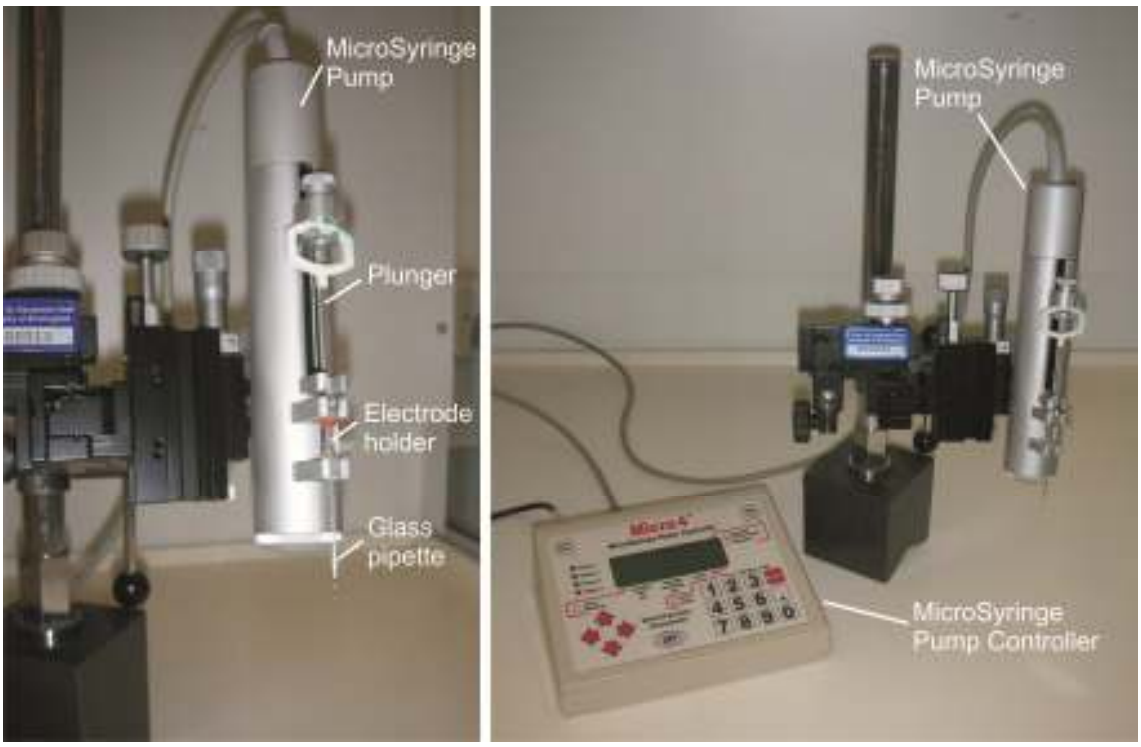

Figure 2.4. MicroSyringe Pump and Controller. These images show the glass pipette with inserted wire plunger held in place by an electrode holder which is clamped into place in the MicroSyringe Pump. This is all controlled by the Micro4™ MicroSyringe Pump Controller shown in the right hand panel.

The slice cultures were positioned under the dissecting microscope and viewed at the highest possible magnification so the cell layers of the slice could be visualised (the cell layers were darker than the surrounding areas). The tip of the pipette was positioned over the str. radiatum of the CA3 and lowered to touch the slice. An injection of 16nl of treatment solution at 2nl/sec was made and the pipette gently raised away from the slice. Injections onto all the slices on the membrane were carried out in one session and returned to the incubator as soon as possible. Plates were handled very gently to prevent too much movement which can cause loss of toxicity of the toxin. Each individual treatment was restricted to slices on the same membrane.

The slices were then left for a minimum of 2 days before the first recordings were carried out. Medium was changed 3 days after treatment and then again every 3-4 days (alternating). Having established the most appropriate treatment method, the investigation of the effects of TeNT on the slice cultures could now begin.

2.3.4 Electrophysiology

2.3.4.1 Field recordings

At 2, 8 and/or 16 days post treatment (±2 days), field recordings on the vehicle and toxin-injected slices were carried out. These recordings were carried out in an Olympus FV1000 confocal microscope with an attached incubation box (Solent Scientific, Segensworth, UK). The temperature of this box was maintained at 30°C and was useful to keep the relative sterility of the slices whilst they were being recorded from. Very few infections were caused as a result of removing slices from the culture inserts and using them for about 45 minutes in this chamber once or multiple times. The stage area consisted of an inflow and outflow of ACSF (in mM: 10

glucose, 125 NaCl, 26 $NaHCO_3$, 3 KCl, 1.25 $NaH_2PO_4H_2O$, 1 $MgCl_2$ and 2 $CaCl_2$) bubbled with 95% O_2-5%CO_2, heated to 30°C with an inline heater (Scientifica, Uckfield, UK) and flowing at 3ml/min. A temperature probe and ground electrode were also present within the stage area. Slices were positioned on the glass coverslip and weighed down to prevent movement during the recordings. The stimulus electrode was a twisted nichrome wire (50μm diameter; Advent, Oxford, UK). Recording electrodes were borosilicate glass electrodes (1.2mm O.D, 0.69mm I.D.; Harvard Apparatus, Kent, UK) pulled on a P-97 horizontal puller (Sutter Instruments, Novato, CA, USA) with resistances of 5-7MΩ. An NPI SEC-10L amplifier (Scientifica), low-pass Bessel filter set at 1kHz (NL-125, Digitimer Ltd., Welwyn Garden City, UK) and Power 1401 (CED) for digitization at 10kHz were all used for recordings. The stimulus electrode was placed in the str. radiatum of the CA3 (Figure 2.5). A recording electrode was then placed in the CA1 str. pyramidale (Figure 2.5). Signal (CED) was used to deliver a square pulse at 0.1 seconds with a length of 0.001 seconds. A stimulus response curve was created with stimuli ranging from 0-70V and a frame length of 30 seconds. The order of the stimuli was random each time and differed from one slice to the next. Stimulus response curves were then repeated in the str. radiatum of the CA1 and the strata pyramidale and radiatum of CA3 (Figure 2.5).

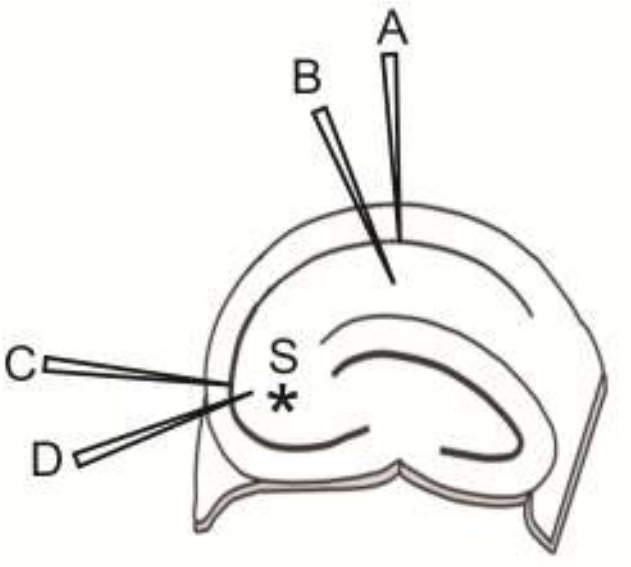

Figure 2.5. Positions of stimulus and recording electrodes for field recordings in organotypic hippocampal slice cultures. Stimulations were made at Position S (marked with asterisk). Recording positions were CA1 str. pyramidale (A), CA1 str. radiatum (B), CA3 str. pyramidale (C) and CA3 str. radiatum (D).

In three cases, particularly robust and regular spontaneous seizure-like activity was seen in the hippocampal slice cultures treated with 50ng/µl TeNT. To confirm this as biological activity, tetrodotoxin (TTX; Alomone Labs, Jerusalem, Israel) was added at a concentration of 1:1000 to the circulating ACSF. Recordings were continued with a 40V stimulus every 30 seconds. When all activity was blocked, the TTX was washed out with fresh ACSF and recordings continued, to look for the return of responses.

A low magnification image was taken after each stimulus response curve to record the position of both the stimulation and recording electrodes. This meant that when recording from a slice on multiple days, the electrodes could be placed in as similar a position to the previous recordings as possible. This would give an indication of the changes, if any, which could occur across the time points of the model within the different treatments.

Following recordings, slices were either fixed (see Section 2.3.5.1) or returned to the Millipore inserts for further recordings on a later day.

2.3.4.2 Analysis of field recordings

Analysis of str. pyramidale field recordings used cursors within Signal (CED) to give an indication of the size of the response. The first cursor was placed at the beginning of the excitatory post synaptic potential (EPSP) and the second cursor at the peak of the population spike. The trough output measures the amplitude of the response, halfway along a tangent that is formed between the start of the EPSP and the peak of the population spike. This gave a value of the size of the population spike in mV. For the str. radiatum recordings, the two cursors were placed on the EPSP within the middle 60% and the slope measurement used, giving a value of mV/ms. This was carried out for all frames within the stimulus response curve and the data plotted in SigmaPlot. For CA1 these measurements were used without problems. However, within the CA3, the largely interconnected network gave rise to both antidromic and orthodromic responses. These multiple components of the response made the measurement of the slope and trough difficult. These different components are not easily differentiated without the use of pharmacological blockers of synaptic activity. Therefore the analysis of CA3 strata pyramidale and radiatum was changed to take into account the difficulty of separation without the use of drugs. A crude measurement of the peak amplitude in relation to baseline was used; positive amplitude for str. pyramidale and negative amplitude for str. radiatum. This took into account the difference between treatment groups in the production of an antidromic response alone or an antidromic and orthodromic response combined, if a difference exists. The presence of an orthodromic response, that produced by synaptic

transmission, is likely to produce a larger positivity and negativity than an antidromic response alone. The proximity of the recording electrode to the stimulating electrode also played a part in the differences between CA1 and CA3 responses and analysis.

Epileptic like activity was seen in a number of slices, across the different treatments. These consisted of evoked afterdischarges that occurred after the stimulation or spontaneous activity not related to the stimulus. Measurements of the durations of these events were taken as well as the stimulation voltage that caused the evoked afterdischarges. An afterdischarge was considered to have occurred if there was activity remaining after the peak of the population spike and continuing to occur more than 0.02 seconds after the stimulation pulse was given.

2.3.4.3 Statistical analysis

A 3 parameter sigmoid curve was fitted to the data, from both types of analysis, to give a read-out of the maximal response size (Vmax) and the voltage required to produce half this maximal response (V50). Statistical analyses of these values were carried out using t-tests or Mann Whitney Rank Sum tests within SigmaPlot. The choice of these tests was due to the data from some conditions not following a normal distribution or showing equal variances with other groups. The significance criterion was 0.05 and the Bonferroni correction was used in cases of multiple comparisons, where stated. This will include comparisons of the four different treatment conditions which results in six different tests, thus requiring a correction of the significance criterion to 0.0083. Comparisons of the three different time points within individual treatment conditions requires three different tests and thus a Bonferroni correction to 0.0167 is made.

2.3.5 Histology

2.3.5.1 Fixation

Slices were fixed following electrophysiological recordings or at time points up to 16 days post injection. Originally, the method used for the fixation of the *ex vivo* slices was also used for the hippocampal slice cultures (1 hour 15 minutes in 4% paraformaldehyde). However the quality of the staining seemed to deteriorate. A number of possible issues were addressed. The fixation time was altered, the concentrations of antibodies changed and antibodies to test for a glial layer across the slice that could prevent penetration of the antibodies were all tested. None of these remedied the problem or provided answers to the problems with immunostaining. Microwave fixation was tried and alleviated the problems.

2.3.5.2 Microwave fixation

The microwave fixation method was as follows. A water-load of 250ml was placed in the centre of the microwave in a glass bottle. The shape of the membrane containing the slices was noted and 3-4 slices placed into a vial of 4ml 4% paraformaldehyde (at 4°C). Two of these vials without the lid on were then placed in each of two small beakers containing 40mls water (room temperature). These were placed on either side of the water-load in the microwave. The slices were then microwaved for 30 seconds, turned off for 15 seconds and finally microwaved again for 15 seconds. Slices were then promptly removed from the paraformaldehyde with a paint brush and put into 0.1M PB in 24 well plates for a 10 minute wash. Slices were then stored in 0.1M PB and thimerosal (0.01%) at 4°C before immunohistochemistry.

2.3.5.3 Immunohistochemistry

The initial washes, blocking solution, primary antibody solution and secondary antibody solution stages were mostly the same as stated in the previous sections however with some slight modifications. Sections were removed from the fridge and washed 3 x 10 minutes in 0.1M PB followed by 2 x 15 min TBST (0.5%) to permeabilise the cells. Blocking solution consisting of 5% NGS in TBST was this time supplemented by 1% BSA to decrease the background staining that was sometimes occurring with these slices. The blocking solution was put on the slices for 45 minutes at room temperature. The primary antibody solution consisting of TBST, 2% NGS, 0.01% thimerosal and the primary antibody of either VAMP1 (1:800 Abcam) or VAMP2 (1:1500; Synaptic Systems) was put on the slices and incubated for three days at 4˚C.

Following the three day incubation, the primary antibody solution was removed and the sections washed 2 x 10 minutes TBST before overnight incubation in the secondary antibody solution; TBST, 0.01% thimerosal and Alexa 488 goat anti-rabbit IgG (1:1000; Molecular Probes). The only difference following incubation with the secondary antibody was that sections were washed 2 x 15 minutes 0.1M PB before incubation in 4',6-Diamidino-2-Phenylindole (DAPI; 1:333) for 10 minutes at room temperature in the dark. A final wash in 0.1M PB and the sections were mounted on glass slides with Mowiol and glass coverslips. Nail varnish was used to seal the slides.

2.3.5.4 Microscopy

The low magnification microscopy protocol was the same as in Section 2.2.2.3. The high magnification microscopy was carried out using a similar protocol to that in

Section 2.2.2.3 but with some differences. Firstly, the exposure time was 0.05 seconds for the organotypic slice cultures. Also, there were no filled cells to use for the positioning of the *Z*-stacks, unlike the slices used in the *ex vivo* experiments. Instead, the images were taken from CA3b and CA1b consistently throughout all slices to correspond with the positioning of the electrodes in the field recordings.

2.3.6 Analysis

2.3.6.1 Analysis of high magnification images

As with the bouton counts in the *ex vivo* batch (Section 2.2.3), boutons within the CA1 and CA3 strata pyramidale and radiatum were analysed. Unfortunately, the analysis method used in the *ex vivo* slices was not suitable for use with the organotypic slice cultures. The automatic bright object count was counting areas of the image that were clearly not boutons but background noise, predominantly within TeNT treated slices. This resulted in the analysis method having to be altered for the purpose of quantitating changes, if any occurred, following treatments with control and the TeNT at different concentrations. As the automatic bright object count in Image-Pro was not successful, the Thresholding tool had to be used. This is the same tool that was used in the grey level analysis. The thresholding level was adjusted to include only objects that appeared to be boutons. There was a clear distinction between boutons and background noise in the way that the pixels appeared. Boutons were clearly groups of pixels in a relatively round formation that appeared at similar brightnesses. The background noise was seen as individual pixels or very small groups of pixels that had no clearly defined shape. Once the threshold had been set to include only those objects that were boutons, the AOI(s) was positioned. These AOIs were the same as used in the analysis of *ex vivo* slices

and positioned in the same way. A count was then conducted which measured the area occupied by the VAMP1 or 2 immunopositive objects within the threshold range already set.

2.3.6.2 Statistical analysis

Statistical analysis used for the bouton areas of the organotypic hippocampal slice cultures were the same as used in Section 2.2.3.3.

2.4 Methodological limitations and considerations

This section will address the limitations that presented themselves throughout the study in regards to methodology and analysis. As with all experiments, there remain limitations of the techniques used and the conclusions that can be drawn from the observed results.

2.4.1 Histology

Throughout the study there were a small number of issues encountered regarding histology, particularly when it came to quantification of TeNT cleavage.

2.4.1.1 Grey level analysis

The grey level analysis included multiple layers from each region of the hippocampus. If some layers were affected by the toxin and others were not then there is the possibility that the TeNT induced cleavage would be diluted by the unaffected layers. Distance from the injection site may also have a similar dilution effect. This was part of the rationale behind the later bouton analyses within individual layers of the hippocampus and also investigating CA1a and CA1c separately whilst correlating with electrophysiological recordings. Overall however the grey level analysis provided an initial insight into the spatiotemporal changes in VAMP isoform expression following treatment with TeNT.

2.4.1.2 Injection position

It is important to remember that within the grey level analysis and the bouton counts, there is likely to be variation between animals. Even though the *in vivo* injections were made using stereotaxic co-ordinates, the injection itself may not always perfectly align within the str. radiatum of the CA3. The same applies for injections

onto the slice cultures. Here, the highest magnification was used with the dissection microscope but there will be some variation because of the judgment of the positioning by eye. Minute differences could result in the effects of the toxin initially targeting different neuronal populations and the position of the injections cannot be confirmed in all animals. The injection track within animals of the day 2 group (ex *vivo*) can mostly be identified, although the exact end point of the injection is not always clear. For those animals within the day 8 and 16 groups, the injection track is not usually still visible and thus there is no confirmation of the correct positioning of the injection. All animals injected *in vivo* and used between 8 and 16 days showed seizures following treatment with the toxin. There is variation between animals relating to the frequency of seizures and the day of onset, similar to previous reports (Mellanby *et al.*, 1977; Jefferys & Whittington, 1996). This further shows that there is variation, whether it is biological variation or as a result of the injection position. Therefore the differences between the grey level distributions and the bouton counts would be expected to vary somewhat, even when all conditions are attempted to be kept consistent.

2.4.1.3 Slice fixation

Unfortunately, the fixation method used within the *ex vivo* slice experiments was not suitable for fixation of the slice cultures due to inconsistent and patchy staining. The microwave protocol used resolved the difficulties and resulted in successful staining. We believe it is unlikely that the fixation method was responsible for the need to change the bouton quantification method in slice cultures as visually the slice cultures appeared very similar to the *ex vivo* slices, and it was only the TeNT treated slices that caused the problem with the automatic bright objects count.

2.4.2 Use of multiple slices from the same animal

Multiple slices from the same animals were used within the same analysis groups, from injections *in vivo* and *in vitro*. This was used to reduce numbers of animals where possible. For recordings and bouton analysis of *ex vivo* slices, more than one area within the animal, e.g. CA1a and CA1c, were used, but from separate slices. It may be suggested that using multiple slices from the same animal would produce more variability because the extent of the toxin's effects may not be included within all slices. However, from the grey scale analysis, it was clear that there was already variation between animals and that the spread of the lesion was quite wide at 8-16 days post injection. Using multiple slices from the same animal for the culturing experiments would produce less variation in the extent of the lesion because each slice was treated individually.

3 INVESTIGATION OF THE SPATIOTEMPORAL EFFECTS OF TETANUS TOXIN FOLLOWING UNILATERAL INTRAHIPPOCAMPAL INJECTION

3.1 Spatiotemporal analysis of the distribution of VAMP1 and VAMP2 in control and TeNT-treated rats

In this section, the distribution of the VAMP1 and VAMP2 immunostaining in ipsilateral and contralateral hippocampal slices will be discussed. This will look at both the control and TeNT injected animals at 2, 8 and 16 days post injection. We will consider the distribution of staining by looking at low magnification images taken at each of the time points and then will move onto discussing the grey level analysis of these sections, looking at the individual areas of the hippocampus; dentate gyrus, CA2/3 and CA1. This will elucidate the changes, if any, which occur in these different regions over the early part of this model. First moment analysis will be used to look at the grey level graphs and analyse each trace as a single number to make comparisons between the changes in overall intensity distribution. Slices that have had the antibody for VAMP1 applied will be looked at first, followed by VAMP2.

3.1.1 Distribution of VAMP1 immunopositivity

In this section we will first establish the distribution of VAMP1 immunopositive areas within the hippocampus in control treated rats. Following this, the effects of TeNT injections will be shown at 2, 8 and 16 days post injection in the ipsilateral and contralateral hippocampi, at both mid and posterior levels within coronal brain sections.

3.1.1.1 Control hippocampus

The immunostaining distribution of VAMP1 in control sections is layer specific throughout the hippocampus (Figure 3.1 upper panels). This staining was consistent with that seen by Raptis *et al.* (2005) who looked at VAMP distribution across the

entire brain. The dentate gyrus shows the highest intensity immunosignal following fluorescent microscopy in the hilus and a lower intensity in the granule cell layer, indicating that the most VAMP1 is present in the hilus. The inner and outer molecular layers show differential immunostaining. The inner layer displays a brighter intensity immunosignal than the very dark outer molecular layer. The str. lacunosum moleculare is also seen as a dark area, similar to that of the outer molecular layer, suggesting a very low level of VAMP1 present.

The CA1 and CA2/3 show the highest immunosignal in the strata radiatum and oriens with a lower intensity in the str. pyramidale. This is consistent along the length of each area. The str. lucidum in the CA3 shows a brighter intensity than the pyramidal layer and is of similar intensity to the adjacent str. radiatum.

This layer specific distribution is consistent at 2, 8 and 16 days post injection (Figure 3.1 upper panels) and is not disrupted by the needle tract (Figure 3.1 marked with asterisks). Around this tract the tissue is of course damaged but the individual layers retain their low or high intensity immunosignal.

The contralateral control slices (Figure 3.2 upper panels) show the same layer specificity as that of the ipsilateral hippocampus and the staining is consistent across the three time points. The distribution of VAMP1 in the posterior sections remains the same as in the mid level sections, both ipsilateral (Figure 3.3 upper panels) and contralateral (Figure 3.4 upper panels). Even though the orientation of parts of the hippocampus has changed, the layer specificity remains. This shows that the spread of the control solution, if there is any spread, has no effect on the VAMP1 synaptic protein.

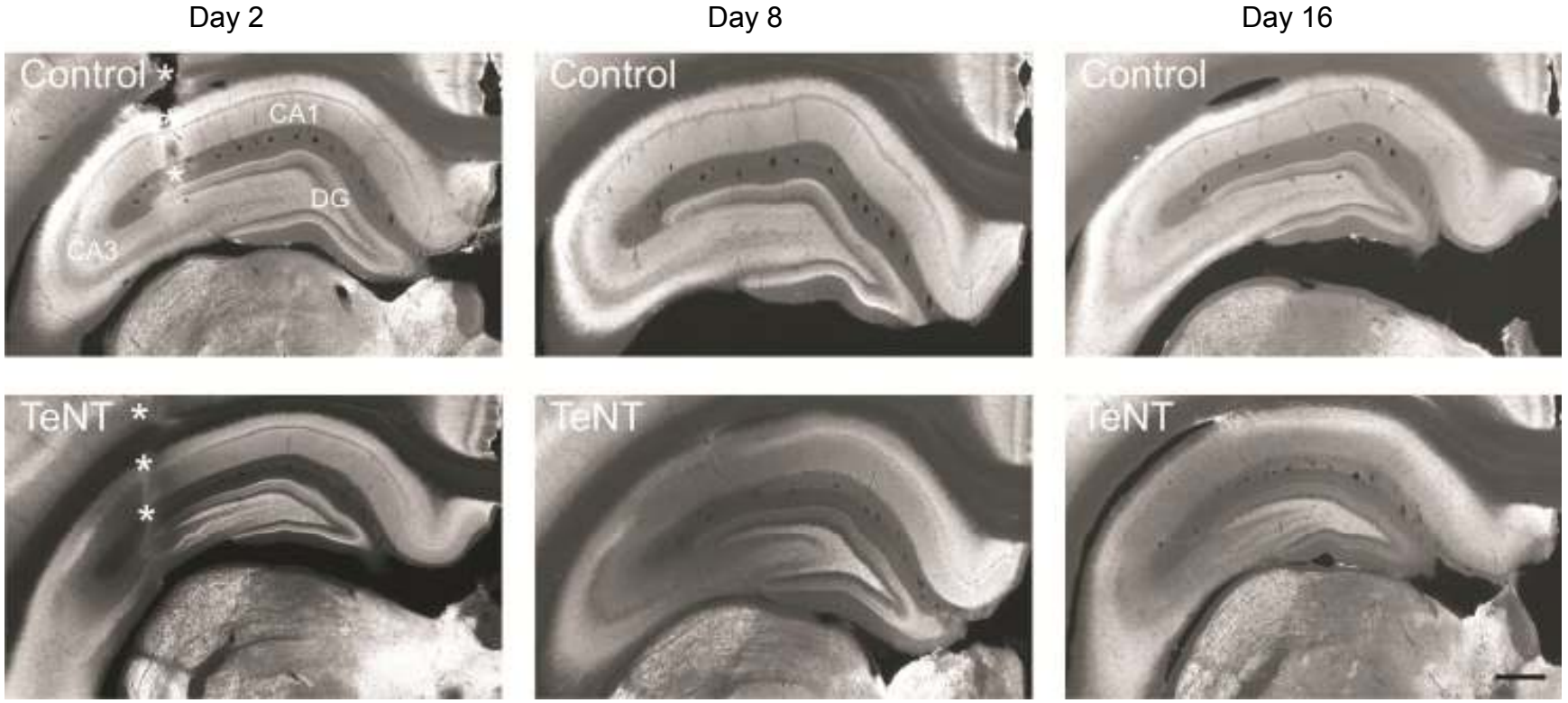

Figure 3.1. Distribution of VAMP1 immunopositivity in mid level ipsilateral hippocampus of rats injected with control or TeNT solutions. Low magnification fluorescent images of ipsilateral (injected) mid level hippocampi stained with antibody against VAMP1 and revealed using an Alexa 488 secondary antibody. Slices from control (upper panels) and TeNT (lower panels) injected animals killed at 2, 8 and 16 days post injection are shown. Asterisks in the day 2 images show the remains of the injection tract caused by the needle. Consistent differential immunostaining is seen across the hippocampi from control animals but there are increasing effects of the toxin seen in the TeNT treated slices, where a focal cleavage of VAMP1 is seen at 2 days post injection which spreads to include a larger area by day 8 and into day 16. Scale bar represents 500μm.

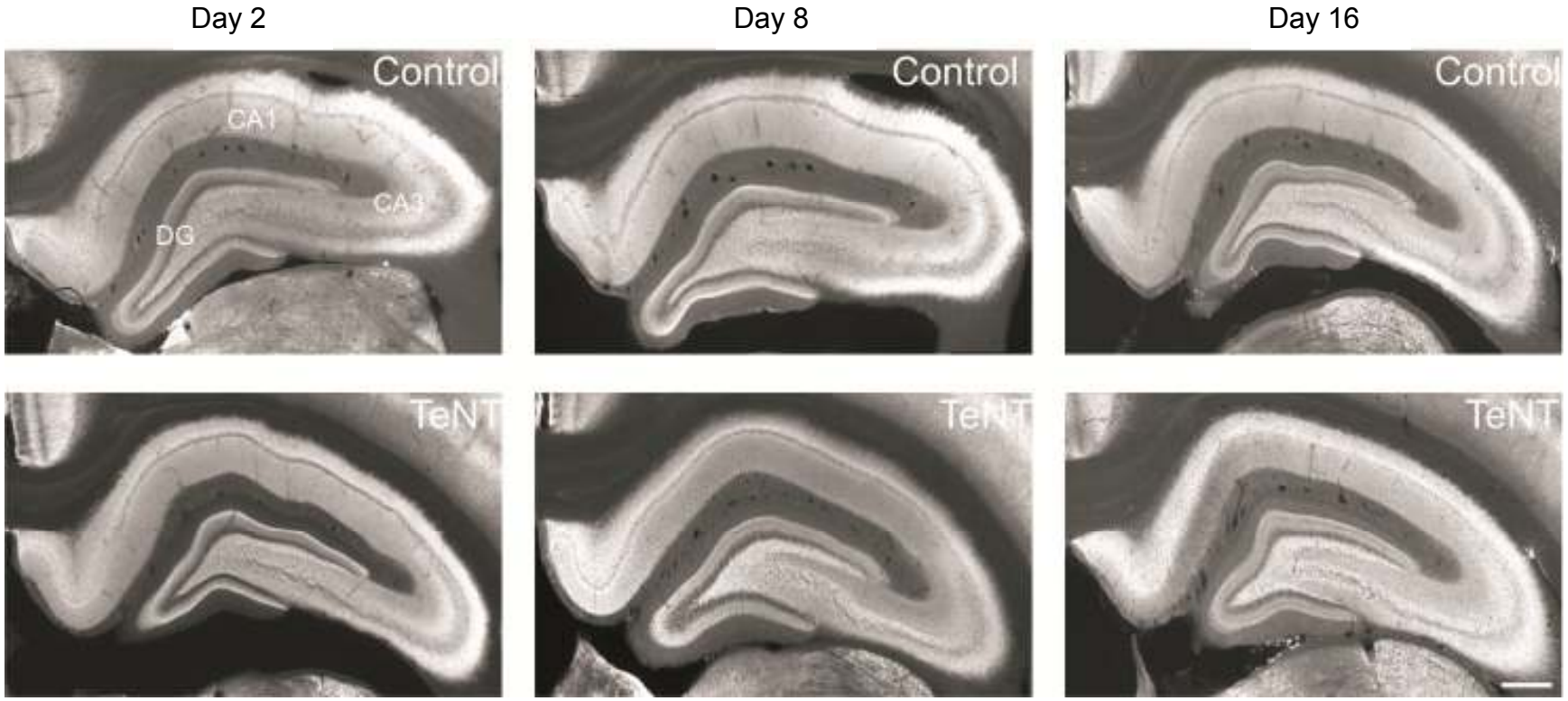

Figure 3.2. Distribution of VAMP1 immunopositivity in mid level contralateral hippocampus of rats injected with control or TeNT solutions. Low magnification fluorescent images of contralateral (uninjected) mid level hippocampi stained for VAMP1. The upper panels show control injected animals and the lower panels show TeNT injected animals at 2, 8 and 16 days post injection. The immunostaining distribution of VAMP1 is layer specific and consistent across the time points in control injected animals. Effects of the TeNT begin to be seen at day 8. Scale bar represents 500μm.

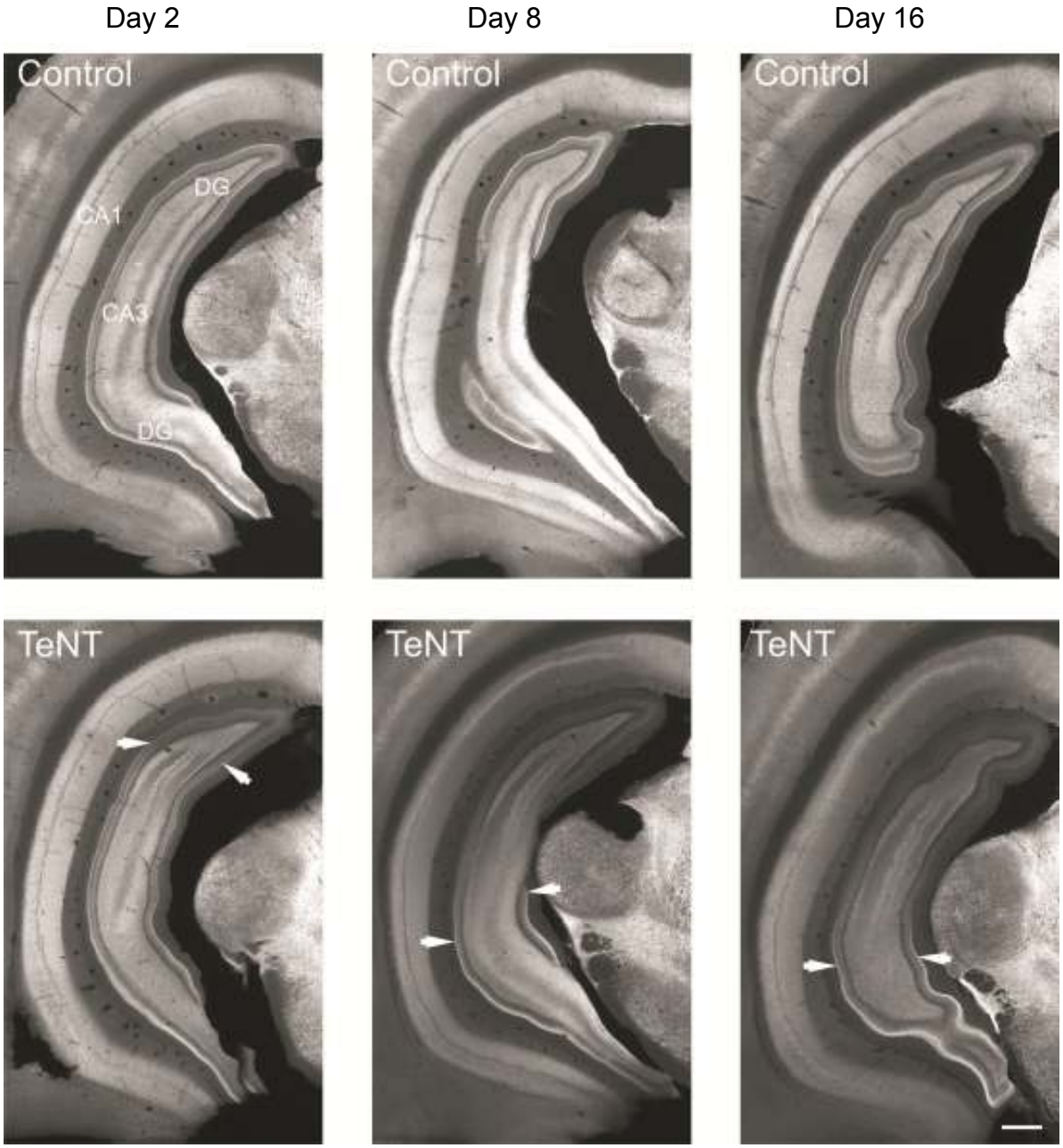

Figure 3.3. Distribution of VAMP1 immunopositivity in posterior level ipsilateral hippocampus of rats injected with control or TeNT solutions. Low magnification fluorescent images of ipsilateral posterior hippocampi immunostained for VAMP1. The secondary antibody used was Alexa 488. Animals were injected with either control (upper panels) or TeNT (lower panels) solutions. Three different groups of animals were used; those killed at 2, 8 and 16 days post injection. The control slices shows consistent differential immunostaining throughout the different layers and areas of the hippocampus. The TeNT slices show cleavage of VAMP1 most prominently at days 8 and 16. Arrowheads in TeNT images indicate that above, within dorsal regions, there is cleavage of VAMP1, particularly in the inner molecular layer, shown by loss of the bright immunosignal. Scale bar represents 500μm.

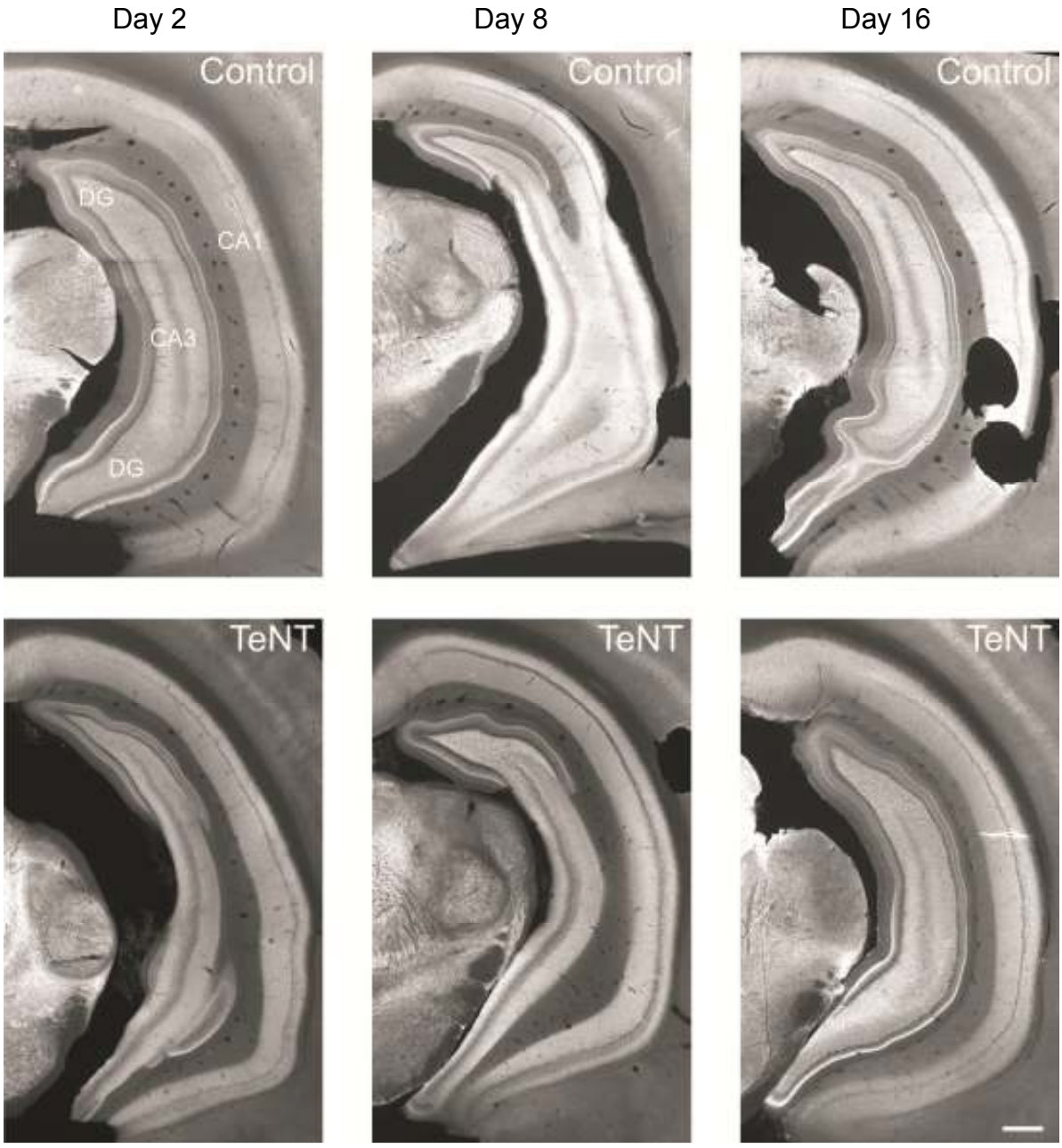

Figure 3.4. Distribution of VAMP1 immunopositivity in posterior level contralateral hippocampus of rats injected with control or TeNT solutions. Low magnification fluorescent images of contralateral posterior hippocampi stained for VAMP1. The upper panels show slices from control injected animals killed at 2, 8 and 16 days post injection respectively. The lower panels show slices from animals injected with TeNT. The controls show consistent staining across the three time points and the TeNT slices show only minimal disruption of staining in the dorsal inner molecular layer at day 16. Scale bar represents 500μm.

3.1.1.2 Mid level ipsilateral hippocampus in TeNT injected rats

Figure 3.1 (lower panels) shows representative mid level ipsilateral sections from TeNT injected animals at 2, 8 and 16 days post injection. Here it is clear that there are changes in pixel intensity in many layers surrounding the needle tract (marked by asterisks), from a focal cleavage at day 2 to a more widespread effect at later stages.

At day 2, there is a slight darkening of the inner molecular layer closest to the injection site, in comparison to the more medial area of this layer. There is also a decrease in the intensity of the immunosignal in the str. radiatum of the CA3, indicated by the stark difference in pixel intensity between the hilus and the str. radiatum. The difference between the two layers is less pronounced in control injected slices. The immunosignal has also decreased in the CA1c region which is in line with the injection tract. Both the strata radiatum and oriens around this area, both sides of the needle tract, are darker than the CA1a end of the hippocampus which is further from the injection site. This could imply that after removal of the needle, some toxin rose up the tract. The darkening of the str. radiatum in the CA3, and to some extent in the CA1, is emphasised by the str. pyramidale immunosignal appearing brighter. The darkening in CA3 and CA1c is not seen around the needle tract in control injected slices indicating that the injection of a solution itself is not causing changes in VAMP1 expression. The CA1a end shows immunostaining that is very similar to the control slices, with the str. pyramidale having a darker immunosignal than the surrounding strata radiatum and oriens. The str. lucidum appears normal in these 2 day slices, with relatively bright fluorescence, particularly in the CA3c. Some decrease in signal intensity may be seen in the str. lucidum of CA3b. These changes are seen in slices that have the needle tract present (n=3) but not to such an extreme

extent in slices without the tract (n=3). Of the 3 animals where slices showed the needle tract, two had corresponding anterior sections (1920µm more caudal) which showed minimal or no changes in the VAMP1 immunosignal. These slices were not included in the analysis as were too anterior. This shows in itself that the focal decrease in immunosignal intensity is localised around the area which received the injection at this early stage of the model. These focal changes in pixel intensity around the injection site are represented further in Figure 3.5.

Figure 3.5 shows slices from control and TeNT injected animals at day 2. The line histograms demonstrate that whilst there is a disruption of the pixel intensities due to the damage of the tissue by the needle tract, the control images show relatively consistent pixel intensities within the str. radiatum, from CA1 continuing into CA3. Within the TeNT slice however, there is a clear decrease in the pixel intensities shown by very dark areas in the image and also by the change in intensities within the graph. It also highlights that whilst the CA3 and CA1c are clearly affected by the toxin; the majority of the CA1 is not, representing the focal nature of the cleavage.

Figure 3.1 also shows a slice from a TeNT injected animal that was killed 8 days post injection. Here, the decrease in the immunosignal that was limited to the area surrounding the needle at day 2 has expanded to include more of the hippocampus. The decrease in the intensity of the immunosignal within the inner molecular layer has spread, although the crest of the dentate gyrus appears to have an immunosignal comparable to controls. The CA3 strata radiatum and oriens as a whole have become much darker than in control sections and this is emphasised by the apparent brightening of the hilus in comparison. The pyramidal layer appears brighter than the surrounding areas. In the CA3, the str. lucidum is also affected by

the toxin, shown by its lack of differential staining compared with the decreased immunosignal in the str. radiatum. More of the CA1 is affected at this time point with the spread of the cleavage extending from CA1c towards CA1a.

The animals in the day 16 group (Figure 3.1, lower right panel) show varying degrees of staining disruption across the hippocampus. This group shows a continued decrease in the brightness of the immunosignal in the inner molecular layer but to differing degrees between the slices. In the majority of cases (4 of 6) the whole layer looks darker but in others it is just the part nearest the CA3 that is affected. The most pronounced effects continue to be seen in the CA3 as a whole, and most of CA1b and c. Consistent with the changes seen at earlier time points of the model, the strata radiatum shows a darkening which makes the str. pyramidale and hilus appear brighter than in the control equivalents.

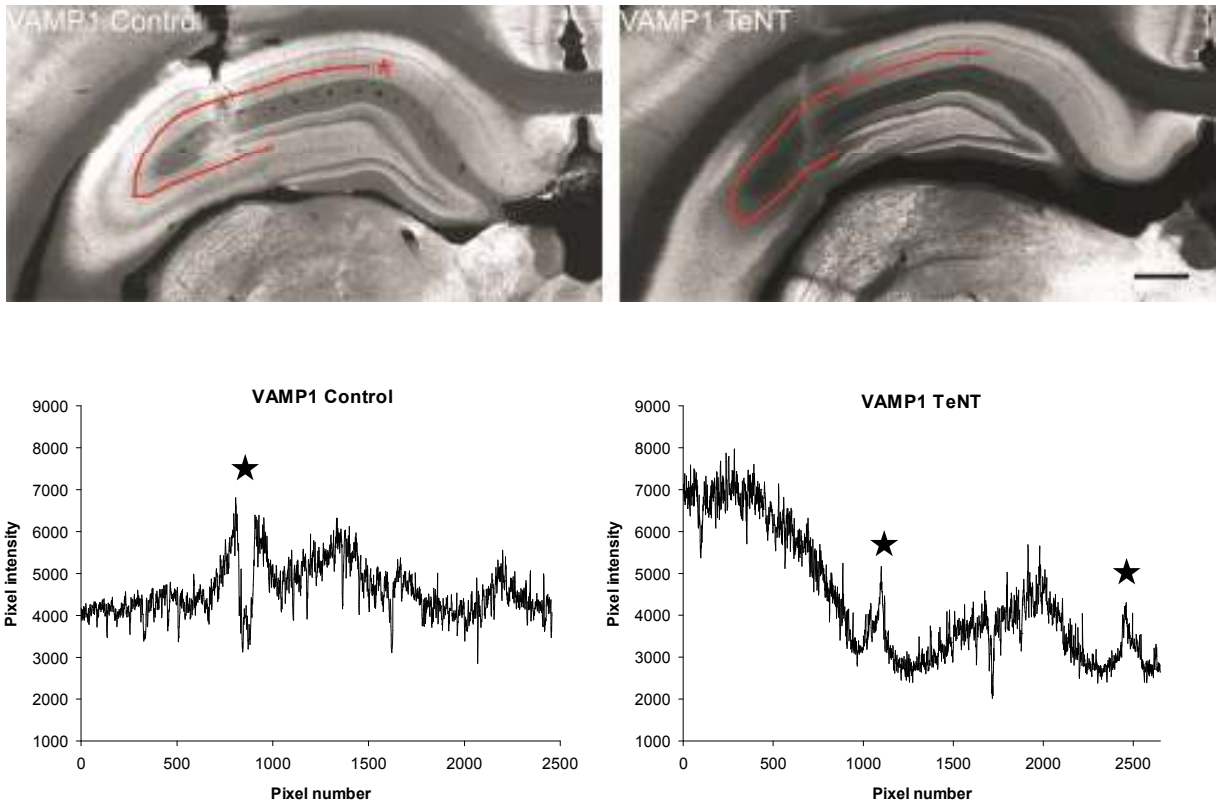

Figure 3.5. Analysis of pixel intensities around the site of control or TeNT injection within VAMP1 immunopositive slices. The images show VAMP1 immunopositive slices from 2 days after injection of control or TeNT solution. The analysis of pixel intensities starts within the CA1 str. radiatum (indicated by the asterisk; VAMP1 Control panel) and corresponds to Pixel 1 in the x axis of the graphs. Note that the sudden deflections (marked by a star) in the pixel intensity relate to the disruption of the tissue by the injection tract. Overall it can be seen that in VAMP1 immunopositive slices, the injection of TeNT causes a dramatic shift towards darker pixel intensities around the injection site, including CA1c and CA3. Scale bar represents 500µm.

3.1.1.3 Mid level contralateral hippocampus in TeNT injected rats

In contrast to the ipsilateral slices, there is no disruption of the staining in the contralateral side at 2 days post injection. The layer specific distribution remains well defined (Figure 3.2, lower panels). This lack of change in the immunosignal is likely to be because the cleavage of the toxin is only seen in a tight area around the injection site at day 2 and has had little time to spread to more remote areas for example the contralateral hippocampus.

By day 8 there are some very slight changes in the contralateral hippocampus but they are not as clear as those seen in the ipsilateral side. As seen in the ipsilateral dentate gyrus, there is a very slight decrease in the immunosignal of the inner molecular layer at the tip of the buried blade. The hilus and part of the str. lucidum appear brighter in comparison to a slight decrease in the immunosignal of the str. radiatum. There is also some darkening in the CA1 strata radiatum and oriens. The grey level analysis later in this chapter will show the changes that occur in the contralateral side in a quantitative manner rather than qualitatively.

Within the day 16 group there is some variation. Whilst there are no dramatic decreases in immunosignal seen, there are some subtle changes particularly within the str. radiatum of CA1 where there is a decrease in the signal (5 of 6 animals). These animals also show decreases in the immunosignal of the inner molecular layer across the majority of the layer rather than just focussed at the tips of the blades.

3.1.1.4 Posterior level ipsilateral hippocampus in TeNT injected rats

Much of the staining in the poster level sections of the day 2 TeNT treated group is very similar to that of the controls (Figure 3.3). The only difference occurs in 2 slices

where the very top of the slice shows a small degree of change. Here the crest of the dentate gyrus shows a darkening of the immunosignal in the inner molecular layer, shown above the arrow heads in the day 2 TeNT slice in Figure 3.3. This shows that the spread of the toxin varies from one animal to another and most likely depends on the exact position of the injection.

In the day 8 group the effects of the toxin on the inner molecular layer begin to spread to a wider area (Figure 3.3). There is a decrease of the immunosignal from this layer for about 2/3rds the length of the dentate gyrus. In two cases the CA3 strata radiatum and oriens is also darkened. The spread of the cleavage in the strata radiatum and oriens in the CA1 is more pronounced in some slices than others. Most of the effects are focused around the dentate gyrus and the CA3 .

The day 16 group, similar to the day 8 group, shows a decrease in the immunosignal from the inner molecular layer (Figure 3.3). Five of 6 slices show a darkening of the strata radiatum and oriens in the CA3 region. Within the CA1, the decrease in immunosignal across the most dorsal regions of the strata radiatum and oriens results in a brighter str. pyramidale.

3.1.1.5 Posterior level contralateral hippocampus in TeNT injected rats

The changes in the posterior contralateral hippocampus are minimal at all time points but when they do occur they are in specific layers of the hippocampus. The day 2 slices show staining that is comparable to that of the control slices (Figure 3.4, lower left panel). At day 8 there is a specific decrease of the immunosignal in the dorsal CA1 strata radiatum and oriens compared with the ventral part of this region. Other than this the TeNT appears not to have affected the other regions at this time point.

By day 16 there is a slight reduction in the immunosignal of the inner molecular layer at the crest of the dorsal dentate gyrus in all slices. In 3 of 6 slices there is also a reduction in the immunosignal in a small area of the dorsal CA1. Other than this, the staining in the CA1 and CA3 remains undisturbed. This all shows that there are minimal changes in the contralateral side but they are localised in the dorsal hippocampus.

3.1.2 Grey level analysis of VAMP1 immunosignal in control and TeNT treated rats

The low magnification fluorescent images from the previous sections (Figures 3.1-3.4) have shown an overview of the staining distributions in control slices and the effects of the TeNT treatment at the different time points. In this following section we will quantify the changes seen. As described in the Materials and Methods section, the grey level analysis looks at the pixel intensities within the individual areas of the hippocampus. The pixel intensities for each slice and each region are divided into 8 different grey levels and the distributions plotted. The graphs in the following sections show the distributions of the immunosignal intensities as an average of all the slices from the same treatment condition and time point (Figures 3.6-3.8). The dentate gyrus, CA2/3 and CA1 are considered as separate regions of the hippocampus and therefore we shall be looking at these areas individually and comparing the treatments and sides within each of these areas, and also considering the middle and posterior sections. The first moment graphs give a representation of the changes at the different time points and between the treatments using a weighted average.

At each survival time, only two rats were injected with the control solution. The rationale behind this was to minimise the numbers of animals used and we had hypothesised that there would be no differences between the controls. This however meant that the number of slices for each time point was low, particularly as one of the day 8 control animals had a very large ventricle which affected the hippocampus and was thus excluded. Statistical analysis (ANOVA) confirmed that there were no differences between the control slices at the different time points. The control data (ipsilateral and contralateral separately) are made up of slices from days 2, 8 and 16 pooled together. Thus, when referring to the control data in the following sections,

looking at the individual areas, the values will be the same at 2, 8 and 16 days post injection.

Each graph contains the data from ipsilateral TeNT, contralateral TeNT and ipsilateral control injected animals. The contralateral control traces are not shown in these graphs as they are very similar to the ipsilateral control traces. The data however is used within statistical analyses.

Due to the number of tests that are used for the comparisons of the different treatments at the three time points, the significance criterion for each individual area, for example mid level dentate gyrus, will be lowered to 0.0167 to be more stringent (using the Bonferroni correction). This reduces the chance of obtaining one or more false positive results to 0.05 after multiple tests. This will be used because within each individual area, three two-way ANOVAs were used, one for each of 2, 8 and 16 days post injection. A single two-way ANOVA was used to look at whether there were any differences between the three time points within the slices from TeNT treated animals, looking at ipsilateral and contralateral sides separately. As only one ANOVA was used for each area, the significance criterion will remain at 0.05. Two-way ANOVAs were used for the comparisons unless otherwise stated.

3.1.2.1 Mid level dentate gyrus

Figure 3.6 (upper panels) shows the grey level graphs for the mid level dentate gyrus at 2, 8 and 16 days post injection, along with the first moment analysis that allows for a direct comparison between the treatment groups and sides of the hippocampus.

The distribution of staining intensity across the controls (pooled data from 2, 8 and 16 days) shows that in the dentate gyrus, the highest percentage of pixels are present in

grey levels 3 and 4. The first moment for ipsilateral control is 3.57±0.08 which shows that the weighted average for the trace rests in grey level 3. This is in the mid to low intensity range and would be expected due to the low immunosignal of the granule cell layer where less VAMP1 is expressed. There is a decrease in the percentage of pixels as you go to the lighter grey levels. This is a trend consistent with the contralateral TeNT treated slices at all three time points. The ipsilateral TeNT trace however shows changes across the time points. At day 2 there is a slight shift to the left, indicating some decrease in the immunosignal (first moment 3.21±0.27). By day 8 there is a further dramatic shift to the left and the first moment has decreased to 2.58±0.18. At this point, the majority of pixels are in grey level 1 and the change is likely due to the cleavage of VAMP1 within the inner molecular layer. At 16 days post injection the trace remains with the majority of pixels at the darkest grey levels and the first moment remains low at 2.70±0.41.

The comparisons graph in Figure 3.6 (upper row, right hand panel) shows the first moments at each of the time points for ipsilateral TeNT (solid line), contralateral TeNT (dotted line) and ipsilateral control (dashed line). Statistical analysis was carried out within each of the time points to compare the treatments and the sides of the hippocampus. This showed that there are significant differences between the ipsilateral control and TeNT slices at 8 days post injection ($p=<0.001$). Controls show significantly higher first moments, and thus have an average weighting in a lighter grey level than that of ipsilateral TeNT slices. There are also significantly higher first moments in contralateral TeNT slices versus ipsilateral TeNT at all three time points; $p=0.014$, $p=<0.001$ and $p=0.006$ as the days increase.

A comparison of the TeNT slices at the different time points (but within the individual sides) showed no significant differences.

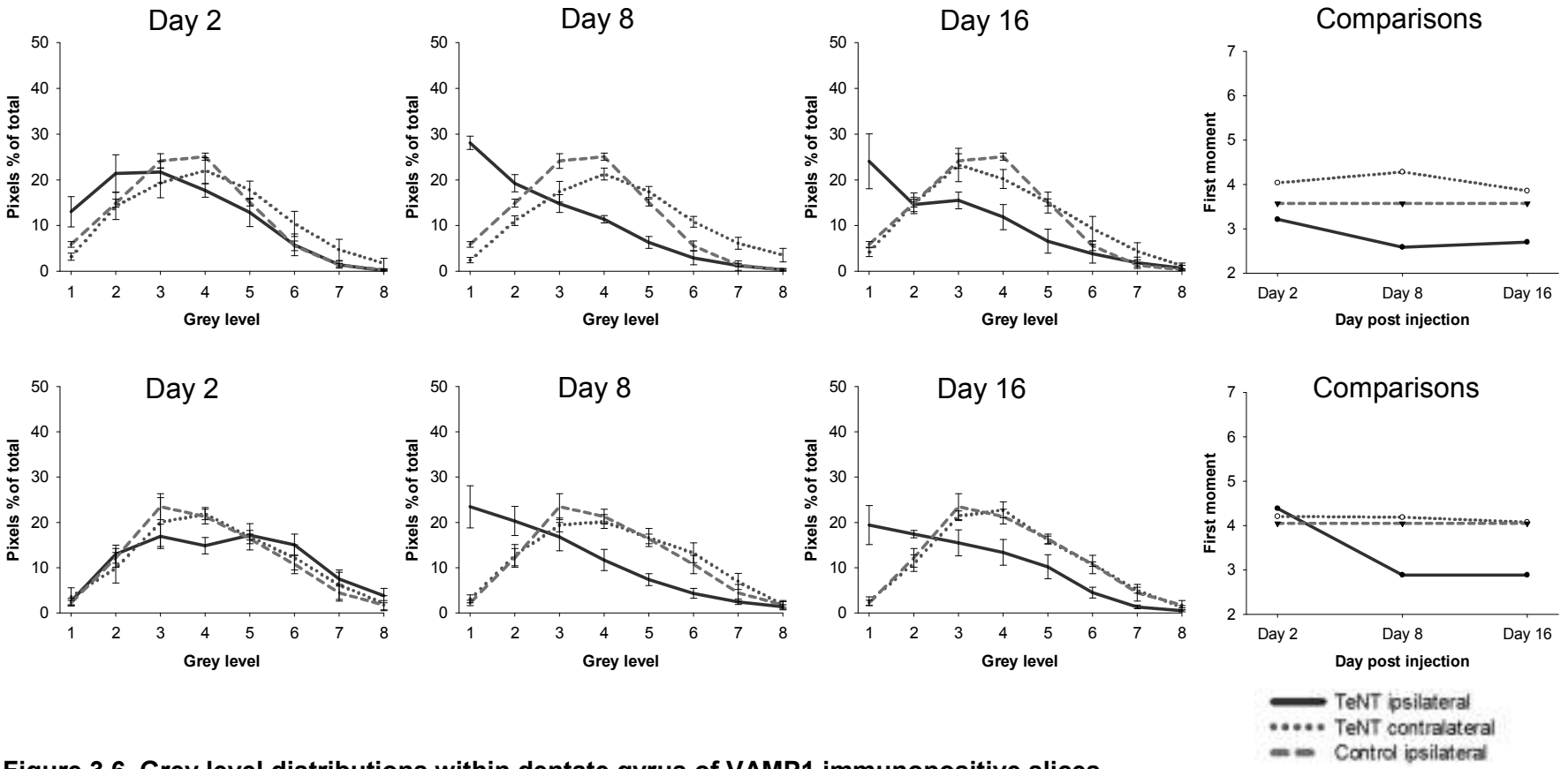

Figure 3.6. Grey level distributions within dentate gyrus of VAMP1 immunopositive slices.
Grey level graphs for the middle (top row) and posterior (bottom row) dentate gyrus at 2, 8 and 16 days post injection from VAMP1 immunostained slices. The distribution of the pixels across the 8 grey levels (1-8; dark-light) is shown for TeNT ipsilateral (solid), TeNT contralateral (dotted) and Control ipsilateral (dashed) conditions. Data presented as mean ± SEM. The right hand panels (Comparisons) shows the first moments for each of the time points and treatment conditions. Control traces contain 6 or 7 slices in both middle and posterior slices (ipsilateral and contralateral). Middle TeNT traces contain 6 slices, except for day 8 TeNT groups which each contain 4 slices. Posterior TeNT groups contain 3, 4 and 6 slices for days 2, 8 and 16 respectively.

3.1.2.2 Posterior level dentate gyrus

The pooled controls for the posterior dentate gyrus shows the highest percentage of pixels in grey level 3 which is towards the darker end (first moment 4.05±0.24) (Figure 3.6, lower panels). As with the middle sections, this will be due to the low immunosignal from the granule cell layer which makes up a large proportion of the dentate gyrus. In the day 2 graphs, the highest percentage of pixels for the contralateral TeNT slices is in grey level 4 and for the ipsilateral TeNT slices is grey level 5. Overall the traces are very similar. These are similar to that seen in the mid level sections, if not a little lighter. By day 8 and continuing into day 16, there is a shift towards the darkest grey level for the ipsilateral TeNT trace (first moments 2.89±0.25 and 2.88±0.31 respectively) whilst the contralateral TeNT (first moments 4.19±0.16 and 4.08±0.12 respectively) remains similar to the control trace.

The comparisons graph (Figure 3.6, lower right panel) shows that within the posterior hippocampus, the effects of the toxin do not begin until day 8. There are no significant differences between the treatment conditions at 2 days post injection, shown by very closely associated first moments in the graph. At days 8 and 16, there are significantly higher first moments in ipsilateral control in comparison to ipsilateral TeNT ($p=0.003$ and $p=0.002$ respectively) and also higher in contralateral TeNT versus ipsilateral TeNT ($p=0.003$ and $p=0.002$ respectively).

Comparisons of the ipsilateral TeNT slices at the different time points shows that within the posterior slices, there are significant differences when comparing day 2 to day 8 ($p=0.010$) and day 2 to day 16 ($P=0.009$), where in both cases the day 2 showed the higher first moment indicating a brighter overall immunosignal. The

decrease in brightness of pixel distribution at the later time points is due to the widespread decrease in immunosignal of the inner molecular layer. In the contralateral side there are no differences between the different time points in toxin treated slices.

3.1.2.3 Mid level CA2/3

The data from the pooled controls in the CA2/3 show the peak of the curve in grey level 5 and the first moment is 5.14±0.14 (Figure 3.7, upper panels). This will be due to the bright immunosignal from the strata radiatum and oriens which makes up the largest percentage of the CA2/3 region. At all three time points, the contralateral TeNT trace remains similar to the controls, with the first moment remaining in grey level 5. The ipsilateral TeNT however starts to show a shift towards the darker grey levels at the earliest time point (first moment 3.95±0.29). By day 8 this shift has dramatically increased with the majority of pixels in the darkest two grey levels, similar to that seen in the dentate gyrus (first moment 2.69±0.39). This is due to the increased area of the toxin's cleavage affects. The trace at day 16 however shows a similar distribution to day 2, indicating that the very intense decrease in immunosignal seen at day 8 has subsided somewhat by day 16 (first moment 4.22±0.50). This is further emphasised in the comparisons graph (Figure 3.7, upper right panel).

There are clear differences between the ipsilateral control and TeNT slices, where the control slices show significantly higher first moments: $p=0.004$, $p=<0.001$ at 2 and 8 days post injection respectively. There is then a recovery towards control levels at day 16, indicated by no significant differences between the treatments in the ipsilateral side. There are significantly higher contralateral TeNT first moments than in the ipsilateral TeNT at all three time points; $p=<0.001$, $p=<0.001$ and $p=0.004$ at days 2, 8 and 16 respectively. Interestingly, the contralateral TeNT trace in the comparisons graph shows a trend similar to that of the ipsilateral TeNT slices, although to a less dramatic extent. It can be seen that at day 8, there is a subtle

reduction in the first moment compared to days 2 and 16. This suggests that the TeNT may have some cleavage effect within the contralateral side, but not to the extent seen within the ipsilateral side, hence no significant differences compared with control slices.

A comparison of the different time points in the ipsilateral TeNT slices showed that there was a significant difference between the first moments of 8 and 16 days post injection ($p=0.044$). There were no significant differences between the time points in the contralateral side.

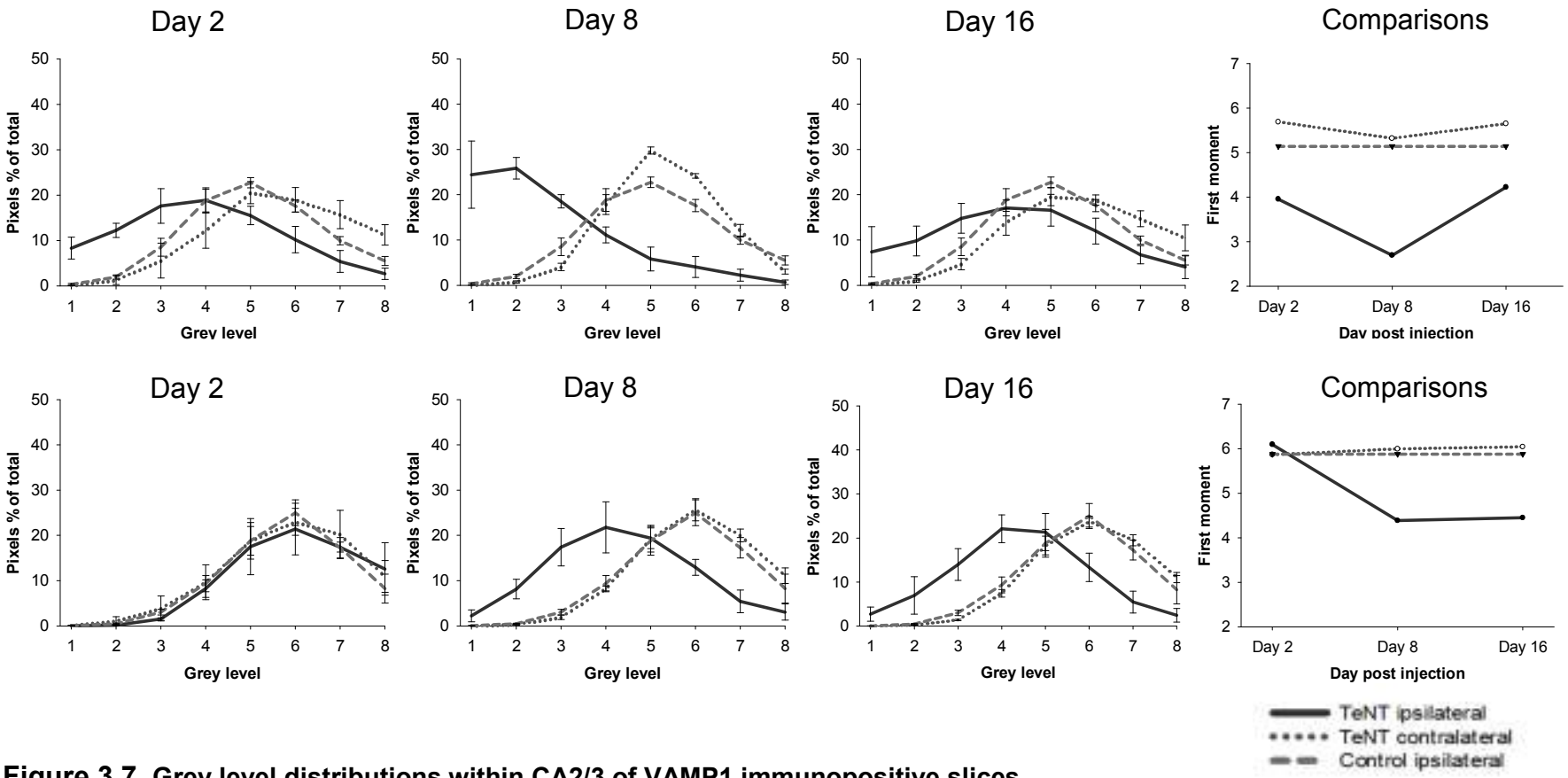

Figure 3.7. Grey level distributions within CA2/3 of VAMP1 immunopositive slices.
Grey level graphs for the middle (top row) and posterior (bottom row) CA2/3 at days 2, 8 and 16 in VAMP1 immunostained slices. The distribution of the pixels in the TeNT ipsilateral (solid), TeNT contralateral (dotted) and Control ipsilateral (dashed) slices are shown across the 8 grey levels (1-8; dark-light). Data presented as mean ± SEM. The Comparisons panels show the first moments for each of the time points and treatment conditions. Control traces contain 6 or 7 slices in both middle and posterior slices (ipsilateral and contralateral). Middle TeNT traces contain 6 slices, except for day 8 TeNT groups which each contain 4 slices. Posterior TeNT groups contain 3, 4 and 6 slices for days 2, 8 and 16 respectively.

3.1.2.4 Posterior level CA2/3

The control slices pooled together for posterior CA2/3 show a peak in the 6th grey level, one of the lighter grey levels (Figure 3.7, lower panels). The first moment for the ipsilateral control slices is 5.88±0.22. The graphs also show that the staining across the CA2/3 is consistent at 2 days post injection in the posterior sections, whether treated with control or TeNT and whether on the ipsilateral or contralateral side. By day 8, the ipsilateral TeNT line has shifted towards the darker grey levels with the peak shown in grey level 4 (first moment 4.39±0.15). The contralateral TeNT and control lines remains focused in the brighter grey levels. At day 16, the peak of the ipsilateral TeNT slices remains in grey level 4 (first moment 4.45±0.35).

There are significantly higher first moments in the ipsilateral control versus TeNT at days 8 and 16 ($p=<0.001$ in both instances). There are also significantly higher contralateral than ipsilateral TeNT first moments at these time points ($p=<0.001$ in both cases).

A comparison of the time points within the TeNT slices shows that in the ipsilateral side, there is a significant difference between days 2 and 8 ($p=0.010$) with day 8 showing a lower first moment value and thus a darkening of the overall area. Day 16 also shows a significantly lower first moment than day 2 ($p=0.011$) indicating a sustained darkening, rather than a recovery as seen in the mid level CA2/3. In the contralateral side there are no differences between the different time points.

3.1.2.5 Mid level CA1

The grouped control slices for CA1 show the highest percentage of pixels in the middle range grey levels (4 and 5) with a first moment of 4.69±0.20 (Figure 3.8, upper panels). The day 2 graphs show the peaks for all three conditions in grey levels 4 or 5. This is similar to the CA3 which would be expected as the layer distribution of the VAMP1 protein is similar throughout the CA3 and CA1, apart from the presence of the str. lucidum in the CA3. Similar to the dentate gyrus and CA2/3, the biggest shift in pixel intensity distribution happens in the ipsilateral TeNT injected animals at day 8. The peak for these slices is in grey level 2 (first moment 2.26±0.09) showing that most pixels are at the darkest end of the spectrum. By day 16, the distribution of pixels in the ipsilateral TeNT slices is less biased towards the darker grey levels than at day 8 and may be recovering towards control values (ipsilateral TeNT first moment 3.65±0.53).

The first moment comparisons graph shows that there are changes in the ipsilateral TeNT from day 2. There are significant differences between the ipsilateral control and TeNT slices at day 8 ($p=<0.001$) however not at days 2 or 16. Contralateral TeNT slices show significantly higher first moments than ipsilateral TeNT slices at all three time points ($p=0.008$, $p=<0.001$ and $p=0.002$ for days 2, 8 and 16 respectively). The day 8 contralateral CA1 shows a significantly higher first moment in the control slices in comparison to TeNT slices ($p=0.001$) suggesting that the TeNT has travelled to the contralateral CA1 and has had its cleavage effect on VAMP1. This trend of a decrease in the first moments of day 8 contralateral TeNT slices was also seen in the CA2/3, although was not significant. It is interesting that this occurs at the peak time of the effect in the ipsilateral side as well. As with the CA2/3, the day 8 shows the

greatest darkening and then some recovery by day 16 in mid level ipsilateral sections.

Comparing the different time points within the TeNT slices shows that there is a significant difference between the first moments at 2 and 8 days post injection ($p=0.025$) in the ipsilateral side. In the contralateral side however, there is a significant difference between the 8 and 16 day slices ($p=0.029$) where the day 16 shows a higher first moment than the day 8 slices, further indicating a cleavage within contralateral CA1 at day 8.

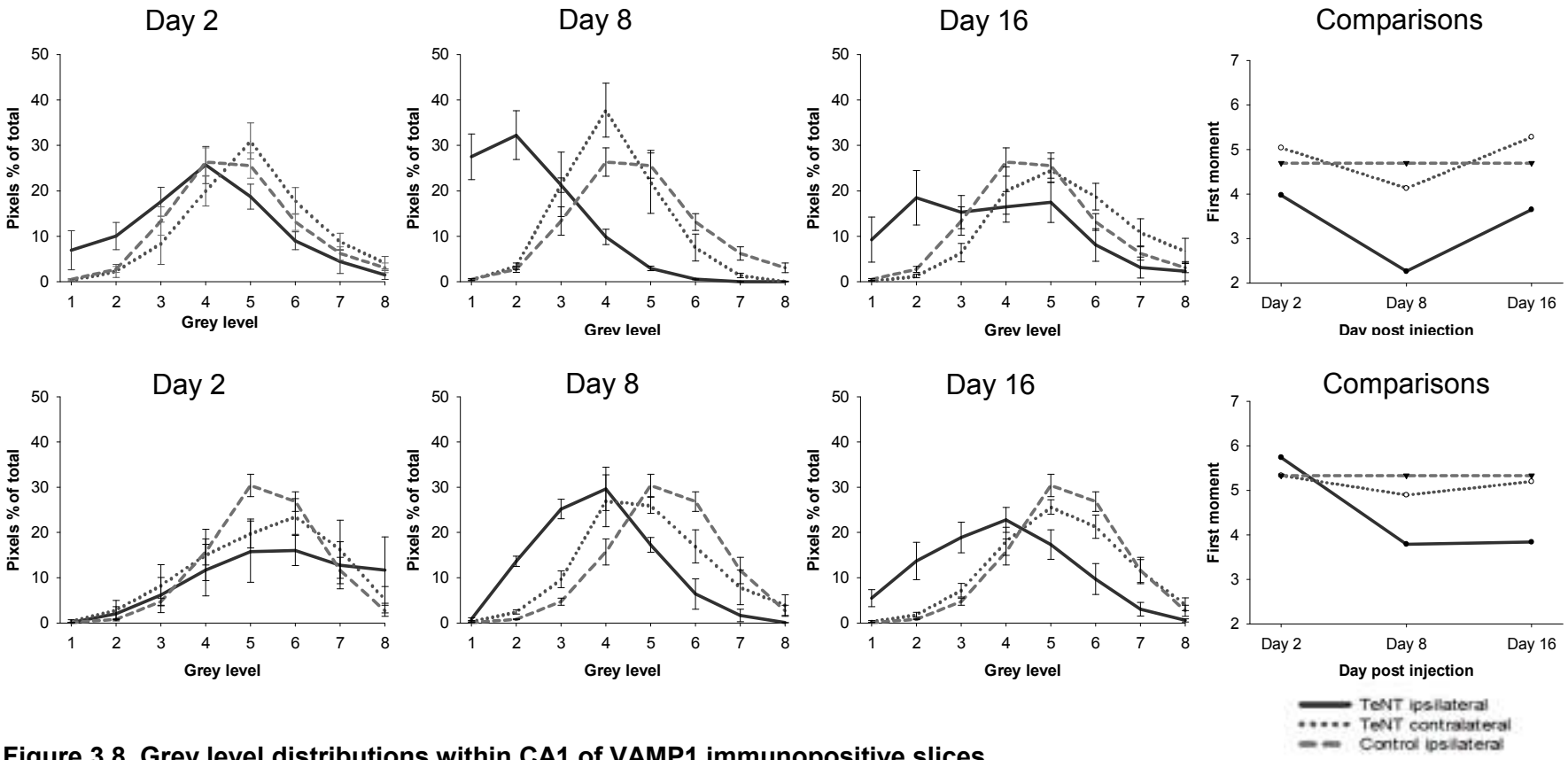

Figure 3.8. Grey level distributions within CA1 of VAMP1 immunopositive slices.
Grey level graphs for VAMP1 immunostained slices from the middle (top row) and posterior (bottom row) CA1. Graphs are shown for 2, 8 and 16 days post injection. The distribution of the pixels across the 8 grey levels (1-8; dark-light) is shown for TeNT ipsilateral (solid), TeNT contralateral (dotted) and Control ipsilateral (dashed) conditions. Data presented as mean ± SEM. Comparisons of the first moments at each of the time points and between the treatment conditions are shown in the right hand panels. Control traces contain 6 or 7 slices in both middle and posterior slices (ipsilateral and contralateral). Middle TeNT traces contain 6 slices, except for day 8 TeNT groups which each contain 4 slices. Posterior TeNT groups contain 3, 4 and 6 slices for days 2, 8 and 16 respectively.

3.1.2.6 Posterior level CA1

The pooled controls show a peak in grey level 5 and a first moment of 5.33±0.16 (Figure 3.8, lower panels). At day 2, the ipsilateral and contralateral TeNT slices have peaks in grey level 6 (first moments 5.74±0.66 and 5.33±0.46 respectively). The day 8 graphs show that the peak pixel intensities of the ipsilateral TeNT slices have shifted towards grey level 4, which remains by day 16 (3.79±0.11 and 3.84±0.32 respectively). The contralateral TeNT trace at day 8 also shows a shift of the peak to grey level 4 but the majority of the pixels remain in the brighter grey levels (first moment 4.89±0.27).

The posterior first moment analysis shows that there are no significant differences between the treatment conditions at 2 days post injection. At days 8 and 16, there are significantly higher first moments in ipsilateral control versus TeNT ($p=<0.001$ at both time points). There are also higher first moments in contralateral versus ipsilateral TeNT at these two time points ($p=<0.001$ in both cases). At day 8, there is a higher first moment in contralateral control in comparison to contralateral TeNT ($p=0.014$). This was also shown in the mid level CA1 and further supports the travel of the toxin to the contralateral hippocampus at a time when the peak cleavage effect is seen in the ipsilateral side.

A comparison of the ipsilateral TeNT slices shows that there is a significant difference between day 2 and day 16 ($p=0.021$ t-test) but not between day 2 and day 8. Day 2 shows the highest first moment and day 16 the lowest, demonstrating that the effect on the posterior hippocampus remains at day 16, whereas in middle sections it

begins to recover. There are no differences between the time points in the contralateral side.

3.1.2.7 Summary of the effects of TeNT on the VAMP1 immunosignal in the ipsilateral and contralateral hippocampi

Overall the low magnification images and grey level analysis have shown that the earliest effect of the toxin on VAMP1 is at 2 days post injection in the mid level CA2/3 of the injected hippocampus. By day 8, the toxin has affected all areas in the mid level ipsilateral hippocampus, however there seems to be some recovery towards control levels by day 16. This is in contrast with the posterior sections, where the initial effect of the toxin is seen at day 8 in ipsilateral sections and remains at day 16, with no recovery seen. This suggests that the spread of the toxin's effects moves away from the initial site of injection between days 2 and 8. Interestingly, at day 8, in both mid level and posterior slices, there are significantly higher first moments in CA1 of contralateral controls than contralateral TeNT slices. This suggests that the toxin's effect has spread to include the contralateral CA1.

3.1.3 Distribution of VAMP2 immunopositivity

In this section we will be considering the distribution of VAMP2 across the different regions of the hippocampus, both ipsilateral and contralateral, at mid and posterior levels within slices from 2, 8 and 16 days post injection.

3.1.3.1 Control hippocampus

The distribution of VAMP2, as with VAMP1, shows layer specificity across the hippocampus (Figure 3.9). However there are differences in the distribution in comparison to VAMP1. The dentate gyrus shows a hilus full of VAMP2 (intense immunosignal) surrounded by a dark granule cell layer indicating a lower presence of the protein. The inner molecular layer has a slightly brighter immunosignal than the granule cell layer and the outer molecular layer is brighter still, showing that VAMP2 rather than VAMP1 is the protein abundant in this area. This corresponds with the results shown by Raptis *et al*. (2005). The str. lacunosum moleculare is of similar immunosignal intensity to the outer molecular layer representative of a high level of VAMP2 also residing here. It is slightly brighter in immunosignal intensity than the str. radiatum in the CA3 and CA1. In these areas, the strata radiatum and oriens are similar in fluorescent intensity to each other across their length. The str. pyramidale that runs through the centre of these areas is darker which shows less VAMP2 present. The str. lucidum is the brightest area of the CA3 indicating an abundance of VAMP2.

These staining distributions are present in all mid level ipsilateral slices across the 2, 8 and 16 day groups (Figure 3.9). This staining is also the same in the mid level control contralateral hippocampus (Figure 3.10) and the control posterior sections; both ipsilateral and contralateral (Figures 3.11 and 3.12 respectively).

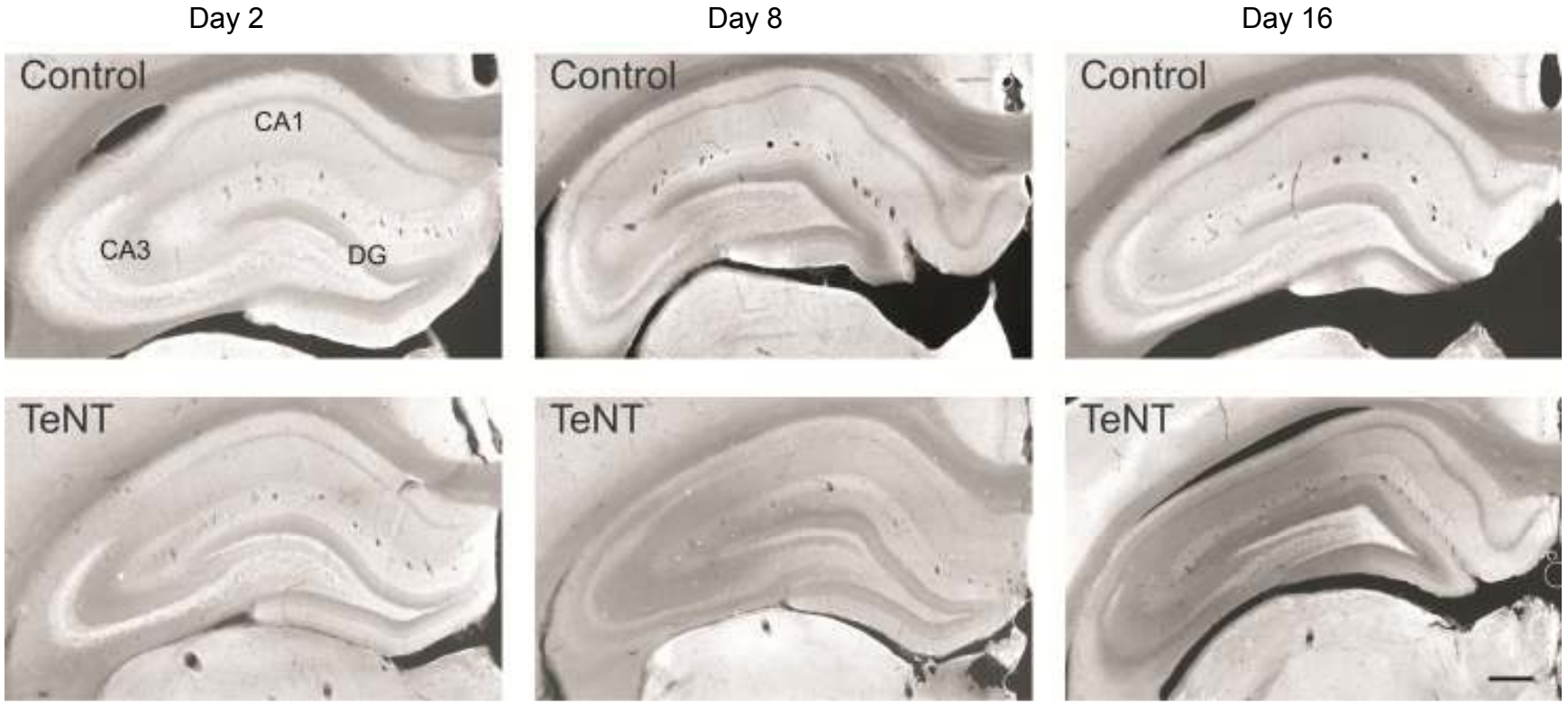

Figure 3.9. Distribution of VAMP2 immunopositivity in mid level ipsilateral hippocampus of rats injected with control or TeNT solutions. Low magnification fluorescent images of ipsilateral (injected) mid level hippocampi immunostained with antibody against VAMP2. The upper panels show control injected and the lower panels TeNT injected animals. Slices were taken from animals killed at 2, 8 and 16 days post injection. The control images show consistent distribution of the VAMP2 in the different layers of the hippocampus across the three time points. A focal cleavage of VAMP2 is seen to start at day 2 and spread to include a wider area by days 8 and 16. Scale bar represents 500μm.

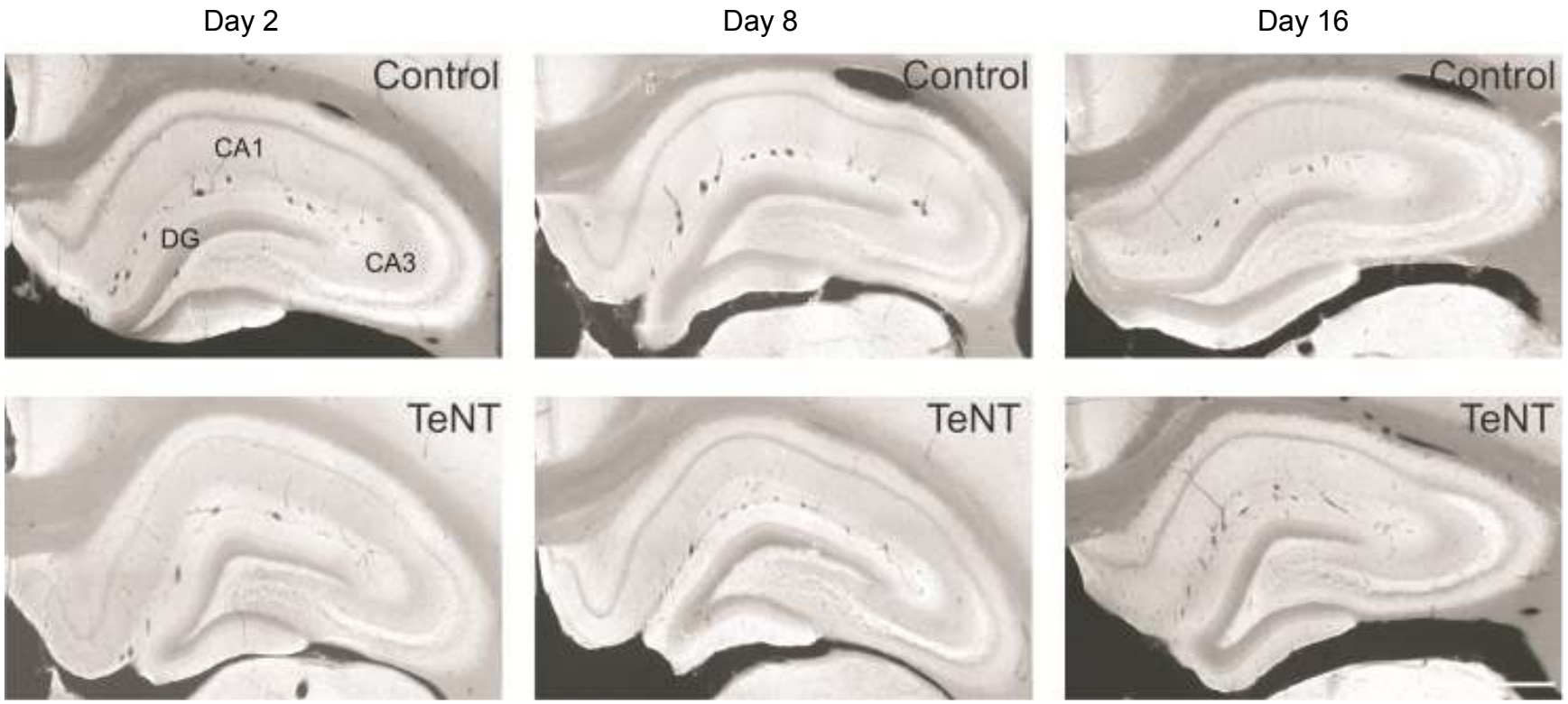

Figure 3.10. Distribution of VAMP2 immunopositivity in mid level contralateral hippocampus of rats injected with control or TeNT solutions. Low magnification fluorescent images of VAMP2 immunostaining from contralateral (uninjected) mid level hippocampi. The upper panels show slices from control injected animals killed at 2, 8 and 16 days post injection. The lower panels show slices from TeNT injected animals. The staining distribution of the TeNT slices is mostly comparable to that of controls, although with subtle differences at day 16. Scale bar represents 500µm.

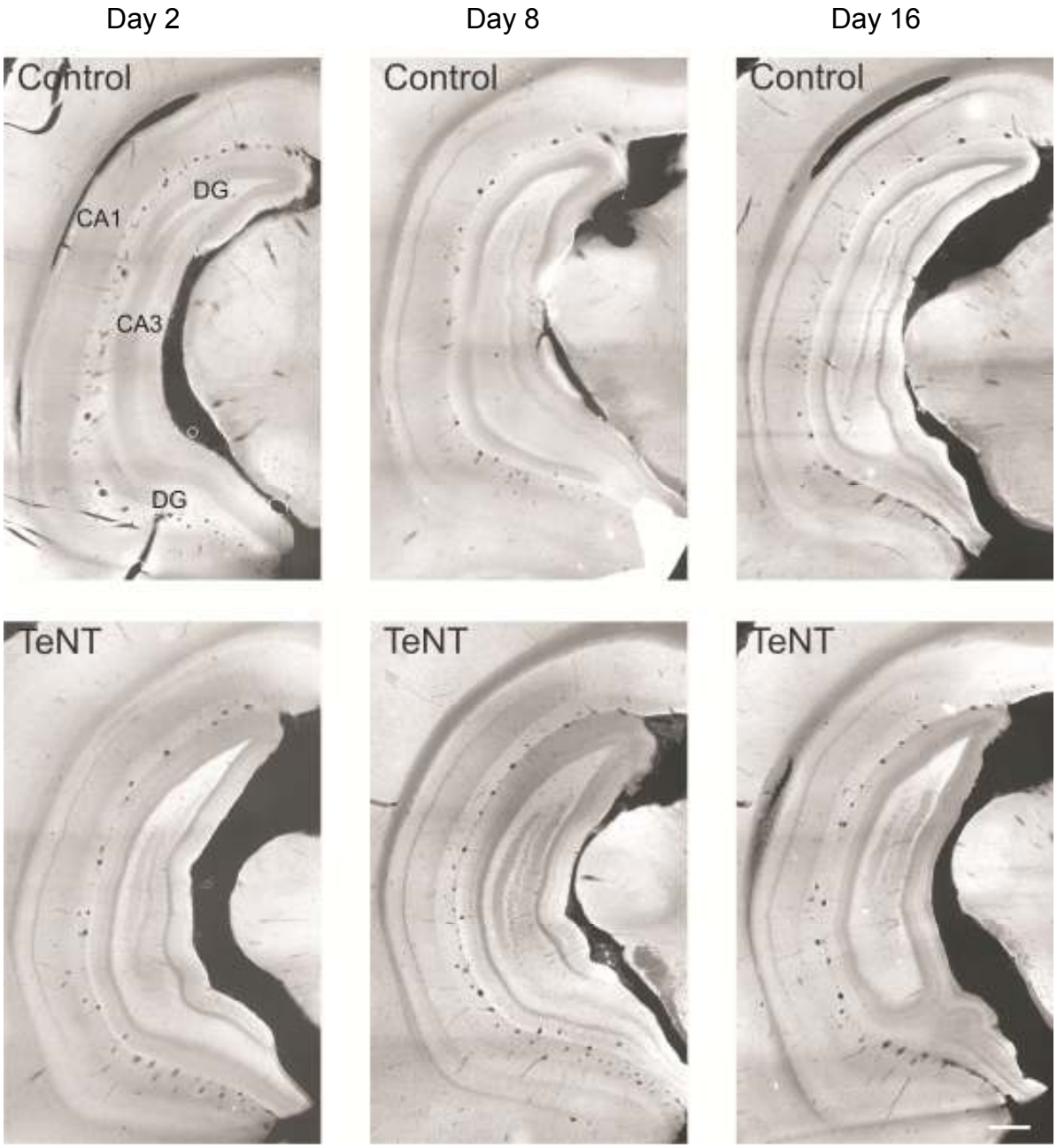

Figure 3.11. Distribution of VAMP2 immunopositivity in posterior level ipsilateral hippocampus of rats injected with control or TeNT solutions. Low magnification fluorescent images from ipsilateral posterior hippocampi. Slices have been immunostained with antibody against VAMP2 and revealed using an Alexa 488 secondary antibody. Images in the upper panels show slices from control injected animals killed 2, 8 and 16 days post injection respectively. Slices from TeNT injected animals at the same time points are shown in the lower panels. The effects of the toxin are seen focally at day 2, predominantly within the inner and outer molecular layers of the dentate gyrus and spread to include a wider area at days 8 and 16. Scale bar represents 500μm.

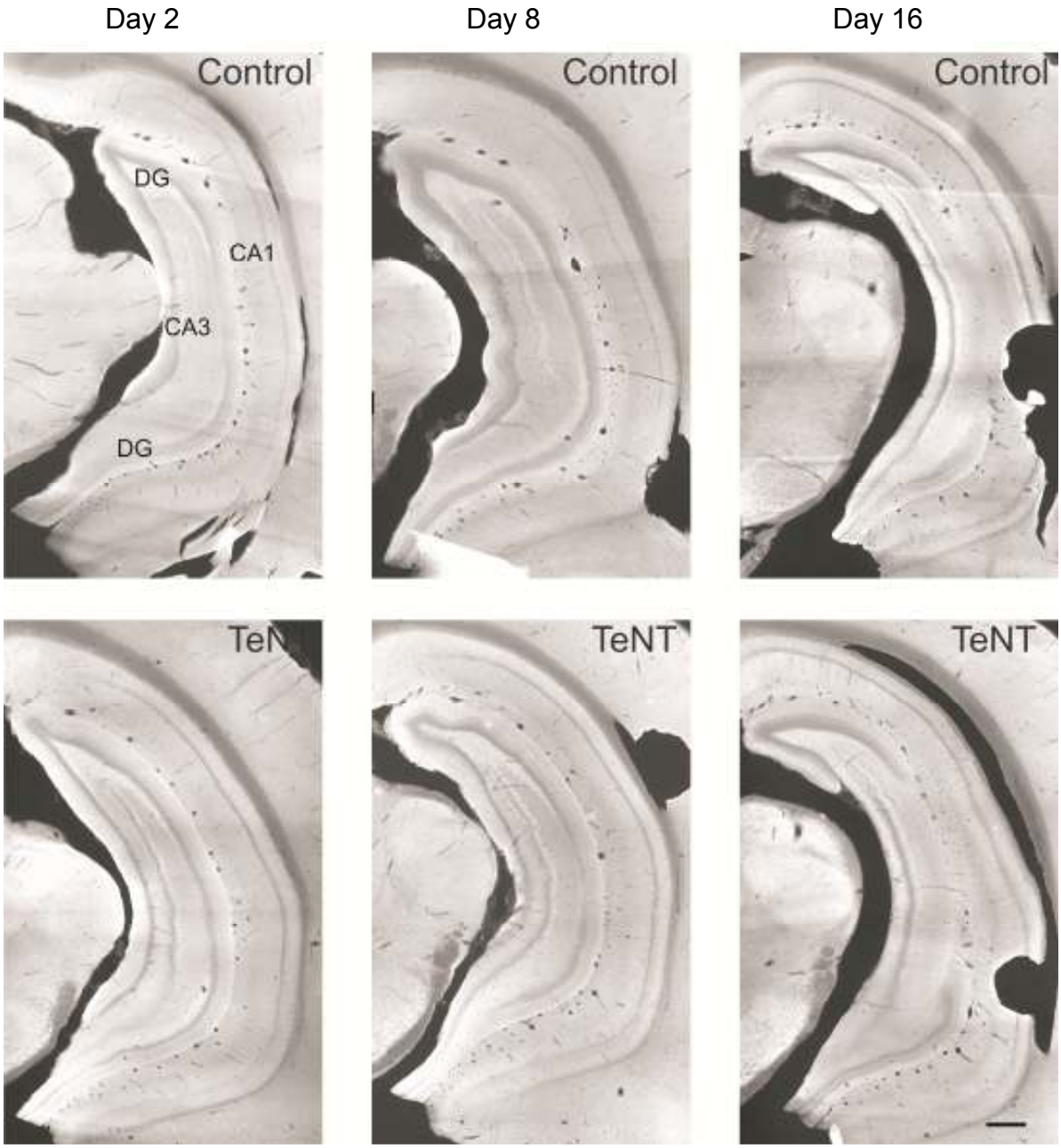

Figure 3.12. Distribution of VAMP2 immunopositivity in posterior level contralateral hippocampus of rats injected with control or TeNT solutions. Low magnification fluorescent images of contralateral posterior hippocampi from control (upper panels) and TeNT (lower panels) injected animals. Animals were killed at three different time points; 2, 8 and 16 days post injection. No effects of the toxin are seen at any of the time points studied. Scale bar represents 500μm.

3.1.3.2 Mid level ipsilateral hippocampus in TeNT injected rats

The day 2 group of animals that were injected with the TeNT and immunostained with antibody against VAMP2 (Figure 3.9 lower panels) show very faint traces of a cleavage but nothing as stark as in the VAMP1 immunostained slices. This is also shown in Figure 3.13 where a line histogram for slices from the control and TeNT injected animals in the day 2 group are compared. This shows the very consistent staining throughout the str. radiatum in control slices and only a minimal decrease in pixel intensity in the TeNT slice, corresponding to area CA3a/b. Here there is a slight decrease in the immunosignal from the str. radiatum. In two slices there is a possible brightening of the str. lucidum (Figure 3.9 lower panels). This coincides with a str. pyramidale which is less clearly differentiated from the str. lucidum, especially when compared to control slices. Overall however, the effects are very small and therefore we will consider the results of the grey level analysis to give a quantitative result in the next sections.

The day 8 group decreases in fluorescent staining intensity around the injection site and to a wider area. The crest of the dentate gyrus remains with the differentiation apparent between each of the layers. In contrast, in the centre part of the hippocampus, the outer and inner molecular layers of the buried blade of the dentate gyrus have decreased in intensity to a level similar to the granule cell layer, thus showing cleavage of VAMP2. The overall brightness of the immunosignal in the CA3 has decreased in all layers. Whilst the str. lucidum remains the brightest region in 2 of 4 slices, its intensity is not as vibrant as in controls. In the other 2 slices, no distinction can be made between the str. lucidum and the adjacent str. radiatum. In the CA1c the str. pyramidale is particularly bright and is the brightest part of this

region, corresponding with the darkening of the strata radiatum and oriens. In all cases, the CA1a region remains undisturbed by the toxin. The differences between the two ends of the CA1 shall be addressed later in this chapter, where high magnification microscopy is used to look with more sensitivity at smaller areas.

By day 16, the effects of the toxin are still visible in the mid level hippocampal slices. The hilus appears bright in contrast with the lower immunosignal of the adjacent granule cell layer and CA3 str. radiatum in all slices. The outer and inner molecular layers show some decrease in immunosignal within the buried blade of the dentate gyrus but this is not apparent at the crest, away from the original injection position. In 3 out of 4 slices in the CA3, the immunosignal from the str. lucidum has decreased in brightness (in CA3a/b) and the str. pyramidale has returned to being the darkest layer of the CA3, although it may show less immunosignal than in controls. The strata radiatum and oriens remain darker than in comparison to controls. The str. pyramidale of the CA1 is dark throughout. In CA1c the strata radiatum and oriens have lower intensity immunosignals than in the CA1a showing that the effects of the toxin are still present around the original injection site but that they are not reaching to the furthest, more medial, parts of the hippocampus.

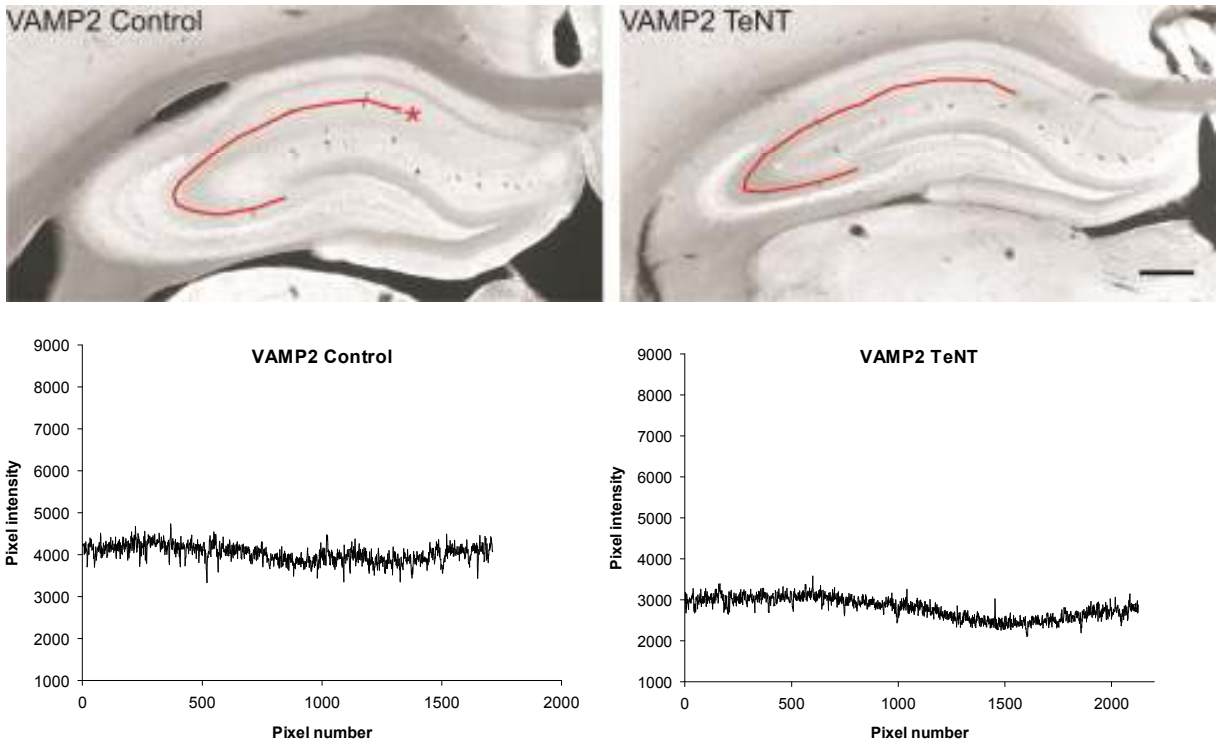

Figure 3.13. Analysis of pixel intensities around the site of control or TeNT injection within VAMP2 immunopositive slices. The images show VAMP2 immunopositive slices from 2 days after injection of control or TeNT solution. Pixel 1 in the x axis of the graph corresponds to the start of the line trace in the CA1 str. radiatum (indicated by the asterisk; VAMP2 Control panel). Only a very subtle decrease in pixel intensity is seen corresponding to the CA3a/b of VAMP2 immunopositive slices following exposure to TeNT. Scale bar represents 500µm.

3.1.3.3 Mid level contralateral hippocampus in TeNT injected rats

The immunosignal of the contralateral hippocampi from the three time points show minimal deviations from controls (Figure 3.10). The only subtle differences are within the str. radiatum of the CA3 and the inner and outer molecular layers of the dentate gyrus in day 16 animals where there appears to be some darkening (3 of 5 animals).

3.1.3.4 Posterior level ipsilateral hippocampus in TeNT injected rats

The day 2 TeNT injected group show posterior slices that have slight changes (Figure 3.11, lower panels). The inner and outer molecular layers at the crest of the dentate gyrus decrease in immunosignal intensity to a level that is similar to the granule cell layer. This effect is focused in the most dorsal parts of the dentate gyrus. A small portion of the str. radiatum in the CA1 also shows some very slight darkening in 2 of 4 slices.

The day 8 posterior slices continue to show a cleavage of the VAMP2 protein in the inner and outer molecular layers at the crest of the dentate gyrus. Here, the outer molecular layer is much darker than the str. lacunosum moleculare whereas they are normally similar in intensity, as seen in the more ventral parts of the slice. The effects have spread to include a larger area of the dorsal part of the hippocampus than in the day 2 group. In the CA3, the strata radiatum and oriens have darker immunosignals than the contained str. lucidum and surrounding hilus, showing a contrast that is much clearer than in control slices. The CA1 area shows mostly homogenous staining throughout the strata radiatum and oriens apart from in the dorsal region where there is some darkening in comparison to the ventral portion.

The day 16 group of slices show similar effects to that seen in the day 8 group. The inner and outer molecular layers at the dorsal crest of the dentate gyrus show a decrease in the immunosignal intensity as the predominant feature along with a darkening of the str. radiatum and oriens in the dorsal CA3 and CA1 (3 of 4 slices).

3.1.3.5 Posterior level contralateral hippocampus in TeNT injected rats

The contralateral posterior VAMP2 immunopositive slices show staining that is unaffected by the TeNT at all time points studied (Figure 3.12). The inner and outer molecular layers that were affected in the ipsilateral posterior slices show no decrease in immunosignal on the contralateral side. This is indicated by an immunosignal that is brighter than the granule cell layer and of comparable brightness to the str. lacunosum moleculare in the case of the outer molecular layer. There is also no cleavage identified in the CA3 or CA1.

3.1.4 Grey level analysis of VAMP2 immunosignal in control and TeNT treated rats

As with the VAMP1 sections, the distribution of VAMP2 across eight different grey levels within the different areas of the hippocampus will be investigated. This allows for a first moment analysis to be carried out giving a weighted average of the staining within the different treatment conditions to determine if there are quantitative differences at the different time points and within the different regions and sides of the hippocampus.

The grey level and first moment analyses for the controls at the three different time points have been pooled together, having tested that there are no significant differences between them (as undertaken in VAMP1 immunopositive slices). The significance criterion remains set at 0.0167, corrected for multiple comparisons, for analysis of the effects of the different treatments within individual time points as before. The significance criterion for the comparison of the three time points within the TeNT treated animals remains at 0.05. As with the VAMP1 grey level analysis, the statistical tests used were two-way ANOVAs unless otherwise stated.

3.1.4.1 Mid level dentate gyrus

The pooled controls show a relatively even distribution across the 8 different grey levels (Figure 3.14 upper panels). The first moment for the control slices is 4.12±0.19. All three conditions included in the graphs for the day 2 slices show very similar pixel distributions across the different grey levels. By day 8, the peak of the graph for the ipsilateral TeNT slices shifts all the way to grey level 1 which is the darkest (first moment 3.29±0.50). This is in comparison to the contralateral TeNT where first moment is 5.27±0.23, thus remaining in the brighter grey levels. The day 16 group also shows the peak of the ipsilateral TeNT in the darkest grey level, but

here the percentage of pixels is even higher than in the day 8 group (first moment 2.44±0.51), suggesting a further darkening in the area which corresponds to the spread of the TeNT effect in the inner and outer molecular layers. Interestingly, the contralateral TeNT line has also shifted to the left, showing the peak in grey level 2 (first moment 3.75±0.52).

The first moment comparisons graph in Figure 3.14 (upper right panel) shows that there are clear differences between the treatment conditions in the dentate gyrus. At 2 and 8 days post injection there are no differences between the treatments in the ipsilateral or contralateral sides. At day 16, there is a difference between the treatments in the ipsilateral side ($p=0.002$) where the controls show a higher first moment. At day 8, there is a significantly higher first moment in the contralateral TeNT compared with the ipsilateral TeNT ($p=<0.001$).

A comparison of the ipsilateral TeNT slices at the three different time points shows that day 2 has a significantly higher first moment, and thus brighter overall staining, than day 16 ($p=0.005$). In the contralateral TeNT slices, there are significant differences between days 2 and 16 ($p=0.037$) and between days 8 and 16 ($p=0.028$) with day 16 showing the lowest first moment in both cases. This data, coupled with the lack of difference between the ipsilateral and contralateral TeNT first moments shows that there is some effect of the toxin in the contralateral dentate gyrus by day 16.

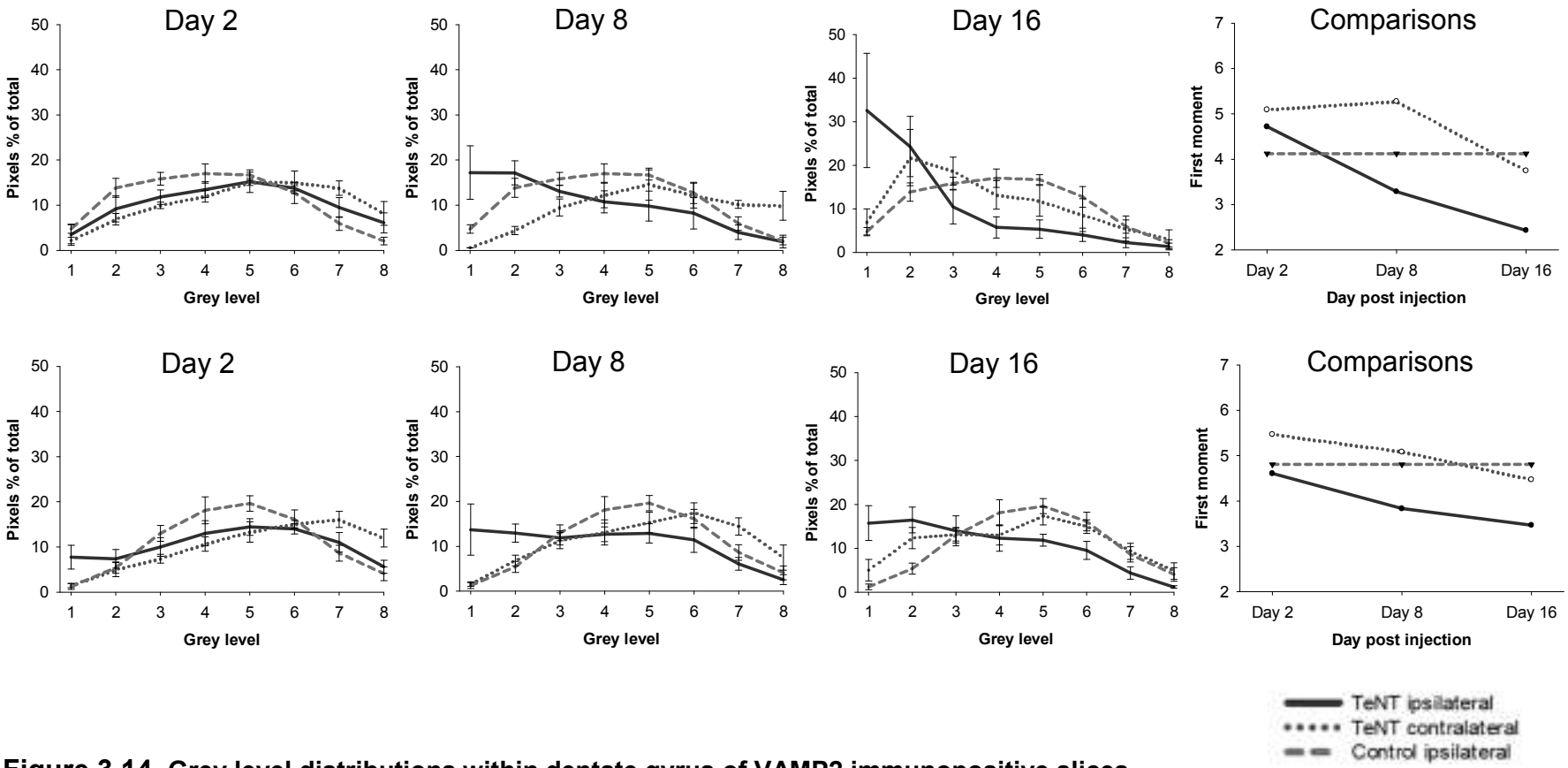

Figure 3.14. Grey level distributions within dentate gyrus of VAMP2 immunopositive slices.
Grey level graphs for the middle and posterior dentate gyrus (upper and lower rows respectively) at days 2, 8 and 16 in VAMP2 immunostained slices. The distribution of the pixels across the 8 grey levels (1-8; dark-light) is shown for TeNT ipsilateral (solid), TeNT contralateral (dotted) and Control ipsilateral (dashed) slices. Data presented as mean ± SEM. The right hand panels show comparisons of the first moments for each of the time points and treatment conditions. Control traces contain 7 slices at each time point, within middle and posterior slices, whilst TeNT traces contain 4 slices.

3.1.4.2 Posterior level dentate gyrus

Pooled controls show a peak in the 5th grey level (Figure 3.14 lower panels) and a first moment of 4.81±0.21. At 2 days post injection the distributions are similar for all treatments. By day 8, as was the trend in the mid level slices, the peak for the ipsilateral TeNT has shifted to the darkest grey level and shows a more equal spread of percentage of pixels across the different intensity grey levels (first moment 3.83±0.38). This shift has increased by day 16 (first moment 3.47±0.16).

The comparisons of the first moments within the different time points shows that in the posterior sections there are significant differences between the treatments in the ipsilateral side at days 8 and 16 ($p=0.010$ and $p=<0.001$ respectively), where the controls show higher first moments. When comparing the ipsilateral and contralateral TeNT slices, there are higher first moments in the contralateral side at 8 and 16 days post injection ($p=0.004$ and $p=0.007$ respectively).

There are no significant differences between the first moments at any of the time points within the ipsilateral TeNT, however there is a significant difference between the day 2 and day 16 first moments in the contralateral side ($p=0.024$). This suggests subtle changes within the dentate gyrus at this latest time point. No changes were observed from the low magnification images.

3.1.4.3 Mid level CA2/3

The pooled controls for CA2/3 show the peak of the distribution in the 4th grey level (Figure 3.15 upper panels) with a first moment of 4.37±0.33. The peak is much higher than in the dentate gyrus and there are fewer pixels in other grey levels whereas in the dentate gyrus the distribution was more evenly spread. This is because of the difference in staining across the two different regions. At 2 days post injection, all three conditions show a relatively similar trend in the distribution of the pixel intensities. The ipsilateral TeNT trace at day 8 shows a shift towards the darker grey levels with the peak in grey level 2 (first moment 2.32±0.36) and intensifying by day 16 (first moment 2.18±0.33). Very few pixels are in grey levels 6-8 showing that there are very few bright areas within the CA3 following the toxin treatment at these time points.

Comparing the treatments within the different time points shows that at day 2 there are no differences between the different sides of the hippocampus or the treatments. At days 8 and 16, there are significantly higher first moments in the ipsilateral control versus ipsilateral TeNT ($p=0.002$ in both cases) and in the contralateral TeNT versus ipsilateral TeNT ($p=<0.001$ in both cases).

A comparison of the three different time points in the TeNT slices shows that in the ipsilateral side there are significant differences between days 2 and 8 ($p=0.004$) and between days 2 and 16 ($p=0.004$). There are no differences between any of the time points in the contralateral side however, overall showing that the TeNT has had no effect there.

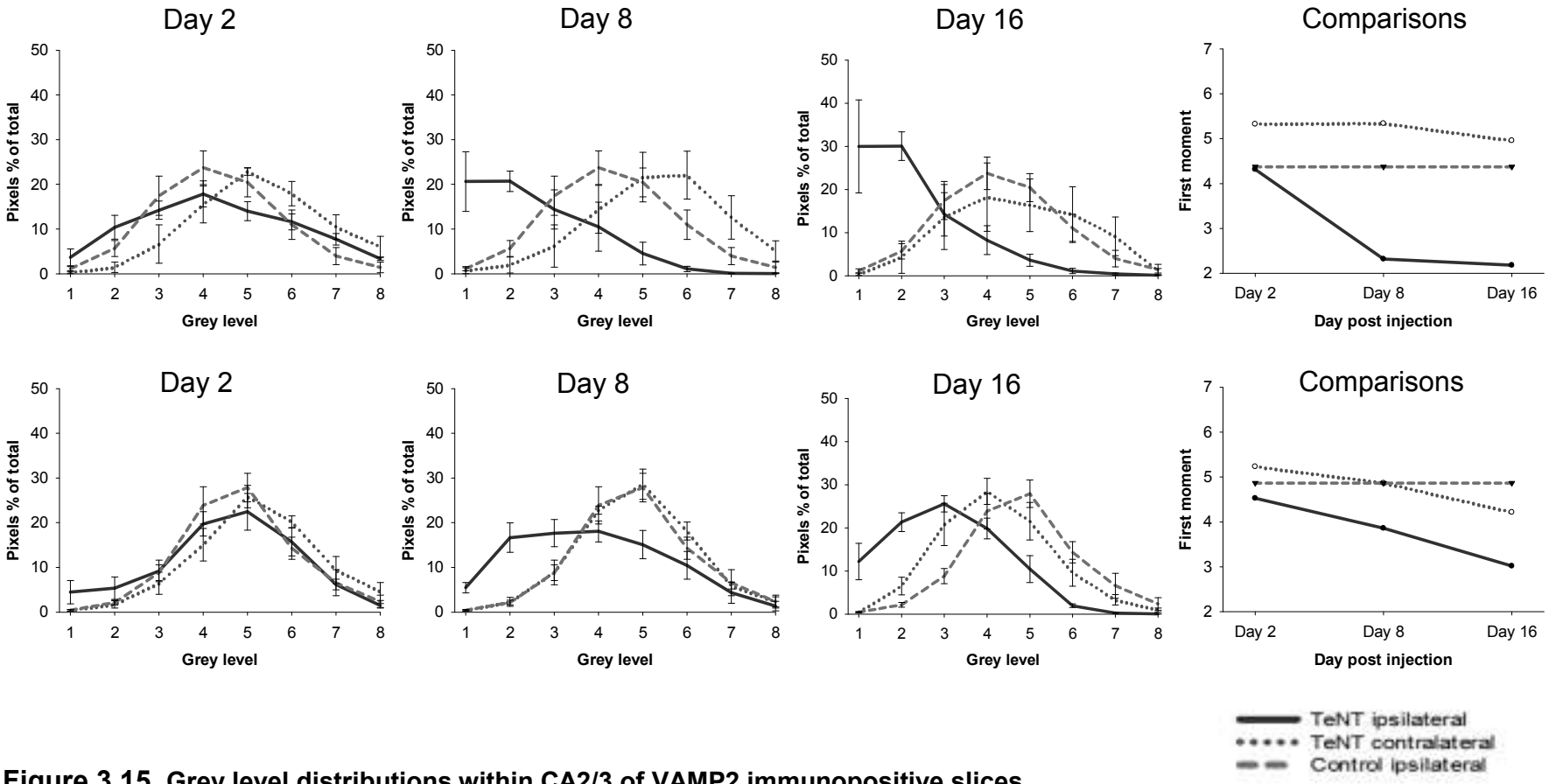

Figure 3.15. Grey level distributions within CA2/3 of VAMP2 immunopositive slices.
Grey level graphs for the middle (upper row) and posterior (lower row) CA2/3 of VAMP2 immunostained slices at 2, 8 and 16 days post injection. The distribution of the pixels across the 8 grey levels (1-8; dark-light) is shown for the different treatment conditions; TeNT ipsilateral (solid), TeNT contralateral (dotted) and Control ipsilateral (dashed). Data presented as mean ± SEM. The Comparisons panels show the first moments for each of the time points and treatment conditions. Control traces contain 7 slices at each time point, within middle and posterior slices, whilst TeNT traces contain 4 slices.

3.1.4.4 Posterior level CA2/3

The pooled control slices in the CA2/3 region show a peak in grey level 5, one of the mid-to-light grey levels (first moment is 4.87±0.25) (Figure 3.15 lower panels). The distribution of pixels across the different grey levels is similar for all three conditions at day 2, with the peak in grey level 5 in all cases. By day 8 there has been a shift of the ipsilateral TeNT slices to include the majority of pixels in the darker grey levels (first moment 3.86±0.28). Again, by day 16, ipsilateral TeNT slices show a further increase in the percentage of pixels in the darkest grey levels: first moment decreasing further to 3.02±0.19, showing that here as well as in the mid level slices there is an increased affect by this latest time point.

The lower right panel of Figure 3.15, comparing the first moments, shows that there are no differences between the treatments or sides at 2 days post injection in the posterior sections, as with the middle sections in the CA2/3. At 8 and 16 days post injection, the control first moment is significantly higher than the TeNT in the ipsilateral side ($p=0.006$ (ANOVA) and $p=0.006$ (Mann Whitney Rank Sum) respectively). The day 16 first moment is the lowest. The ipsilateral slices show significantly lower first moments than the contralateral slices in the TeNT treatments at day 8 ($p=0.014$).

Comparing the time points within the TeNT slices show that there is a difference between days 2 and 16 in the ipsilateral ($p=0.013$) and contralateral sides ($p=0.025$) suggesting a cleavage of VAMP2 in the CA2/3 of both sides of the brain.

3.1.4.5 Mid level CA1

Pooled controls in the CA1 show a peak in grey level 4 with a first moment of 4.49±0.34 (Figure 3.16 upper panels). The peaks for all three lines are within grey levels 4 and 5 at 2 days post injection. The distribution of the pixels either side of these peaks decreases in a steady manner. At day 8 in the CA1, as was seen in the dentate gyrus and CA2/3, there is a shift towards the darker grey levels for the ipsilateral TeNT (first moment reducing to 3.17±0.32). The peaks for the control and contralateral TeNT slices remain in grey levels 4 and 5 respectively. The day 16 group also shows that the shift towards the darker grey levels has remained for the ipsilateral TeNT slices (first moment of 2.77±0.65), and has further increased the percentage of pixels in the darkest two grey levels.

A comparison of the first moments within the middle CA1 shows that there are no differences between the treatments or the sides of the brain at any of the time points studied. This suggests that the effect of the TeNT within CA1c is not great enough to cause a significant shift in the distribution of pixels within the CA1 region as a whole. The differences between the CA1a and CA1c regions may account for the larger variations between the data within the day 16 ipsilateral TeNT group and thus is responsible for the lack of difference compared with control slices.

Comparing the days within the TeNT slices shows no differences between the time points in the ipsilateral or contralateral sides. This is interesting as it is the only mid level area within VAMP2 immunopositive slices where this is true and is likely to do with the larger variation within the day 16 ipsilateral TeNT data.

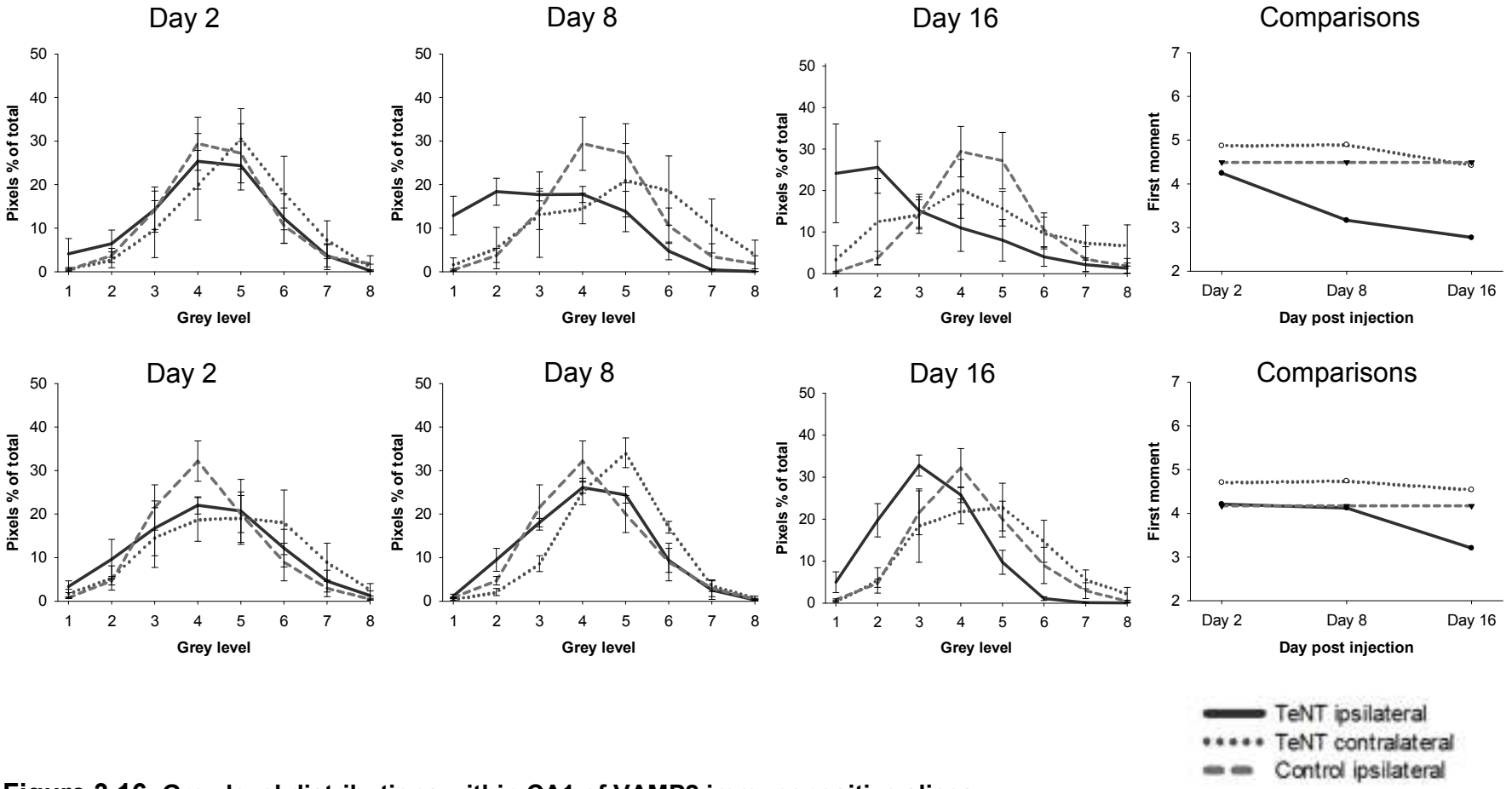

Figure 3.16. Grey level distributions within CA1 of VAMP2 immunopositive slices.
Grey level graphs for the middle and posterior CA1 (upper and lower rows respectively) at days 2, 8 and 16 in VAMP2 immunostained slices. The distribution of the pixels across the 8 grey levels (1-8; dark-light) are shown for TeNT ipsilateral (solid), TeNT contralateral (dotted) and Control ipsilateral (dashed) slices. Data presented as mean ± SEM. The right hand panels compare the first moments for each of the time points and treatment conditions. Control traces contain 7 slices at each time point, within middle and posterior slices, whilst TeNT traces contain 4 slices.

3.1.4.6 Posterior level CA1

The pooled controls for the posterior CA1 region show a peak in grey level 4 and a first moment of 4.17±0.25 (Figure 3.16 lower panels). At day 2 the spread of the percentage of pixels in each grey level is similar across the three traces. At day 8 there is no shift to the left in the CA1 of the ipsilateral TeNT slices (first moment 4.12±0.19) showing that the posterior CA1 is not affected at this time point. By day 16, a slight shift can be seen for the ipsilateral TeNT (first moment decreasing to 3.21±0.17), however not as dramatic as in the CA2/3.

In the posterior sections of the CA1, there are no significant differences between the sides or the treatments at 2 and 8 days post injection. In all the other posterior areas, there have been differences between the treatments in the ipsilateral side and between the sides in the TeNT slices at day 8, but here there are not. At day 16 however, the ipsilateral TeNT shows the lowest first moment in comparison to ipsilateral control ($p=0.015$) and contralateral TeNT slices ($p=0.004$).

A comparison of the different time points within the TeNT slices show that there are no significant differences in either the ipsilateral or contralateral slices.

3.1.4.7 Summary of the effects of TeNT on the VAMP2 immunosignal in the ipsilateral and contralateral hippocampi

Overall, this section has shown that the VAMP2 is cleaved by TeNT and as with the VAMP1, the cleavage is layer specific. The inner and outer molecular layers are the most affected regions of the dentate gyrus, and the strata radiatum and oriens of the CA2/3 and CA1. The str. lucidum shows a greater susceptibility in VAMP2 positive slices compared with the VAMP1 equivalents, likely due to the higher abundance of

the VAMP2 protein in this layer. The grey level analysis has shown that the toxin has no significant effect in any of the hippocampal areas at 2 days post injection. In mid level hippocampus, by day 8, changes are seen in the CA2/3 where ipsilateral control first moments are significantly higher than those of ipsilateral TeNT slices. By day 16 this has spread to include the dentate gyrus as well. Both the dentate gyrus and the CA2/3 show that the day 16 first moments are significantly lower than those of day 2, which shows that in VAMP2, the peak effect of the toxin is seen at 16 days post injection (compared with day 8 for VAMP1). In the posterior hippocampus, ipsilateral control values are significantly higher than ipsilateral TeNT in the dentate gyrus and CA2/3 at 8 and 16 days, and this spreads to include CA1 by 16 days. Contralateral cleavage of VAMP2 is suggested to occur in both the mid and posterior level dentate gyrus and the posterior CA2/3 at 16 days post injection. Interestingly, these changes were observed only in a small number of low magnification images, if at all, which suggest that the grey level analysis is suitable for uncovering more subtle changes.

3.2 Differential expression of VAMP isoforms in inhibitory and excitatory neurons

We have seen in the previous sections that both the VAMP1 and VAMP2 proteins have been affected by TeNT, albeit at different time points. Considering that much of the literature refers to TeNT having an affinity for inhibitory neurons and that VAMP2 is the substrate for the toxin, our group chose to look at whether the VAMP1 and VAMP2 were localised in specific subsets of neurons. The initial work was carried out by Dr Alex Ferecsko and he found that inhibitory neurons (GAD65 expressing) most predominantly expressed VAMP1, whereas the VAMP2 was mostly co-localised with VGLUT1 (excitatory marker) immunopositive neurons (unpublished data). These results were interesting in that they contradict what is stated in much of the literature. We have shown that both the VAMP proteins are cleaved by the TeNT and thus both inhibitory and excitatory neurons are affected, however perhaps to varying degrees and on a differing time scale. These findings led us to investigate the functional effects of the toxin on neurons within the CA1 at 8-16 days post injection.

3.3 Functional effects of intrahippocampal TeNT injection and corresponding bouton analysis

Having shown that both VAMP1 and VAMP2 are cleaved by the injection of TeNT into the hippocampus, and that these two proteins are differentially expressed and co-localised with VGLUT1 and GAD, it leads to the hypothesis that both inhibition and excitation are affected by the TeNT injections. Previous data and clinical evidence has suggested that the toxin has an affinity for inhibitory neurons (Mellanby & Green, 1981; Farrar *et al.*, 2000; Turillazzi *et al.*, 2009). To further investigate this we undertook a group of experiments to look at the functional consequences of these injections. Here we couple electrophysiological recordings with immunohistochemistry for VAMP1 and VAMP2. This will give a further insight into the functional changes that occur and how these relate to the changes in the expression of the two proteins.

3.3.1 Electrophysiological recordings from CA1 of control and TeNT injected rats

Dr Andrew Powell and Dr Wei-Chih Chang carried out the electrophysiology on the acute *ex vivo* hippocampal slices from 8-16 day post injection rats. These slices were then processed for immunohistochemistry. For technical reasons, neurons from CA1a and CA1c were whole-cell patch clamped, but not from CA3 because in adult rats this area proves very difficult for patch clamp recordings. The electrophysiology results shall be briefly summarised below.

3.3.1.1 Ipsilateral hippocampus

Whole-cell patch clamp recordings were carried out in CA1a (away from injection site) and CA1c (adjacent to injection site). The results of the electrophysiology show

that evoked inhibitory post synaptic currents (IPSCs) were completely abolished (amplitude was zero), whilst the evoked excitatory post synaptic current (EPSC) maximal amplitude fell to 22% of controls in CA1c. There were no effects of the toxin in CA1a, where evoked responses were similar to controls. Spontaneous IPSCs (sIPSC) and EPSCs (sEPSC) were also recorded and showed that although the amplitude remained at levels comparable to controls, the frequency was severely reduced in the CA1c area for both sEPSCs and sIPSCs (falling to ~36% and ~2% of control values respectively).

3.3.1.2 Contralateral hippocampus

The same recordings were carried out in contralateral slices, although from a separate batch of animals. These recordings showed that there were no significant differences between the spontaneous or evoked recordings within the CA1a or CA1c when comparing controls to TeNT slices.

Having established that there are significant changes in the functional abilities in ipsilateral CA1c of TeNT injected animals, we next move on to looking at the boutons in the areas that were recorded from to gain a better insight into the effects of the TeNT, focusing on the cleavage of VAMP1 and VAMP2. We also looked at the boutons in CA3 to investigate the changes which occurred here. We did not have the electrophysiological data to go with this from the current experiments, but previous work has looked at the physiological effects of TeNT in the CA3 area (Jefferys & Empson, 1990; Empson & Jefferys, 1993; Whittington & Jefferys, 1994).

3.3.2 High magnification microscopy and analysis of VAMP1 immunopositive boutons in control and TeNT injected animals

High magnification oil immersion microscopy allowed boutons in the different areas to be revealed. Bouton counts will be considered from the strata pyramidale and radiatum of the CA1a, CA1c and CA3. Analysis of the bouton counts within these different regions will compare the ipsilateral and contralateral sides, as well as control and TeNT treatments. Within each region this will consist of 4 tests and thus the significance criterion will be lowered to 0.0125 (Bonferroni correction for multiple comparisons). Comparisons of the bouton counts will then be made between the different regions, and here 3 tests are used so the significance criterion has been set at 0.0167 (Bonferroni correction for multiple comparisons). Unless stated, the test used will be a t-test.

3.3.2.1 Str. pyramidale

Within the CA1a str. pyramidale (Figure 3.17, panels A and B) there are no differences between the two sides of the hippocampus in control or TeNT slices. When comparing the ipsilateral control to the ipsilateral TeNT slices however, there are significantly fewer boutons in the TeNT condition ($p=<0.001$). This is likely to be due to spread of the toxin effect by 8-16 days that has spread from CA1c along towards the more medial area of CA1. There are no differences between the control and TeNT treatment in the contralateral CA1a, showing that this region is unaffected by the toxin.

The str. pyramidale of CA1c (Figure 3.17, panels C and D) shows some differences to the CA1a. Here there are no differences between control and TeNT bouton counts within the ipsilateral hippocampus ($p=0.014$ which is non-significant after the lowered

significance criterion). The ipsilateral TeNT group only contained 3 slices. This was because the cell bodies within the str. pyramidale in the other images were not clear and therefore were not consistent and were excluded from the analysis. Of the 3 slices that were included, there was a large variation, with bouton counts of 7, 8 and 22. This would suggest that two slices showed significant cleavage of VAMP1 positive boutons but that the other was not so affected by the toxin. There are fewer boutons in the ipsilateral TeNT slices compared with the contralateral TeNT treatment ($p=0.012$) which would suggest that there may indeed be cleavage in the ipsilateral TeNT slices. Further experiments to increase the number of slices in this treatment condition will validate this. Conversely, there are significantly fewer boutons in the contralateral control slices in comparison to the ipsilateral controls ($p=0.006$; Mann Whitney Rank Sum).

The CA3 str. pyramidale (Figure 3.17, panels E and F) of control slices show a significant difference between the two sides, where there are fewer boutons in the contralateral side compared with the ipsilateral ($p=0.011$). This value is quite near to the significance criterion so should be analysed with caution but as will be mentioned in the next section, the same result is also seen in the CA3 of VAMP2 immunopositive slices. There are no differences between the two hippocampal sides within the TeNT slices. Comparisons of control with TeNT slices show that there are significantly fewer boutons in the TeNT slices in both the ipsilateral and contralateral sides ($p=0.003$ (Mann Whitney Rank Sum) and $p=0.009$ respectively). This shows that the toxin is having a cleavage affect on the VAMP1 immunopositive boutons on both sides of the hippocampus, but with a greater effect on the ipsilateral side, which is to be expected.

3.3.2.2 Comparison of str. pyramidale in the different hippocampal regions

Within this section, the CA1a, CA1c and CA3 will be compared to each other within one side of the brain and an individual treatment, for example the ipsilateral control slices. Three tests will be used for each of these conditions and thus the significance criterion has been set at 0.0167 (Bonferroni correction for multiple comparisons).

There are no differences between the three regions in the ipsilateral control slices or within the contralateral control or contralateral TeNT slices. The ipsilateral TeNT bouton counts show that there are significantly fewer boutons in the CA1c compared with CA1a ($p=0.009$) but no differences comparing the other regions. Conclusions should be made cautiously because only 3 slices were included in the CA1c TeNT group, but the comparisons of the areas would suggest that in fact the CA1c does show a cleavage hence the significantly lower bouton counts compared with CA1a. The counts for CA3 lie between those of CA1a and CA1c which would identify why there are no differences between CA3 and either of the CA1 regions.

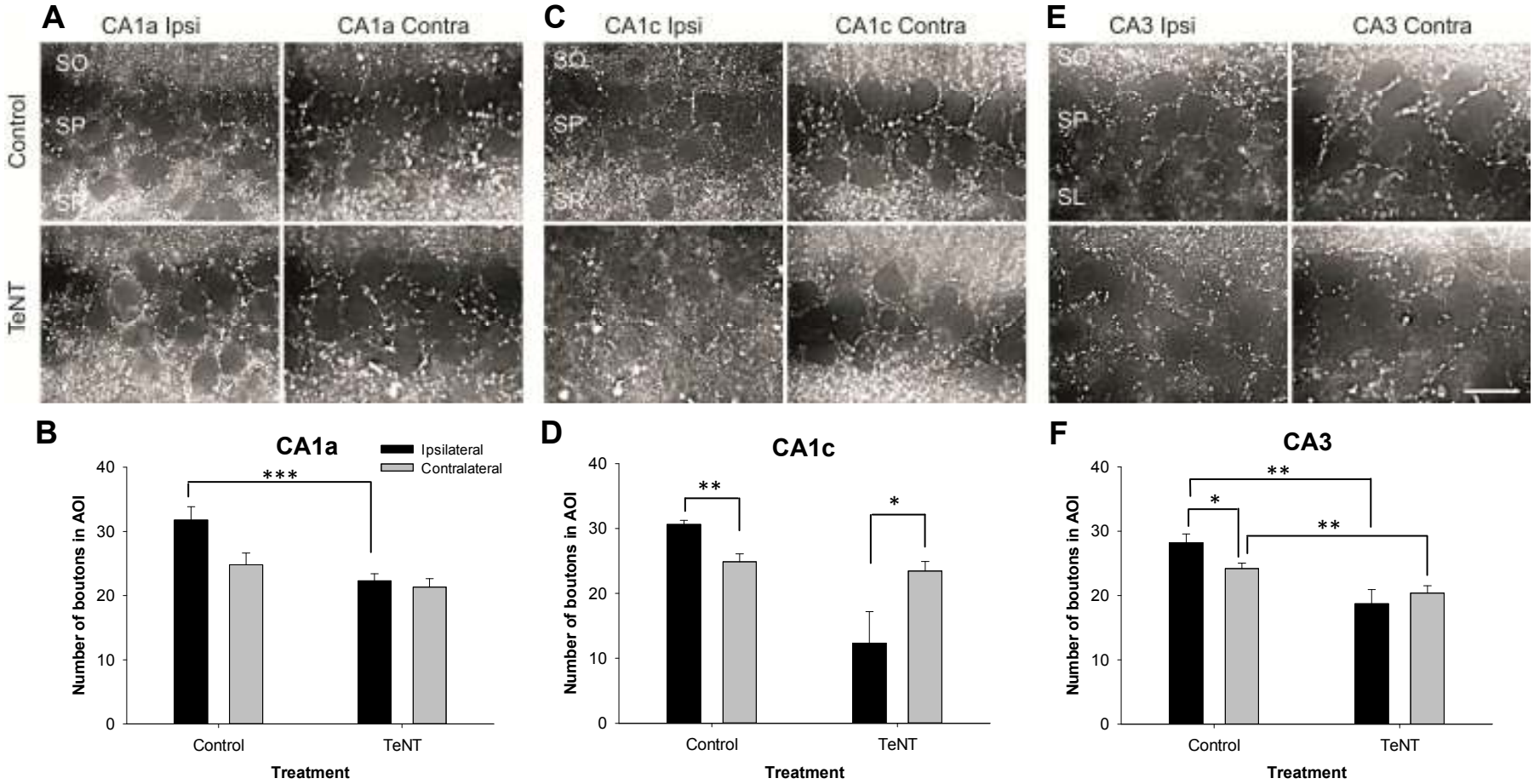

Figure 3.17. VAMP1 immunopositive boutons in str. pyramidale of CA1a, CA1c and CA3. Panels A, C and E show high magnification images taken from the CA1a, CA1c and CA3 respectively, ipsilateral (black bars) and contralateral (grey bars) to the injection. Below, panels B, D and F show the bouton counts made within an area of interest (AOI; 15x60µm) placed within the str. pyramidale (SP). Data in graphs shown as mean ± SEM. * $p<0.05$, ** $p<0.01$ and *** $p<0.001$. Scale bar represents

20μm. The number of slices analysed is as follows, with ipsilateral then contralateral: CA1a Control 4, 9; CA1a TeNT 15, 14; CA1c Control 10, 16; CA1c TeNT 3, 9; CA3 Control 14, 25 and CA3 TeNT 15, 25. Abbreviations: SO, Str. Oriens; SP, Str. Pyramidale; SR, Str. Radiatum and SL, Str. Lucidum.

3.3.2.3 Str. radiatum

The CA1a str. radiatum (Figure 3.18, panels A and B) shows significantly more boutons in the contralateral side compared with the ipsilateral side in both the control and TeNT slices (p=0.008 and p=0.004 respectively). There are no differences between the two treatments when compared within the individual sides of the brain which emphasises the differences between the counts in the individual sides but also shows that the toxin has no effect in the CA1a region of str. radiatum, unlike str. pyramidale.

The CA1c region (Figure 3.18, panels C and D) also shows differences between the two sides, with the contralateral side again showing the greater bouton counts. This is present in both controls and TeNT slices (p=<0.001 and p=0.010 (Mann Whitney Rank Sum) respectively). There are significantly fewer boutons in the ipsilateral TeNT slices compared with ipsilateral control (p=0.001) but no differences in the contralateral side between the treatments. These data identify that the toxin is having a cleavage effect within the ipsilateral CA1c but not within the contralateral side and that there is a discrepancy between contralateral and ipsilateral boutons within control slices, as in the CA1a.

There are no differences between the hippocampi on the two different sides of the brain in controls or TeNT slices within the CA3 (Figure 3.18, panels E and F). There are however significantly fewer boutons in TeNT slices compared with controls in both the ipsilateral and contralateral hippocampi (p=<0.001 and p=0.009 respectively). This shows that the toxins most prominent effect is within the ipsilateral

hippocampus but its effects are also seen on the contralateral side, specifically in the CA3.

3.3.2.4 Comparison of str. radiatum in the different hippocampal regions

The bouton counts in the ipsilateral hippocampi show no differences between the three different regions, in control or TeNT slices. In the contralateral control however, there are significantly fewer boutons in the CA3 compared with both the CA1a and CA1c ($p=0.004$ and $p=<0.001$respectively). This is also seen in the TeNT slices ($p=0.014$ and $p=0.004$; CA1a vs CA3 and CA1c vs CA3 respectively). There are significantly more boutons in CA1c versus CA1a in the str. radiatum ($p=0.007$). This all suggests that the numbers of boutons with the str. radiatum is not consistent across the length of the hippocampus and should therefore be compared with caution. This difference is understandable considering that neurons within the different regions receive differing innervations.

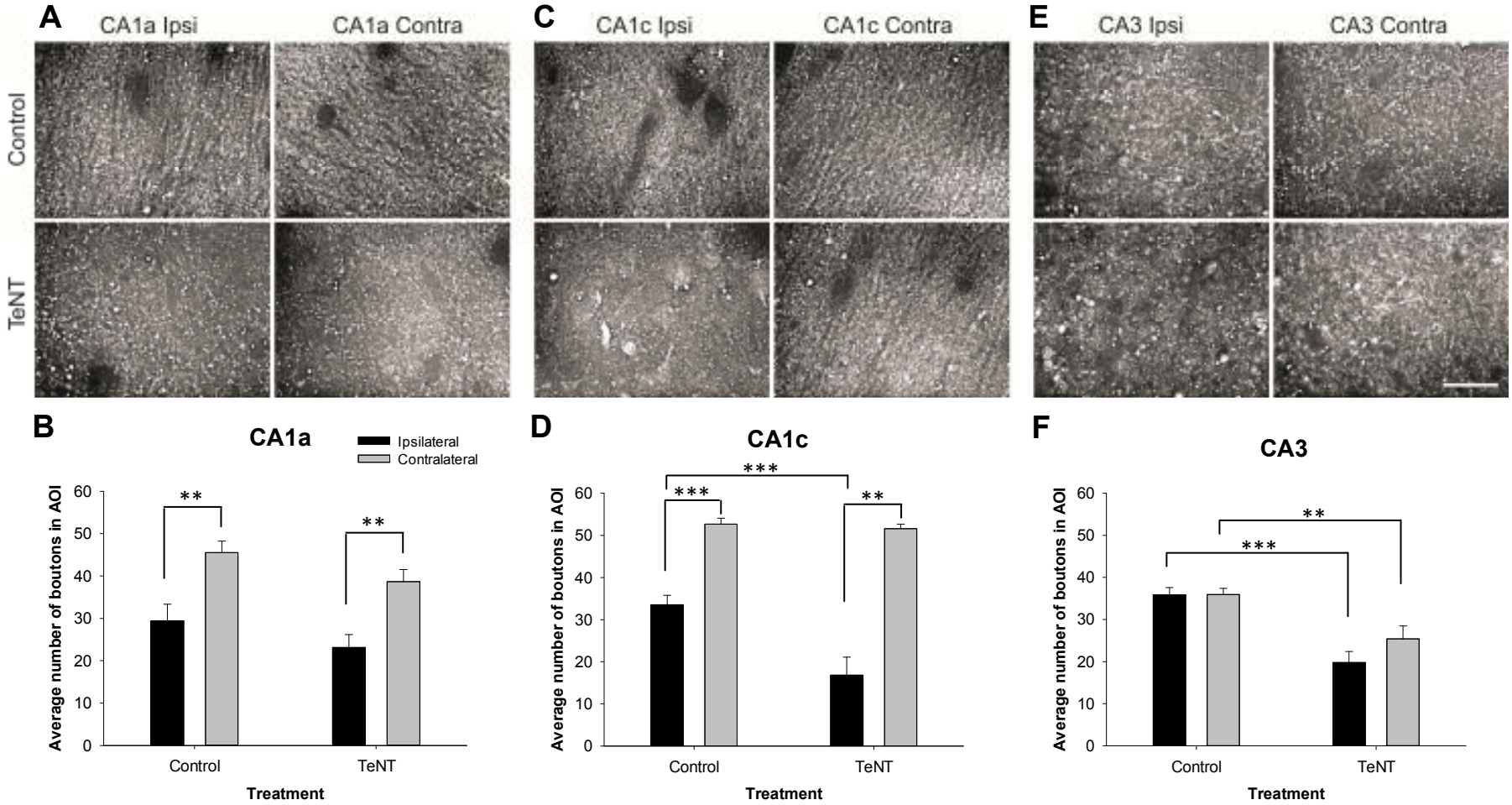

Figure 3.18. VAMP1 immunopositive boutons in str. radiatum of CA1a, CA1c and CA3. High magnification images (panels A, C and E) show boutons within the CA1a, CA1c and CA3. Control and TeNT slices are shown from ipsilateral (black bars) and contralateral (grey bars) hippocampi. The associated average bouton counts made from an area of interest (AOI; 10x10μm)

randomly placed in four positions throughout each image are shown in panels B, D and F. Data shown as mean ±SEM. * $p<0.05$, ** $p<0.01$ and *** $p<0.001$. Scale bar represents 20μm. The number of slices analysed is as follows, with ipsilateral then contralateral: CA1a Control 4, 6; CA1a TeNT 10, 6; CA1c Control 11, 8; CA1c TeNT 6, 4; CA3 Control 6, 12 and CA3 TeNT 6, 12.

3.3.2.5 Summary of the effects of TeNT in hippocampal regions on VAMP1 immunopositive bouton counts

Overall, the bouton counts have shown that the toxin is able to cleave VAMP1 in the CA3 of both the ipsilateral and contralateral hippocampus in the strata pyramidale and radiatum, with the more prominent effects seen in the ipsilateral side. There is also evidence of cleavage in ipsilateral CA1a and CA1c of the str. pyramidale and CA1c of the str. radiatum. We have also seen differences between the counts in the sides of the brain which shall be considered in the discussion.

3.3.3 High magnification microscopy and analysis of VAMP2 immunopositive boutons in control and TeNT injected animals

The previous section showed the changes in bouton counts within the different hippocampal regions for VAMP1 immunopositive boutons. In this section, the same comparisons will be made but for VAMP2 immunopositive boutons.

3.3.3.1 Str. pyramidale

As shown in low magnification microscopy (Section 3.3), the distribution of VAMP2 is somewhat different to VAMP1. This is further highlighted at high magnification, where VAMP1 immunopositive boutons encircle the cell bodies, but here VAMP2 immunopositive boutons fill the area between the cell bodies rather than encircling them. The CA3 images show a bright area in the bottom section. This is where the mossy fibres are coming into the str. lucidum and show very high VAMP2 labelling. When the AOI is positioned, the str. lucidum area is avoided and the str. pyramidale layer focused upon.

The CA1a str. pyramidale (Figure 3.19, panels A and B) shows no differences between the two sides of the brain in control slices but there are significantly more boutons in ipsilateral TeNT versus contralateral TeNT ($p=0.004$; Mann Whitney Rank Sum). This would seem like an unusual result but overall when coupled with results showing no difference between the control and TeNT slices in ipsilateral or contralateral slices it suggests that the TeNT has had no effect on the CA1a str. pyramidale and the difference in TeNT slices is due to hippocampal side differences.

The toxin has cleaved VAMP2 immunopositive boutons in the CA1c (Figure 3.19, panels C and D). There are significantly fewer boutons in the TeNT slices compared with controls in both the ipsilateral and contralateral hippocampi ($p=0.008$ and

p=0.005 respectively). There are no differences between the two sides in control slices or TeNT slices.

The CA3 region (Figure 3.19, panels E and F) shows significantly higher bouton counts in the ipsilateral control slices compared with contralateral controls (p=0.004), a result that mirrors that seen in the VAMP1 immunostained slices. There are no differences between the sides in the TeNT slices. Significant differences between controls and TeNT slices are seen in both the ipsilateral and contralateral hippocampi (p=<0.001 in both cases) and show that both sides are robustly affected by the toxin.

3.3.3.2 Comparison of str. pyramidale in the different hippocampal regions

Within ipsilateral control slices, there are no differences between the three regions. In the ipsilateral TeNT str. pyramidale, there are significantly fewer boutons in CA3 versus CA1a (p=<0.001). This would be expected as the previous section showed that CA1a was unaffected by the toxin, and yet CA3 boutons were cleaved. In the contralateral hippocampus, the CA3 has significantly fewer boutons again in comparison to the CA1a, but here in control as well as TeNT slices (p=0.014 and p=<0.001 respectively). The results from the control slices should be approached with caution as it is quite close to the significance criterion and therefore no strong conclusions should be drawn from this. It is plausible that CA3 str. pyramidale may show fewer boutons than CA1a in the contralateral side, but without further tests in other batches of animals, this cannot be fully concluded. The difference in the contralateral TeNT slices however shows a clear difference and this further emphasises the effects of the toxin in the contralateral CA3 as well as the ipsilateral.

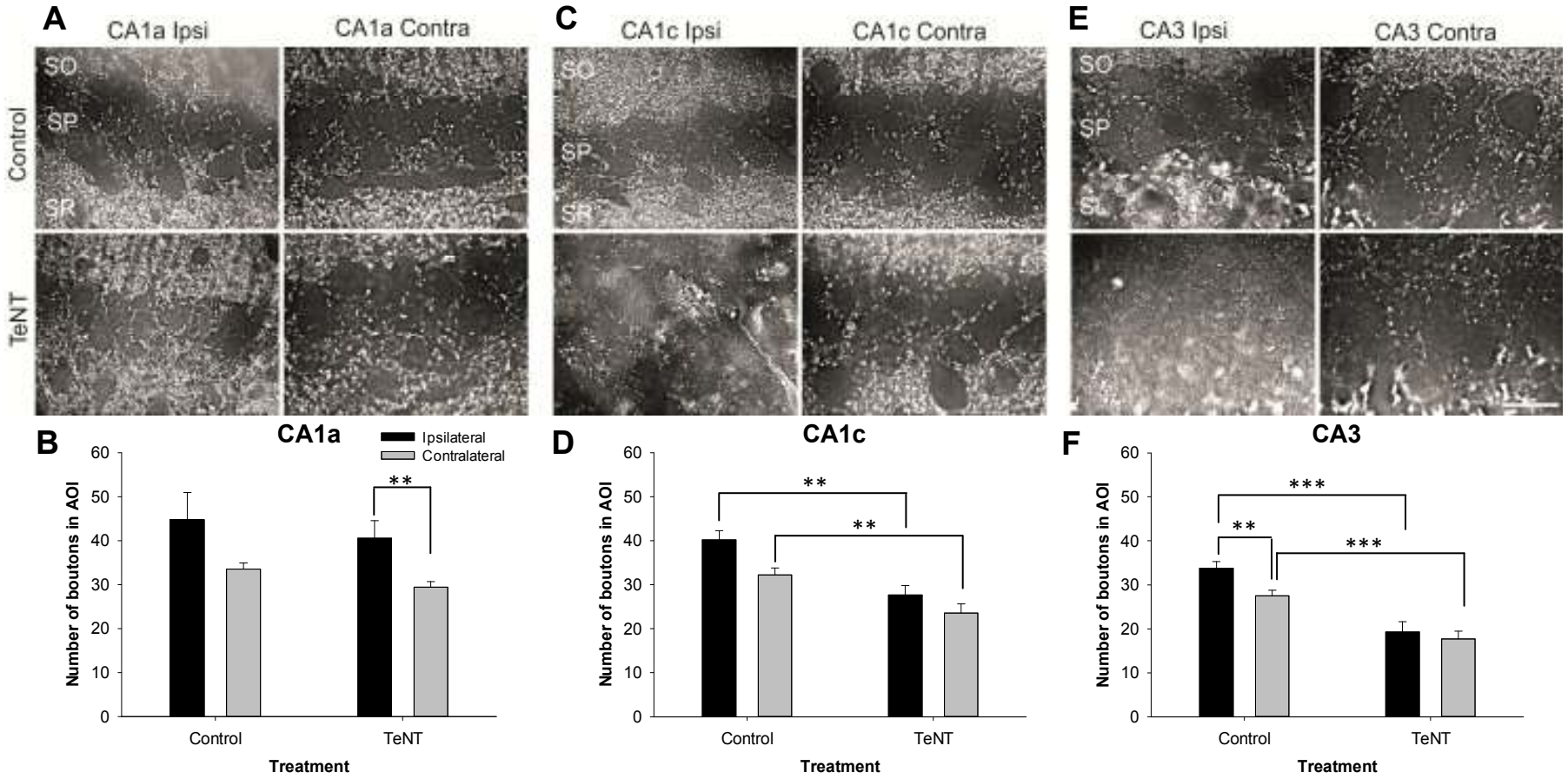

Figure 3.19. VAMP2 immunopositive boutons in str. pyramidale of CA1a, CA1c and CA3. Panels A, C and E show high magnification images from CA1a, CA1c and CA3 of VAMP2 immunostained hippocampal slices. Control and TeNT slices are represented, along with both the ipsilateral (black bars) and contralateral (grey bars) sides. Panels, B, D and F show the associated bouton counts for the different treatments, areas and side of the brain taken within an area of interest (AOI; 15x60µm) placed within the str. pyramidale. Data shown as mean ± SEM. * $p<0.05$, ** $p<0.01$ and *** $p<0.001$.Scale bar

represents 20μm. The number of slices analysed is as follows, with ipsilateral then contralateral: CA1a Control 4, 9; CA1a TeNT 9, 17; CA1c Control 6, 14; CA1c TeNT 3, 7; CA3 Control 14, 26 and CA3 TeNT 7, 23. Abbreviations: SO, Str. Oriens; SP, Str. Pyramidale; SR, Str. Radiatum and SL, Str. Lucidum.

3.3.3.3 Str. radiatum

Bouton counts within the str. radiatum of the control CA1a (Figure 3.20, panels A and B) show that there are significantly fewer VAMP2 immunopositive boutons in ipsilateral CA1a versus contralateral (p=0.009). There are no differences between the sides in TeNT slices and no differences between control and TeNT treatments in either side of the brain. Overall this suggests the toxin has no effect in CA1a but that contralateral str. radiatum has an increased number of boutons in control slices compared with the opposite side.

The CA1c (Figure 3.20, panels C and D) also shows a higher number of boutons in the contralateral side, but here in both control and TeNT slices (p=0.002 and p=<0.001 respectively). The ipsilateral TeNT slices show fewer boutons than ipsilateral controls (p=0.003), indicating that the toxin affects the ipsilateral CA1c but not the contralateral.

There are no differences between CA3 (Figure 3.20, panels E and F) in the two sides of the brain for control or TeNT slices. There are however significantly fewer boutons in the TeNT slices compared with controls in both the ipsilateral and contralateral sides (p=0.001 in both cases).

3.3.3.4 Comparison of str. radiatum in the different hippocampal regions

Comparisons between the different areas indicate no differences in the ipsilateral side of control or TeNT slices. In the contralateral side, there are significantly fewer boutons in the CA3 compared with the CA1a and CA1c in both the control (p=<0.001 and p=0.004 (Mann Whitney Rank Sum) respectively) and TeNT slices (p=0.002 in both cases).

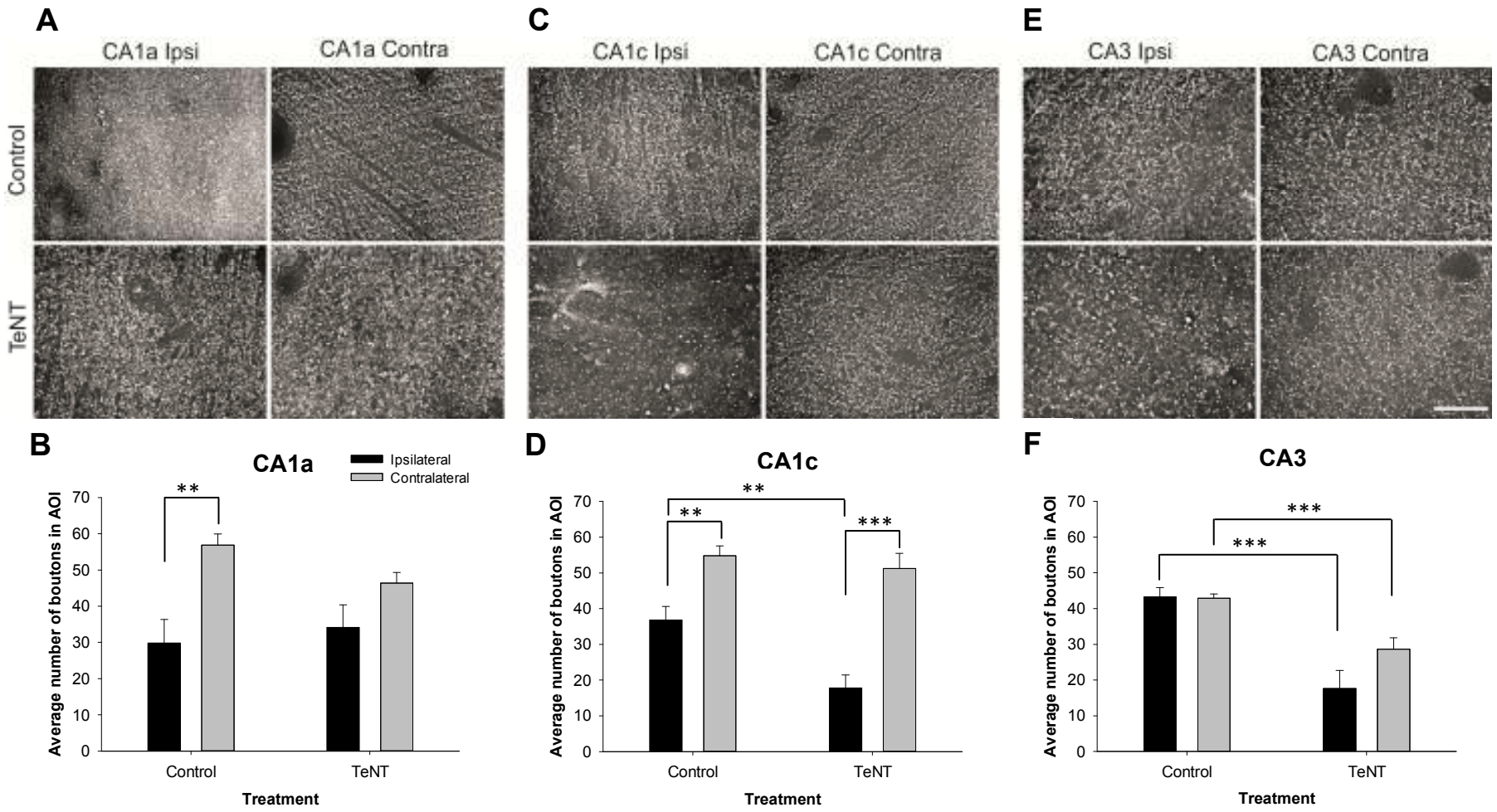

Figure 3.20. VAMP2 immunopositive boutons in str. radiatum of CA1a, CA1c and CA3. High magnification images of the str. radiatum of the CA1a, CA1c and CA3 are shown in panels A, C and E respectively. The associated bouton counts collected from areas of interest (AOI; 10x10μm) within control and TeNT slices, from the ipsilateral (black bars) and contralateral (grey bars) hippocampi. Data shown as mean ± SEM. * p<0.05, ** p<0.01 and *** p<0.001. Scale bar represents 20μm. The number

of slices analysed is as follows, with ipsilateral then contralateral: CA1a Control 4, 4; CA1a TeNT 8, 7; CA1c Control 9, 9; CA1c TeNT 7, 4; CA3 Control 6, 12 and CA3 TeNT 5, 11.

3.3.3.5 Summary of the effects of TeNT in hippocampal regions on VAMP2 immunopositive bouton counts

Overall, the VAMP2 immunopositive bouton counts show that the CA3 is affected by the toxin in both the ipsilateral and contralateral sides of strata pyramidale and radiatum. The CA1c is also affected by the toxin in both these layers of the ipsilateral hippocampus, along with contralateral str. pyramidale. As in the VAMP1 immunostained slices, there are differences between the bouton counts in the two sides of the brain in control sections, dependent on the area.

3.3.4 Summary of the VAMP1 and VAMP2 immunopositive bouton analysis in the strata pyramidale and radiatum in control and TeNT injected rats

The bouton counts from both the VAMP1 and VAMP2 immunostained slices have highlighted that there are differences between the sides of the brain. In the str. pyramidale, the ipsilateral side shows the most boutons within CA3, significantly higher than the contralateral side, in both VAMP1 and VAMP2. With one exception (VAMP1 CA1c), the CA1a and CA1c regions do not show differences between the two halves of the brain in control str. pyramidale. The str. radiatum however shows the contralateral side to have significantly higher counts than the ipsilateral side, but this time within the CA1a and CA1c, and no differences in the CA3. These results have highlighted that there are differences, not only between the sides of the brain, but also between the different regions within that side. These data will be further reviewed in relation to asymmetry in Chapter 5 (Discussion).

The CA3 strata pyramidale and radiatum analysis shows that the TeNT cleavage occurs in both the ipsilateral and contralateral sides in VAMP1 and VAMP2 positive

sections. The only other region that shows cleavage in the contralateral side is the CA1c str. radiatum in VAMP2 positive sections.

3.4 Summary of the effects of in vivo TeNT injections within the first 16 days of the epileptic syndrome

This chapter has highlighted that intrahippocampal injection of TeNT causes a disruption of VAMP1 and VAMP2 positive boutons, which are differentially localised in inhibitory and excitatory neuronal populations respectively. Imaging and grey level analysis of slices at 2, 8 and 16 days has demonstrated the spatiotemporal progression of VAMP1 and VAMP2 cleavage following toxin injections. The electrophysiology and high magnification imaging of boutons at the later time points (8-16 days) have indicated that the toxin disrupts both inhibition and excitation, to differing levels, within the CA1c, closest to the injection. Immunohistochemistry has also clearly shown that VAMP1 and VAMP2 immunopositive boutons are cleaved in both the ipsilateral and contralateral hippocampi.

4 INVESTIGATION OF THE EFFECTS OF FOCAL TETANUS TOXIN INJECTIONS ONTO ORGANOTYPIC HIPPOCAMPAL SLICE CULTURES

4.1 Rationale for the use of organotypic hippocampal slice cultures to investigate the effects of TeNT

The use of *in vivo* TeNT injections has many benefits for studying the effects of the toxin. However, there would be advantages to having an *in vitro* method for the toxin injections. This method could allow the study of changes across multiple time points as well as possibly providing a medium throughput method for the testing of antiepileptic and anticonvulsive drugs. The aim of this part of the project was to set up an *in vitro* method of TeNT injections and to establish whether the electrophysiological and immunohistochemical changes that are seen in the *in vivo* model are also seen in organotypic hippocampal slice cultures.

4.2 Investigation into the effects of TeNT on organotypic hippocampal slice cultures using extracellular field recordings

To investigate the physiological changes that may occur following treatment with the different toxin concentrations, extracellular recordings were carried out in organotypic hippocampal slice cultures. Recordings of the field potentials in the CA1 and CA3, in the str. pyramidale and str. radiatum, were undertaken at 2, 8 and/or 16 days post injection. Electrophysiological recordings from *ex vivo* slices that have been taken from TeNT injected animals are regularly undertaken and thus provide a good comparison for this new method of focal treatment *in vitro.*

4.2.1 Multiple recordings from individual slices

Organotypic hippocampal slice cultures allow repeated recordings from the same slice over many days. To test whether these repeated recording sessions damaged the slices, statistical analysis compared slices used on multiple occasions with those

that were used only once. T-tests or Mann Whitney Rank Sum tests were used. Overall, at all time points and within all areas and all treatments, there were no significant differences between the slices used multiple times and those used only once, showing no detriment to the responses recorded. However the power is very low for these calculations because sometimes there are only 2 or 3 slices in each group. For now all the slices have been grouped together within the respective time points, regardless of whether they were used multiple times or not. If further experiments are carried out in the future then this is an issue that needs to be considered further, particularly when larger numbers of slices are used in each group to see if there is a difference. The following sections use this pooled data.

For the comparisons between the different treatment groups at individual time points, the significance criterion will be lowered to 0.0083 using the Bonferroni correction for multiple comparisons. This is because there will be 6 tests performed at each time point and thus lowering the significance criterion makes the chance of getting one or more false positives over these multiple tests 0.05. For statistical tests looking at the differences between the time points within individual treatments there will be 3 tests each and so the Bonferroni correction for multiple comparisons will be used to lower the significance criterion to 0.0167.

In the next sections, the results from the CA1 and CA3 str. pyramidale and str. radiatum shall be considered separately, firstly looking at response sizes, then moving onto the additional effects of the toxin on slices.

4.2.2 CA1 str. pyramidale

The most noticeable differences between the treatments in recordings from the CA1 str. pyramidale is the lack of responses or very small responses seen in the 50ng/µl TeNT treated slices (Figure 4.1). At all three time points, these slices show significantly smaller maximal responses (Vmax) than control slices, p=<0.001, p=<0.001 (both Mann Whitney Rank Sum) and p=0.002 (t-test) for 2, 8 and 16 days post injection respectively (Figure 4.2). There are also significantly smaller responses in the 25ng/µl TeNT slices compared with controls at 8 and 16 days post injection (p=<0.001 and p=0.002; t-test and Mann Whitney Rank Sum respectively). At day 8 the 5ng/µl slices also show significantly larger responses than 50ng/µl TeNT treated slices (p=0.004; Mann Whitney Rank Sum).

The V50 values for the 50ng/µl TeNT slices are significantly smaller than controls at days 2 and 8 (p=<0.001 in both cases; Mann Whitney Rank Sum) (Figure 4.2). At 2 days post injection there are also larger V50 values in controls compared with the 25ng/µl TeNT slices (p=0.003; Mann Whitney Rank Sum) and at day 8 the 5ng/µl TeNT slices show larger V50 values than 50ng/µl TeNT slices (p=0.004; Mann Whitney Rank Sum). In these cases, a lower V50 shows that the tissue is more sensitive to stimulation. Considering that the Vmax for the higher doses of toxin slices are significantly lower than in controls, then coupling this with the lower V50s shows that the responses from the TeNT slices are significantly affected by the application of toxin and that synaptic transmission in the CA1 str. pyramidale is lost or significantly decreased.

When comparing the size of the responses within individual treatments but between the time points, there are no significant differences between the maximal sizes of the

responses or the V50 values in any of the treatment groups. This shows that if the TeNT is having an effect on the responses (as has been shown when comparing the controls with 25 and 50ng/µl TeNT treatments) then the effect remains across all three time points.

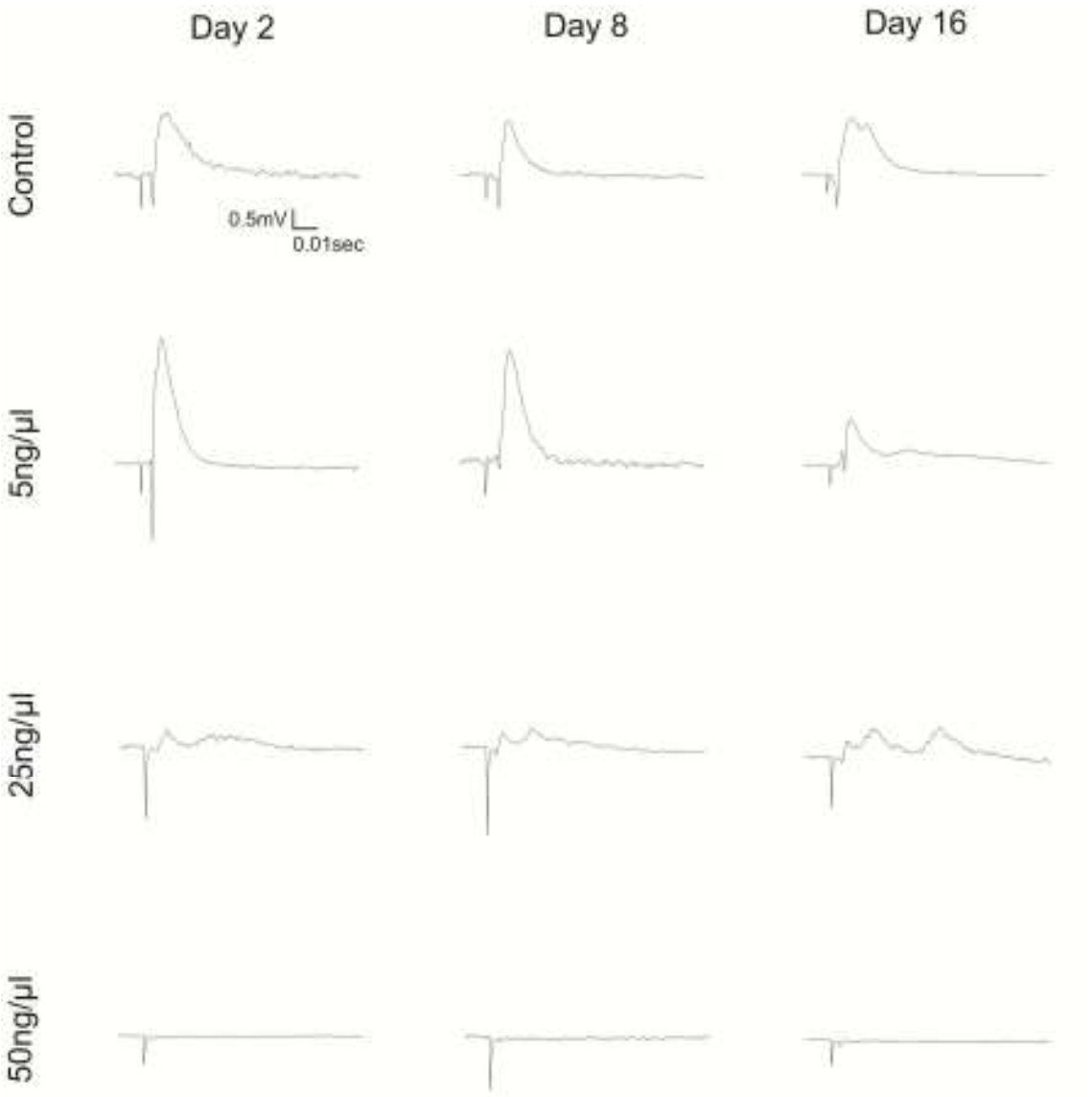

Figure 4.1.Field recordings from CA1 str. pyramidale of organotypic hippocampal slice cultures. Field recordings from control and 5, 25 and 50ng/µl TeNT treated slices from the CA1 str. pyramidale. These are representations of traces recorded at 2, 8 and 16 days post injection following a stimulus of 50V directed at the CA3 str. radiatum. Population spikes are affected by toxin treatment in a concentration dependent manner.

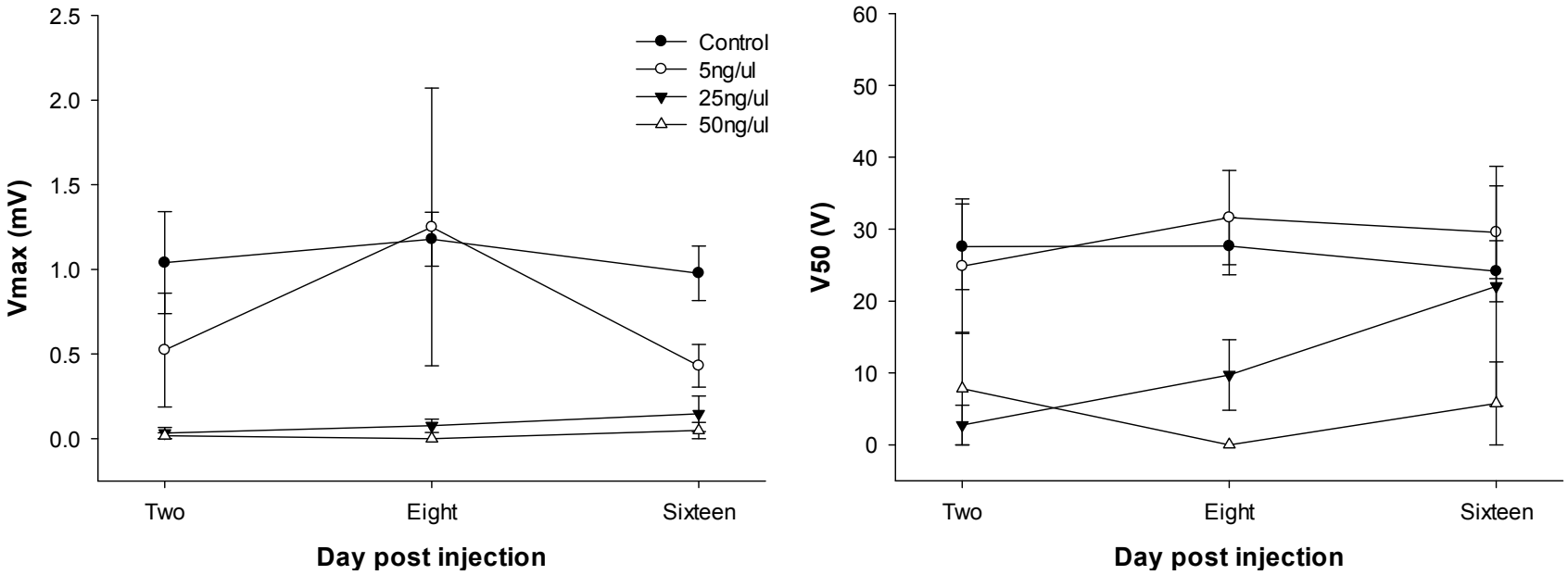

Figure 4.2. Analysis of CA1 str. pyramidale responses. These graphs show the maximal response sizes (Vmax) and the voltage required to evoke half the maximal response (V50) in the CA1 str. pyramidale of organotypic hippocampal slice cultures. The slices had been treated focally with control or 5, 25, or 50ng/µl TeNT solution and recordings made at 2, 8 and 16 days post injection. The data points indicate the mean ± SEM. The number of recordings for each of the treatments at the time points of 2, 8 and 16 days post injection respectively are: Controls 7, 11 and 7 slices; 5ng/µl 7, 5 and 6 slices; 25ng/µl 5, 7 and 6 slices, and 50ng/µl 7, 6 and 4 slices.

4.2.3 CA1 str. radiatum

Similar to the str. pyramidale of the CA1, there are reductions in the maximal sizes of the responses in the CA1 str. radiatum of slices treated with the highest two concentrations of TeNT (Figure 4.3). At days 2, 8 and 16, the controls show significantly larger maximal responses than the 50ng/µl TeNT slices ($p=<0.001$, $p=<0.001$ and $p=0.002$; all Mann Whitney Rank Sum) (Figure 4.4). At days 8 and 16 the control responses are also greater than the 25ng/µl TeNT slices ($p=0.008$ and $p=0.003$; both Mann Whitney Rank Sum). There are no differences between the lowest TeNT concentration and the higher concentrations at any of the three time points.

The differences between the treatment groups are less apparent when comparing the V50 values. There are only differences between the highest concentration of TeNT and the control slices at 8 days post injection ($p=0.003$; Mann Whitney Rank Sum) (Figure 4.4).

As seen in the str. pyramidale, there are no differences between the response sizes or the V50 values at the different time points within each treatment group. This again shows that if an effect is present, then it remains throughout all the time points studied.

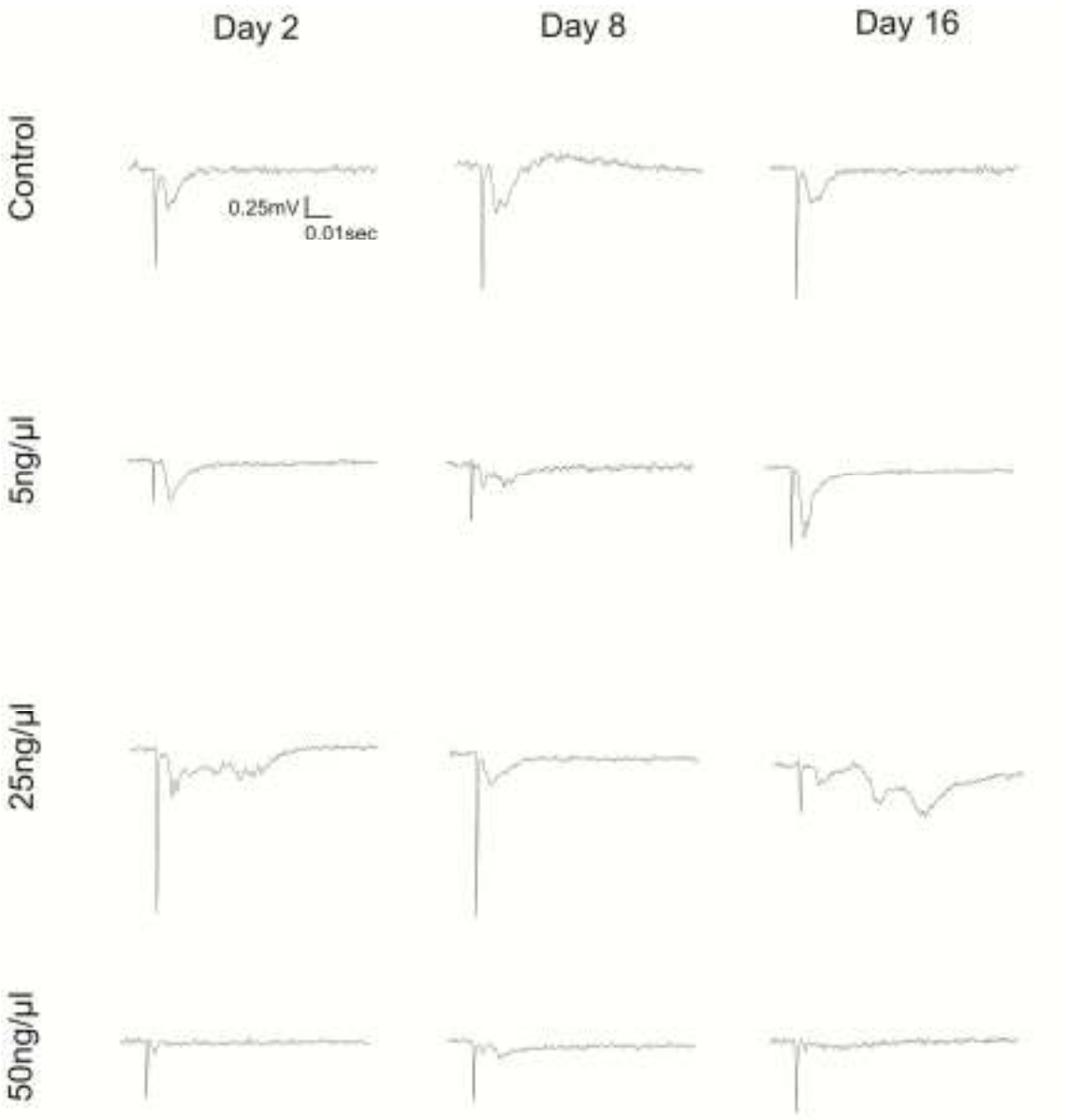

Figure 4.3. Field recordings from CA1 str. radiatum of organotypic hippocampal slice cultures. These traces show evoked responses within the CA1 str. radiatum following a stimulus of 50V in the CA3 str. radiatum. Slices had been treated focally with control or 5, 25 or 50ng/µl TeNT solutions and recordings were made at 2, 8 and 16 days post injection. Concentration dependent effects are seen in toxin treated slices from the three different groups compared with controls.

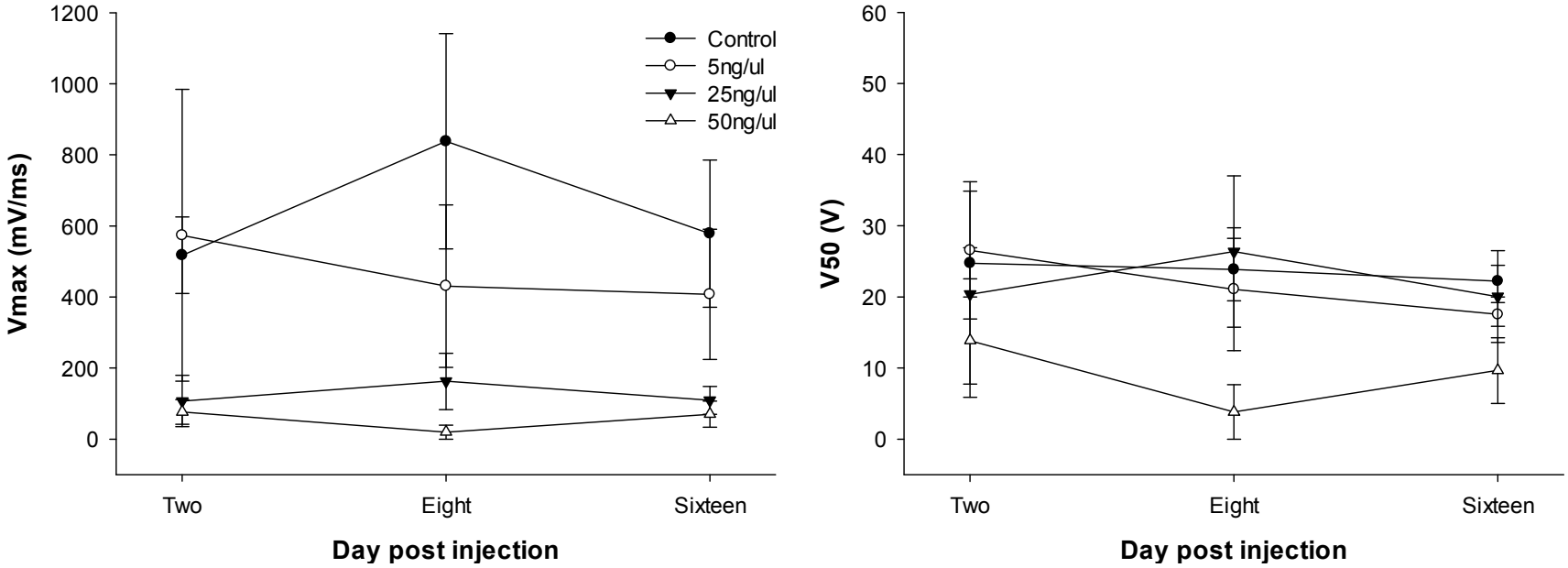

Figure 4.4. Analysis of CA1 str. radiatum responses. These graphs show the maximal size of responses (Vmax) evoked within the CA1 str. radiatum and the stimulus size required to evoke half this maximal response (V50). Organotypic hippocampal slice cultures had been treated with control solution or TeNT solution at concentrations of 5, 25 or 50ng/µl and recordings made at 2, 8 and 16 days post injection. Data points indicate mean ± SEM. The number of recordings for each of the treatments at the time points of 2, 8 and 16 days post injection respectively are: Controls 11, 11 and 10 slices; 5ng/µl 5, 6 and 6 slices; 25ng/µl 4, 6 and 8 slices, and 50ng/µl 11, 8 and 7 slices.

4.2.4 CA3 str. pyramidale

As explained in the Materials and Methods section, the analysis for the CA3 recordings differed from that of CA1 to take account of their different components. Within the CA3 str. pyramidale the peak positive amplitude was used. At all three time points control slices showed significantly larger maximal amplitudes than 50ng/µl TeNT treated slices ($p=<0.001$ Mann Whitney Rank Sum, at all time points) (Figures 4.5 and 4.6). At days 8 and 16 the control responses were also significantly larger than 25ng/µl TeNT slices ($p=0.008$ and $p=<0.001$ respectively, both Mann Whitney Rank Sum) and at day 2 they were also larger than the slices treated with the lowest dose of TeNT, 5ng/µl ($p=<0.001$, Mann Whitney Rank Sum). The voltage required to evoke half the maximal amplitude (V50) showed minimal differences between the treatment groups. There was only a significantly greater V50 in the 25ng/µl TeNT treatment group compared to controls at 16 days post injection ($p=0.003$). A comparison of the three time points within each individual treatment condition showed that there were no differences between the maximal amplitudes of the responses (Vmax) or the V50.

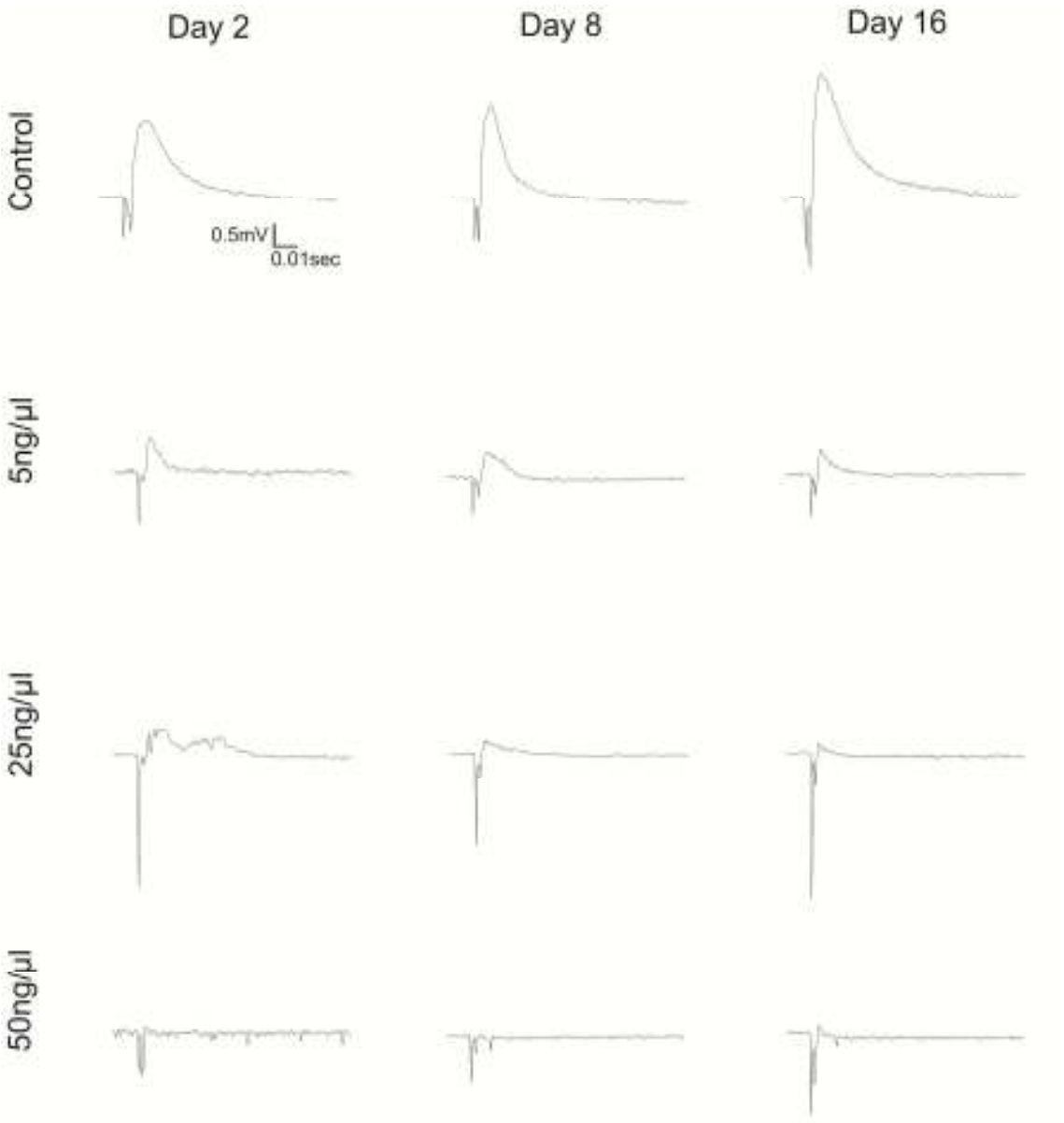

Figure 4.5. Field recordings from CA3 str. pyramidale of organotypic hippocampal slice cultures. Evoked responses following a stimulus of 50V in the CA3 str. radiatum at 2, 8 and 16 days post injection in slice cultures treated with control or TeNT solution (5. 25 or 50ng/µl). As with the CA1, the TeNT treated slices show concentration dependent effects.

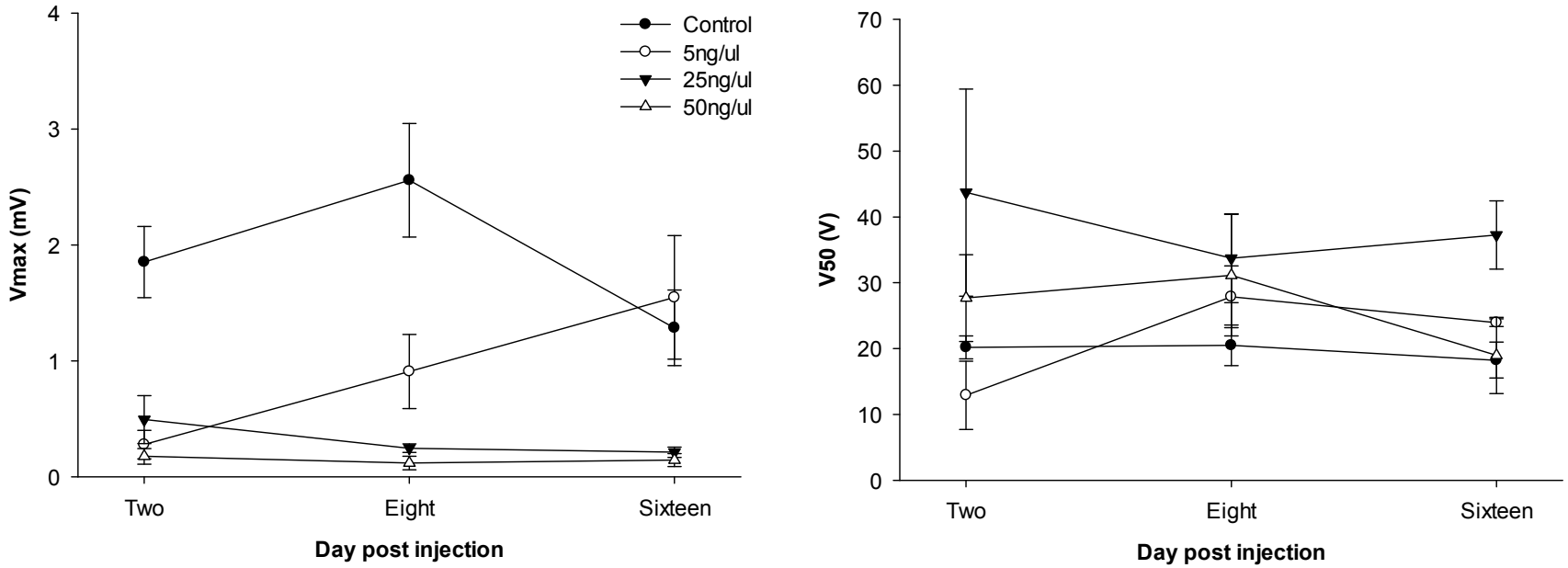

Figure 4.6. Analysis of CA3 str. pyramidale responses. These graphs show the comparisons of the maximal amplitudes of responses (Vmax) within the CA3 str. pyramidale and the stimulus required to evoke half the maximal response amplitude (V50). These measurements differ to those within the CA1 due to the disruption of measurements by the antidromic component of the response that is clearly present as well as the orthodromic. Organotypic hippocampal slice cultures had been treated with either control or TeNT (5, 25, or 50ng/µl) solutions and recordings made at 2, 8 and 16 days post injection. Data is plotted as mean ± SEM. The number of recordings for each of the treatments at the time points of 2, 8 and 16 days post injection respectively are: Controls 13, 12 and 11 slices; 5ng/µl 8, 8 and 5 slices; 25ng/µl 6, 7 and 8 slices, and 50ng/µl 10, 8 and 8 slices.

4.2.5 CA3 str. radiatum

As mentioned in the previous section, the analysis within the CA3 str. radiatum also had to differ from that of the CA1. The analysis of the peak negativity within the CA3 str. radiatum shows differences similar to that in the str. pyramidale. All three time points show larger maximal amplitudes of responses in control slices than 50ng/µl TeNT slices (p=<0.001, p=<0.001 and p=0.003 respectively as time increases, Mann Whitney Rank Sum) (Figures 4.7 and 4.8). At 2 days post injection there are also greater responses in controls compared with both 5 and 25ng/µl slices (p=0.002 and p=<0.001 respectively). Day 8 control also shows a greater response than the 25ng/µl slices (p=<0.001). These results are interesting as it suggests that at the earliest time point all concentrations of TeNT affect the synaptic transmission within this region but there is a dose dependent effect on the time at which the responses remain affected. This demonstrates that only the higher concentration effects last into the later time points, or that there is some recovery of synaptic transmission in the lower concentration treated slices.

The V50 analysis showed differences between control and 50ng/µl TeNT slices at days 8 and 16 (p=<0.001 and p=0.003 respectively, Mann Whitney Rank Sum) and between the 5 and 50ng/µl slices at day 16 (p=0.010, Mann Whitney Rank Sum). However these results show that the 50ng/µl V50 had the lowest V50 because it was zero at these time points. This shows that minimal or no synaptic transmission is detected at days 8 and 16 following treatment with the highest dose of the toxin in the majority of slices.

There are no differences within the individual treatments when comparing the different time points, in the analysis of Vmax or V50 which suggests that when changes occur, they continue or are similar to the other time points.

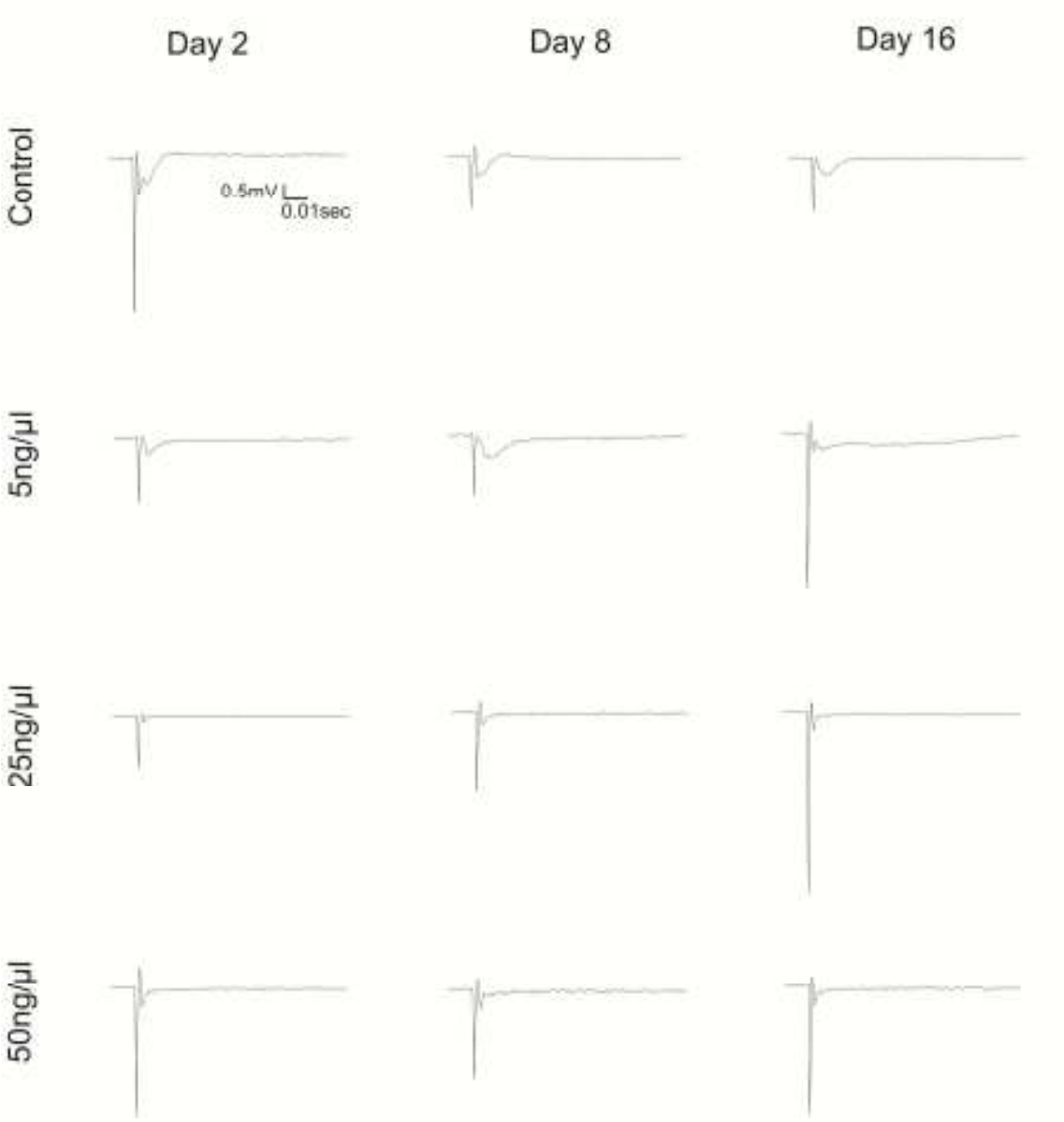

Figure 4.7. Field recordings from CA3 str. radiatum of organotypic hippocampal slice cultures. These traces show the responses from slice cultures treated with control or 5, 25, or 50ng/µl TeNT solutions. Recordings were made at 2, 8 and 16 days post injection. Traces shown indicate responses following a 50V stimulus to the CA3 str. radiatum. Dramatic decreases in responses are seen in slices that received the higher concentrations of TeNT.

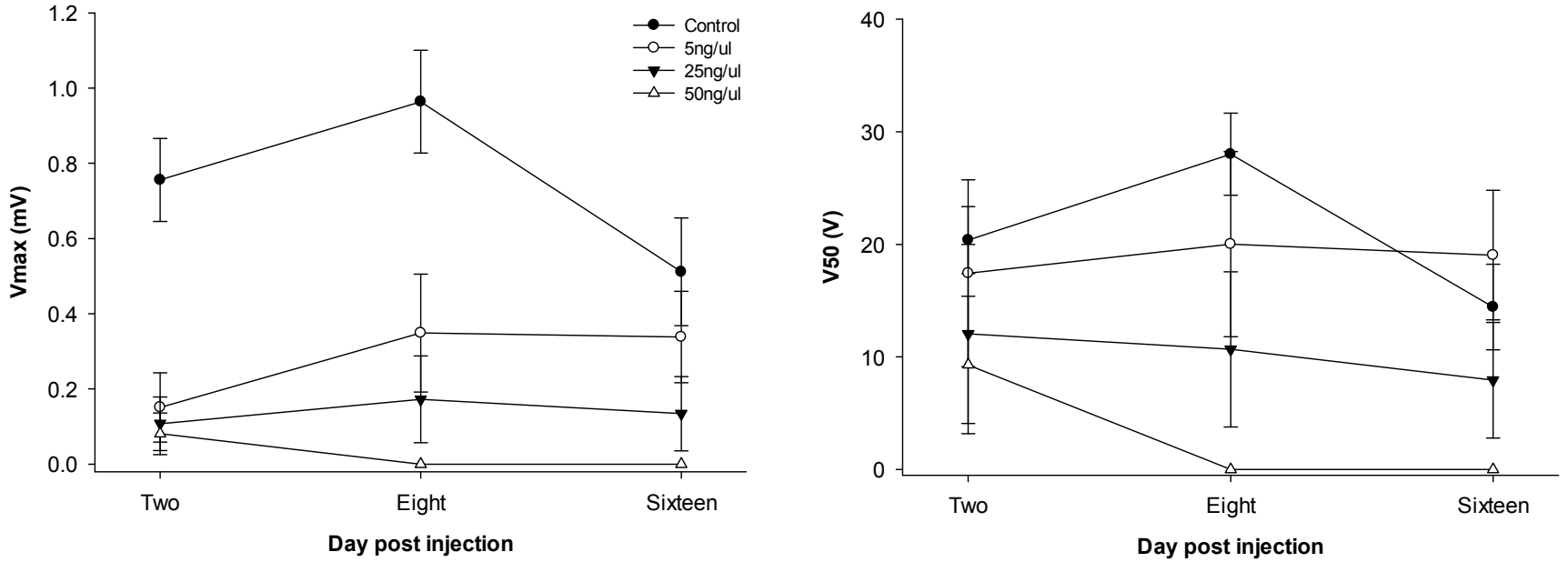

Figure 4.8. Analysis of CA3 str. radiatum responses. The graphs show the maximal amplitude of responses from baseline to peak negativity (Vmax) and the stimulus required to evoke half this maximal amplitude response (V50) for organotypic hippocampal slice cultures at 2, 8 and 16 days post injection. These measurements are different to those from the CA1 due to the overlap of the antidromic and orthodromic components. Slices had been treated with control or TeNT (5, 25 or 50ng/µl) solutions. Data plotted indicates mean ± SEM. The number of recordings for each of the treatments at the time points of 2, 8 and 16 days post injection respectively are: Controls 10, 10 and 9 slices; 5ng/µl 6, 8 and 8 slices; 25ng/µl 6, 7 and 7 slices, and 50ng/µl 8, 8 and 8 slices.

4.2.6 TeNT treatment results in epileptic activity in organotypic hippocampal slice cultures

We have already shown that the synaptic transmission is affected by the toxin, particularly the highest dose, but that the effects vary within the region studied and the different time points. As well as these changes in evoked synaptic transmission, epileptic activity was also seen in these slice cultures. This occurred in many slices and examples of it could be seen in all regions of the hippocampus recorded from and in a variety of slices from the different treatment groups. However it presented itself in different forms even within slices from the same treatment groups. These consisted of evoked afterdischarges and/or spontaneous activity. Both these forms however showed two distinct types within them.

4.2.6.1 Evoked afterdischarges

The evoked afterdischarges could last less than 1 second or continue for up to 8 seconds before returning to baseline. The characteristics of these two types of responses differed; one consisted of multiple spikes and the other represented seizure-like after-bursts. Examples of these responses can be seen in Figure 4.9 panels A and B.

The afterdischarges were dependent on a threshold stimulus. This threshold varied between slices and between the areas of the hippocampus but was always between 20 and 45V for both the interictal-type and the seizure-like discharges. Table 4.1 shows the percentages of slices that displayed afterdischarges. Whilst this table shows that control slices did show epileptic activity, it only occurred in a minority of recordings (5 from a total of 122 recordings across all three time points, counting each region of the hippocampus as a separate recording). It is also clear that the

majority of the epileptic activity was in slices treated with 25ng/μl TeNT (16 of 71 recordings), although many afterdischarges were also seen in 5ng/μl TeNT slices (14 of 78 recordings). The 50ng/μl slices showed minimal afterdischarges (3 of 93 recordings) which can be attributed to the nearly complete disruption of evoked synaptic transmission suggested by the field recording analysis, particularly at the later time points. Whilst the time points and the four areas recorded from have been combined within Table 4.1, it overall suggests that the application of the toxin has effects on the slices, although to varying degrees, dependent on concentration.

Table 4.2 indicates the spread of the effects of the toxin. Whilst there are some slices that only show afterdischarges (interictal-type and seizure-like pooled) within a single hippocampal region, it is clear that the 5 and 25ng/μl TeNT treatments cause epileptic activity in a widespread area, affecting both the CA1 and CA3 in the majority of slices affected. Interestingly, in all treatment conditions, the str. radiatum of the CA1 and CA3 is not affected alone.

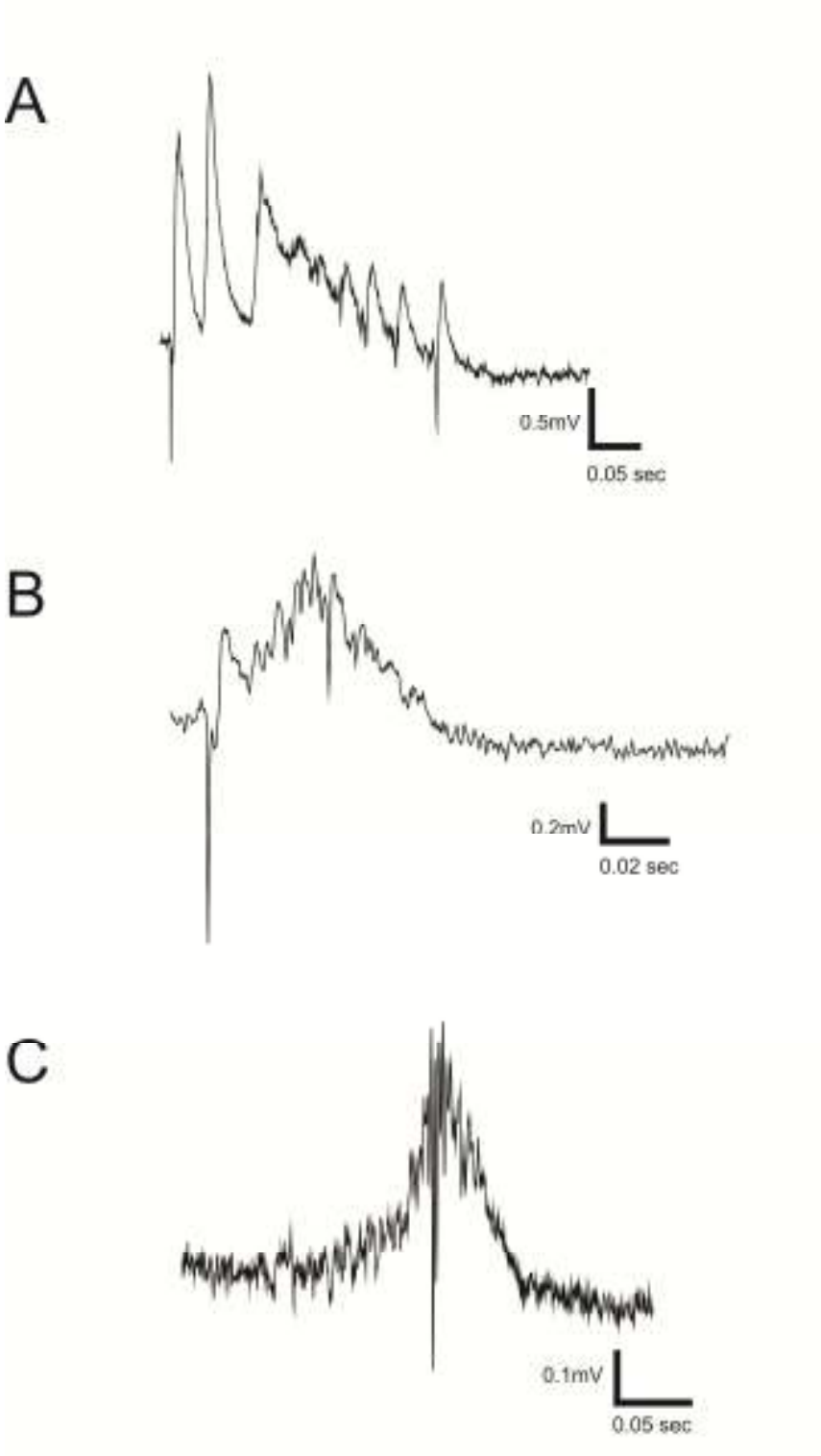

Figure 4.9. Different forms of epileptic activity within slice cultures. These traces show the variations in epileptic activity seen in slice cultures. Seizure-like evoked afterdischarges (A) and multiple spike evoked afterdischarges (B) from 16 days post TeNT injection slices after a stimulus of 35V. A spontaneous discharge is shown in C from a 2 day post TeNT injected slice.

Afterdischarges	Control (%)	5ng/µl TeNT (%)	25ng/µl TeNT (%)	50ng/µl TeNT (%)
CA1 SP	8.00	22.22	50.00	11.76
CA1 SR	3.13	17.65	16.67	0.00
CA3 SP	5.56	23.81	23.81	3.85
CA3 SR	0.00	9.10	10.00	0.00
Mean	4.17	18.20	25.12	3.90

Table 4.1. Evoked afterdischarges in organotypic hippocampal slice cultures. Table to show the percentage of recordings which showed afterdischarges in the different treatment groups and in the different areas across the hippocampus. This data consists of days 2, 8 and 16 grouped together. If afterdischarges were seen then they always occurred in a number of frames and were dependent on reaching a threshold stimulus. This table includes both types of evoked afterdischarges.

Afterdischarges	CA1 str. pyramidale alone	CA1str. radiatum alone	Both CA1 strata pyramidale and radiatum	CA3 str. pyramidale alone	CA3 str. radiatum alone	Both CA3 strata pyramidale and radiatum	Both CA1 and CA3
Control	0	0	0	1	0	0	2
5ng/µl TeNT	1	0	0	0	0	1	4
25ng/µl TeNT	1	0	1	1	0	0	4
50ng/µl TeNT	1	0	0	0	0	0	1

Table 4.2. Localisation of evoked afterdischarges within organotypic hippocampal slice cultures. This table indicates the number of slices where evoked afterdischarges were observed in recordings from the different regions. Each slice is only included in one of the columns thus giving a representation of whether individual areas or multiple areas most commonly showed epileptic activity.

4.2.6.2 Spontaneous activity

The spontaneous activity also showed two forms. One consisted of very short lived bursts which lasted usually less than 1 second, and most commonly less than 0.3 seconds (Figure 4.9 panel C). These were similar to interictal spontaneous activity recorded in *ex vivo* slices taken from adult rats that had received intrahippocampal TeNT injections at infancy (Lee *et al.*, 1995; Smith *et al.*, 1998). These could occur up to 5 times within 30 seconds (frame length), but more commonly 1-2 times. The other type showed more prolonged activity that was seen in clusters that ranged in duration from 2-14 seconds (Figure 4.10 panel A). These clusters were seen at a particularly high frequency in three of twenty six recordings that had been made in the CA3 str. pyramidale from slices treated with 50ng/µl TeNT. Here, robust spontaneous seizure-like activity was seen only at 2 days post injection (ten recordings within the CA3 str. pyramidale) (Figure 4.10). TTX was added to these TeNT slices to confirm that what was seen was biological activity and indeed it was. The responses were abolished during the TTX application and when washed out they returned, albeit with fewer clusters per frame (Figure 4.11). In the slice that shows the most robust seizure-like activity, the clusters occurred every 1-2 seconds. In the other two slices the clusters were observed 0-10 times within a 30 second frame. The amplitude of the individual deflections within the clusters most commonly ranged from 0.2-0.3mV. Recordings were also made from these 3 slices at 8 and 16 days post injection but the robust spontaneous seizure-like activity was not seen again, nor any evoked afterdischarges.

Whilst this epileptic activity was seen in three slices treated with the 50ng/µl TeNT, only two other slices treated with this highest concentration showed any epileptic

activity. When it did occur in these two slices is was the spontaneous activity of the much shorter duration (less than 0.3 seconds) and none showed evoked afterdischarges.

There is a greater occurrence of spontaneous activity within 25ng/µl TeNT slices and it varied between the clusters and short bursts (22 of 71 recordings). The repetitive and consistent type clusters that were seen in the three slices from 50ng/µl TeNT slices were not present in slices from any other treatment group. As with the afterdischarges, there was some activity in control treated slices but only in 4 of 122 recordings across all the time points studied. The activity in two of these recordings consisted of the short burst, with durations and amplitudes that were similar to those in TeNT slices, although region and time matched equivalents from TeNT were not available at all concentrations for direct comparison. Within the other recordings, there were periods of spontaneous activity that ranged from 4-10 seconds and these consisted of larger overall amplitudes than see in TeNT slices. Only 8 of these long spontaneous bursts were seen within the 15 frames used for analysis. The 5ng/µl TeNT slices only showed spontaneous activity in 10 of 78 recordings, which suggests that the afterdischarges predominate slightly at this lower concentration.

The spontaneous activity occurred in recordings regardless of the stimulus given, contrasting to that of afterdischarges. Table 4.3 shows the percentages of slices that displayed spontaneous activity. As with the afterdischarges, the 25ng/µl slices show the most spontaneous activity. Table 4.4 shows the localisations of the spontaneous activity. The most widespread activity is seen in the 25ng/µl TeNT treated slices, where the majority of slices show spontaneous activity in both the CA1 and CA3. The

spontaneous activity within slices treated with 50ng/µl TeNT is focussed mainly within the CA3 str. pyramidale.

Overall, grouping all the treatments together showed that spontaneous activity was most commonly seen at 2 days point injection but evoked afterdischarges at 16 days post injection (data not shown). However, with such low incidences of this activity, statistical analysis has not been carried out.

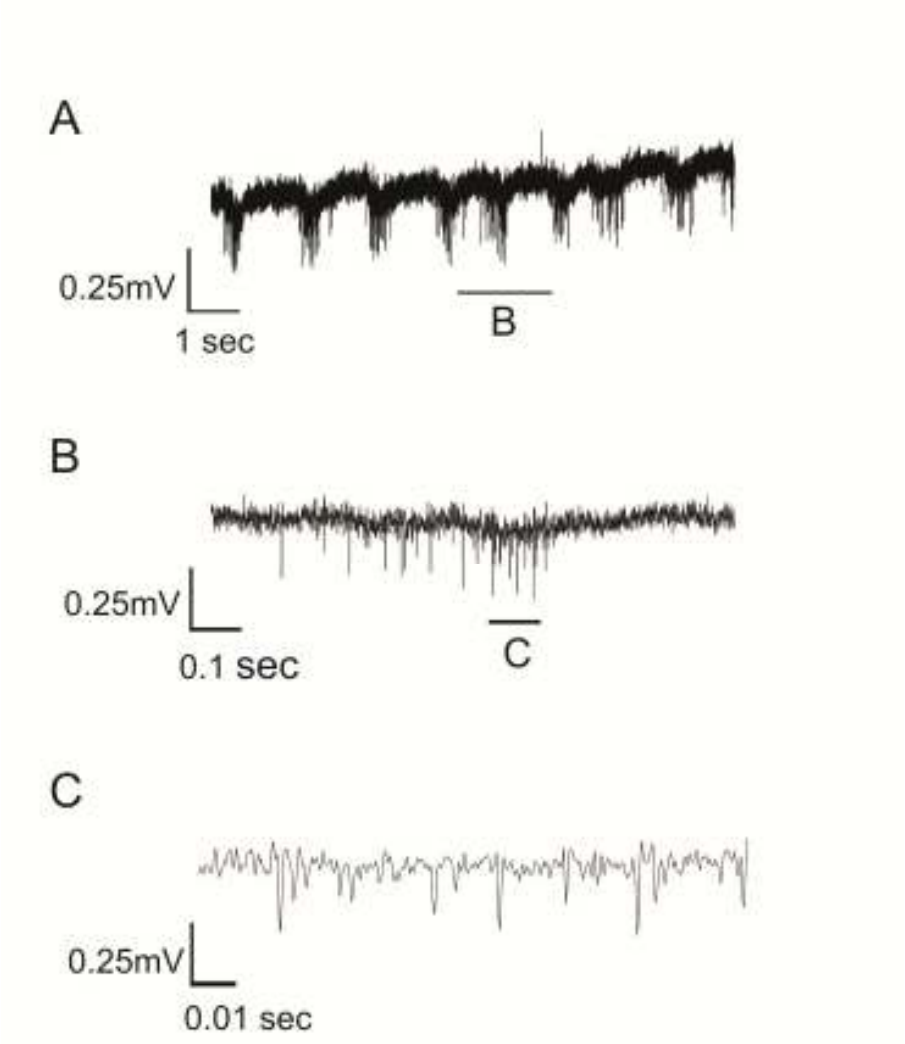

Figure 4.10. Seizure-like activity in organotypic hippocampal slice cultures. The top panel shows spontaneous seizure-like activity within the CA3 str. pyramidale of a slice culture injected with 50ng/µl and recording made at 2 days post injection. This was taken during 10 seconds following a stimulus of 50V to the CA3 str. radiatum. Panel B shows the corresponding portion from panel A expanded, and similarly for panel C.

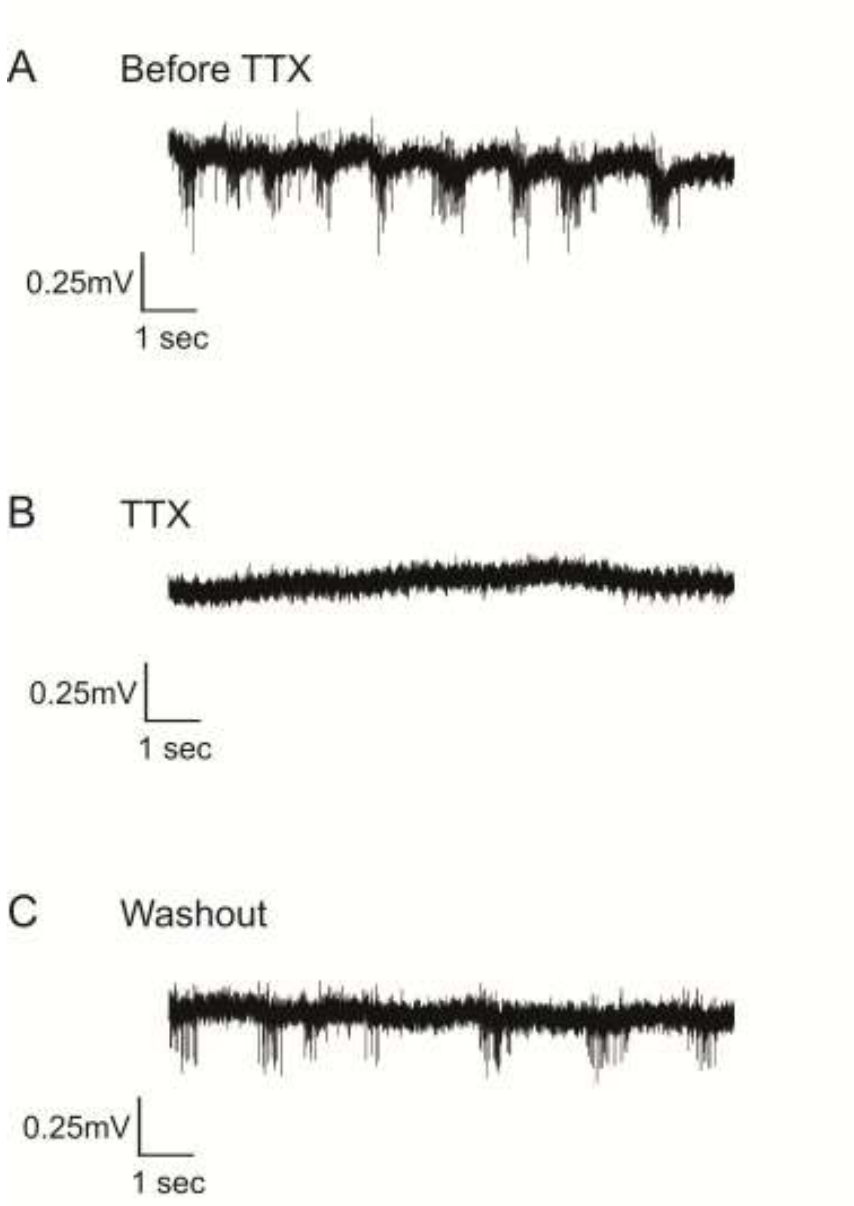

Figure 4.11. Seizure-like activity abolished by TTX. These panels show the spontaneous seizure-like activity (A), followed by the addition of TTX to the ACSF (B) which abolished seizure-like activity. After washout (C) the seizure-like activity returned. These traces are from the same slice as shown in Figure 4.10 (50ng/µl at 2 days post injection) but with a stimulation of 40V given every 30 seconds throughout the addition of TTX and washout.

Spontaneous	Control (%)	5ng/µl TeNT (%)	25ng/µl TeNT (%)	50ng/µl TeNT (%)
CA1 SP	0.00	5.56	41.67	11.76
CA1 SR	3.13	17.65	33.33	0.00
CA3 SP	2.78	9.52	28.57	11.54
CA3 SR	6.901	18.18	25.00	4.17
Mean	3.20	12.73	32.14	6.87

Table 4.3. Spontaneous activity in organotypic hippocampal slice cultures. Table shows the percentage of recordings which showed spontaneous activity in the different treatment groups and in the different areas across the hippocampus. This data consists of days 2, 8 and 16 grouped together. When spontaneous activity occurred, it appeared in many frames (each 30secs long) and was not dependent on the stimulus strength. This table includes spontaneous activity whether short bursts or clustered.

Spontaneous	CA1 str. pyramidale alone	CA1 str. radiatum alone	Both CA1 strata pyramidale and radiatum	CA3 str. pyramidale alone	CA3 str. radiatum alone	Both CA3 strata pyramidale and radiatum	Both CA1 and CA3
Control	0	0	0	0	2	0	1
5ng/µl TeNT	0	1	0	1	2	0	2
25ng/µl TeNT	0	2	0	1	1	1	5
50ng/µl TeNT	2	0	0	4	1	0	0

Table 4.4. Localisation of spontaneous activity within organotypic hippocampal slice cultures. This table indicates the number of slices where spontaneous activity was observed in recordings from the different regions. Each slice is only included in one column which indicates whether individual areas or multiple areas are most commonly exhibiting epileptic activity.

4.2.7 Summary of the effects of different concentrations of TeNT on field recordings up to 16 days

The results from the field recordings show that treatment with the highest two concentrations of TeNT, 25 and 50ng/µl, cause decreases in the maximal sizes of responses in both the CA1 and CA3 strata pyramidale and radiatum in comparison to control treated slices. These effects are seen at all three time points for the 50ng/µl TeNT treated slices. The effects of the 25ng/µl TeNT are seen at the first two time points in the CA3 str. radiatum but not until the later two time points in all other regions. The effects of the lowest dose of toxin are only seen in the CA3 and at the earliest time point. This suggests that the higher concentration of the toxin has an earlier, longer lasting and more widespread effect. This has also been shown after *in vivo* intrahippocampal TeNT injections (Mellanby *et al.*, 1977).

It is interesting to see that epileptic activity is seen in a variety of forms in the different slices and is most prominent at the middle TeNT concentration. The robust seizure-like activity however was only seen in the highest dose of toxin and at the earliest time point.

4.3 Investigation into the effects of TeNT on the distribution of VAMP1 and VAMP2 immunopositivity within organotypic hippocampal slice cultures.

Having collected electrophysiological recordings from the hippocampal slice cultures treated with control or different concentrations of TeNT, we can now look at the effects that the toxin had on the VAMP1 and VAMP2. Considering that there are significant changes in synaptic transmission and observations of epileptic activity within the different areas following TeNT treatment that are concentration dependent, it questions whether effects on VAMP1 and VAMP2 may also be dependent on the concentration used. The results of the immunohistochemistry in Chapter 3 showed that VAMP1 and VAMP2 were both cleaved in *ex vivo* slices in a temporal and spatial manner. At 2 days post injection there were very focal effects that spread to include a wider area by day 8 and continued to be present at day 16, although with a different profile for the two different isoforms. In this section we consider the presence and extent of VAMP1 and VAMP2 cleavage in the organotypic hippocampal slice cultures following focal treatment with the toxin and control solutions. This will allow comparisons of the two models in relation to the immunohistochemistry. It will also allow any correlations with the electrophysiological responses to be made.

The first part of the following section gives an overview of the immunostaining of VAMP1 at a low magnification. The later sections will look at higher magnification within the slices to give a more detailed representation of the effects of the toxin across the slice cultures and allow for quantitative analysis. These will then be repeated to consider the VAMP2 immunopositive slices.

4.3.1 Distribution of VAMP1 immunopositivity within control slices at low magnification

The staining distribution across the hippocampal slice cultures in control treated slices shows a layer specific distribution, but less clear differentiation between layers than in the *ex vivo* slices (Figure 4.12, top row). The darkest area, showing a mostly immunonegative layer, is the granule cell layer of the dentate gyrus. Adjacent to this is the molecular layer which is also quite dark. The str. pyramidale is a darker region which runs through the strata radiatum and oriens, the brightest regions of the slice which show a large immunopositive population. The str. pyramidale is not always very clear throughout its length at low magnification.

4.3.2 Distribution of VAMP1 immunopositivity within TeNT treated slices at low magnification

The other images shown in Figure 4.12 are representations of the staining at each TeNT concentration. In some cases there are variations between the effects seen in slices from within the same group. This was also the case when using *ex vivo* slices.

The 5ng/µl slices (Figure 4.12 row two) show overall immunostaining that is similar to that of the control slices. The granule cell layer remains the darkest area and generally the strata radiatum and oriens of the CA1 and CA3 are of similar intensities. The 25ng/µl TeNT slices (Figure 4.12 row three) however show some differences to the control slices, particularly at 2 days post injection. Here, much of the CA1 has darkened to a level that is of similar intensity to the molecular layers of the dentate gyrus, indicating a cleavage of the VAMP1 within the CA1. The brightest area is part of the CA3. At all three time points the differentiation between the granule cell layer of the dentate gyrus and the surrounding areas is less clear than in control

sections, suggesting that there may have been an overall decrease of the VAMP1 immunopositivity following treatment with this concentration of toxin.

The 50ng/µl TeNT treated slices (Figure 4.12 row four) show a darkening of much of the CA3 layer to intensities similar to the dentate gyrus at 2 days post injection in 3 of the 5 slices. The other two slices show immunostaining that at this magnification does not appear affected. At 8 days post injection all 5 slices show a darkening around the CA3 area. By day 16 the effects are smaller and localised just around the edge of the dentate gyrus into the CA3 but are still present.

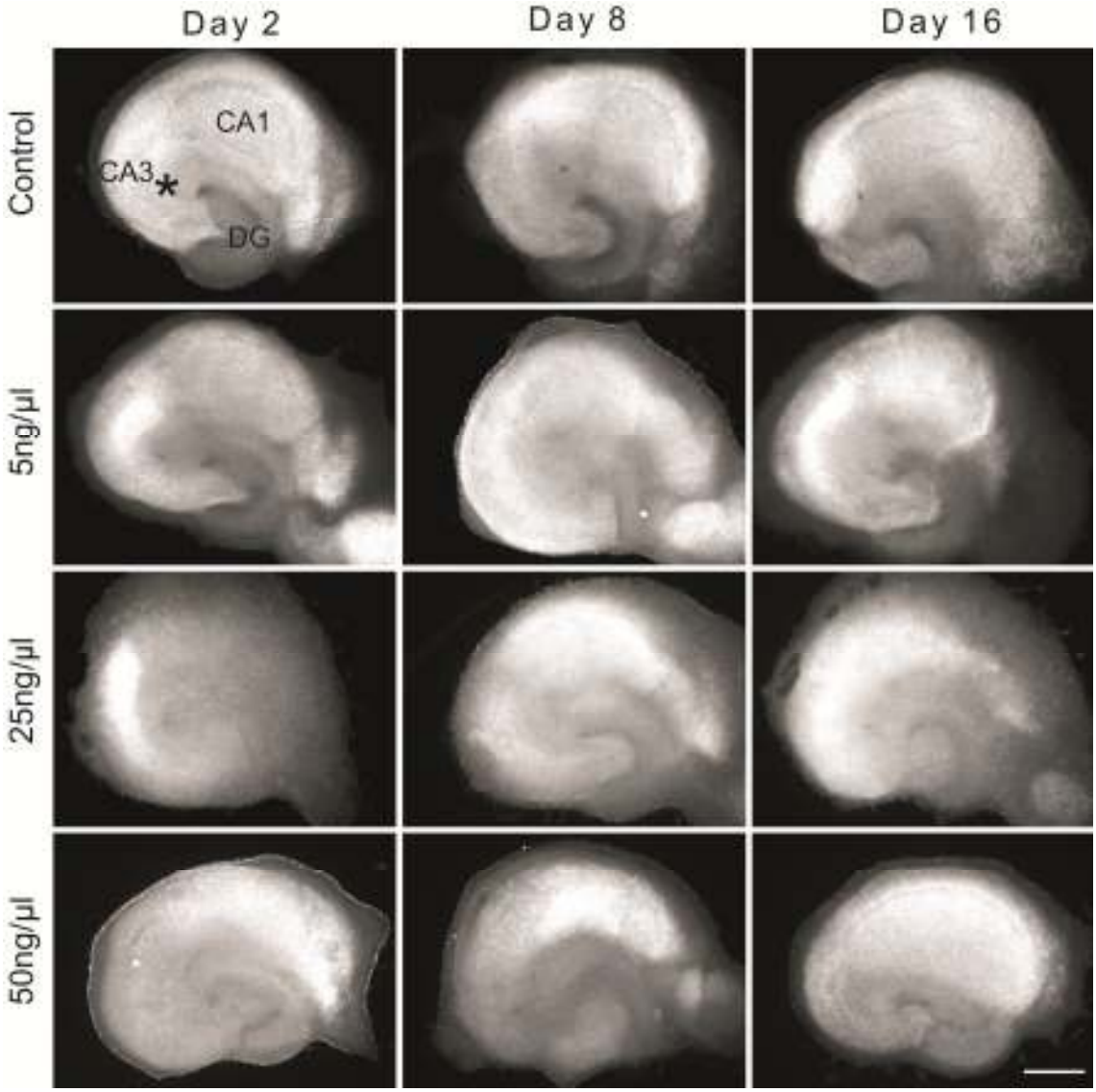

Figure 4.12. VAMP1 immunopositive organotypic hippocampal slice cultures. These VAMP1 immunopositive organotypic hippocampal slice cultures are from control and 5, 25 and 50ng/µl TeNT slices at 2, 8 and 16 days post injection. Staining within control slices is consistent across the three time points but variations occur within toxin treated slices. The injection site is represented by an asterisk and applies to all images. Scale bar represents 400µm.

4.3.3 High magnification investigation of VAMP1 immunopositive boutons and the effects of different TeNT concentrations

Having looked at the low magnification images of the VAMP1 immunopositive slices, we shall now look at high magnification images to consider the boutons present and whether the effects of the toxin can be seen at this level in the different areas and at the different time points. This will give a better representation of the effects of the toxin at different doses. As with the slices from those animals injected *in vivo* (Chapter 3), these data together with the electrophysiology allows consideration of the functional effects of the toxin when injected in hippocampal slice cultures.

The analysis method for the bouton counts within slice cultures had to be adapted from that used in the *ex vivo* slices. The reasons for this have already been discussed in the Materials and Methods (Chapter 2). The analysis in this section uses the thresholding tool within ImagePro to specify only those bright objects that are considered to be boutons (see Materials and Methods, Chapter 2). There is a clear distinction between the appearance of boutons and background noise based on the clusters of pixels that are present. The area that is occupied by the VAMP1 or 2 immunopositive boutons is calculated within the relevant area of interest (AOI): 15x60μm within the str. pyramidale or six AOIs (10x10μm) placed randomly throughout the image in the str. radiatum. A value showing a larger area within the following sections shows a greater immunopositivity than images that show a very small area occupied by VAMP immunopositive boutons.

In this section, all comparisons are made with a t-test unless stated and the significance criterion has been corrected for multiple comparisons using the Bonferroni correction. For comparisons made of the time points within individual

treatment groups the significance criterion has been lowered to 0.0167 (as 3 tests will be carried out). The criterion for comparing the treatments within a time point have been lowered to 0.0083 as 6 tests will be carried out.

4.3.3.1 CA1 str. pyramidale

Figure 4.13 shows representations of the VAMP1 immunopositive boutons within the CA1 str. pyramidale and the corresponding bouton area for all slices. There were no significant differences between the values at the three time points within control or TeNT treated slices (graph in Figure 4.13). A comparison of the treatments within the individual time points highlights a significant decrease in the area covered by VAMP1 immunopositive boutons in the 50ng/µl TeNT slices in comparison to controls and 5ng/µl slices ($p=0.005$ and $p=0.003$ respectively) at 2 days post injection. At day 8, the area is significantly lower in 25ng/µl versus 5ng/µl slices ($p=0.003$) but there are no differences at the day 16 time point.

4.3.3.2 CA1 str. radiatum

Figure 4.14 shows images from the CA1 str. radiatum of VAMP1 immunopositive slices from all treatments. Comparisons of the different time points within the individual treatments show that there are only differences between the day 2 and 16 time points within slices treated with 5ng/µl TeNT ($p=0.015$). Other than this, there are consistent areas covered by the boutons at the three time points within individual treatments.

When comparing the different treatments, there are clear differences at all three time points. At day 2, both control and 5ng/µl slices show larger area values than the 50ng/µl slices ($p=<0.001$ in both cases). The 5ng/µl also has a significantly larger area than the 25ng/µl slices ($p=0.002$). The control slices at day 8 continue to show a larger area than 50ng/µl slices ($p=0.005$) as well as those treated with 25ng/µl TeNT ($p=0.002$). At day 16, the 5ng/µl slices show a smaller area than the controls ($p=0.008$) suggesting a later occurring effect in this lowest toxin dose.

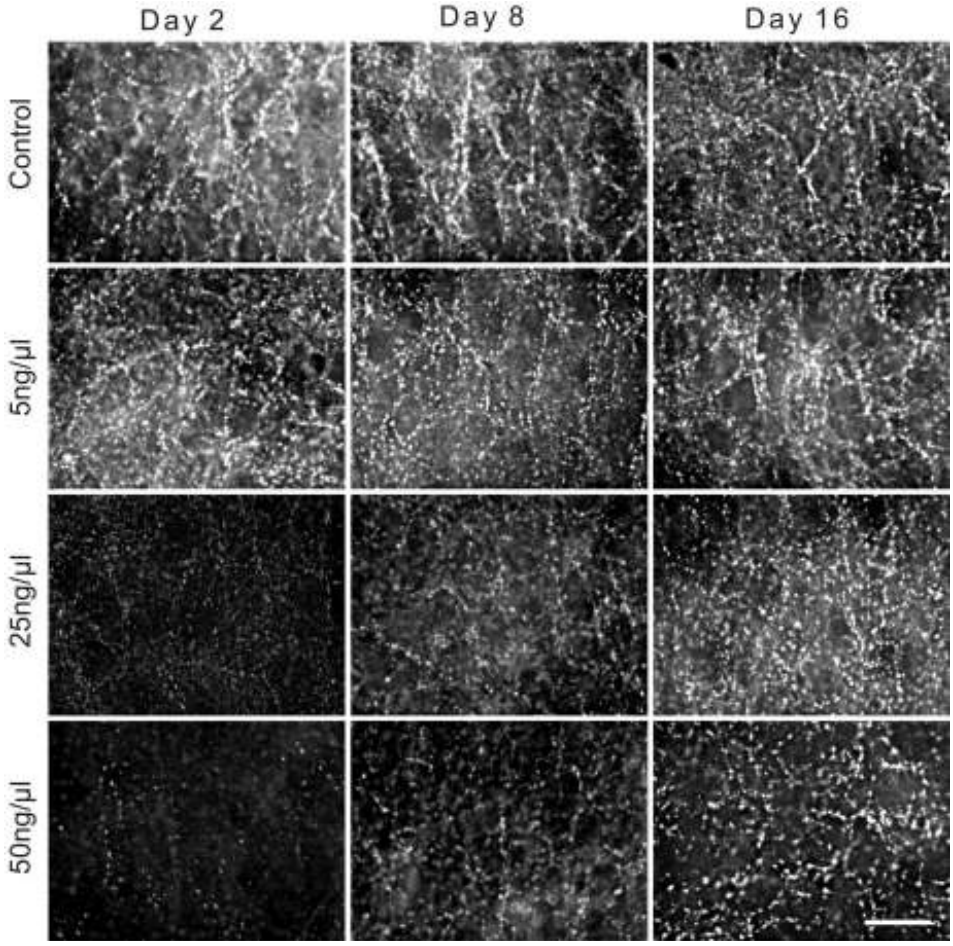

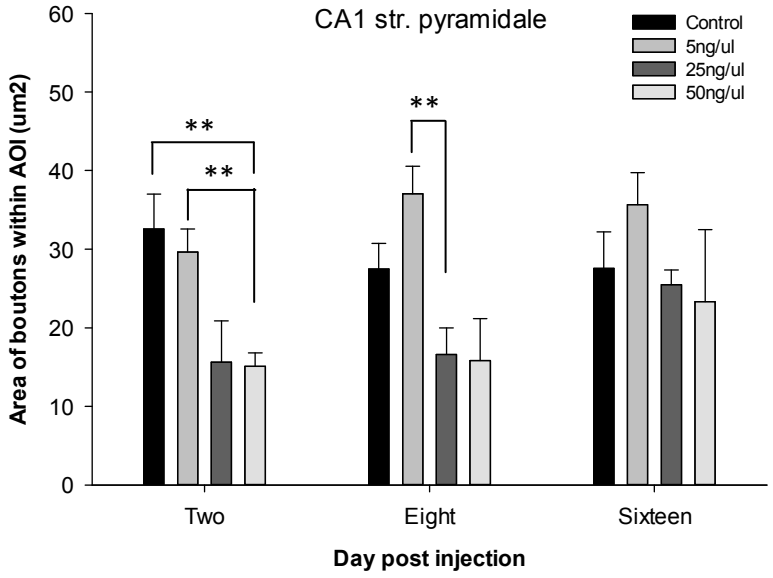

Figure 4.13. VAMP1 immunopositive boutons in CA1 str. pyramidale. Examples of high magnification images at 2, 8 and 16 days post injection from the different treatment groups. The graph shows the area occupied by VAMP1 immunopositive boutons within the area of interest (AOI; 15x60µm) at each of the time points and

treatments. Data plotted as mean ± SEM and the number of slices in each condition was 4 or 5. ** indicates p=<0.01. Scale bar represents 20μm.

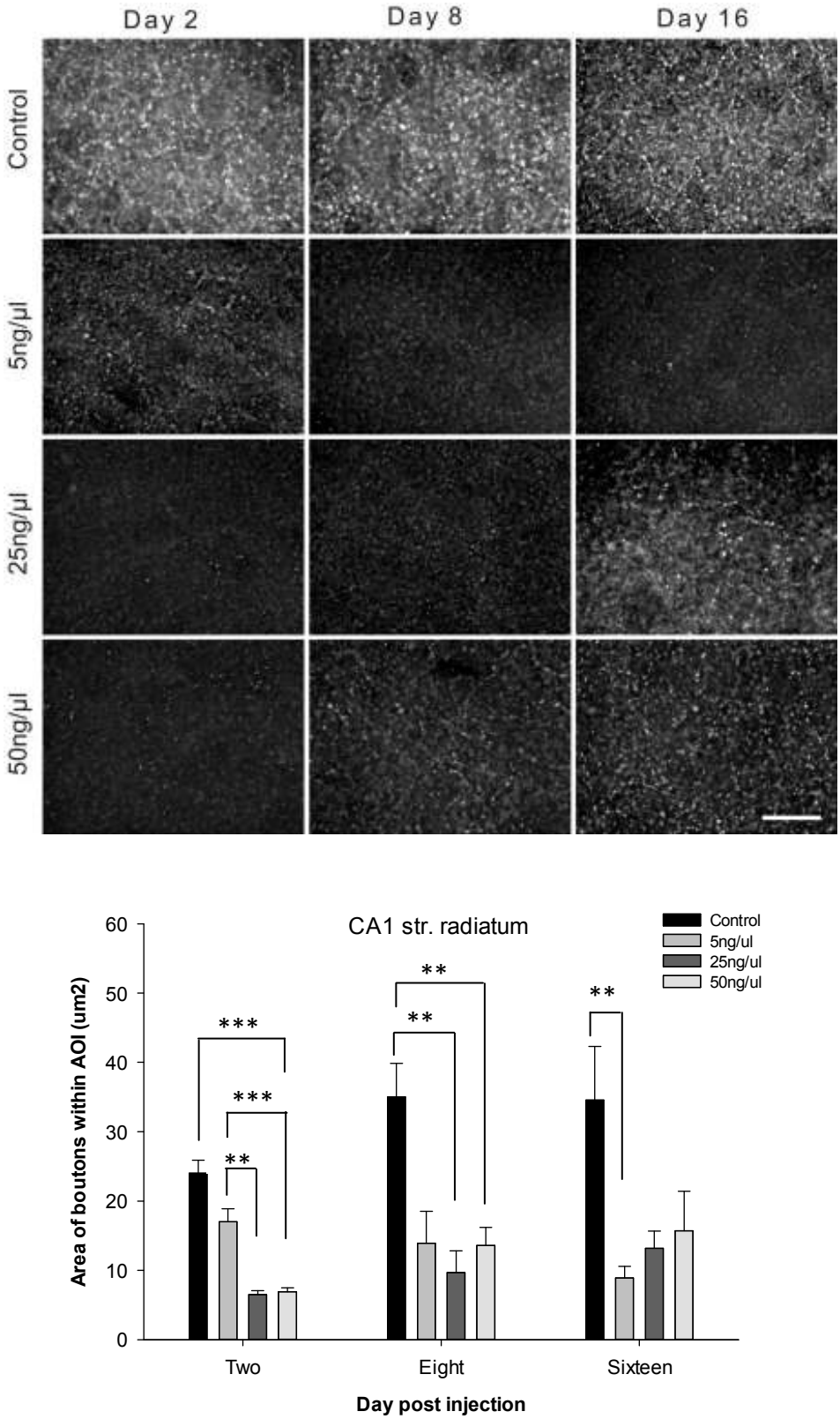

Figure 4.14. VAMP1 immunopositive boutons in CA1 str. radiatum. High magnification images with associated graph showing the areas occupied by VAMP1

immunopositive boutons within six AOIs (10x10μm) positioned randomly across the image. Data includes each of the time points and the individual treatment groups. Data plotted as mean ± SEM and the number of slices for each group was 4 or 5 with the exception of control day 2 which was 3. ** shows p=<0.01 and *** indicates p=<0.001. Scale bar represents 20μm.

4.3.3.3 CA3 str. pyramidale

High magnification images of the CA3 str. pyramidale VAMP1 positive boutons are shown in Figure 4.15. As was the general trend in the CA1, there are no differences between the three time points within each treatment group in the CA3 str. pyramidale. Although there are large differences between the controls and the higher two concentrations of TeNT slices at 2 and 8 days post injection, the differences are not significant. This is likely due to a large variation and a low sample number in the control group (n=3) for the day 2 data. At day 8 however, the 5ng/µl slices show a larger VAMP1 immunopositive area compared to both the 25 and 50ng/µl TeNT slices ($p=0.001$ and $p=0.002$ respectively). There are no differences at day 16.

4.3.3.4 CA3 str. radiatum

The bouton counts at the different time points with the CA3 str. radiatum show that within the controls and the three different TeNT concentrations there are no differences. Whilst there are no differences between the treatment groups at 2 and 16 days post injection, the controls show a significantly larger area than the 25 and 50ng/µl TeNT slices at day 8 ($p=0.008$ in both cases, Mann Whitney Rank Sum) (Figure 4.16). The lack of significant differences between the control and different TeNT concentrations at day 2 is likely due to the low sample number of the controls (n=3) as in the CA3 str. pyramidale.

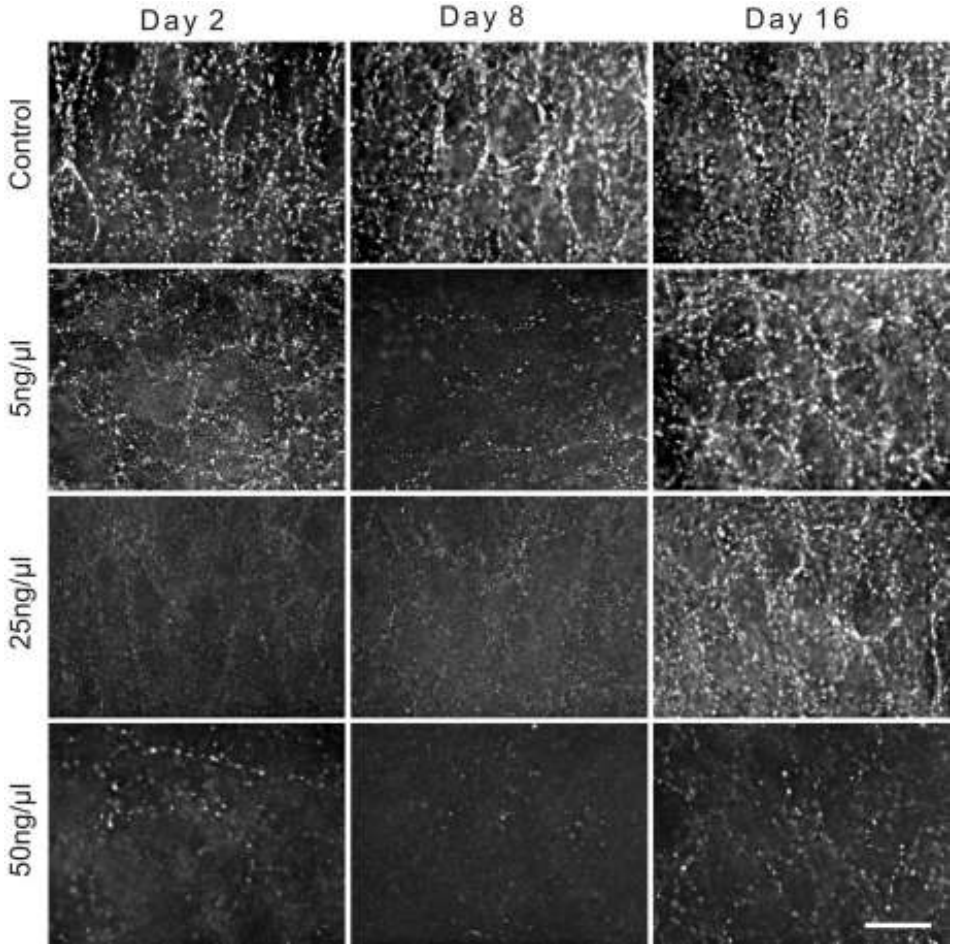

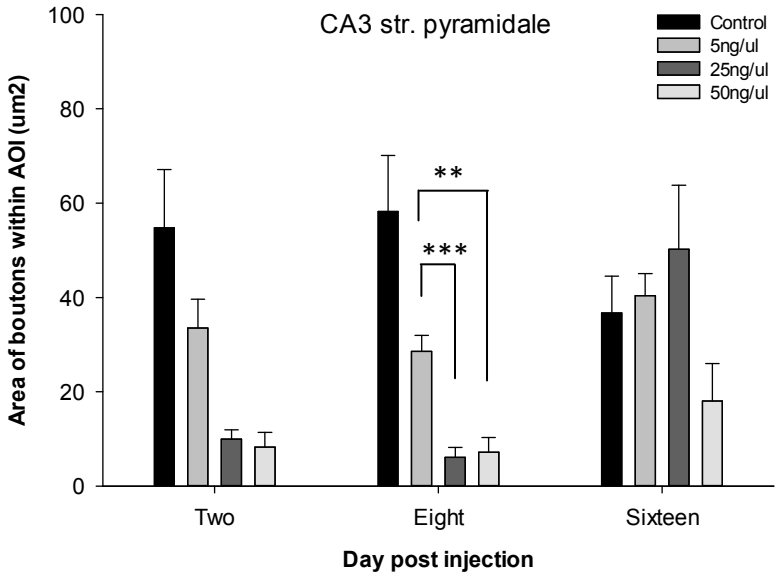

Figure 4.15. VAMP1 immunopositive boutons in CA3 str. pyramidale. High magnification images to show the boutons in each of the treatment conditions and at

2, 8 and 16 days post injection. The area of VAMP1 immunopositive boutons within a 15x60μm AOI are shown within the graph. Data plotted as mean ± SEM. The number of slices was 4 or 5 in each group, with the exception of control day 2 which was 3. ** shows p=<0.01 and *** indicates p=<0.001. Scale bar represents 20μm.

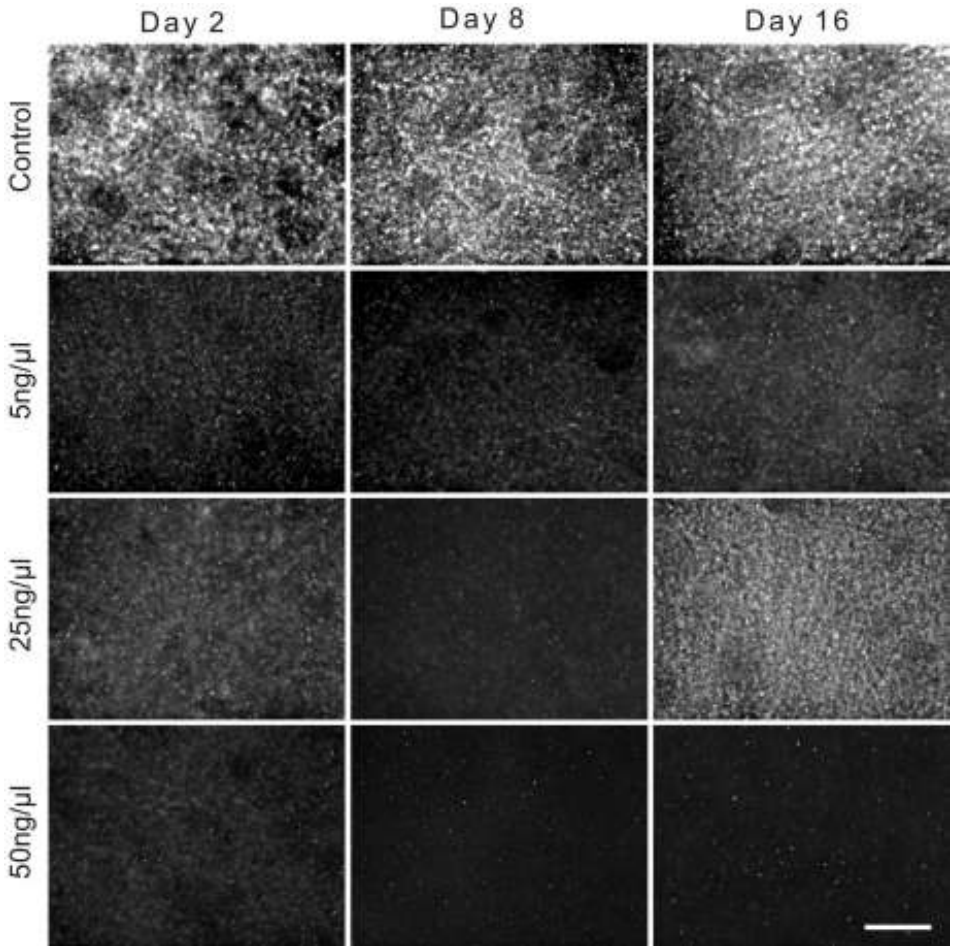

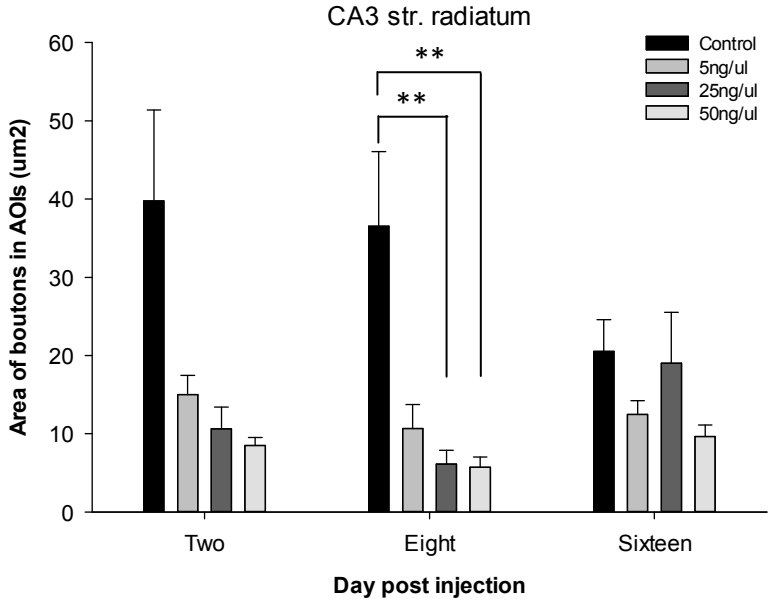

Figure 4.16. VAMP1 immunopositive boutons in CA3 str. radiatum. High magnification images showing boutons at the different time points and within the different treatment

conditions. The associated graph shows the area occupied by VAMP1 immunopositive boutons in six AOIs (10x10μm) positioned randomly across the image. Data plotted as mean ± SEM. The number of slices was 4 or 5 in each condition, with the exception of control day 2 which was 3. ** shows p=<0.01. Scale bar represents 20μm.

4.3.3.5 Summary of the effects of TeNT on the different areas of the slice culture in VAMP1 immunopositive slices

Across all the areas of the hippocampus, the main effects of the toxin are focussed at 8 days post injection. Interestingly, effects at day 2 were only seen in the CA1 (both strata pyramidale and radiatum). The 50ng/µl TeNT concentration shows the most effects, indicated by the smallest areas covered by VAMP1 immunopositive boutons, with the 25ng/µl closely behind. Very few differences are seen between controls and 5ng/µl TeNT, and when this does occur (CA1 str. radiatum), it only occurs at the latest time point studied suggesting that the lower dose of toxin requires a longer incubation to cause a significant difference from controls.

4.3.4 Distribution of VAMP2 immunopositivity within control slices at low magnification

The slice cultures showing VAMP2 immunopositivity shall now be investigated. It was shown in Chapter 3 that robust changes in VAMP2 immunopositivity occurred across the hippocampus of TeNT treated animals, with most changes seen at 8 and 16 days post injection.

The lowest immunosignal within the control hippocampal slice cultures stained with the antibody against VAMP2 is from the granule cell layer of the dentate gyrus and the str. pyramidale of the CA3 and CA1 (Figure 4.17, top row). Whilst the granule cell layer is clearly visible, the str. pyramidale can be less clear in some slices at low magnification. This layer of the CA1 often spreads into a wider layer than the granule cell layer. The str. radiatum and str. oriens are bright areas, as are the molecular layers of the dentate gyrus.

4.3.5 Distribution of VAMP2 immunopositivity within TeNT treated slices at low magnification.

Looking at the 5ng/µl TeNT treated slices, it can be seen that the hilus and the str. lucidum become very bright, particularly at 2 and 8 days post injection (Figure 4.17 row two). This was also seen in *ex vivo* slices from TeNT injected animals. These layers in the control slices are not seen as such a contrast to the surrounding layers.

The day 2 slices of the 25ng/µl TeNT group (Figure 4.17 row three) show some variations. Three slices show staining that is comparable to control slices but the other 3 show a darkening within the CA3 area. The day 8 and 16 groups again show the brightening of the mossy layer and hilus, although this may stretch into the CA3

str. pyramidale as well. There is some darkening of the surrounding layers which was not seen in all the 5ng/µl slices even when a brightening of the str. lucidum was seen.

The 50ng/µl TeNT treatment group (Figure 4.17 row four) shows that at 2 days post injection the bright mossy layer is not apparent but that overall the contrast between the different layers is not very clear at all, suggesting an overall decrease in VAMP2 immunosignal. The day 8 and 16 slices again show the brightening of the mossy layer and also a decrease in the immunopositivity of the surrounding layers.

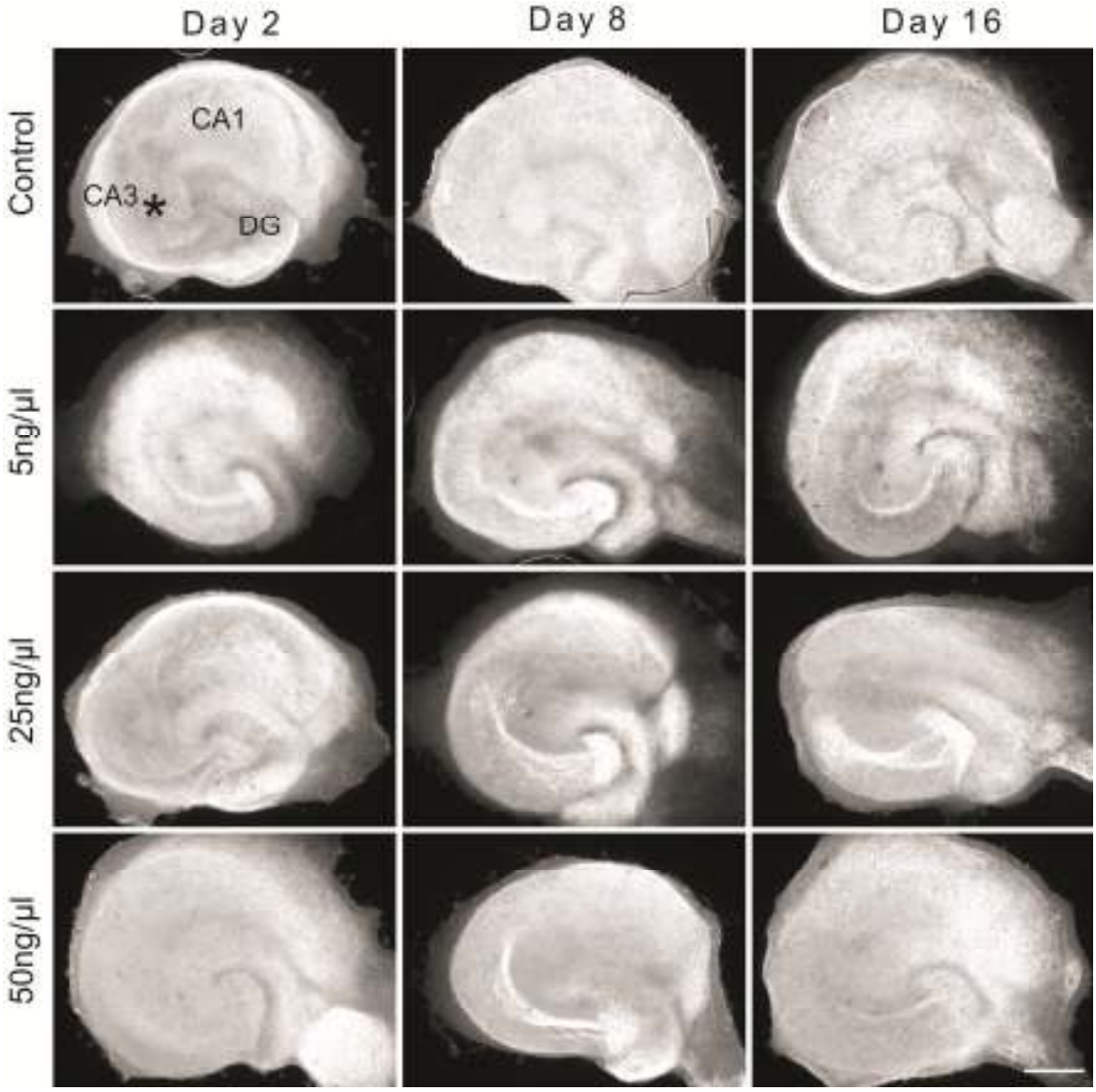

Figure 4.17. Organotypic hippocampal slice cultures immunostained with antibody against VAMP2. Low magnification fluorescent images of VAMP2 immunostained organotypic hippocampal slice cultures treated with injection to the CA3 SR (asterisk) of control solution or 5, 25 or 50ng/µl of TeNT solution. Control slices show consistent staining across the three time points but variations are seen within the different TeNT concentrations. Scale bar represents 400µm.

4.3.6 High magnification investigation of VAMP2 immunopositive boutons and the effects of different TeNT concentrations

As with the VAMP1 immunopositive slices, the area occupied by the VAMP2 immunopositive boutons shall be used as a measure of the effects of the toxin within slices injected with different concentrations of TeNT and compared with those of control slices.

4.3.6.1 CA1 str. pyramidale

The CA1 str. pyramidale shows only minimal changes in these VAMP2 immunopositive slices (Figure 4.18). There is a significantly lower VAMP2 immunopositive area in day 8 compared to day 2 in 25ng/µl slices ($p=0.010$). All other treatment groups show no differences between the time points. At 2 days post injection, the 25ng/µl slices have a larger VAMP2 immunopositive area than slices treated with 5ng/µl TeNT ($p=0.003$). Other than this, there are no significant differences between the other treatment groups at any of the time points.

4.3.6.2 CA1 str. radiatum

Within the CA1 str. radiatum of VAMP2 immunostained hippocampal slice cultures (Figure 4.19) there are also no differences between the bouton counts of the different treatments at any of the time points studied. There are also no differences between the different time points when compared within the individual treatment groups. At 2 and 8 days post injection, this is likely due to the large variation seen within a number of the treatment groups (shown by the large error bars in Figure 4.19).

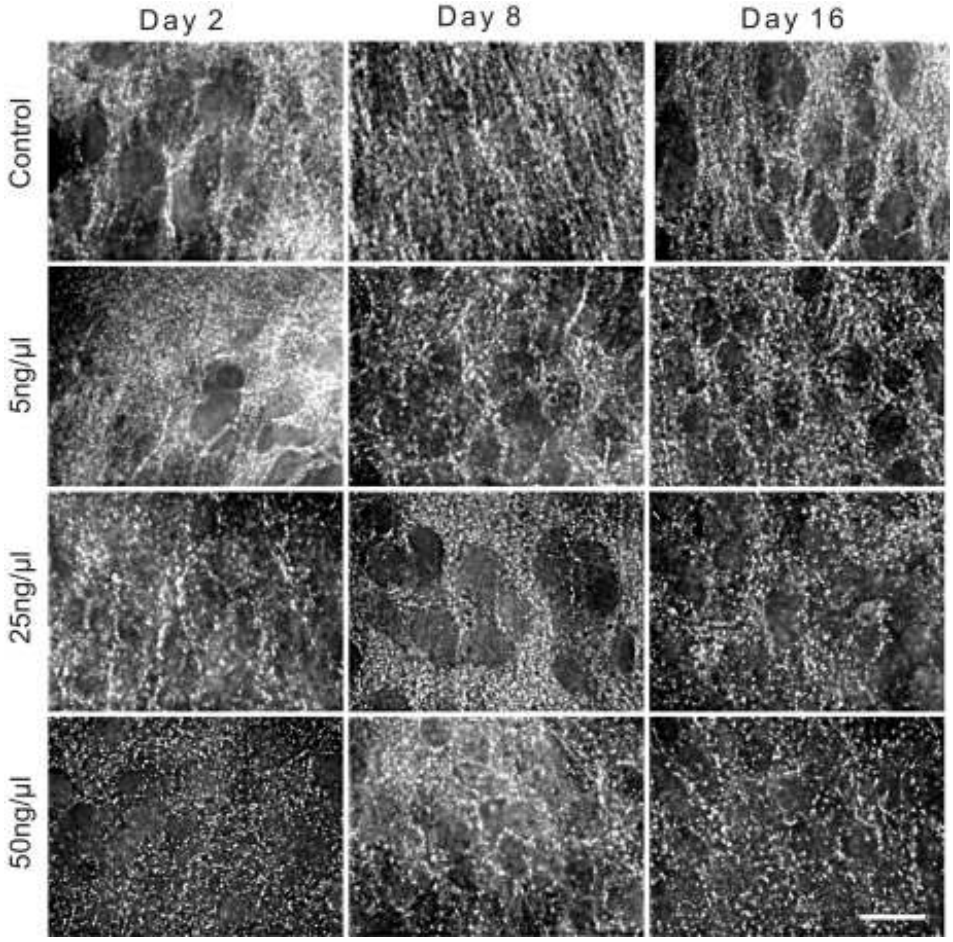

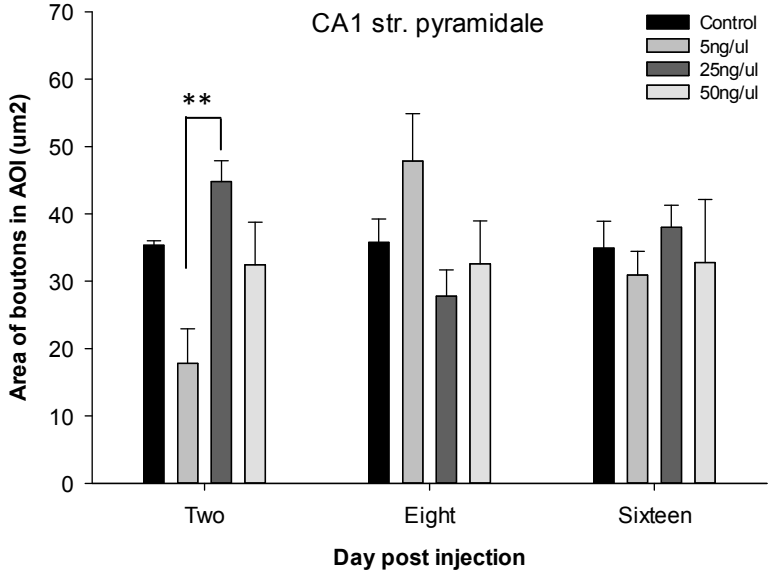

Figure 4.18. VAMP2 immunopositive boutons in CA1 str. pyramidale. High magnification images within the different treatments and time points. The associated

graph shows the area occupied by VAMP2 immunopositive boutons within a 15x60μm area of interest (AOI) placed within the str. pyramidale. Data plotted as mean ± SEM. The number of slices in each group is as follows, with days 2, 8 and 16 listed respectively: Control 6, 4 and 8; 5ng/μl 3, 3, and 4; 25ng/μl 5, 4 and 7; and 50ng/μl 7, 4 and 6. ** shows p=<0.01. Scale bar represents 20μm.

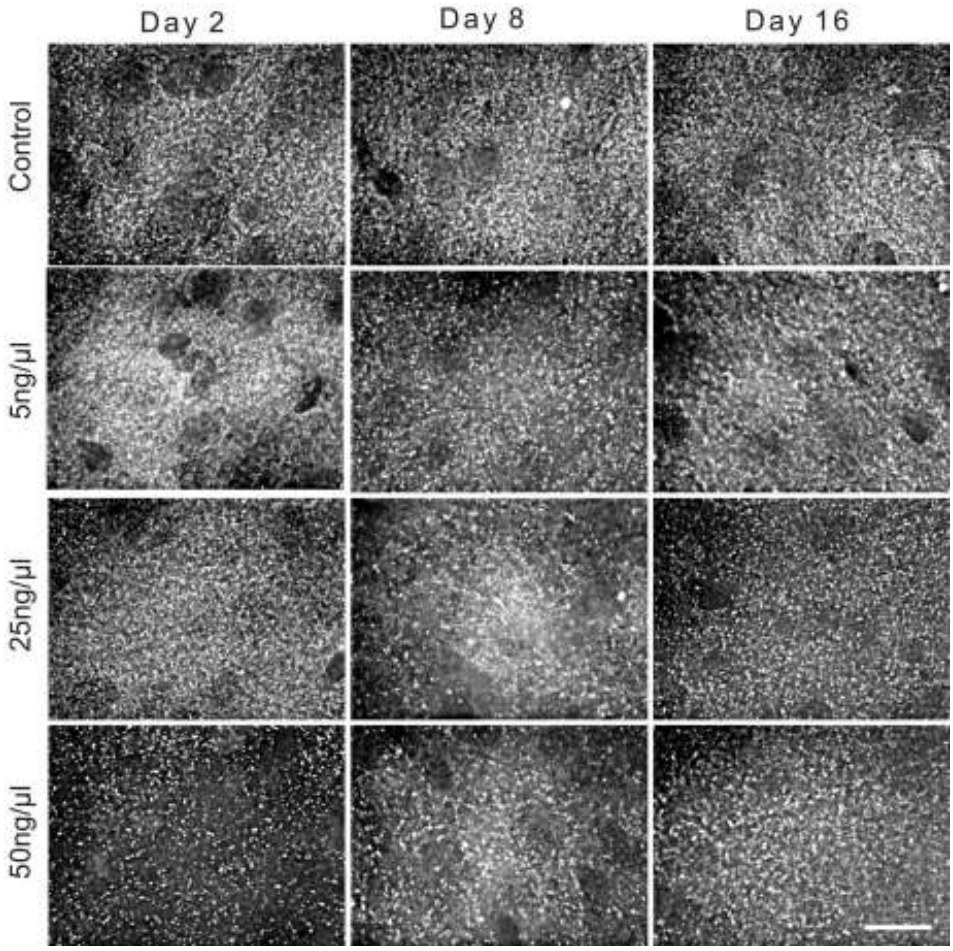

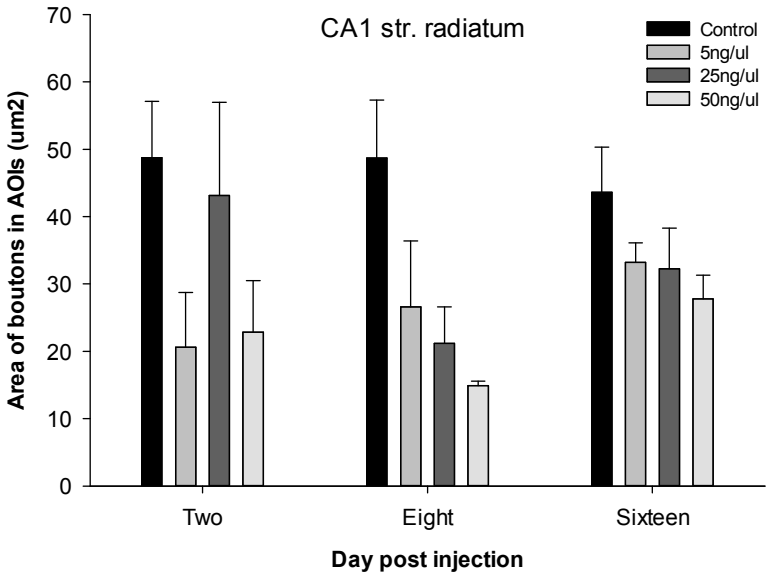

Figure 4.19. VAMP2 immunopositive boutons in CA1 str. radiatum. Images of boutons at high magnification from slices exposed to different treatments and at the three time

points studied. The graph below shows the area covered by VAMP2 immunopositive boutons within six AOIs (10x10μm) randomly positioned within the image. Data plotted as mean ± SEM. The number of slices in each group is as follows, with days 2, 8 and 16 listed respectively: Control 6, 5 and 8; 5ng/μl 4, 3 and 4; 25ng/μl 5, 5, and 7; and 50ng/μl 7, 4 and 6. ** shows p=<0.01 and *** indicates p=<0.001. Scale bar represents 20μm.

4.3.6.3 CA3 str. pyramidale

The CA3 str. pyramidale shows no differences between the time points within individual treatments. However there are large differences between the area occupied by boutons in control slices and those of the different treatments (Figure 4.20). At day 2, the area covered by VAMP2 immunopositive boutons in control slices is significantly larger than all of the 5, 25 and 50ng/µl TeNT slices ($p=<0.001$, $p=0.001$ and $p=<0.001$ respectively). By day 8 however the only difference occurs between control and 5ng/µl slices ($p=0.004$) and by day 16 there are no differences between the treatments, suggesting some recovery from the effects of the toxin.

4.3.6.4 CA3 str. radiatum

Comparisons of the time points within the individual treatment groups show that there are no differences in the area covered by boutons across the length of the study in CA3 str. radiatum of VAMP2 immunostained slices (Figure 4.21). At 2 days post injection, both the control and 25ng/µl slices show larger VAMP2 immunopositive areas than the 50ng/µl slices ($p=0.001$ and 0.003 respectively, Mann Whitney Rank Sum in both cases). No differences are seen at day 8 but at day 16 the difference between control and 50ng/µl slices occurs again, albeit to a lesser extent ($p=0.008$).

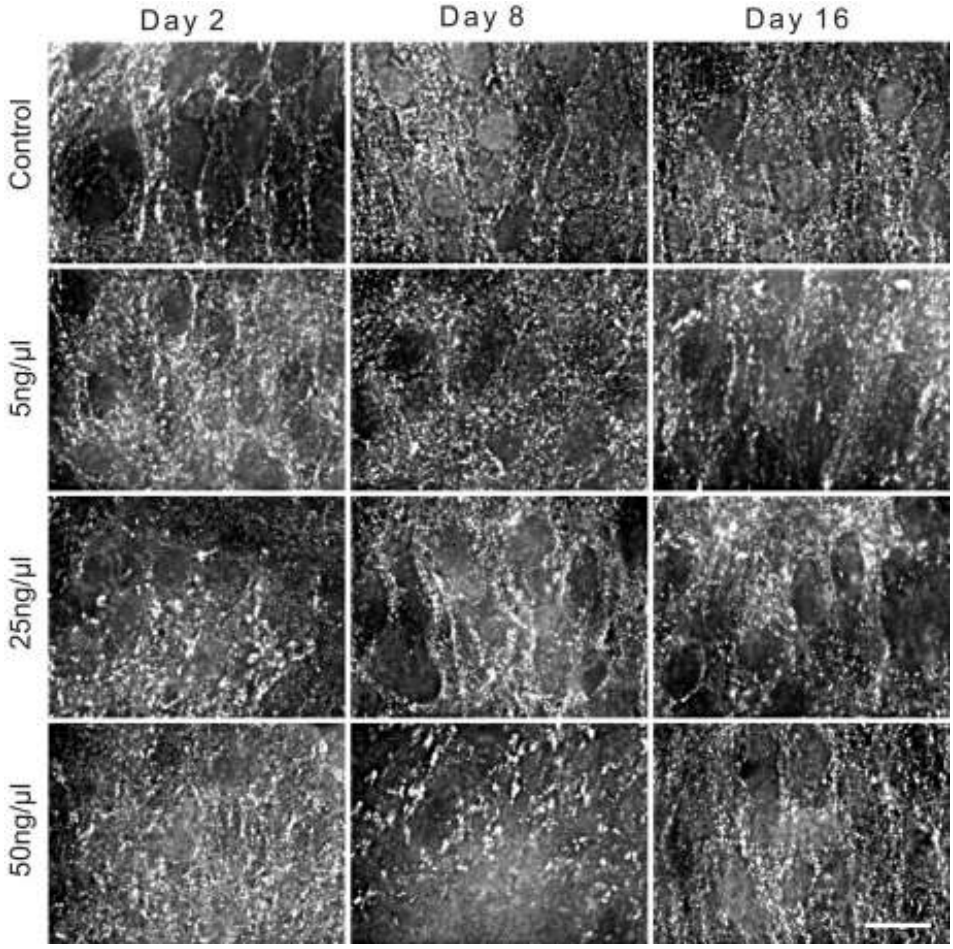

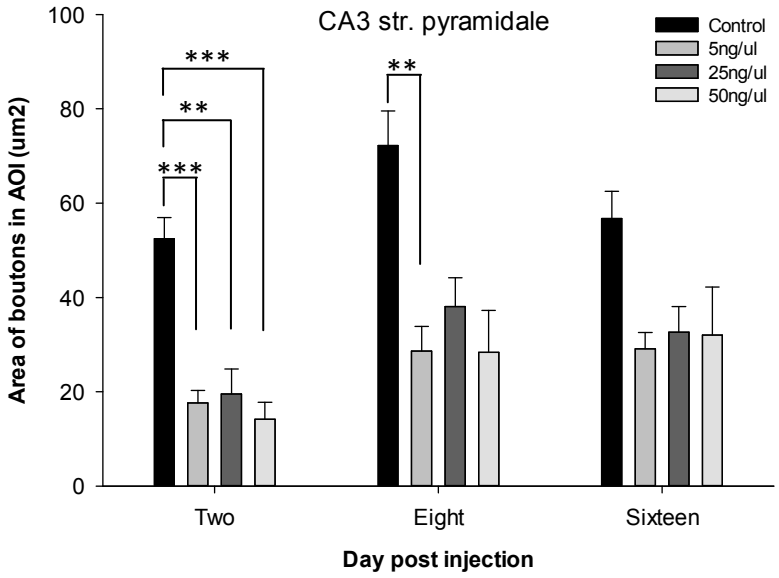

Figure 4.20. VAMP2 immunopositive boutons inCA3 str. pyramidale. High magnification images from the different treatments at days 2, 8 and 16. The

associated graph shows the differences between the area occupied by theVAMP2 immunopositive boutons within a 15x60µm AOI from slices of different treatment groups. Data plotted as mean ± SEM. The number of slices in each group is as follows, with days 2, 8 and 16 listed respectively: Control 6, 3 and 8; 5ng/µl 4, 4, and 4; 25ng/µl 5, 5, and 7; and 50ng/µl 6, 4 and 6. ** shows p=<0.01 and *** indicates p=<0.001. Scale bar represents 20µm.

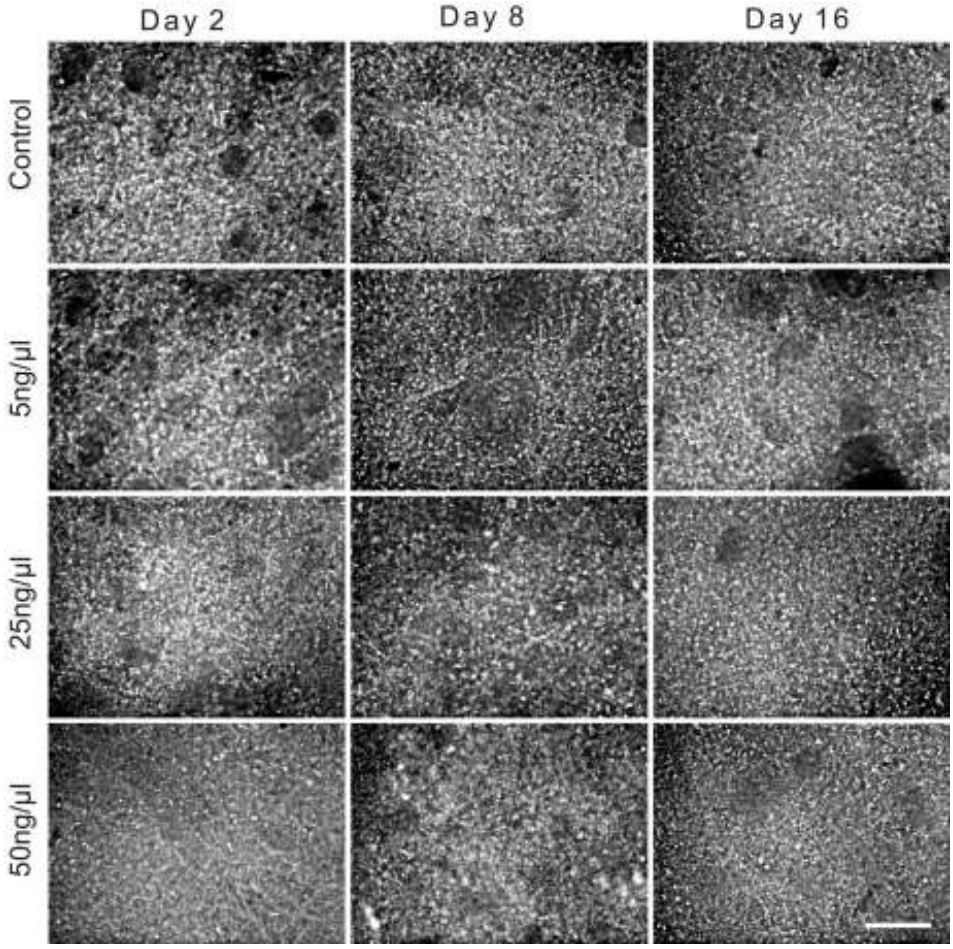

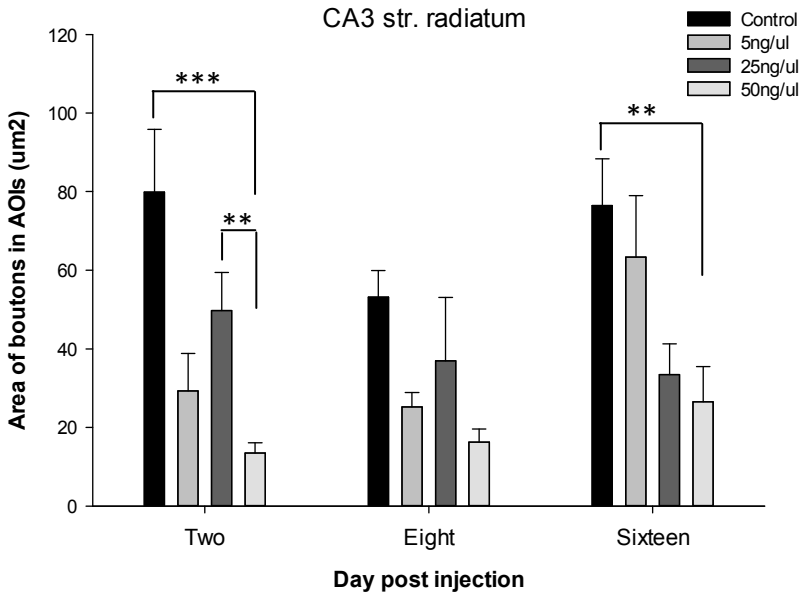

Figure 4.21. VAMP2 immunopositive boutons in CA3 str. radiatum. VAMP2 immunopositive boutons shown at high magnification at days 2, 8 and 16 from the

different treatment groups. The graph below shows the area occupied by VAMP2 immunopositive boutons within six AOIs (10x10μm) placed across the image and the differences between the treatment conditions. Data plotted as mean ± SEM. The number of slices in each group is as follows, with days 2, 8 and 16 listed respectively: Control 6, 5 and 8; 5ng/μl 3, 3, and 4; 25ng/μl 5, 5, and 7; and 50ng/μl 7, 4 and 6. ** shows p=<0.01 and *** indicates p=<0.001. Scale bar represents 20μm.

4.3.6.5 Summary of the effects of TeNT on the different areas of the slice culture in VAMP2 immunopositive slices

In VAMP2 immunopositive slices, the changes in CA1 are minimal, which differs when comparing to the VAMP1 immunopositive slices. Interestingly, again in contrast to the VAMP1 sections, the main effects of the toxin on VAMP2 are focussed at day 2 in the CA3. The 50ng/µl TeNT concentration shows effects that last into the latest time point in the CA3 str. radiatum, an effect not seen in slices treated with the lower two concentrations or in other regions of the hippocampus.

4.4 Summary of the effects of TeNT on organotypic hippocampal slice cultures

Overall, the experiments and results in this chapter have shown that the toxin has robust effects on synaptic transmission and results in epileptic activity in a number of slices, also indicating a concentration dependent effect. The toxin can also be associated with the cleavage of VAMP1 and VAMP2 within these slice cultures. The use of three concentrations of toxin has highlighted differences in the temporal effects as well as the toxins specificity for VAMP1 and VAMP2.

5 DISCUSSION

The effects of TeNT injection, both *in vivo* and *in vitro,* during the first 16 days of the epilepsy model have been shown within the last two chapters. In this chapter, the results shall be considered in relation to the current literature and the impact of the findings will be discussed.

There is a large literature available that focuses on TeNT. This includes comparisons of its effects in the periphery and central nervous system (CNS), the mechanisms of entry into a variety of cells, its actions once within the cell, and the resulting effects that this can have on a system. Constant improvements to experimental methods are allowing more of an understanding of all of these issues, but there still remain a number of discrepancies and un-answered questions that revolve around this toxin and its effects. This is particularly relevant to the understanding of the epileptic syndrome induced by injections of minute amounts of toxin into regions of the brain. The data presented in this thesis goes some way to increasing the understanding of the early stage mechanisms in this chronic epileptic syndrome, however it also raises a number of further questions.

5.1 Temporal and spatial cleavage of VAMP1 and VAMP2 by in vivo TeNT injection

A prominent finding of this study is the evidence of TeNT cleaving both VAMP1 and VAMP2. The extent of the cleavage however differs between the two isoforms and is dependent on the time point studied, the region and position within the hippocampus and the side of the brain relative to injection.

5.1.1 Time course of TeNT effects

5.1.1.1 Ipsilateral hippocampus

A difference in the temporal cleavage of VAMP1 and VAMP2 compared with controls was observed in the ipsilateral hippocampus. This highlighted the minimal cleavage of VAMP2 at 2 days post injection, in contrast with robust changes occurring in the VAMP1 immunostained slices centred around the injection site, as shown by grey level analysis. Significant differences between control and TeNT slices in the ipsilateral hippocampus at 2 days post injection are only seen within the CA3 of VAMP1 immunostained slices. This indicates that whilst changes are seen in other areas, they either do not affect a large enough area or the focal and intense cleavage in a small area is not enough to cause a drastic decrease in the immunosignal that will affect the overall grey level distribution. Whether the initial cleavage of VAMP1 before VAMP2 is due to the uptake of toxin into inhibitory neurons earlier than excitatory neurons is uncertain. Yeh *et al.* (2010) showed differential expression of SV2A and B within the two populations within the cortex (and spinal cord) but without confirmation within the hippocampus we cannot say whether SV2 isoform expression and the subsequent binding of TeNT differs in hippocampal neuronal populations.

Jefferys (1989) showed that slices from animals injected 1-2 days previously had no changes in the electrophysiology. This is supported by minimal changes seen in VAMP expression at this early stage in our experiments, and suggests that the significant focal cleavage in CA3 of VAMP1 positive slices is not enough to cause epileptic activity. A small network of neurons may be affected by the toxin, but the chance of positioning electrodes in this area is minimal. A focal cleavage of VAMP1 may be responsible for the start of the initial epileptogenesis. Here, the beginnings of

a disruption in the inhibition-excitation ratio may take place which over the coming days develops further to include both VAMP1 and VAMP2, ultimately resulting in seizures. Overall this suggests that a threshold level of cleavage of the VAMP1 and/or VAMP2 may exist that must be surpassed before abnormal recordings are observed.

Following the initial cleavage bias towards VAMP1 at day 2, the peak cleavage is also seen at an earlier time point in mid level VAMP1 immunopositive slices compared with VAMP2; day 8 versus day 16 respectively. By day 16, there is some recovery of VAMP1 immunosignal in mid level slices. In posterior sections however, the cleavage of both VAMP1 and VAMP2 does not occur until day 8 onwards and within the time scale of the study, no recovery is seen of either isoform. This suggests that whilst there may be some recovery of the VAMP1 around the injection site by 2 weeks, the direct and/or indirect effects of the toxin may be more focused in the posterior sections at this time point. Electrophysiological recordings within more posterior slices to investigate this in future experiments would provide further information, as well as a longer term immunohistochemical analysis to observe whether the cleavage spreads further into the ventral hippocampus. The delay of the cleavage of VAMP2 within mid level sections may signify that even though recovery occurs focally in VAMP1, the inhibition-excitation ratio is not restored because there is still an imbalance throughout the hippocampus. This may play an important role in the epileptic syndrome as the activation of interneurons may remain disrupted because of the cleavage of VAMP2 in excitatory neurons. This failure of activation of interneurons has been suggested previously, although it has not been correlated with

a direct effect of TeNT on excitatory neurons in these studies (Jordan & Jefferys, 1992; Whittington & Jefferys, 1994; Jefferys & Whittington, 1996).

The ipsilateral bouton analysis from days 8-16 show robust cleavage of VAMP1 and VAMP2 in the strata pyramidale and radiatum of CA3, consistent with the grey level analysis. The CA1c closest to the injection site, shows cleavage of both isoforms in the str. radiatum but only of the VAMP2 in the str. pyramidale. The lack of cleavage in the str. pyramidale of VAMP1 immunopositive slices is likely due to the low sample size that resulted from some difficult images that could not be analysed and the large variation within the slices that were analysed, where two showed robust cleavage whilst the other showed none. As shown in the grey level analysis, there is variation in the extent of the lesion across the time ranges of 8-16 days therefore a sample of three is not enough to draw strong conclusions.

5.1.1.2 Contralateral hippocampus

Within the contralateral side, the effects of the toxin occur later than in the ipsilateral side, and again the VAMP2 cleavage generally lags behind that of VAMP1. However some interesting differences between the ipsilateral and contralateral sides are seen within grey level and bouton analyses. In the grey level analysis of contralateral CA1 of VAMP1 immunostained slices at day 8, there is significant cleavage in TeNT slices at both mid and posterior levels. This suggests transport of the toxin via commissural fibres from the ipsilateral CA3 or CA1 to the contralateral CA1. It is interesting that this effect occurs at the time when the peak effect is also seen in the ipsilateral side (day 8) indicating a wide spread of the toxin's actions. By day 16 this effect is not still observable. Considering that there are commissural fibres from CA3 to contralateral CA3, as well as to contralateral CA1 (Amaral & Lavenex, 2007), it begs the question

of why contralateral cleavage is not seen in the grey level analysis of CA3. The bouton counts however shows opposite results to the grey level analysis. It indicates a significant cleavage of both VAMP1 and VAMP2 in the contralateral CA3 and yet the only significant cleavage in contralateral CA1 is of VAMP2 in the str. pyramidale of CA1c.

High magnification imaging has the potential to reveal details and therefore is more likely to uncover subtle changes in VAMP1 and 2 expression. The layer specific staining of both the VAMP1 and 2 antibodies creates a mixture of brightnesses in the grey level analysis at low magnification. This affects the pixel distribution across the 8 grey levels within individual regions. Layers unaffected by the toxin may dilute the effects in other layers. In the high magnification bouton counts however, an individual layer can be focussed upon and thus subtle changes are more noticeable. The bouton data is from a range of 8-16 days which encompasses the two different time points from the grey level analysis. Given that there are differences between 8 and 16 days in the low magnification images, the bouton counts from a range of days may result in individual differences between the two extremes being lost as the expression of the VAMP isoforms changes across the 8 days included. Where the CA3 contralateral cleavage of either isoform was not detected using the grey level analysis, this may be because only a focal region was affected, and thus was not enough to cause a dramatic shift in the pixel distribution.

5.1.2 Layer specificity of TeNT effects

The low magnification images have shown that there are layers within the hippocampus that are more susceptible to the TeNT than others. This may be due to the neuronal populations present, but most likely due to the connections between

these layers and others, providing easy access or not for the toxin. The str. lacunosum moleculare for example shows a bright immunosignal in VAMP2 immunopositive sections that remains unaffected by the toxin. However, apical dendrites of most CA1 and CA3 pyramidal neurons terminate in the str. lacunosum moleculare where they receive innervations from str. oriens lacunosum-moleculare (O-LM) interneurons (Leao *et al.*, 2012). This would provide a route for the spread of the toxin by retrograde transport to O-LM interneurons which would likely affect the VAMP present in the axons of these interneurons. This would be dependent on the CA1 pyramidal cells containing the toxin however. The str. lacunosum moleculare shows minimal VAMP1 immunostaining, which considering it contains inhibitory synapses is surprising. The presence of VAMP2 however is prominent, suggesting that these interneurons may use VAMP2 instead. However the projection from the entorhinal cortex may account for the high VAMP2 presence (Amaral & Lavenex, 2007; Spruston & McBain, 2007). The lack of cleavage in the str. lacunosum moleculare suggests that the toxin has not spread to include this population of neurons and is also unlikely to have travelled to the entorhinal cortex within the timeframe studied. Longer-term studies looking at 4, 6 and 8 weeks, following the progression of the epileptic syndrome from peak epileptic activity through to remission would identify whether the lesion of VAMP1 and VAMP2 spreads to include the str. lacunosum moleculare within the course of the model. The time point at which it may appear could have important implications for the spread of seizure activity to other regions of the brain.

The clear difference between the populations of neurons in different layers of the hippocampus is particularly highlighted by the effects of the toxin on the outer

molecular layer of the dentate gyrus. Within VAMP1 immunopositive slices, the outer molecular layer appears very dark, showing a low immunosignal. This is in contrast to the inner molecular layer which has a bright immunosignal and within TeNT slices shows cleavage of VAMP1. In VAMP2 immunopositive slices however, both the inner and outer molecular layers have bright immunosignals in control slices and in TeNT slices both layers show a cleavage of VAMP2. This highlights that the neurons within different layers have separate VAMPs present and the cleavage of the relevant VAMP in these layers likely has an impact on the network.

5.1.3 VAMP1 and VAMP2 expression in distinct populations – involvement in epileptic syndrome

The above discussion has shown that there are differential effects of the toxin on the two VAMP isoforms, the position within the hippocampus and the side of the brain relative to the injection. All of these may have an involvement in the generation of the epileptic syndrome, as well as its continuation. Data from our laboratory (unpublished) has shown that VAMP1 and VAMP2 are differentially, but not exclusively, expressed in different populations of neurons within the hippocampus. VAMP1 is seen to co-localise with the marker for inhibitory neurons, whilst VAMP2 is mostly expressed in excitatory neurons. Bragina *et al.* (2010) showed that there were differential co-localisations between various synaptic proteins within the cortex so this phenomenon is not entirely unexpected. However, differences between the populations in the cortex are less distinct than in our observations of the hippocampus. Much of the literature has focused on the effects of the toxin on inhibition, but here we have shown that both inhibition and excitation are likely affected.

5.1.4 Specific observations following high magnification imaging of VAMP immunopositive boutons

The counts of the boutons within the different regions of the ipsilateral and contralateral hippocampi in the different treatment conditions have highlighted aspects which are discussed in the following sub-section.

5.1.4.1 Asymmetry of synaptic protein expression

Asymmetry of the expression of VAMP1 and VAMP2 within the ipsilateral and contralateral hippocampi has been observed at high magnification. The extent of asymmetry varies between the region and the layer within that region. This occurs within control sections, therefore is not a result of TeNT treatment. It is also seen in some regions of TeNT treated slices however. Overall, the differences in the str. pyramidale appear to be focused in the CA3 whereas in the CA1 the differences are within the str. radiatum. It is also noteworthy that the side showing the higher bouton counts is opposite for the two layers: ipsilateral for str. pyramidale and contralateral for str. radiatum. Considering that both the VAMP1 and VAMP2 positive sections show these differences and that the differences vary in the dominant side between the layers, suggests that these are not due to an issue with the analysis or an anomaly. Asymmetry within the brain has been suggested previously in normal healthy rats, however no mention of VAMP1 or VAMP2 specifically has been found. Some groups have focused on the thickness of the hippocampus (Diamond *et al.*, 1982; Diamond *et al.*, 1983) showing a right hippocampus bias in male rats, others have counted the neurons in the principal cell layers (Lister *et al.*, 2006) showing significantly more neurons in the left hand CA1 and CA3 compared with the right. This was also shown in the CA3 of dog hippocampus (Ragbetli *et al.*, 2010). Others have focussed on proteomics (Samara *et al.*, 2011) and gene expression (Moskal *et*

al., 2006) and have shown a majority of a right hand bias. Overall these findings vary, with Diamond *et al.* (1982) showing that the differences were dependent on age, where a smaller difference occurred during sexual maturity which overall continued to decrease with age. If more cells reside in the pyramidal layers of the left (contralateral) hippocampus then that could explain the fewer boutons seen in the CA str. pyramidale regions because a greater amount of the area of interest would be occupied by the cell bodies. An increase in the pyramidal cell numbers in the CA3 and CA1 would account for increases in the density of boutons within the str. radiatum, resulting in increased bouton counts in the contralateral versus ipsilateral hippocampus.

5.1.5 Correlation of bouton analysis and electrophysiological data

The coupling of the electrophysiological and immunohistochemical techniques has allowed for a specific insight into the changes caused by TeNT injections at 8-16 days post injection.

5.1.5.1 Effects of TeNT on evoked neurotransmission in CA1

The observed changes in evoked responses, such as abolition of IPSCs and a significant decrease in EPSCs, can be attributed to the significant cleavage of VAMP1 and VAMP2 proteins in the strata pyramidale and radiatum of CA1c. The stimulating electrode in these recordings was placed in the str. radiatum so the cleavage of the VAMP1 and VAMP2 in this layer will impact on the neurotransmitter release onto the dendrites of the pyramidal cell being recorded from. The cleavage of the VAMP1 in str. pyramidale of CA1c (in 2 of the 3 analysed slices) for example has important implications for the changes in the evoked IPSCs. This is the VAMP isoform localised in inhibitory neurons, thus synapses of basket cells and axo-axonic cells onto pyramidal neurons in the str. pyramidale will be affected, shown by the abolishment of evoked IPSCs.

Electrophysiology in the CA1a of TeNT slices remained normal, and was associated with bouton counts comparable to control slices, except in the VAMP1 str. pyramidale where significantly fewer boutons were seen in TeNT slices. This may suggest that a spread of the toxin's effect to include the CA1a in some slices had occurred. This scenario is likely as the boundary for the spread of the toxin is variable, particularly at 8-16 days after injection. There is also variation in the position of the cells and their proximity to the injection site.

Interestingly, Vreugdenhil *et al.* (2002) showed that at 5 months after TeNT injection, population spike amplitude was still reduced in the CA1. They attribute this as an anti-epileptic mechanism which may be due to a reduced efficacy of excitatory synapses. A similar hypothesis was also presented by Hawkins & Mellanby (1987). It was suggested that its presence in the later stage of the model, after seizures have remitted, is likely to play a role in the learning impairments that still remain (Jefferys & Williams, 1987). However, considering that we have seen both VAMP isoforms cleaved at the early stages of the model indicates that the changes in excitation at 5 months may not be anti-epileptic but rather a direct result of the protease action of the toxin within excitatory synapses as well as the inhibitory population. Experiments to investigate this later time point in the model coupling electrophysiological and immunohistochemical techniques are planned for the future.

5.1.5.2 Effects of TeNT on spontaneous neurotransmission in CA1

The reduction in the frequency, but preservation of the amplitude, of IPSCs and EPSCs in ipsilateral CA1c has been shown in previous studies using TeNT (Mellanby & Thompson, 1972; Duchen & Tonge, 1973). In these studies, as in ours, evoked responses have been abolished or drastically reduced. These differences between evoked and spontaneous release suggest one of two options: 1) that the cleavage of VAMP1 or VAMP2 is not complete in all neurons or within the local network or 2) that a protein other than VAMP1 or VAMP2 is responsible for the spontaneous release, possibly from a different pool of vesicles. The possibility that the cleavage within individual boutons is not complete does not seem to be appropriate given that evoked IPSCs at least are completely abolished. However, there is ongoing investigation as to whether spontaneous and evoked release is reliant on the same

or separate mechanisms (Chung *et al.*, 2010; Ramirez *et al.*, 2012). The cleavage within the local population however is not complete, shown by the remaining presence of some VAMP positive boutons in all images. These boutons may be enough to maintain spontaneous neurotransmission, but at a reduced frequency.

There is also emerging evidence that SNAREs other than those forming the classic SNARE complex of VAMP2, syntaxin1 and SNAP25, may be involved in exocytosis (Fasshauer *et al.*, 1999; Yang *et al.*, 1999; Bragina *et al.*, 2007; Benagiano *et al.*, 2011; Tsai *et al.*, 2011; Raingo *et al.*, 2012; Ramirez & Kavalali, 2012; Ramirez *et al.*, 2012). Whilst some disagree whether there are differences between the proteins contained in GABAergic and glutamatergic neurons (Verderio *et al.*, 2004; Frassoni *et al.*, 2005; Delgado-Martinez *et al.*, 2007), the possibility of a variety of combinations being made between the different components of the SNARE complexes, and differences between those expressed in different neuronal populations, offers possibilities that there may be a compensation or additive mechanism when VAMP1 and 2 are cleaved by TeNT. The non-canonical SNAREs that may be candidates for evoked asynchronous or spontaneous neurotransmitter release include VAMP4 (Raingo *et al.*, 2012), VAMP7 (Scheuber *et al.*, 2006) and Vps10p-tail-interactor-1a (vti1a) (Ramirez *et al.*, 2012). Whether these are responsible for some of the remaining spontaneous neurotransmission in our slices is uncertain at this stage. The use of the organotypic slice culture method would allow for slices to be obtained from VAMP4, VAMP7 or vti1a knockout mice that could then be treated with TeNT in the way described in this project. A further reduction in the frequency or a reduction in the amplitude of spontaneous release may identify a compensatory mechanism provided by these non-canonical SNAREs.

5.1.5.3 Effects of TeNT in CA3

In the present study, patch clamp recordings were not carried out in the CA3 region but our bouton data can be related to sharp-electrode intracellular recordings from previous work. Empson & Jefferys (1993) showed that the contralateral CA3 produced significantly more spontaneous epileptic bursts within 'mirror' foci than the ipsilateral side in experiments at 10-18 days post injection. Whilst we have shown that both VAMP isoforms are significantly cleaved by the toxin in CA3 of both hippocampi (in strata pyramidale and radiatum) within this time range, we have not seen a greater decrease in the contralateral bouton count compared with the ipsilateral side. Empson & Jefferys suggest that inhibitory neurons on the contralateral side may be functional, shown by the preservation of monosynaptic fast and slow IPSPs within CA3 during pharmacological block of EPSPs. This was not the case in the ipsilateral side. The depression of GABA release in the ipsilateral but not the contralateral side highlights the possible differences in mechanisms for epileptic foci on the two sides of the brain (Jefferys & Empson, 1990; Empson & Jefferys, 1993). Considering that we have seen robust cleavage of VAMP1 and VAMP2 immunopositive boutons in CA3 on both sides of the brain to similar levels also questions why there are different mechanisms in the separate hippocampi and would suggest that both inhibitory and excitatory neurons are directly affected by the toxin. The contralateral hippocampus receives both excitatory and inhibitory commissural inputs from the ipsilateral hippocampus and therefore both populations in the contralateral hippocampus have the possibility of being directly exposed to TeNT (Ribak *et al.*, 1986). Differences in the time points included in each study or differences in the overall strengths of toxin and resulting epileptic syndromes may

play a role in the discrepancies between our study and that of Empson & Jefferys. Whole-cell patch clamp recordings within the CA3 of both hippocampi and the corresponding bouton analysis around recorded and filled cells after injection with our current toxin batch may highlight if there are variations in the effects between the two experiments. These results would also apply more directly to our current CA1 study by coupling electrophysiology and immunohistochemistry.

Whittington & Jefferys (1994) also showed that whilst epileptic activity takes longer to occur in the contralateral CA3, and recovers faster, the peak time point for epileptic activity was at 2 weeks. The robust cleavage of VAMP1 and VAMP2 boutons at 8-16 days corresponds with this electrophysiology, although analysis of later time points would indicate whether the peak effect on boutons has indeed occurred here or later.

Empson & Jefferys (1993) suggest that extra CA3 pyramidal cell connections may be made, and that these may happen more efficiently in the side that has no direct contact with the toxin. However, the cleavage of the boutons that we have seen in the contralateral CA3 suggests that the toxin does in fact travel to the contralateral hippocampus and thus will be having a direct effect at synapses within the CA3. This is also contradictory to work by Mellanby (1989) who showed that up to 3 days post injection, no radiolabelled TeNT was detected in the hippocampus contralateral to injection, however later time points were not mentioned. It was also shown that by 9 days post injection, only 1.5% of the radioactivity remained and this was focused around the injection site in the ipsilateral hippocampus. These results from Mellanby may be different to ours due to their injections being targeted to the ventral hippocampus, where commissural projections differ to the dorsal hippocampus (Amaral & Lavenex, 2007). The fact that we have seen significant cleavage in the

contralateral side indicates that the toxin must have travelled there, at least in the dorsal hippocampus.

5.1.5.4 Potential changes in VAMP1 and VAMP2 expression as the epileptic syndrome progresses

Considering that most animals injected with TeNT show remission from seizures at about 6-8 weeks (Mellanby *et al.*, 1977; Brace *et al.*, 1985; Empson & Jefferys, 1993) implies that a recovery from the effects of the initial cleavage would have occurred by this stage. What requires further investigation, is that the recovery from disinhibition in the ipsilateral CA3 (8 weeks) occurs before recovery from epileptic activity evoked in slices (16 weeks) (Whittington & Jefferys, 1994). It has been suggested previously that the continued presence of reduction in polysynaptic activation onto CA3 pyramidal cells and dentate gyrus granule cells at 8 weeks following TeNT injection, at a time when monosynaptic IPSCs have recovered, may be due to a decrease in intrinsic excitability of the interneurons, or that excitatory connections on the interneurons are failing (Jordan & Jefferys, 1992; Whittington & Jefferys, 1994; Jefferys & Whittington, 1996). Having shown that the VAMP2, primarily located in excitatory terminals, in our slices is cleaved by the toxin, it suggests the latter; that the reduction in polysynaptic activation is likely due to a failure of the excitatory connections onto interneurons. Whether the recovery from cleavage of VAMP1 coincides with the recovery from disinhibition (monosynaptic recovery), and recovery from epileptic activity occurs in line with normal VAMP2 expression being re-established at a later time, would be a very interesting route to investigate. It would also be interesting to look at the expression of the VAMP isoforms at a time when the

animals have remitted from motor seizures (6-8 weeks), but a behavioural and electrophysiological impairment remains (Jefferys & Williams, 1987).

Without further investigation into the expression of VAMP1 and VAMP2 at later time points (up to 16 weeks) in this model we cannot say how long the protease effect continues or remains. This is currently being addressed in our laboratory, however a recent study showed the presence of VAMP2 cleavage in protein extracts from mouse visual cortex up to 35 days after injection with TeNT (Mainardi *et al.*, 2012). This would suggest that the effects of the toxin could continue into much later time points than the 16 days studied in this project, in our intrahippocampally injected slices. A really interesting study would use double-labelling of VAMP1 and VAMP2 to directly compare and contrast the cleavage of the two proteins within the same slice. This is likely to demonstrate key differences between the time scales of cleavage, particularly by extending the study to many weeks.

Whittington & Jefferys (1994) also suggest that the pyramidal and granule cells could have a hypertrophy of excitatory synapses onto them which could overpower any inhibition. From the bouton counts that we have carried out from *ex vivo* slices prepared from chronically epileptic rats that have been used for whole-cell patch clamp recordings, we have not seen increases in the number of VAMP1 or VAMP2 positive boutons in TeNT slices and therefore feel it unlikely that there is an increase in these excitatory connections. Immunohistochemistry using synaptophysin, a marker for synaptic boutons, (Muzerelle *et al.*, 2003) would further confirm this. Comparing our results with that of Whittington & Jefferys must be done cautiously as we have not completed work to look at later time points in relation to the cleavage of VAMP1 and VAMP2 and so differences may be encountered at this later stage.

5.2 The use of organotypic hippocampal slice cultures as a model of TeNT-induced epilepsy

The addition of organotypic hippocampal slice cultures to this project has allowed a further insight into the functions of the toxin. As mentioned in the introduction, organotypic hippocampal slice cultures are being used more regularly for disease models. Whilst epilepsy has been studied in these slices following application of kainic acid to the culture medium (Bausch & McNamara, 2004; Reid *et al.*, 2008) or perfusion with low Mg^{2+} solution (Gutierrez *et al.*, 1999; Kovacs *et al.*, 1999; Wahab *et al.*, 2009), no focal application of a convulsant or otherwise has been made to slice cultures. The idea behind carrying out the experiments within our study was to see whether an *in vitro* model could be produced that would mimic the electrophysiology and immunohistochemistry results from *ex vivo* slices taken from previously injected rats. The results presented show that there are some differences between the two models, but it highlights that this technique could prove very useful in the future after further investigation has been carried out. There is the potential that the *in vitro* model could be used as a drug screen and could drastically decrease the number of animals used in drug application studies as only those that showed an effect *in vitro* would be initially tried in the whole animal.

5.2.1 Effects of TeNT on field potentials within slice cultures

The use of field recordings from the organotypic hippocampal slice cultures provided the first evidence of similarities between the effects of TeNT in slice cultures and *ex vivo* slices following *in vivo* injection.

5.2.1.1 Consistent results in control slices across the study

Encouraging results from the field recordings of the organotypic hippocampal slice cultures show that there is no deterioration in the size of the responses within control slices across the three time points studied. This implies that the time spent in culture, up to 30 days, does not result in a decrease in the viability of slices. This has also been seen in preliminary recordings made at 32 days post injection (up to 46 days in culture; data not shown). This has important implications if the model were to be used to further assess the effects of the toxin at later time points than addressed in this study. This would be useful considering that the TeNT effects following *in vivo* injections result in a syndrome that lasts for weeks.

5.2.1.2 Concentration dependent effects of TeNT

The field recordings from the different areas of the slice cultures highlighted that the toxin was able to disrupt synaptic transmission, particularly at the highest two toxin concentrations. Within the region closest to the injection site, the CA3 str. radiatum, all three concentrations appeared to have an effect at the earliest time point of day 2. This was followed by a recovery of the 5ng/µl TeNT slices by day 8 and the 25ng/µl TeNT slices by day 16, suggesting a dose dependent continuation of the disruption or recovery at the lower doses. The region most distal to the injection site, the CA1, showed significant disruptions in synaptic transmission in both the strata pyramidale and radiatum in 25 and 50ng/µl TeNT slices, but not within the lowest dose, again suggesting a dose dependent effect of the toxin.

The failure of the 5ng/µl TeNT injection to cause significant disruptions in synaptic transmission within the CA1, unlike the higher concentrations, offers evidence that the injection of the toxin does not spread across the slice but remains focal. If the

injection solution was to disperse across the majority of the surface of the slice then you would not expect to see this regional difference in responses. The effects of the higher concentrations of toxin on synaptic transmission within the CA1 are therefore likely to be due to the transport of the toxin to this region within neurons. The chance of this is higher due to the higher concentrations of toxin available. Alternatively, the higher concentrations may cause a block of synaptic transmission in a greater proportion of CA3 neurons which therefore has an indirect effect on the CA1. Considering that the stimulating electrode is within the CA3 for all recordings then this may apply.

The use of three different concentrations of toxin in this study highlights another advantage offered by organotypic hippocampal slice cultures. It has allowed us to study the similarities and/or differences between the effects of the toxin at different concentrations. The use of concentrations that vary by a factor of ten could not be used *in vivo* for long term studies due to the toxin's very poisonous nature, as shown by Bagetta *et al.* (1990) where high doses resulted in the death of most animals after only a few days. Each batch of toxin is different and the potency needs to be considered carefully for use in live animals. The use of multiple concentrations highlighted that the spatial spread as well as the time scale of the toxin's effects is dependent on the concentration. These differences are likely to continue into time points later than 16 days and may play important roles as the epileptic-type syndrome progresses.

Our concentration dependent results also highlight that differing results throughout the literature regarding TeNT use may be very dependent on the concentration and

toxicity of the particular batch of toxin used. Standardising this, however, would likely prove difficult.

5.2.1.3 Epileptic activity

The epileptic activity that has been seen within the slice cultures is interesting. The different types of activity, evoked afterdischarges and spontaneous activity, which are consistent with observations from *ex vivo* slices (Jefferys, 1989), albeit on a different time scale, offer encouraging evidence for the use of slice cultures as a tool to study TeNT induced epilepsy. Given that both types of activity exhibited two distinct forms highlights biological variation, not just between slices from different animals but also from slices within the same animal. Whether it is dependent on very subtle differences in the positioning of the injection and the neuronal network that is targeted initially is uncertain. This is something that could be investigated in the future, possibly through the use of tracers and targeting specific populations of neurons using genetically modified animals and injections at a higher magnification for greater accuracy. This has implications for epilepsy in general in that small differences in the position of the epileptic focus could result in different forms of seizure activity. Using these slice cultures to test drug applications and to see if the different forms of seizure activity are affected by the drugs in the same or different ways would provide important evidence to support this.

We have shown that in organotypic hippocampal slice cultures the spontaneous activity occurs most commonly at 2 days post injection and the afterdischarges at day 16, although the power was not enough to test whether differences were significant.

Future experiments to establish whether the afterdischarges begin at the highest dose at later time points should be carried out. This may give some indication of a recovery of the VAMPs, and may coincide with an increase in the synaptic responses following stimulation. Coupling electrophysiological and immunohistochemical analyses will help elucidate this. Another interesting future experiment would be to make multiple simultaneous recordings from the CA1 and CA3 to see whether the spontaneous activity or afterdischarges in the CA3 can spread to influence the CA1. Jefferys (1989) showed that spontaneous activity in the CA3 could trigger epileptic bursts in the CA1. If this also occurred in the slice cultures treated with TeNT then it would offer further evidence for the similarities between the two protocols.

5.2.1.4 Epileptic activity in a minority of control treated slice cultures

There was evidence of some epileptic activity within a small number of control slices. This may be due to the time spent in culture or a degeneration of part of the slice that led to these responses. Another possible explanation is the penicillin that is contained within the culture medium. However, because these responses are not consistent across all slices, it is unlikely that the penicillin plays a role. The final concentration of penicillin contained within our culture medium (100 U/ml) is also lower than concentrations that have been shown to cause epileptic activity (Lueders *et al.*, 1980; Schwartzkroin & Prince, 1980). Within each well, 6-8 slices would have been exposed to the same culture medium and yet only a minority of control slices showed epileptic activity. The majority of this activity is focussed on TeNT treated slices and shows concentration dependent occurrences, thus we are confident that the epileptic activity in the majority of slices is a direct result of the toxin.

5.2.2 Time scale of TeNT effects relative to in vivo injections

The effects of TeNT injections onto the slice cultures resulted in changes in responses from as early as 2 days post injection. These effects at 2 days post injection in the slice cultures may show an earlier onset of changes than TeNT injections *in vivo,* although reports from *in vivo* studies vary. Whilst slice recordings from adult rats injected *in vivo* have shown that there are no electrophysiological changes until the third day post injection onwards (Jefferys, 1989), electrodes implanted in the hippocampi of infant (Lee *et al.*, 1995; Anderson *et al.*, 1997) or adult (Anderson *et al.*, 1997) rats has shown that there are variations. Electrographic seizures begin within 1-3 days in infant rats and between days 1-7 in adult rats. The onset of behavioural seizures also vary from the first 24 hours (Lee *et al.*, 1995) to the third day post injection (Rashid *et al.*, 1999) in infant rats and not until days 3-7 in adult rats (Jefferys & Whittington, 1996). Behavioural seizures do not always accompany electrographic seizures in either age group (Anderson *et al.*, 1997). Changes in *ex vivo* slices may occur later than changes *in vivo* because an isolated slice from the animal only provides a small representation of the affected hippocampus. It may not contain large groups of neurons affected by the toxin at this early stage, thus detection is difficult (Jordan & Jefferys, 1992), whereas *in vivo* the intact connections would make the observations easier as the spread of the activity is uninterrupted. This may also be the reason that we see changes in the slice cultures earlier than in *ex vivo* slices, because the severed connections have reformed in slice cultures and there is a finite area that can be affected by the toxin. The lack of extrahippocampal inputs may also result in less dampening of seizure activity (Coulter *et al.*, 2011). The other possibility is that our slice cultures are in fact a closer

model for infant TeNT induced epilepsy rather than adult. As mentioned in Chapter 4, the epileptic activity seen in the slice cultures is similar to that in adult slices, whether taken from animals injected during infancy and allowed to mature to adulthood (Lee *et al.*, 1995; Smith *et al.*, 1998) or from those injected as adults (Jefferys, 1989). This is something that needs to be investigated further, using adult slice cultures to compare with our current results, but also exploring these infant slice cultures in more detail, starting with intracellular recordings. Whole-cell patch clamp recordings from slice cultures would allow for comparisons of epileptic activity with slices from *in vivo* intrahippocampally injected adult animals. This would help to show whether the epileptic activity seen is similar in the two preparations or whether the young age of the animals used for culturing show differences because of a less mature network.

As mentioned previously, at day 2 in the sections taken from *in vivo* injected animals there was a focal cleavage of VAMP1, particularly seen around the injection site, suggesting that this is not enough to cause an imbalance in the inhibition-excitation ratio. In our treated slice cultures however, we have seen robust effects of the toxin on both VAMP1 and VAMP2, starting as early as day 2. This may be due to the smaller network contained within a single slice of hippocampus, as well as the knowledge that the injection site is situated near to the recording, which cannot always be confirmed after *in vivo* injection. Therefore *ex vivo* slices may not show changes until the time of behavioural seizures because by that point a larger area is affected by the toxin and therefore recordings are more likely to be undertaken from a region affected.

5.2.3 Focal application of TeNT versus incubation in culture medium

Focal injections of TeNT onto organotypic hippocampal slice cultures were meant to mimic *in vivo* injections in that a small area was initially exposed to the toxin. Previous work has only used TeNT application into culture medium (500ng/ml for 72 hours) (Scheuber *et al.*, 2006). Although seizure-like activity was not reported, incubation in the TeNT-containing medium was shown to abolish EPSCs in the CA1 evoked by stimulation of Schaffer collaterals and within the CA3 where mossy fibre stimulation produced unreliable asynchronous responses (Scheuber *et al.*, 2006). Scheuber *et al.* (2006) also showed spontaneous miniature EPSCs (mEPSCs) were significantly decreased in frequency. These results show that the TeNT is able to have its protease effect within slice cultures from mice when applied to the culture medium that will affect the whole slice. In relation to our focal experiments, the initial concentration of the toxin used by Scheuber *et al.* is 100 times lower than our highest concentration (500ng/ml versus 50ng/µl).

The Scheuber *et al.* results differ slightly from the results of the patch clamp experiments in our *ex vivo* slices as their group have shown a total abolishment of EPSCs whereas we saw only a significant reduction, but a total abolishment of IPSCs. This is likely due to the different application of toxin: the entire slice culture in the Scheuber *et al.* study compared with a spread from a focal intrahippocampal injection. Our recordings were also made 7-15 days later so there may be some recovery of the responses by this time. The different concentrations of toxin are also likely to be important. The field recordings from our focally treated slice cultures offer similar results to that of Scheuber *et al.* in that population spike sizes were significantly reduced in toxin treated slices at the highest doses and these are

predominantly EPSPs. Future whole-cell patch clamp recordings from focally treated organotypic slice cultures will allow comparisons to be made between our results and those of Scheuber *et al.* It will also then allow comparisons to be made between the intracellular recordings within slice cultures and those from our slices from chronically epileptic rats.

There is a possibility that following injection of TeNT onto slice cultures, there may be leakage of the toxin through the membrane into the culture medium. This would result in a greatly diluted concentration. The electrophysiological evidence already presented that shows regional and concentration dependent effects focussed around the injection site argues against this however. The immunohistochemical results showing a lack of homogeneous cleavage of VAMP1 and VAMP2, which would be expected to be seen if the entire slice was directly exposed to the toxin, also prove this leakage unlikely. Experiments that looked at the binding and internalisation of the toxin showed that incubation with radiolabelled toxin and warming of cells to 37°C resulted in nearly 70% of the radiolabelled toxin being resistant to digestion by incubation with pronase (a protease) within 10 minutes (Staub *et al.*, 1986). This suggests that the binding and internalisation of the toxin occurs rapidly and as our slice cultures were incubated at this temperature then the likelihood of the binding and internalisation of the toxin occurring shortly after injection is high.

5.2.4 Advantage of multiple recordings in slice cultures

Most importantly, the results from the electrophysiology within the slice cultures shows that the TeNT is able to severely affect synaptic transmission and is able to cause epileptic activity in different forms. These results offer the great advantage of the ability to use the same slice at multiple occasions and follow the progression of

the changes induced by TeNT. This will be particularly important for detailed investigations of the actions of the toxin many weeks after injection. Recordings starting early in the model and repeated once every 1-2 weeks could really show the changes that occur across the course of the epileptic syndrome. This is something that is not possible in acute slices prepared from epileptic animals, but utilising both methods together will lead to deeper insights into the mechanisms and actions of TeNT.

5.2.5 Immunohistochemical analysis of VAMP immunopositive boutons in slice cultures

To further understand the effects of the toxin on slice cultures, immunohistochemical analysis of VAMP1 and VAMP2 cleavage were also carried out in a similar way to that of *ex vivo* slices. This offered further data to compare with *ex vivo* slices and also to understand more of the effects of the toxin at different concentrations within a culture setting.

5.2.5.1 Consistent measurements across the time course of the study

As with the electrophysiology, there were no differences between the immunohistochemical results within control slice cultures at the three different time points studied, in VAMP1 or VAMP2, across any of the regions. Again this has encouraging implications for further use of this model to study later time points as the viability of the slices seem unaffected up to 4-5 weeks and therefore have potential uses for further days or weeks.

5.2.5.2 Distribution of VAMP1 and VAMP2 immunopositivity in slice cultures

Overall, the distribution of VAMP1 and VAMP2 was layer specific within slice cultures, particularly at high magnification, and showed immunopositive and negative layers comparable to those from the *ex vivo* slices and Raptis *et al.* (2005). The str. pyramidale of the CA1 in these slice cultures was not always particularly clear at low magnification (Muller *et al.*, 1993). This is because the pyramidal cells of the CA1 spread into a layer within the middle of the slice rather than remaining piled on top of each other as in the CA3 (Stoppini *et al.*, 1991; Buchs *et al.*, 1993). As this was consistent across slices, comparisons of the bouton quantification between the CA1 str. pyramidale of different treatment conditions could still be carried out.

5.2.5.3 Differential cleavage of VAMP1 and VAMP2 by TeNT within slice cultures

The analysis of the boutons within the VAMP1 and VAMP2 immunostained slices have shown some differences between the regions and time points most affected by the toxin. The most robust cleavage is seen within VAMP1 immunostained slices. Here, the highest two toxin concentrations consistently show the lowest area occupied by VAMP1 immunopositivity, although not always significantly lower than control slices. The differences between the treatments are focussed around days 2 and 8, with minimal differences seen at day 16. This suggests a degree of recovery of the VAMP1 by this time point, consistent with the low magnification images. This matches the time scale of changes that appeared from the grey level analysis of the VAMP1 immunostaining in *ex vivo* slices from epileptic rats. The significant differences seen at day 2 only occur within the CA1 of 25 and 50ng/µl TeNT slices, and not within the CA3. Considering that the electrophysiology would suggest that the CA3 is affected by all concentrations of toxin, and the CA1 by only these highest two doses, it would have been expected that the CA3 would show significantly lower VAMP1 positive areas occupied by boutons at this earliest time point. The raw data shows that both the higher doses of toxin have very small VAMP1 positive areas within the CA3 compared with controls. However, the control data shows quite a large degree of variation in both the CA3 strata pyramidale and radiatum because only 3 slices could be included in the analysis, which is a particularly low number. Future experiments to increase the sample size for control CA3 will provide a more definitive answer as to the differences between control and the toxin doses. These results within the CA1 showing that only the two highest toxin concentrations cause a

significant decrease in the immunopositive bouton area, and not the 5ng/µl TeNT, are consistent with the electrophysiological data.

The VAMP2 immunoprofile differs to that of VAMP1. The effects of the high toxin concentration on VAMP2 remain throughout the course of the study around the injection site however the cleavage of VAMP2 is minimal in distal regions (CA1), even in slices that received the highest concentration of toxin. This region specific effect of the toxin in VAMP2 is interesting, especially considering that the effect of the toxin on VAMP1 is so widespread. It suggests that similar to the *ex vivo* slices; there is a lag in the spread of cleavage of VAMP2 compared with VAMP1. The recurrent excitatory connections that exist within the CA3 may also result in the cleavage of VAMP2 remaining focussed in a network local to the injection site.

5.2.5.4 Comparison of ex vivo slices and slice culture bouton analysis

The differences between the two populations of VAMP seen in slice cultures differ slightly to that from the *ex vivo* slices mentioned earlier. Without further investigation into later time points, it is difficult to say whether the VAMP2 is less affected in slice cultures, or whether the extent of the cleavage has not reached its peak within the 16 days studied. It was shown in the *ex vivo* slices that the cleavage of VAMP2 lagged behind that of VAMP1. Considering that many similarities have been seen between the results using the two different protocols, particularly in the electrophysiology and the effects of the toxin on VAMP1, it would suggest that the VAMP2 may well be affected at a later time point and within the length of our current study we have not seen the full extent. However, the focal cleavage of VAMP2 within the CA3 of our slice cultures at the earliest time point is something that was not seen in the grey level analysis of *ex vivo* slices. Having said this, a very focal cleavage may not have

been enough to cause a change in the distribution of the entire area within that low magnification analysis. Without bouton counts within *ex vivo* slices from 2 days post injection, it is difficult to compare the results from the two protocols at this earliest time point to see whether an early cleavage of VAMP2 occurs in *ex vivo* slices.

5.2.5.5 Comparison of electrophysiological and immunohistochemical data within slice cultures

Interestingly, within the 5ng/µl TeNT slices the most epileptic activity (afterdischarges and spontaneous) is within the CA3 str. pyramidale, whereas for 25 and 50ng/µl TeNT slices the greatest amount of epileptic activity occurs within the CA1 str. pyramidale. This is likely to be because whilst synaptic transmission is severely affected by the toxin at the highest two concentrations in the CA1, it is to a lesser degree than in the CA3. As synaptic transmission is virtually abolished by these high concentrations of toxin within the CA3, then the establishment of afterdischarges or spontaneous activity is very unlikely to be seen. Therefore higher rates of epileptic activity are seen in the CA1 where the disruption of synaptic transmission is not as prominent, but is still affected. The lesser cleavage of VAMP2 within the slice cultures in CA1 may also play a role in the epileptic activity, indicating that excitatory transmission may predominate over inhibition. The changes in electrophysiology depend on the release of neurotransmitters from neurons and thus VAMP1 and VAMP2 are important, but because the stimulating electrode was in the CA3 str. radiatum even for CA1 recordings, the activation of CA1 which could depend on excitation of CA3 may be disrupted by the cleavage of VAMP1 and/or VAMP2 within the CA3. Simultaneous recordings within the CA1 and CA3 may uncover this. For the lowest TeNT concentration, the most epileptic activity occurs in the CA3 because this

is the area that is shown to have been affected by the toxin, but to a much lesser extent. The CA1 is unaffected by the toxin at this concentration and therefore epileptic activity is not seen.

5.2.5.6 Both inhibition and excitation are affected by TeNT in slice cultures

The electrophysiology showed significantly decreased synaptic transmission in the highest doses of toxin in all areas of the hippocampus and epileptic activity in a number of slices, suggesting that both excitation and inhibition are affected. If just inhibition was affected then it would be expected that the response to stimulation was increased, rather than decreased, as the inhibitory mechanisms would not be present to dampen any excitatory responses. This would also account for the epileptic activity as the network would have lost its inhibitory regulation. The dramatic and significant decreases in responses to stimulation at the higher doses of toxin show that the excitation is also affected by the toxin. Coupling the electrophysiological recordings and the cleavage of both VAMP1 and VAMP2 confirm this.

5.2.6 Considerations for the use of slice cultures

Whilst the use of organotypic hippocampal slice cultures offers a number of advantages, there are some areas that need consideration to be able to utilise them to their full potential.

5.2.6.1 Choice of animal age

As mentioned in Chapter 2, the age of the animals used for culturing impacts on slice viability (Gahwiler *et al.*, 2001; Fuller & Dailey, 2007). Whilst the use of infant animals for our culturing study may not be ideal in an experiment that compares to results from adult animals injected intrahippocampally with TeNT, the methods for adult

cultures are relatively new and less established. Adult cultures are limited by the poor survival of slices or shorter term use, however the research is ongoing and advances are being made (Finley *et al.*, 2004; Legradi *et al.*, 2011; Kim *et al.*, 2013). In the future, it may be possible to culture slices from adult animals that received *in vivo* intrahippocampal TeNT injections. That way, a more detailed and longer term study of the changes may be conducted using the slice culture method. This would allow for slices to be taken at different stages of the epileptic syndrome *in vivo* and then to record from the slices at multiple time points throughout their time in culture. Whether the features of the epileptic syndrome *in vivo* would continue in parallel *in vitro* would be very interesting to determine. It may be dependent on the time after injection that the slices were isolated.

5.2.6.2 Difficulties with analysis of responses

There are some difficulties with using field recordings in organotypic slices that are both very small and also have a degree of recurrent connectivity that is not present in acute *ex vivo* slices. This was shown to be an issue when recording from the CA3 region, where the recording electrode was in such close proximity to the stimulus electrode. The CA3-CA3 recurrent connections occur at a higher frequency than CA1-CA1 connections in both acutely prepared (Deuchars & Thomson, 1996) and organotypic hippocampal slices (Debanne *et al.*, 1995), adding another compounding factor. These issues meant that the recording of responses from the CA3, both within the strata pyramidale and radiatum resulted in responses that showed an antidromic component, and in the cases of controls and some TeNT slices, also an orthodromic component. Whilst the orthodromic component is reliant on synaptic transmission, the antidromic is not. Brace *et al.* (1985) showed the antidromic response remained

when orthodromic spikes were depressed in intrahippocampal TeNT injected animals. This also indicated that the changes in orthodromic responses were as a result of changes in synaptic transmission rather than neuronal loss because the antidromic response was still present and at sizes comparable to control animals. Therefore for the purposes of understanding the effects of the toxin within our slice cultures, it was important that if the two components could not easily be distinguished within the response then a method of analysis needed to be used that could take into account the different components. For this reason, the analysis of the field recordings for the CA3 regions were based on the amplitude of the responses (positive or negative for strata pyramidale and radiatum respectively) rather than the trough and slope measurements that were used within the CA1. Using the amplitudes from baseline was the best available measurement for the mainly synaptic or orthodromic component from evoked field potentials, because of the overlap with the antidromic spike. In future experiments, pharmacological tools (for example NBQX and bicuculline) could be used to isolate the antidromic responses by blocking all synaptic transmission to show that the responses that remained were truly antidromic. Within the 50ng/µl TeNT slices for example, the blocking of synaptic transmission using pharmacological means would be expected to show very little difference to the recordings made without this intervention, because of the effects of the toxin.

5.2.6.3 Variation in recordings procedures

There are differences between the protocols from different laboratories when carrying out electrophysiological recordings from hippocampal slice cultures. Some perfuse with culture medium (Wahab *et al.*, 2009; Dyhrfjeld-Johnsen *et al.*, 2010), others with ACSF (Kovacs *et al.*, 1999; Ziobro *et al.*, 2011; Berdichevsky *et al.*, 2012). Similarly,

some use the submerged technique (Wahab *et al.*, 2009; Berdichevsky *et al.*, 2012) whereas others use interface chambers for recordings (Kovacs *et al.*, 1999; Dyhrfjeld-Johnsen *et al.*, 2010; Ziobro *et al.*, 2011). Whether the conditions of the recordings and the perfusion solution used makes a difference in recordings is uncertain. We used the submerged technique as this was the only option available with a fitted incubator box to try and maintain the environment and relative sterility of the slices. In the future however, if access to an interface chamber with a fitted incubator box was available then it would be interesting to see if the recordings differed between the two techniques. This would be particularly relevant to the presence and type of epileptic activity seen. Considering that many of the recordings from acute *ex vivo* slices are made using the interface method, it would also be important to compare results from slice cultures using this technique to show whether the type of recording chamber effects the epileptic activity observed.

5.2.6.4 Reorganisation of slices and its impact on the model

One issue regarding slice cultures is that whilst they maintain the overall organisation of the normal hippocampus, there is some reorganisation within layers, particularly the CA1 (Stoppini *et al.*, 1991; Buchs *et al.*, 1993). The responses recorded from this layer can vary with only small movements of the electrode, whether within one plane or changing the depth (Muller *et al.*, 1993). In a number of our slice cultures, typical str. radiatum responses were difficult to locate within the CA1. Small movements could change from a positive response to negative response (Muller *et al.*, 1993) and sometimes a str. radiatum negative response could not be found. This is likely because of the reorganisation of the CA1 pyramidal layer (Buchs *et al.*, 1993). Within control slices, some movement within the area was required to find the expected

population spikes and PSPs although often they were immediately identified. In TeNT slices however this was trickier as even when multiple sites within the area were tested, responses were often not found. To ensure that the lack of response was due to a disruption in synaptic transmission rather than an integral problem with the slice, multiple positions within the region were tried before carrying out the stimulus response curve. Only slices that appeared visually healthy were used for experiments to try and minimise the chance of a false negative recording.

The development of slice cultures has been studied previously and has suggested that whilst there is a reorganisation within the cultures following the slicing procedure, the morphological and synaptic activity development has been preprogrammed by 5 days of post natal life, at least in the CA1 pyramidal cells (De Simoni *et al.*, 2003). After 1 week in culture, the development of slices begins to parallel that *in vivo* (De Simoni *et al.*, 2003). By 21 days *in vitro*, similar dendritic morphologies in regards to spine density and dendritic trees were observed, as well as comparable synaptic currents. The development in culture is said to continue normally, despite there being no input from an external environment that an animal would normally be exposed to in its first weeks of life. The differences that occur within that first week after culturing are likely to be due to the manipulation of the slices during the culturing process. For example the slicing procedure will result in the severing of axons and therefore over the next week a degree of rearrangement will occur. These findings are very encouraging for the use of slice cultures as they offer a parallel to the *in vivo* situation and may be more representative than acute slices. Acute slices cannot recover from the slicing procedure in the same way as slice cultures and therefore slice cultures show a more physiological state and organisation because innervations have been

re-established. No manipulation of our slices was made until at least 10 days in culture to allow for the rearrangements to occur.

5.3 TeNT and its disruption of both inhibitory and excitatory neurotransmission

As reviewed, the general consensus in the literature was that the TeNT effects are targeted to inhibitory neurons. However the results from the bouton analysis and the electrophysiology have shown this not to be the case in our study and that both inhibition and excitation are affected by TeNT injections.

5.3.1 Selectivity of TeNT

The key paper that introduced the idea that rat VAMP1 was insensitive to TeNT and VAMP2 was the sole target of the toxin was that of Schiavo *et al.* (1992). Here they stated that the cleavage site of the TeNT was between the peptide bonds at the Gln76-Phe77 position within VAMP2. These amino acids do not exist at these positions within VAMP1, therefore questioning how it is that we have seen cleavage of this isoform in our slices. It is unlikely that there is any overlap between the two antibodies that we have used, firstly because the two N-terminal sequences that are recognised by the antibodies are very different, and secondly, there were clear differences in the specificity of the individual antibodies for different layers within the hippocampus.

What is interesting however is that the sequences for mouse and human VAMP1 contain the Gln-Phe peptide bonds, although at amino acid positions 78-79 rather than 76-77 as in the rat VAMP2. Shone & Roberts (1994) showed that botulinum type B neurotoxin (BoNT B) was able to cleave human VAMP1, and actually at a faster rate than VAMP2. This was further shown by Yamamoto *et al.* (2012) where the light chain of BoNT B was able to cleave human VAMP1, VAMP2 and VAMP3

(cellubrevin). The Gln-Phe bond in VAMP3 is at positions 59-60. This suggests that the Gln-Phe peptide bond may be required for the action of this toxin, but its exact position within the sequence may not be important. Considering that the BoNT B and TeNT cleavage sites are thought to be at the same peptide bond, it is therefore indicative that the TeNT would also be able to cleave human VAMP1, and most likely mouse.

The amino acid sequences surrounding the cleavage site are also thought to be important in the binding and cleavage properties of the toxin (Chen *et al.*, 2008b). The recognition sequences, however, vary between the BoNT B and TeNT (Chen *et al.*, 2008b). Interestingly the specific sequences that are required for VAMP2 recognition by TeNT are also contained in the rat VAMP1 sequence, although at slightly different amino acid positions. This may play an important part in the VAMP1 cleavage, even though the cleavage site is different from VAMP2.

Overall, this all still raises questions as to why our data has shown a cleavage of rat VAMP1, considering that the Gln-Phe peptide bond is not present. Whether there is a difference in the methodology that could produce the discrepancy is uncertain. Schiavo *et al.* (1992) used highly purified synaptic vesicles from the cerebral cortex and Western blots whereas we have focused on whole tissue and looked at only one region of the brain. Shone & Roberts (1994) used peptides that were synthesised, and Yamamoto *et al.* (2012) used recombinant proteins and the light chains of the botulinum toxins.

Our findings that the VAMP1 and VAMP2 are both cleaved by the toxin opens up further need for investigation into the cleavage site of TeNT in rat VAMP1. The data

we also have that the two isoforms are expressed in separate populations counteracts previous suggestions as well. Not only are both isoforms affected in our experiments, but if it was VAMP2 that was the primary target, then our data would suggest that these were mainly excitatory neurons.

5.3.2 Differential effects on inhibitory and excitatory neurons

The differing degrees of TeNT effect on inhibitory and excitatory populations, particularly suggested by the intracellular recordings in *ex vivo* slices, may be explained by the difference in population numbers within the hippocampus. Inhibitory neurons make up about 10% of the hippocampal neurons (Freund & Buzsaki, 1996). A widespread cleavage of VAMP1 (predominantly inhibitory) by day 8 could thus result in the majority of inhibitory neurons being affected by the toxin, supported by the complete abolishment of the evoked IPSCs within the CA1c of the ipsilateral hippocampus (8-16 days post injection). In contrast, the excitatory neurons, making up the majority of the hippocampus would require a much larger population to be affected to abolish all responses. The evoked responses fell to 22% of controls, suggesting that a considerable proportion of the population was affected, but not the entirety. This is also supported by the later effect of the toxin on VAMP2 shown in the grey level analysis. The significantly reduced responses in the slice cultures after treatment with the highest concentration of toxin also supports the idea that both inhibitory and excitatory neurotransmission are affected given that no prolonged field potentials or afterdischarges are seen. Taking into account the vast network of synapses within the hippocampus, particularly *in vivo*, it is likely that the toxin does not travel to, and thus does not have a direct effect on, all neurons. The indirect effects of the toxin are likely to affect a larger proportion of the hippocampal neurons.

A minority of other groups have also shown that excitation can be affected by the toxin, following different applications. This was shown by reduced excitability and smaller population spikes after intrahippocampal injection (Brace *et al.*, 1985; Hawkins & Mellanby, 1987), reduced excitatory responses after intramuscular injection in cats (Kanda & Takano, 1983) and a decrease in the frequency of mini end-plate potentials seen in the neuromuscular junction after injections into the hind leg of mice (Duchen & Tonge, 1973). All this was early evidence that the TeNT was able to affect excitatory as well as inhibitory responses after injection in the periphery or directly into the brain. More recently, Scheuber *et al.* (2006) have shown that hippocampal slice cultures, pre-treated with TeNT for 72 hours, has effects on both evoked and spontaneous excitatory transmission. However the focus of many groups remained on inhibitory neurons due to the clinical effects of infection by TeNT: spastic paralysis, thought to be caused by blocking inhibitory neurotransmitter release onto motoneurons.

Interestingly, differential TeNT effects on mEPSCs and mIPSCs have been shown between cortical neuronal cultures and spinal cord cultures (Yeh *et al.*, 2010). In cortical neuronal cultures, there were greater decreases in excitation than inhibition following TeNT treatment, but the reverse occurs in spinal cord cultures. SV2, a protein considered to be involved in TeNT entry into neurons, has also been shown to have different isoforms present on different neuronal populations, although not exclusively. In both the cortical and spinal cord neurons, SV2A was mostly present in inhibitory neurons, whereas SV2B co-localised with excitatory neurons (Yeh *et al.*, 2010). However this did not explain the opposite effects of the toxin seen in the spinal cord versus cortical neurons. A differential expression of VAMP1 and VAMP2

in the different regions may offer an explanation if investigated. If SV2 is the mechanism of entry for the TeNT, then a differential presence of SV2A and SV2B in separate populations may also account for the temporal differences in cleavage of VAMP1 and VAMP2 if different rates of uptake exist. Investigation of the overlap of the VAMPs and SV2 proteins in the hippocampus would provide further insight.

5.3.3 Inhibition and excitation affected at different time points

Considering that we have seen both VAMP1 and VAMP2 affected in rat and mouse hippocampal slices, along with decreases in both evoked inhibition and excitation, albeit to varying degrees, further suggests that both populations are affected by injections of TeNT. Our grey level analysis of *ex vivo* slices and bouton analysis of slice cultures also signify an interesting differential cleavage of the two isoforms based on the time after injection.

A number of very early papers looking at the effects of TeNT had shown that there was a differential effect of the toxin on excitatory and inhibitory neurons based on time (Albus & Habermann, 1983; Kanda & Takano, 1983; Bergey *et al.*, 1987). The preparations vary in these papers, from injections peripherally that focus on motoneurons (Kanda & Takano, 1983), to spinal cord neuronal cultures (Bergey *et al.*, 1987) and particles of forebrain cortex (Albus & Habermann, 1983). However, they all show that inhibitory neurons are affected at an earlier time point than excitatory neurons. This difference ranged from an hour (Albus & Habermann, 1983) to days (Kanda & Takano, 1983), although this is likely dependent on the preparation. It is possible, that other laboratories or experiments have not witnessed the effects on excitation as well as inhibition, because either their experiments did not last long enough, or because they did not look specifically for changes in excitation:

probably because of the general consensus that inhibitory neurons were the target of the toxin. This difference in the time scale of effects on the different populations is consistent with what we have shown in our grey level analysis. Here we saw that the peak effect of the toxin on inhibitory neurons (VAMP1) occurred earlier than in excitatory neurons (VAMP2). The slice cultures also showed that VAMP1 boutons were cleaved in a wider area than VAMP2 within the course of the study. Whether the VAMP2 cleavage would occur to a greater degree after 16 days is something that requires further investigation. The time scale of the current study did not allow us to see if the full recovery of one population occurred before the other. High magnification imaging of boutons from day 2 animals in *ex vivo* slices would also allow investigation to support focal effects of the toxin occurring earlier in inhibitory neurons.

Differences in methodology may be responsible for some reports that excitatory responses are not affected by TeNT. For example, Shin *et al.* (2012) looked at the effects of TeNT on a nucleus from the spinal cord, and showed that both evoked and spontaneous inhibitory responses were affected by the TeNT but that glutamatergic responses were not. It may be that due to their methodology, where TeNT was applied to the slices directly for less than one hour during recordings, there was only a very short time for the TeNT to cleave either VAMP and thus the disruption of inhibition predominated. Differences in concentration may also be important. Jordan & Jefferys (1992) showed that EPSPs within CA3 remained intact when IPSPs were decreased at 8-18 days after injection of toxin, likely due to a very low concentration used (2-5ng).

It is likely that there will be variations between the different laboratories and experiments that use TeNT. Whether this is because of injections into different parts of the body or species, different sources or concentrations of toxin, these may influence the results. TeNT is one of the most poisonous substances but even so, there are likely to be differences between the effects of high and low doses.

5.4 Statistical analysis

The different parts of this study contained many different variables. Multiple comparisons between these variables were required. Whilst the data from some sections of the project followed a normal distribution and groups showed equal variance allowing for two way ANOVAs to be used, data from other sections did not. In these cases t-tests (for those data that were normally distributed) or Mann Whitney Rank Sum tests (for those data that were not normally distributed) were required. Corrections for multiple comparisons were made where a cohort of data received more than one statistical test. The Bonferroni correction for multiple comparisons reduces the significance criterion to minimise the risk of obtaining one or more false positives. Multiple univariate tests rather than a single multivariate test were carried out on this data to include the numerous variables that were being tested. These univariate tests offered clarity within the large datasets, for example focussing on treatment and side of the brain within individual time points. This could then be followed by a comparison of time points within TeNT data, as control data was grouped to reduce the number of animals and therefore did not require the comparison of time points.

5.5 Future directions

A number of future avenues could be taken from the results presented within this thesis. As well as the extended investigations and studies already mentioned within this Chapter, there remain other directions to be explored.

The slice cultures are now at a stage at which they can be used for longitudinal investigations of the full duration of the TeNT model. These studies would

complement parallel work *in vivo* and *ex vivo*. Co-cultures (Law *et al.*, 2010) could be used as an additional tool to look at the spread of the toxin's effects from one slice to another, using both immunohistochemical and electrophysiological analyses. Slice cultures also have the potential for screening of both anticonvulsant and antiepileptogenic drugs. This would reduce the numbers of animals used for drug screening studies. Comparison of the effects of carbamazepine and levetiracetam in slice cultures to those already established *in vivo* would provide a starting point (Doheny *et al.*, 2002; Halliday *et al.*, 2013). Using genetically modified mice would aid all these studies and would offer a further level of manipulation, particularly if using lines that are lethal in early life.

The issue of species difference is currently being addressed in our laboratory by intrahippocampal TeNT injections into mouse brain *in vivo.* This will give a greater insight into the consistency of effects of the toxin in rats and mice, furthering what we have shown from current experiments which suggests a great deal of overlap between the effects of the toxin on the two species, even within animals from separate age groups. Further investigation is required, using both *in vivo* injections in mice and using infant rats for slice cultures.

5.6 Implications for human epilepsy

The results in the project have provided further evidence for the mechanisms of epilepsy in the TeNT-induced chronic model. This has implications for human epilepsy in that growing knowledge of the area of the hippocampus affected and the spread of foci to contralateral hippocampi and extrahippocampal regions in the brain can help understand the disease in greater details. The potential of the slice cultures

to act as drug screens for new antiepileptics is also very important for human sufferers. This TeNT model has the unique capability of modelling non-lesional epilepsy and thus is a key tool for research into this form of the disease. The complication of hippocampal sclerosis in other models therefore does not provide a sound model for patients who do not present with this pathology. Whilst there is still much to learn about TeNT-induced epilepsy, any insight into the changes that occur during epilepsy, including epileptogenesis and the propagation of seizures can only be of benefit to patients suffering from the disease.

5.7 Conclusions

There has been a wealth of experiments following intrahippocampal injection of TeNT. What is new in our studies is that this electrophysiological activity has been directly collaborated with immunohistochemical investigation at the bouton level. We have also established that *in vitro* TeNT injections onto slice cultures offer a method to study the effects of the toxin that shows similarities to data already published. These results will deepen our understanding of published results. Overall, our data has shown:

- Both VAMP1 and VAMP2 are cleaved by TeNT injections after *in vivo* intrahippocampal injection and within *in vitro* slice cultures, in rats and mice respectively. This counters previous reports that the toxin specifically targets VAMP2. The two isoforms have also been shown to co-localise in separate neuronal populations; VAMP1 mainly in inhibitory neurons and VAMP2 predominantly in excitatory neurons.

- Inhibition and excitation are disrupted by the toxin, albeit to different degrees, and with evoked and spontaneous activity differentially affected. The disruption can be related to the changes in VAMP1 and VAMP2 expression.

- The VAMP1 cleavage occurs earlier and shows a more widespread effect, with the cleavage of VAMP2 delayed. Future studies into later time points, particularly many weeks post injection will clarify the importance of the difference in peak cleavage times of the two isoforms in relation to the development, continuation and recovery from the epileptic syndrome.

- Contrary to previous suggestions, the mirror foci seen in the contralateral hippocampus is likely to be the direct result of toxin cleavage of VAMPs rather than indirect mechanisms as previously suggested.

- Focal application of TeNT onto organotypic slice cultures produces characteristics of the TeNT induced epilepsy model that are comparable to slices taken from animals injected *in vivo.* This technique offers a useful adjunct for future studies of the toxin.

The use of both *in vivo* and *in vitro* TeNT treatments in this study has complemented each other. Whilst they both have advantages and disadvantages regarding their ease and flexibility of use, duration of use, suitability to relate to *in vivo,* cost and the reduction of animal usage, the combination of the two will help further the knowledge of the effects of TeNT and other substances, whilst improving insights into the mechanisms involved in epilepsy and other diseases.

6 LIST OF REFERENCES

Albus K, Wahab A & Heinemann U. (2008). Standard antiepileptic drugs fail to block epileptiform activity in rat organotypic hippocampal slice cultures. *Br J Pharmacol* **154,** 709-724.

Albus U & Habermann E. (1983). Tetanus toxin inhibits the evoked outflow of an inhibitory (GABA) and an excitatory (D-aspartate) amino acid from particulate brain cortex. *Toxicon* **21,** 97-110.

Alekseyenko OV, Chan YB, Li R & Kravitz EA. (2013). Single dopaminergic neurons that modulate aggression in Drosophila. *Proc Natl Acad Sci U S A* **110,** 6151-6156.

Amaral D & Lavenex P. (2007). Hippocampal Neuroanatomy. In *The Hippocampus Book*, First edn, ed. Andersen P, Morris R, Amaral D & O'Keefe J, pp. 37-. Oxford University Press, Oxford.

Amaral DG, Dolorfo C & Alvarez-Royo P. (1991). Organization of CA1 projections to the subiculum: a PHA-L analysis in the rat. *Hippocampus* **1,** 415-435.

Anderson AE, Hrachovy RA & Swann JW. (1997). Increased susceptibility to tetanus toxin-induced seizures in immature rats. *Epilepsy Res* **26,** 433-442.

Aull-Watschinger S, Pataraia E, Czech T & Baumgartner C. (2008). Outcome predictors for surgical treatment of temporal lobe epilepsy with hippocampal sclerosis. *Epilepsia* **49,** 1308-1316.

Bagetta G, Corasaniti MT, Nistico G & Bowery NG. (1990). Behavioural and neuropathological effects produced by tetanus toxin injected into the hippocampus of rats. *Neuropharmacology* **29,** 765-770.

Bausch SB & McNamara JO. (2004). Contributions of mossy fiber and CA1 pyramidal cell sprouting to dentate granule cell hyperexcitability in kainic acid-treated hippocampal slice cultures. *J Neurophysiol* **92,** 3582-3595.

Benagiano V, Lorusso L, Flace P, Girolamo F, Rizzi A, Bosco L, Cagiano R, Nico B, Ribatti D & Ambrosi G. (2011). VAMP-2, SNAP-25A/B and syntaxin-1 in glutamatergic and GABAergic synapses of the rat cerebellar cortex. *BMC Neurosci* **12,** 118.

Berdichevsky Y, Dzhala V, Mail M & Staley KJ. (2012). Interictal spikes, seizures and ictal cell death are not necessary for post-traumatic epileptogenesis in vitro. *Neurobiol Dis* **45,** 774-785.

Berg AT & Scheffer IE. (2011). New concepts in classification of the epilepsies: entering the 21st century. *Epilepsia* **52,** 1058-1062.

Bergey GK, Bigalke H & Nelson PG. (1987). Differential effects of tetanus toxin on inhibitory and excitatory synaptic transmission in mammalian spinal cord neurons in culture: a presynaptic locus of action for tetanus toxin. *J Neurophysiol* **57,** 121-131.

Blum FC, Chen C, Kroken AR & Barbieri JT. (2012). Tetanus toxin and botulinum toxin a utilize unique mechanisms to enter neurons of the central nervous system. *Infect Immun* **80,** 1662-1669.

Blumcke I, Beck H, Lie AA & Wiestler OD. (1999). Molecular neuropathology of human mesial temporal lobe epilepsy. *Epilepsy Res* **36,** 205-223.

Blume WT, Luders HO, Mizrahi E, Tassinari C, van Emde Boas W & Engel J, Jr. (2001). Glossary of descriptive terminology for ictal semiology: report of the ILAE task force on classification and terminology. *Epilepsia* **42,** 1212-1218.

Brace HM, Jefferys JG & Mellanby J. (1985). Long-term changes in hippocampal physiology and learning ability of rats after intrahippocampal tetanus toxin. *J Physiol* **368,** 343-357.

Bragina L, Candiracci C, Barbaresi P, Giovedi S, Benfenati F & Conti F. (2007). Heterogeneity of glutamatergic and GABAergic release machinery in cerebral cortex. *Neuroscience* **146,** 1829-1840.

Bragina L, Giovedi S, Barbaresi P, Benfenati F & Conti F. (2010). Heterogeneity of glutamatergic and GABAergic release machinery in cerebral cortex: analysis of synaptogyrin, vesicle-associated membrane protein, and syntaxin. *Neuroscience* **165,** 934-943.

Buchs PA, Stoppini L & Muller D. (1993). Structural modifications associated with synaptic development in area CA1 of rat hippocampal organotypic cultures. *Brain Res Dev Brain Res* **71,** 81-91.

Cascino GD. (2008). When drugs and surgery don't work. *Epilepsia* **49 Suppl 9,** 79-84.

Cavalheiro EA, Leite JP, Bortolotto ZA, Turski WA, Ikonomidou C & Turski L. (1991). Long-term effects of pilocarpine in rats: structural damage of the brain triggers kindling and spontaneous recurrent seizures. *Epilepsia* **32,** 778-782.

Chen C, Baldwin MR & Barbieri JT. (2008a). Molecular basis for tetanus toxin coreceptor interactions. *Biochemistry* **47,** 7179-7186.

Chen C, Fu Z, Kim JJ, Barbieri JT & Baldwin MR. (2009). Gangliosides as high affinity receptors for tetanus neurotoxin. *J Biol Chem* **284,** 26569-26577.

Chen S, Hall C & Barbieri JT. (2008b). Substrate recognition of VAMP-2 by botulinum neurotoxin B and tetanus neurotoxin. *J Biol Chem* **283,** 21153-21159.

Choi H, Sell RL, Lenert L, Muennig P, Goodman RR, Gilliam FG & Wong JB. (2008). Epilepsy surgery for pharmacoresistant temporal lobe epilepsy: a decision analysis. *Jama* **300,** 2497-2505.

Chow DM, Theobald JC & Frye MA. (2011). An olfactory circuit increases the fidelity of visual behavior. *J Neurosci* **31,** 15035-15047.

Chung C, Barylko B, Leitz J, Liu X & Kavalali ET. (2010). Acute dynamin inhibition dissects synaptic vesicle recycling pathways that drive spontaneous and evoked neurotransmission. *J Neurosci* **30,** 1363-1376.

Cook TM, Protheroe RT & Handel JM. (2001). Tetanus: a review of the literature. *Br J Anaesth* **87,** 477-487.

Coulter DA, Yue C, Ang CW, Weissinger F, Goldberg E, Hsu FC, Carlson GC & Takano H. (2011). Hippocampal microcircuit dynamics probed using optical imaging approaches. *J Physiol* **589,** 1893-1903.

De Simoni A & Edwards FA. (2006). Pathway specificity of dendritic spine morphology in identified synapses onto rat hippocampal CA1 neurons in organotypic slices. *Hippocampus* **16,** 1111-1124.

De Simoni A, Griesinger CB & Edwards FA. (2003). Development of rat CA1 neurones in acute versus organotypic slices: role of experience in synaptic morphology and activity. *J Physiol* **550,** 135-147.

Debanne D, Guerineau NC, Gahwiler BH & Thompson SM. (1995). Physiology and pharmacology of unitary synaptic connections between pairs of cells in areas CA3 and CA1 of rat hippocampal slice cultures. *J Neurophysiol* **73,** 1282-1294.

Delgado-Martinez I, Nehring RB & Sorensen JB. (2007). Differential abilities of SNAP-25 homologs to support neuronal function. *J Neurosci* **27,** 9380-9391.

Deuchars J & Thomson AM. (1996). CA1 pyramid-pyramid connections in rat hippocampus in vitro: dual intracellular recordings with biocytin filling. *Neuroscience* **74,** 1009-1018.

Diamond MC, Johnson RE, Young D & Singh SS. (1983). Age-related morphologic differences in the rat cerebral cortex and hippocampus: male-female; right-left. *Exp Neurol* **81,** 1-13.

Diamond MC, Murphy GM, Jr., Akiyama K & Johnson RE. (1982). Morphologic hippocampal asymmetry in male and female rats. *Exp Neurol* **76,** 553-565.

Doheny HC, Whittington MA, Jefferys JG & Patsalos PN. (2002). A comparison of the efficacy of carbamazepine and the novel anti-epileptic drug levetiracetam in the tetanus toxin model of focal complex partial epilepsy. *Br J Pharmacol* **135,** 1425-1434.

Duchen LW & Tonge DA. (1973). The effects of tetanus toxin on neuromuscular transmission and on the morphology of motor end-plates in slow and fast skeletal muscle of the mouse. *J Physiol* **228,** 157-172.

Dyhrfjeld-Johnsen J, Berdichevsky Y, Swiercz W, Sabolek H & Staley KJ. (2010). Interictal spikes precede ictal discharges in an organotypic hippocampal slice culture model of epileptogenesis. *J Clin Neurophysiol* **27,** 418-424.

Elger CE. (2002). Epilepsy: disease and model to study human brain function. *Brain Pathol* **12,** 193-198.

Empson RM & Jefferys JG. (1993). Synaptic inhibition in primary and secondary chronic epileptic foci induced by intrahippocampal tetanus toxin in the rat. *J Physiol* **465,** 595-614.

Engel J, Jr. (2001). Mesial temporal lobe epilepsy: what have we learned? *Neuroscientist* **7,** 340-352.

Engel J, Jr. (2006). Report of the ILAE classification core group. *Epilepsia* **47,** 1558-1568.

Engel J, Jr. & Pedley TA. (1997). *Epilepsy: A Comprehensive Textbook*, vol. 1. Lippincott-Raven, Philadelphia.

Farrar JJ, Yen LM, Cook T, Fairweather N, Binh N, Parry J & Parry CM. (2000). Tetanus. *J Neurol Neurosurg Psychiatry* **69,** 292-301.

Fasshauer D, Antonin W, Margittai M, Pabst S & Jahn R. (1999). Mixed and non-cognate SNARE complexes. Characterization of assembly and biophysical properties. *J Biol Chem* **274,** 15440-15446.

Figueiredo DM, Hallewell RA, Chen LL, Fairweather NF, Dougan G, Savitt JM, Parks DA & Fishman PS. (1997). Delivery of recombinant tetanus-superoxide dismutase proteins to central nervous system neurons by retrograde axonal transport. *Exp Neurol* **145,** 546-554.

Finley M, Fairman D, Liu D, Li P, Wood A & Cho S. (2004). Functional validation of adult hippocampal organotypic cultures as an in vitro model of brain injury. *Brain Res* **1001,** 125-132.

Fisher RS, van Emde Boas W, Blume W, Elger C, Genton P, Lee P & Engel J, Jr. (2005). Epileptic seizures and epilepsy: definitions proposed by the International League Against Epilepsy (ILAE) and the International Bureau for Epilepsy (IBE). *Epilepsia* **46,** 470-472.

Frassoni C, Inverardi F, Coco S, Ortino B, Grumelli C, Pozzi D, Verderio C & Matteoli M. (2005). Analysis of SNAP-25 immunoreactivity in hippocampal inhibitory neurons during development in culture and in situ. *Neuroscience* **131,** 813-823.

French JA. (2007). Refractory epilepsy: clinical overview. *Epilepsia* **48 Suppl 1,** 3-7.

Freund TF & Buzsaki G. (1996). Interneurons of the hippocampus. *Hippocampus* **6,** 347-470.

Fuller L & Dailey ME. (2007). Preparation of rodent hippocampal slice cultures. *CSH Protoc* **2007,** pdb prot4848.

Gahwiler BH. (1981). Organotypic monolayer cultures of nervous tissue. *J Neurosci Methods* **4,** 329-342.

Gahwiler BH, Thompson SM & Muller D. (2001). Preparation and maintenance of organotypic slice cultures of CNS tissue. *Curr Protoc Neurosci* **Chapter 6,** Unit 6 11.

Gambardella A, Labate A, Giallonardo A & Aguglia U. (2009). Familial mesial temporal lobe epilepsies: clinical and genetic features. *Epilepsia* **50 Suppl 5,** 55-57.

Gulyas AI, Toth K, McBain CJ & Freund TF. (1998). Stratum radiatum giant cells: a type of principal cell in the rat hippocampus. *Eur J Neurosci* **10,** 3813-3822.

Gutierrez R, Armand V, Schuchmann S & Heinemann U. (1999). Epileptiform activity induced by low Mg2+ in cultured rat hippocampal slices. *Brain Res* **815,** 294-303.

Gutierrez R & Heinemann U. (1999). Synaptic reorganization in explanted cultures of rat hippocampus. *Brain Res* **815,** 304-316.

Halliday AJ, Campbell TE, Nelson TS, McLean KJ, Wallace GG & Cook MJ. (2013). Levetiracetam-loaded biodegradable polymer implants in the tetanus toxin model of temporal lobe epilepsy in rats. *J Clin Neurosci* **20,** 148-152.

Hawkins CA & Mellanby JH. (1987). Limbic epilepsy induced by tetanus toxin: a longitudinal electroencephalographic study. *Epilepsia* **28,** 431-444.

Hayashi T, McMahon H, Yamasaki S, Binz T, Hata Y, Sudhof TC & Niemann H. (1994). Synaptic vesicle membrane fusion complex: action of clostridial neurotoxins on assembly. *Embo J* **13,** 5051-5061.

Helting TB & Zwisler O. (1977). Structure of tetanus toxin. I. Breakdown of the toxin molecule and discrimination between polypeptide fragments. *J Biol Chem* **252,** 187-193.

Humeau Y, Doussau F, Grant NJ & Poulain B. (2000). How botulinum and tetanus neurotoxins block neurotransmitter release. *Biochimie* **82,** 427-446.

Hussain S & Davanger S. (2011). The discovery of the soluble N-ethylmaleimide-sensitive factor attachment protein receptor complex and the molecular regulation of synaptic vesicle transmitter release: the 2010 Kavli Prize in neuroscience. *Neuroscience* **190,** 12-20.

Janz R & Sudhof TC. (1999). SV2C is a synaptic vesicle protein with an unusually restricted localization: anatomy of a synaptic vesicle protein family. *Neuroscience* **94,** 1279-1290.

Jefferys J & Walker M. (2006). Tetanus Toxin Model of Focal Epilepsy. In *Models of Seizures and Epilepsy*, ed. Pitkänen A, PA S & Moshé S, pp. 407-414. Academic Press, Burlington.

Jefferys JG. (1989). Chronic epileptic foci in vitro in hippocampal slices from rats with the tetanus toxin epileptic syndrome. *J Neurophysiol* **62,** 458-468.

Jefferys JG & Empson RM. (1990). Development of chronic secondary epileptic foci following intrahippocampal injection of tetanus toxin in the rat. *Exp Physiol* **75,** 733-736.

Jefferys JG, Evans BJ, Hughes SA & Williams SF. (1992). Neuropathology of the chronic epileptic syndrome induced by intrahippocampal tetanus toxin in rat:

preservation of pyramidal cells and incidence of dark cells. *Neuropathol Appl Neurobiol* **18,** 53-70.

Jefferys JG & Whittington MA. (1996). Review of the role of inhibitory neurons in chronic epileptic foci induced by intracerebral tetanus toxin. *Epilepsy Res* **26,** 59-66.

Jefferys JG & Williams SF. (1987). Physiological and behavioural consequences of seizures induced in the rat by intrahippocampal tetanus toxin. *Brain* **110 (Pt 2),** 517-532.

Jiruska P, Finnerty GT, Powell AD, Lofti N, Cmejla R & Jefferys JG. (2010). Epileptic high-frequency network activity in a model of non-lesional temporal lobe epilepsy. *Brain* **133,** 1380-1390.

Jiruska P, Shtaya AB, Bodansky DM, Chang WC, Gray WP & Jefferys JG. (2013). Dentate gyrus progenitor cell proliferation after the onset of spontaneous seizures in the tetanus toxin model of temporal lobe epilepsy. *Neurobiol Dis* **54,** 492-498.

Jordan SJ & Jefferys JG. (1992). Sustained and selective block of IPSPs in brain slices from rats made epileptic by intrahippocampal tetanus toxin. *Epilepsy Res* **11,** 119-129.

Jung YJ, Suh EC & Lee KE. (2012). Oxygen/Glucose Deprivation and Reperfusion Cause Modifications of Postsynaptic Morphology and Activity in the CA3 Area of Organotypic Hippocampal Slice Cultures. *Korean J Physiol Pharmacol* **16,** 423-429.

Kamada M, Li RY, Hashimoto M, Kakuda M, Okada H, Koyanagi Y, Ishizuka T & Yawo H. (2004). Intrinsic and spontaneous neurogenesis in the postnatal slice culture of rat hippocampus. *Eur J Neurosci* **20,** 2499-2508.

Kanda K & Takano K. (1983). Effect of tetanus toxin on the excitatory and the inhibitory post-synaptic potentials in the cat motoneurone. *J Physiol* **335,** 319-333.

Kim H, Kim E, Park M, Lee E & Namkoong K. (2013). Organotypic hippocampal slice culture from the adult mouse brain: A versatile tool for translational neuropsychopharmacology. *Prog Neuropsychopharmacol Biol Psychiatry* **41,** 36-43.

Kitamura M, Takamiya K, Aizawa S, Furukawa K & Furukawa K. (1999). Gangliosides are the binding substances in neural cells for tetanus and botulinum toxins in mice. *Biochim Biophys Acta* **1441,** 1-3.

Kobayashi T, Kai N, Kobayashi K, Fujiwara T, Akagawa K, Onda M & Kobayashi K. (2008). Transient silencing of synaptic transmitter release from specific neuronal types by recombinant tetanus toxin light chain fused to antibody variable region. *J Neurosci Methods* **175,** 125-132.

Kovacs R, Gutierrez R, Kivi A, Schuchmann S, Gabriel S & Heinemann U. (1999). Acute cell damage after low Mg2+-induced epileptiform activity in organotypic hippocampal slice cultures. *Neuroreport* **10,** 207-213.

Laurberg S & Sorensen KE. (1981). Associational and commissural collaterals of neurons in the hippocampal formation (hilus fasciae dentatae and subfield CA3). *Brain Res* **212,** 287-300.

Law S, Raisman G & Li D. (2010). Organotypic slice co-cultures reveal that early postnatal hippocampal axons lose the ability to grow along the fimbria, while retaining the ability to invade and arborise in septal neuropil. *Eur J Neurosci* **31,** 1352-1358.

Leao RN, Mikulovic S, Leao KE, Munguba H, Gezelius H, Enjin A, Patra K, Eriksson A, Loew LM, Tort AB & Kullander K. (2012). OLM interneurons differentially modulate CA3 and entorhinal inputs to hippocampal CA1 neurons. *Nat Neurosci* **15,** 1524-1530.

Lee CL, Hrachovy RA, Smith KL, Frost JD, Jr. & Swann JW. (1995). Tetanus toxin-induced seizures in infant rats and their effects on hippocampal excitability in adulthood. *Brain Res* **677,** 97-109.

Legradi A, Varszegi S, Szigeti C & Gulya K. (2011). Adult rat hippocampal slices as in vitro models for neurodegeneration: studies on cell viability and apoptotic processes. *Brain Res Bull* **84,** 39-44.

Lister JP, Tonkiss J, Blatt GJ, Kemper TL, DeBassio WA, Galler JR & Rosene DL. (2006). Asymmetry of neuron numbers in the hippocampal formation of prenatally malnourished and normally nourished rats: a stereological investigation. *Hippocampus* **16,** 946-958.

Loscher W. (1997). Animal models of intractable epilepsy. *Prog Neurobiol* **53,** 239-258.

Loscher W & Brandt C. (2010). High seizure frequency prior to antiepileptic treatment is a predictor of pharmacoresistant epilepsy in a rat model of temporal lobe epilepsy. *Epilepsia* **51,** 89-97.

Lothman EW & Collins RC. (1981). Kainic acid induced limbic seizures: metabolic, behavioral, electroencephalographic and neuropathological correlates. *Brain Res* **218,** 299-318.

Lueders H, Bustamante L, Zablow L, Krinsky A & Goldensohn ES. (1980). Quantitative studies of spike foci induced by minimal concentrations of penicillin. *Electroencephalogr Clin Neurophysiol* **48,** 80-89.

Mainardi M, Pietrasanta M, Vannini E, Rossetto O & Caleo M. (2012). Tetanus neurotoxin-induced epilepsy in mouse visual cortex. *Epilepsia* **53,** e132-136.

Majores M, Schoch S, Lie A & Becker AJ. (2007). Molecular neuropathology of temporal lobe epilepsy: complementary approaches in animal models and human disease tissue. *Epilepsia* **48 Suppl 2,** 4-12.

Mellanby J, George G, Robinson A & Thompson P. (1977). Epileptiform syndrome in rats produced by injecting tetanus toxin into the hippocampus. *J Neurol Neurosurg Psychiatry* **40,** 404-414.

Mellanby J & Green J. (1981). How does tetanus toxin act? *Neuroscience* **6,** 281-300.

Mellanby J & Thompson PA. (1972). The effect of tetanus toxin at the neuromuscular junction in the goldfish. *J Physiol* **224,** 407-419.

Mellanby JH. (1989). Elimination of ^{125}I from rat brain after injection of small doses of ^{125}I-labelled tetanus toxin into the hippocampus. *Neuroscience Letters* **36 [Supplement]**.

Mitchell J. (1998). Tetanus toxin-enhanced GABA immunoreactivity in living neurons. *J Histochem Cytochem* **46,** 321-326.

Moskal JR, Kroes RA, Otto NJ, Rahimi O & Claiborne BJ. (2006). Distinct patterns of gene expression in the left and right hippocampal formation of developing rats. *Hippocampus* **16,** 629-634.

Muller D, Buchs PA & Stoppini L. (1993). Time course of synaptic development in hippocampal organotypic cultures. *Brain Res Dev Brain Res* **71,** 93-100.

Murray AJ, Sauer JF, Riedel G, McClure C, Ansel L, Cheyne L, Bartos M, Wisden W & Wulff P. (2011). Parvalbumin-positive CA1 interneurons are required for spatial working but not for reference memory. *Nat Neurosci* **14,** 297-299.

Muzerelle A, Alberts P, Martinez-Arca S, Jeannequin O, Lafaye P, Mazie JC, Galli T & Gaspar P. (2003). Tetanus neurotoxin-insensitive vesicle-associated membrane protein localizes to a presynaptic membrane compartment in selected terminal subsets of the rat brain. *Neuroscience* **122,** 59-75.

Paxinos G & Watson C. (1998). *The rat brain in stereotaxic coordinates*. Academic Press, London.

Racine RJ. (1972). Modification of seizure activity by electrical stimulation. II. Motor seizure. *Electroencephalogr Clin Neurophysiol* **32,** 281-294.

Raedt R, Van Dycke A, Van Melkebeke D, De Smedt T, Claeys P, Wyckhuys T, Vonck K, Wadman W & Boon P. (2009). Seizures in the intrahippocampal kainic acid epilepsy model: characterization using long-term video-EEG monitoring in the rat. *Acta Neurol Scand* **119,** 293-303.

Ragbetli MC, Aydinlioglu A, Koyun N, Yayici R & Arslan K. (2010). Total neuron numbers in CA1-4 sectors of the dog hippocampus. *Indian J Med Res* **131,** 780-785.

Raingo J, Khvotchev M, Liu P, Darios F, Li YC, Ramirez DM, Adachi M, Lemieux P, Toth K, Davletov B & Kavalali ET. (2012). VAMP4 directs synaptic vesicles to a pool that selectively maintains asynchronous neurotransmission. *Nat Neurosci* **15,** 738-745.

Ramirez DM & Kavalali ET. (2012). The role of non-canonical SNAREs in synaptic vesicle recycling. *Cell Logist* **2,** 20-27.

Ramirez DM, Khvotchev M, Trauterman B & Kavalali ET. (2012). Vti1a identifies a vesicle pool that preferentially recycles at rest and maintains spontaneous neurotransmission. *Neuron* **73,** 121-134.

Raptis A, Torrejon-Escribano B, Gomez de Aranda I & Blasi J. (2005). Distribution of synaptobrevin/VAMP 1 and 2 in rat brain. *J Chem Neuroanat* **30,** 201-211.

Rashid S, Lee I, Anderson AE, Hrachovy RA & Swann JW. (1999). Insights into the tetanus toxin model of early-onset epilepsy from long-term video monitoring during anticonvulsant therapy. *Brain Res Dev Brain Res* **118,** 221-225.

Reid CA, Adams BE, Myers D, O'Brien TJ & Williams DA. (2008). Sub region-specific modulation of synchronous neuronal burst firing after a kainic acid insult in organotypic hippocampal cultures. *BMC Neurosci* **9,** 59.

Ribak CE, Seress L, Peterson GM, Seroogy KB, Fallon JH & Schmued LC. (1986). A GABAergic inhibitory component within the hippocampal commissural pathway. *J Neurosci* **6,** 3492-3498.

Rossetto O, Seveso M, Caccin P, Schiavo G & Montecucco C. (2001). Tetanus and botulinum neurotoxins: turning bad guys into good by research. *Toxicon* **39,** 27-41.

Roux E & Borrel A. (1898). Tétanos cérébral et immunité contre le tétanos. *Annales de l'Institut Pasteur* **4,** 126-138.

Ruban D, Byrne RW, Kanner A, Smith M, Cochran EJ, Roh D & Whisler WW. (2009). Chronic epilepsy associated with temporal tumors: long-term surgical outcome. *Neurosurg Focus* **27,** E6.

Samara A, Vougas K, Papadopoulou A, Anastasiadou E, Baloyanni N, Paronis E, Chrousos GP & Tsangaris GT. (2011). Proteomics reveal rat hippocampal lateral asymmetry. *Hippocampus* **21,** 108-119.

Scheuber A, Rudge R, Danglot L, Raposo G, Binz T, Poncer JC & Galli T. (2006). Loss of AP-3 function affects spontaneous and evoked release at hippocampal mossy fiber synapses. *Proc Natl Acad Sci U S A* **103,** 16562-16567.

Schiavo G, Benfenati F, Poulain B, Rossetto O, Polverino de Laureto P, DasGupta BR & Montecucco C. (1992). Tetanus and botulinum-B neurotoxins block neurotransmitter release by proteolytic cleavage of synaptobrevin. *Nature* **359,** 832-835.

Schwartzkroin PA & Prince DA. (1980). Changes in excitatory and inhibitory synaptic potentials leading to epileptogenic activity. *Brain Res* **183,** 61-76.

Shao XM & Feldman JL. (2007). Efficient measurement of endogenous neurotransmitters in small localized regions of central nervous systems in vitro with HPLC. *J Neurosci Methods* **160,** 256-263.

Sharma AK, Reams RY, Jordan WH, Miller MA, Thacker HL & Snyder PW. (2007). Mesial temporal lobe epilepsy: pathogenesis, induced rodent models and lesions. *Toxicol Pathol* **35,** 984-999.

Shin MC, Nonaka K, Wakita M, Yamaga T, Torii Y, Harakawa T, Ginnaga A, Ito Y & Akaike N. (2012). Effects of tetanus toxin on spontaneous and evoked transmitter release at inhibitory and excitatory synapses in the rat SDCN neurons. *Toxicon* **59,** 385-392.

Shone CC & Roberts AK. (1994). Peptide substrate specificity and properties of the zinc-endopeptidase activity of botulinum type B neurotoxin. *Eur J Biochem* **225,** 263-270.

Smith AT & Drew SJ. (1995). Tetanus: a case report and review. *J Oral Maxillofac Surg* **53,** 77-80.

Smith KL, Lee CL & Swann JW. (1998). Local circuit abnormalities in chronically epileptic rats after intrahippocampal tetanus toxin injection in infancy. *J Neurophysiol* **79,** 106-116.

Sollner T, Whiteheart SW, Brunner M, Erdjument-Bromage H, Geromanos S, Tempst P & Rothman JE. (1993). SNAP receptors implicated in vesicle targeting and fusion. *Nature* **362,** 318-324.

Spruston N & McBain C. (2007). Structural and Functional Properties of Hippocampal Neurons. In *The Hippocampus Book*, First edn, ed. Andersen P, Morris R, Amaral D & O'Keefe J, pp. 133-. Oxford University Press, Oxford.

Staub GC, Walton KM, Schnaar RL, Nichols T, Baichwal R, Sandberg K & Rogers TB. (1986). Characterization of the binding and internalization of tetanus toxin in a neuroblastoma hybrid cell line. *J Neurosci* **6,** 1443-1451.

Stoppini L, Buchs PA & Muller D. (1991). A simple method for organotypic cultures of nervous tissue. *J Neurosci Methods* **37,** 173-182.

Sudhof TC. (2004). The synaptic vesicle cycle. *Annu Rev Neurosci* **27,** 509-547.

Sugino K, Hempel CM, Miller MN, Hattox AM, Shapiro P, Wu C, Huang ZJ & Nelson SB. (2006). Molecular taxonomy of major neuronal classes in the adult mouse forebrain. *Nat Neurosci* **9,** 99-107.

Tsai PS, van Haeften T & Gadella BM. (2011). Preparation of the cortical reaction: maturation-dependent migration of SNARE proteins, clathrin, and complexin to the porcine oocyte's surface blocks membrane traffic until fertilization. *Biol Reprod* **84,** 327-335.

Turillazzi E, Neri M, Pomara C, Riezzo I & Fineschi V. (2009). An immunohistochemical study on a tetanus fatal case using toxin fragment C (TTC). Should it be a useful diagnostic tool? *Neuropathology* **29,** 68-71.

Turski WA, Cavalheiro EA, Bortolotto ZA, Mello LM, Schwarz M & Turski L. (1984). Seizures produced by pilocarpine in mice: a behavioral, electroencephalographic and morphological analysis. *Brain Res* **321,** 237-253.

Umezaki Y, Yasuyama K, Nakagoshi H & Tomioka K. (2011). Blocking synaptic transmission with tetanus toxin light chain reveals modes of neurotransmission in the

PDF-positive circadian clock neurons of Drosophila melanogaster. *J Insect Physiol* **57,** 1290-1299.

van Groen T & Wyss JM. (1990). Extrinsic projections from area CA1 of the rat hippocampus: olfactory, cortical, subcortical, and bilateral hippocampal formation projections. *J Comp Neurol* **302,** 515-528.

Verderio C, Pozzi D, Pravettoni E, Inverardi F, Schenk U, Coco S, Proux-Gillardeaux V, Galli T, Rossetto O, Frassoni C & Matteoli M. (2004). SNAP-25 modulation of calcium dynamics underlies differences in GABAergic and glutamatergic responsiveness to depolarization. *Neuron* **41,** 599-610.

Vermoesen K, Smolders I, Massie A, Michotte Y & Clinckers R. (2010). The control of kainic acid-induced status epilepticus. *Epilepsy Res* **90,** 164-166.

Vincent P & Mulle C. (2009). Kainate receptors in epilepsy and excitotoxicity. *Neuroscience* **158,** 309-323.

Vreugdenhil M, Hack SP, Draguhn A & Jefferys JG. (2002). Tetanus toxin induces long-term changes in excitation and inhibition in the rat hippocampal CA1 area. *Neuroscience* **114,** 983-994.

Wahab A, Heinemann U & Albus K. (2009). Effects of gamma-aminobutyric acid (GABA) agonists and a GABA uptake inhibitor on pharmacoresistant seizure like events in organotypic hippocampal slice cultures. *Epilepsy Res* **86,** 113-123.

Whittington MA & Jefferys JG. (1994). Epileptic activity outlasts disinhibition after intrahippocampal tetanus toxin in the rat. *J Physiol* **481 (Pt 3),** 593-604.

Xiong Y, Lv H, Gong Z & Liu L. (2010). Fixation and locomotor activity are impaired by inducing tetanus toxin expression in adult Drosophila brain. *Fly (Austin)* **4,** 194-203.

Yamamoto H, Ida T, Tsutsuki H, Mori M, Matsumoto T, Kohda T, Mukamoto M, Goshima N, Kozaki S & Ihara H. (2012). Specificity of botulinum protease for human VAMP family proteins. *Microbiol Immunol* **56,** 245-253.

Yamasaki S, Baumeister A, Binz T, Blasi J, Link E, Cornille F, Roques B, Fykse EM, Sudhof TC, Jahn R & et al. (1994). Cleavage of members of the synaptobrevin/VAMP family by types D and F botulinal neurotoxins and tetanus toxin. *J Biol Chem* **269,** 12764-12772.

Yang B, Gonzalez L, Jr., Prekeris R, Steegmaier M, Advani RJ & Scheller RH. (1999). SNARE interactions are not selective. Implications for membrane fusion specificity. *J Biol Chem* **274,** 5649-5653.

Yeh FL, Dong M, Yao J, Tepp WH, Lin G, Johnson EA & Chapman ER. (2010). SV2 Mediates Entry of Tetanus Neurotoxin into Central Neurons. *PLoS Pathog* **6,** e1001207.

Ziobro JM, Deshpande LS & Delorenzo RJ. (2011). An organotypic hippocampal slice culture model of excitotoxic injury induced spontaneous recurrent epileptiform discharges. *Brain Res* **1371,** 110-120.

7 APPENDIX

7.1 Grey level data for the grouping of control slices

7.1.1 VAMP1 control data

Middle

Ipsilateral	P value
DG	0.067
CA2/3	0.067
CA1	0.200

Contralateral	P value
DG	0.200
CA2/3	0.067
CA1	0.333

Posterior

Ipsilateral	P value
DG	0.160
CA2/3	0.933
CA1	0.467

Contralateral	P value
DG	0.362
CA2/3	0.468
CA1	0.524

The above data shows the p values after comparison of the control data from days 2, 8 and 16. These are shown within each region of interest and within the mid and posterior levels of VAMP1 immunostained slices. One way ANOVAs were used to compare the three different time points.

7.1.2 VAMP2 control data

Middle

Ipsilateral	P value
DG	0.148
CA2/3	0.448
CA1	0.206

Contralateral	P value
DG	0.419
CA2/3	0.251
CA1	0.342

Posterior

Ipsilateral	P value
DG	0.487
CA2/3	0.450
CA1	0.329

Contralateral	P value
DG	0.426
CA2/3	0.398
CA1	0.698

The above data shows the p values after comparison of the control data from days 2, 8 and 16. These are shown within each region of interest and within the mid and posterior levels of VAMP2 immunostained slices. The tests were One way ANOVAs in all cases.

7.2 Conference abstracts

7.2.1 British Neuroscience Association Meeting 2011

Alteration of VAMP1 and VAMP2 synaptic protein expression and lack of inhibitory cell loss in tetanus toxin induced temporal lobe epilepsy

Lucy Foss, Alex S. Ferecsko, Premysl Jiruska, John G.R. Jefferys, Attila Sik

Intrahippocampal injection of tetanus toxin (TeTX) induces a chronic model of temporal lobe epilepsy. While the majority of rats lack obvious neuronal loss, it remains possible that a selective loss of inhibitory cells contributes to the epilepsy. We investigated the neuronal death and the spatiotemporal dynamics of VAMP1 and VAMP2 synaptic proteins, the substrates of TeTX. The chronic epileptic syndrome was induced by TeTX injection into the CA3 region of the hippocampus *in vivo* (under the UK Animals (Scientific Procedures) Act (1986)). TUNEL assay was used to reveal the spatial and temporal distribution of apoptotic and necrotic cells and immunofluorescent staining to identify TUNEL expression in parvalbumin (PV) and calretinin (CR)-expressing inhibitory neurons. Immunohistochemical labelling for VAMP1 and VAMP2 proteins was performed on control and TeTX injected rats post injection 2, 8 and 16 days. Apoptotic and necrotic cells could be found in control and TeTX injected animals; some of the TeTx-injected rats at days 8 and 16 appeared to have more positive cells, but this difference between groups was only significant for pooled contralateral hippocampal regions on day 16, and no correlation was found between cell death and seizure severity or frequency. No co-localisation of TUNEL stained cells with either PV or CR labelled interneurons was observed. The labelling of VAMP1 and VAMP2 proteins showed the lowest intensity focally and increased with distance from the injection site. The extent of the regions lacking the VAMP1 and VAMP2 labelling along the anterior-posterior dimension varied considerably between days 2 (320±80μm), 8 (1360±160μm) and 16 (1573±166μm). GABA, glutamate and neurofilament 68k expression were unaltered even in the focus of the injection. These data indicate that disruption of both VAMP1 and VAMP2 proteins rather than the lack of available neurotransmitter or inhibitory cell loss underlie the development of the seizures in TeTX model.

7.2.2 Neuroscience 2011

Differential distribution of hippocampal VAMP1 and VAMP2 isoforms and their cleavage by tetanus toxin.

Lucy Foss, Alex S. Ferecsko, Premysl Jiruska, John G.R. Jefferys, Attila Sik

Tetanus toxin (TeTx) is known to cleave vesicle associated membrane protein (VAMP). It is widely held that TeTx acts preferentially at inhibitory interneurons in brain and spinal cord. Two isoforms of the VAMP exist within the brain, VAMP1 and VAMP2, however previous reports do not agree on which isoform is the target of TeTx, whether it is both or just VAMP2. Here we tested the effects of the toxin on the VAMP proteins by incubating rat synaptosomes in TeTx, followed by denaturing and run on an SDS-PAGE gel followed by western blotting. Detection using enhanced chemiluminescence showed that the TeTx cleaved both the VAMP1 and VAMP2 proteins. To test this on neurons *in vitro,* we carried out focal injections of TeTx onto the surface of the CA3 region of organotypic hippocampal slice cultures from mice followed by immunohistochemical staining for the VAMP2 protein. Results show that the VAMP2 protein is indeed cleaved by TeTx in this condition. To test the specificity *in vivo*, intrahippocampal injections of toxin were then made into the CA3 of rats and *post mortem* immunohistochemical staining carried out for both isoforms. The results show that both VAMP isoforms are cleaved in a spatiotemporal manner. To establish whether there was a differential expression of the two isoforms between inhibitory and excitatory neurons within the hippocampus we carried out co-localisation studies in paraformaldehyde perfused rat brains. VAMP1 and VAMP2 proteins were double labelled with antibodies against glutamic acid decarboxylase 65 (GAD65) and vesicular glutamate transporter 1 (VGLUT1), markers for inhibitory and excitatory neurons respectively. These results showed that VAMP1 is most commonly associated with inhibitory neurons and the VAMP2 with excitatory neurons. Overall these results show that the TeTx is responsible for the cleavage of both isoforms of the VAMP protein, contradicting what has previously been reported. They also show that the isoforms are differentially distributed within the hippocampus. The implication that both inhibitory and excitatory neurons are affected by the toxin poses interesting questions relating to the TeTx model of temporal lobe epilepsy, suggesting that it is not simply due to inhibitory dysfunction.